Production of fuels and chemicals from a solar driven pyrolysis of animal and agricultural wastes

By

Haftom Weldekidan

Department of Environmental Sciences

Faculty of Science and Engineering

Macquarie University

Supervisor:

Prof. Vladimir Strezov

Other supervisors:

Prof. Graham Town and Dr. Tao Kan

This thesis is presented for the degree of Doctor of Philosophy

April, 2019

Declaration

I certify that the work in this thesis has not previously been submitted for a degree nor has it been submitted as part of requirements for a degree to any other university or institution other than Macquarie University.

I also certify that the thesis is an original piece of research and it has been written by me. Any help and assistance that I have received in my research work and the preparation of the thesis itself have been appropriately acknowledged.

In addition, I certify that all information sources and literature used are indicated in the thesis.

_____

Haftom Asmelash Weldekidan

12-June-2019

Acknowledgements

Glory be to the Almighty God! This PhD has come to its end.

I am so fortunate to be a student of Vlad for my PhD. Vlad, I really appreciate your support that you have been doing to me starting from providing the opportunity to pursue my PhD degree in Macquarie University to all the trainings in the research and academic writings. With your endless insightful feedbacks logical thinking and intrinsic encouragements, I am able to build such a solid track record and finish this PhD with publication in top journals. Vlad you are not only an outstanding Prof with extraordinary skills but also an excellent and able educator. I will be forever thankful to you.

I would also like to thank my other supervisors Prof. Graham Town and Dr. Tao Kan who have been available to me whenever I need them. They greatly helped me to formulate my project, edit my many mistakes and provide me thoughtful comments and suggestions which added great value to this PhD.

My stay in this beautiful Australia was amazingly enjoyable because of my friends, colleagues and staffs of the department of Environmental Sciences. Thank you so much!

To my whole family, who has been with me spiritually throughout this PhD program; to the lovelies Eset and Snit, let me assure that I will spend more time with you to compensate your love after my graduation.

Not least of all, I should acknowledge the International Macquarie Research Scholarship of the Macquarie University for the scholarship. I should also acknowledge Macquarie University for the generous PGRF and HDR funding schemes which allowed me travel overseas for experiments and presentation of my findings to the science community and visit some wonderful places on the planet.

Dedication

I would like to dedicate this work to my brilliant grandmother, Zwedu Natnael, who passed away in my last year of PhD. She loved me abundantly, raised and taught me to be the person who I am now. I wish she was still alive and enjoyed my achievements now.

I also want to remember my elder brother, Abera Asmelash, who lost his life in an accident. He was the most unpretentious person with unlimited integrity who could even sacrifice himself for others. You left the whole family in nowhere! Your life was so short, but I will never forget you as long as I exist. My best! I will always miss you all beyond words. May the Almighty God rest your soul in peace!

Amen!!!

Table of Contents

List of Figures

List of Tables

Abstract

Energy is very important in meeting our basic needs. It is also one of the fundamental requirements in the industrial, transportation and agricultural sectors which determine the overall economic development of nations. In this work pyrolysis of different types of wastes, mainly chicken litter and rice husk, was performed at different heating rates and ranges of temperature obtained from a concentrated solar radiation.

Review of solar based technologies and their applications to solar-assisted biomass utilization and conversion technologies were performed to identify the gaps and study the type of bio-fuels that can be produced from solar driven biomass pyrolysis. Prospective solar concentrators were assessed for their efficiency, maximum temperature and applications. Based on the information obtained from the literature and the gaps identified in the review, parabolic dish was selected as a prospective solar concentrator that can achieve higher temperatures at relatively better concentration ratio. Thus a parabolic dish of 1.8 m aperture diameter and a focal length at 0.655 m was designed and manufactured at Macquarie University. The dish was laminated with an 88% reflective aluminium polyethylene terephthalate (PET) and mounted on a rotating structure for adjusting the height and azimuth angles of the sun. Experiments were conducted to measure the maximum achievable temperature and select reactors from different types of materials which should be placed at the focal region. Quartz glass and stainless steel tubes were the best performing reactors, achieving maximum temperature of 1100°C at 900 to 1000 W/m^2.

The feedstock (chicken litter and rice husk) were collected from Carlingford, Sydney then dried and crushed to a sieve size of 280 µm and then packed separately in the quartz glass reactor for the solar pyrolysis experiments which were conducted at different solar temperatures (500 to 900°C).

Gases were the main products obtained from the pyrolysis of the chicken-litter waste, generated in the range of 45–59 wt% followed by bio-char (16–40 wt%) and bio-oils (14–36 wt%). The pyrolysis gas was composed of CO_2, CO, CH_4, H_2 and other light weight hydrocarbons, while the bio-oils which contained phenols, acids and N-containing compounds can be applied to produce solvents, cleaning agents, paint removers, detergents as well as in the synthesis of dyes, aspirin and plastics. Bio-oil and bio-char were the dominant yields in solar pyrolysis, reaching up to 44 wt.% and 43 wt.%, respectively. The bio-char had large glass-like cylindrical holes with many porous and loose structures which are the required properties for the bio-char to be a candidate material for contaminant adsorbent in waste water treatment.

The quality of the solar pyrolysis products was further upgraded using CaO and char catalysts. The catalysts were separately applied in different proportions in an *in-situ* and *ex-situ* modes with the chicken litter, and subjected to the solar pyrolysis at 500 to 800°C. In all cases there was substantial

decrease in CO_2 accompanied by an increase in the formation of CO from 10 to 63 wt% and H_2 from 1 to 15 wt%. Similarly, addition of CaO exhibited considerable deoxygenation performance of the fatty acids up to 3%.

Solar pyrolysis experiments performed on the chicken litter and rice husk biomass at higher temperatures (800 to 1600°C) and heating rates (10 to 500°C/min) produced highly combustible gases with higher heating values of 7255 ± 566 kJ/kg.

Overall, the obtained results revealed that solar-assisted pyrolysis of biomass could be a promising technology for fuel and chemical production.

Chapter 1: Introduction

Energy is considered as one of the significant factors for economic development and its demand is increasing due to the rapid population growth and improved living standards. It has been projected that world energy consumption will grow by 124% at the end of this millennia (Deign, 2018) which is approximately equivalent to 343 petawatt-hours of energy. Currently, fossil fuels are the main sources of energy and they will still remain the dominant source through 2030 and well beyond (Bajwa *et al*., 2018). Keeping the current laws, regulations and policies of energy consumption, the fossil fuel reserve will be depleted after 70 years (Weldekidan *et al*., 2018). Moreover, in 2040 energy related greenhouse gas (GHG) emissions are estimated to increase by 46%, reaching 45 billion metric tons. The heavy reliance on fossil fuel will bring significant climate change and seriously damage the environment (Lim *et al*., 2012).

To address these concerns, producton of fuels and chemicals with renewable energy is receiving intensive attention. Biomass is considred as one promising source of renewble energy due to its availability and carbon neautrality. Biomass can be converted to different types of bio-fuels through a thermochemical treatment process, called pyrolysis. Pyrolysis is a process of heating biomass without oxygen at temperature ranges of 300 to 700°C. Gases, liquid bio-oil and bio-chars are the main products obtained from biomass pyrolysis which can offer different advantages including supply reliablity, fuel diversity, carbon sequestration and many more. Pyrolysis is an endothermic process during which the heat requied to perform pyrolysis is generally supplied either from fossil based fuels or by combusting part of the biomass which compromises the quality and quantity of the pyrolysis products.

On the other side, we have solar energy which can be captured and become available for biomass pyrolysis. Integrating these two sources can therefore, bring substantial benefits by making the whole energy generation process emission free and renewable.

1.1 Thesis Outline

This thesis describes an experimental study aimed at producing different types of fuels and chemicals from organic wastes using solar assisted thermochemical conversion processes. Solar energy has been concentrated to supply process heat to perform pyrolysis of different agricultural wastes, chicken-litter waste and rice husk at different operating conditions. Pyrolysis gases, bio-oil and bio-chars were sufficiently produced and characterized to pinpoint possible areas of applications. It was found that solar assisted pyrolysis can generate fast heating rates and high temperatures which favour production of significant amount of pyrolytic

gases with higher energy values which can be used as a substitute for fossil fuels in many applications.

This thesis is presented in 9 chapters. The general introduction, thesis structure and outlines are presented in Chapter one. In the second chapter, solar based technologies and their applications to solar assisted biomass utilization and conversion are thoroughly reviewed. Chapter 3 includes design and manufacturing of the solar system used in this study. Different types of absorber reactors were evaluated for their performance to produce solar fuels from biomass pyrolysis under the concentrated solar radiation. The fourth chapter comprises studies that examined fast pyrolysis of chicken-litter waste at different temperatures achieved with the solar concentrator. Production and analysis of fuels and chemical from the pyrolysis of rice husk, and the properties of pyrolysis gases, bio-oils and chars at different temperatures are discussed in Chapter 5. Chapters 4 and 5 were conducted at moderate pyrolysis temperatures which produced pyrolysis gases highly dominated with CO_2. It is known that CO_2 is one of the unwanted gas which should be removed from the gas mix to increase the energy content of the pyrolytic gases. Moreover, the bio-oils produced in the previous experiments were highly oxygenated and unstable. The sixth chapter was therefore aimed at upgrading quality of the pyrolysis products with the application of catalysts. Different types of catalysts have been utilized in different modes to improve the quality of the pyrolysis gases and bio-oil compounds. Solar pyrolysis experiments performed at higher temperatures and fast heating rates are discussed in Chapter 7. The influence of process parameters on the yield and composition of solar pyrolysis products are also assessed in Chapter 7. Chapter 8 presents the energy conversion efficiency of the pyrolysis of chicken litter and rice husk feedstocks. These 8 chapters provide an all-encompassing study of the interlinking aspects of biomass pyrolysis under the concentrated solar radiation. The last chapter (Chapter 9) provides the general conclusion and recommendations.

The thesis is formatted as a thesis by publications containing the following publications that resulted from the work:

1.2 List of publications

The following publications resulted from this thesis:

Weldekidan, H., Strezov, V., & Town, G. (2018). Review of solar energy for biofuel extraction. *Renewable and Sustainable Energy Reviews*, 88, 184-192.

Weldekidan, H., Strezov, V., & Town, G., (2018). Solar energy for biofuel extraction, in *Renewable Energy Systems from Biomass: Efficiency, Innovation, and Sustainability* ed. by V. Strezov and H.M. Anawar, CRC Press, Boca Raton, USA, pp 191-208, ISBN 978-1-4987-6790-3.

Weldekidan, H., Strezov, V., & Town, G. (2017). Performance evaluation of absorber reactors for solar fuel production. *Chemical Engineering Transaction*, 61, 1111-1116.

Weldekidan, H., Strezov, V., Kan, T., & Town, G. (2018). Waste to energy conversion of chicken litter through a solar-driven pyrolysis process. *Energy & Fuels*, 32(4), 4341-4349.

Weldekidan, H., Strezov, V., Town, G., & Kan, T. (2018). Production and analysis of fuels and chemicals obtained from rice husk pyrolysis with concentrated solar radiation. *Fuel*, 233, 396-403.

Weldekidan, H, Strezov, V., Kan, T., Kumar, R., He, J., and Town,. G., (2019). Solar assisted catalytic pyrolysis of chicken-litter waste with in-situ and ex-situ loading of CaO and char. *Fuel, 246, 408-416.*

Weldekidan, H, Strezov, V., Li, R., Kan, T., Town, G., Kumar, R., He, J., Flamant, G., (2018). Distribution of solar pyrolysis products and product gas composition produced from agricultural residues at different operating parameters. Submitted *to Renewable Energy.*

Weldekidan, H, Strezov, V., He, J., Kumar, R., Asumadu-Sarkodie, S., Doyi, I., Jahan, S., Kan, T., Town, G., (2018). Energy conversion efficiency of pyrolysis of chicken litter and rice husk biomass. *Energy & Fuels*, http://dx.doi.org/10.1021/acs.energyfuels.9b01264.

List of peer reviewed conferences

Weldekidan, **H**., Strezov, V., Kan, T., and Town, G., Comparison of chicken-litter waste and rice husk pyrolysis under concentrated solar radiation. The 256th American Chemical Society (ACS) National Meeting, 19–23 August 2018, Boston, USA.

Weldekidan, **H**., Strezov, V., Kan, T., Kumar, R., He, J., and Town, G., Catalytic pyrolysis of chicken-litter biomass using calcium oxide and bio-char catalysts assisted by solar energy, 6th International Conference on Biomass Energy, 16–19 October 2018, Wuhan, China.

Weldekidan, H., Strezov, V., Kan, T., and Town, G., Waste to energy valorization of chicken litter through solar-driven pyrolysis process. 6th Sino-Australian Symposium on advanced coal and biomass utilization technologies, 4–8 December 2017, Perth, Western Australia.

Weldekidan, **H**., Strezov, V., Town, G., Kan, T., Ray tracing characterization of solar-assisted biomass pyrolysis reactors. Chemeca 2017 – Innovation through science and engineering, 23–26 July 2017, Melbourne, Australia.

Weldekidan, **H**., Strezov, V., Town, G., Performance evaluation of absorber reactors for solar fuel production. 20th conference process integration, modeling and optimization for energy saving and pollution reduction, 21–24 August 2017, Tianjin, P. R. China.

1.3 References

Bajwa, D. S., Peterson, T., Sharma, N., Shojaeiarani, J., & Bajwa, S. G. (2018). A review of densified solid biomass for energy production. *Renewable and Sustainable Energy Reviews, 96*, 296-305.

Deign, J. (2018). The "silly" demand coming for the earth's resources. Retrieved from https://www.greentechmedia.com/articles/read/energy-needs-in-2100-even-fossil-fuels-will-not-cut-it#gs.LVRbO4MG.

Lim, J. S., Abdul Manan, Z., Wan Alwi, S. R., & Hashim, H. (2012). A review on utilisation of biomass from rice industry as a source of renewable energy. *Renewable and Sustainable Energy Reviews, 16*(5), 3084-3094.

Weldekidan, H., Strezov, V., & Town, G. (2018). Review of solar energy for biofuel extraction. Renewable and Sustainable Energy Reviews, 88, 184-192.

Chapter 2: Review of solar energy for biofuel extraction

In this chapter, review of solar-assisted pyrolysis of organic feedstock for converting solar energy into different types of solar fuels and chemicals is presented. Different types of solar concentrating technologies with potential to capture the solar heat to drive pyrolysis of different types of organic materials are studied. Review of solar assisted gasification and distillation process performed to date are further presented in this chapter. Additionally, a comprehensive study of the different products obtained from the pyrolysis and gasification of different types of feedstock under the concentrated solar radiation are performed. Contemporary developments on solar-assisted thermochemical conversion technologies and their products as well as the advantages of pyrolysis with respect to other thermochemical conversion processes are given in Appendix 1. In addition, discussion on solar towers is incorporated in Appendix 2.

The idea of this work was initiated by my supervisor Prof. Vladimir and developed and written by myself. Major editing and reviewing were performed by Prof. Vladimir and Prof. Graham, and published as a review paper in *Renewable and Sustainable Energy Reviews*.

Publication:

Weldekidan, H. (65%) Strezov, V. (25%) & Town, G. (10%). Review of solar energy for biofuel extraction, ***Renewable and Sustainable Energy Reviews (2018), 88: 184-192.***

Adopted for this thesis with the exclusive rights from Elsevier.

The paper was republished with permission from Elsevier as:

Weldekidan, H. (65%) Strezov, V. (25%) & Town, G. (10%) (2018). Solar Energy for Biofuel Extraction, in *Renewable Energy Systems from Biomass: Efficiency, Innovation, and Sustainability* ed. by V. Strezov and H.M. Anawar, CRC Press, Boca Raton, USA, pp 191-208, ISBN 978-1-4987-6790-3.

Review of solar energy for biofuel extraction

Haftom Weldekidan[a], *Vladimir Strezov*[a*], *Graham Town*[b]

[a] Department of Environmental Sciences, Faculty of Science and Engineering, Macquarie University, Sydney, NSW 2109, Australia

[b] School of Engineering, Faculty of Science and Engineering, Macquarie University, Sydney, NSW Australia

*vladimir.strezov@mq.edu.au

Abstract

One of the most complex challenges of today is managing greenhouse gas emissions produced by excessive use of fossil fuels as energy source. With fossil fuels dominating the energy production, the sustainable and environmental problems will continue unless alternative sources of energy are put in place. Biomass is considered as a promising sustainable energy source which can be introduced to our energy mix. One way of converting raw biomass to higher value biofuels is following the thermochemical conversion processes, which include pyrolysis, gasification, torrefaction, combustion and distillation. However, these processes typically require heat energy to treat the biomass, which is often supplied from non-renewable energy sources. This greatly reduces the conversion efficiency and causes environmental problems. Utilization of solar energy for assisting the biomass conversion through thermochemical conversion process significantly improves the overall sustainability and process performance. This work reviews the solar based technologies and their application to solar assisted biomass utilization and conversion technologies. The review then discusses outcomes of different solar assisted biomass pyrolysis and gasification processes performed to date. It also presents the status of solar assisted distillation for improving ethanol concentration.

Keywords: solar thermal, biomass, biofuel, thermochemical conversion, pyrolysis, gasification

2.1 Introduction

Due to the rapid global population growth and rising living standards, there has been a significant increase in energy demand and consumption over the last several decades (Chen *et al.*, 2015). By 2040, the total energy use is expected to grow by about 40% of the current use. Even though the share of fossil fuels in the entire energy mix is expected to fall, it will still remain the dominant source of energy with oil, coal and gas each expected to account to over 25% of the global energy needs (Cronshaw, 2015). It is also estimated that the world population will reach 9.3 billion by 2050 (Morales *et al.*, 2014). This rapid population growth will increase the energy demand while fossil fuels, being dominant energy sources, are estimated to significantly deplete after 70 years (Metzger & Hüttermann, 2009). It is inevitable that sustainability and environmental challenges will continue, unless an alternative source of energy is put in place ahead of time. The existing pattern of energy supply cannot be sustained in the near future because of the depletion of fossil fuel reserves and also environmental impacts from their use (Rahman *et al.*, 2014). According to Morales *et al.* (2014) one of the most complex challenges faced today is managing and halting climate changes produced by the over-exploitation of natural resources.

Biomass is seen as the most promising energy source to mitigate greenhouse gas emissions. Substantial adoption of this ubiquitous energy source could alleviate the environmental, social, and economic problems faced by the modern society (Khan *et al.*, 2009). Many researchers have shown the possibility of a substantial contribution of biomass to our energy demand for the years to come. Until 2012, global biomass use was 8-14% of the world final energy consumption. The annual availability of biomass is estimated to reach as high as 108 Gtoe, which is almost ten times the world's current energy requirement (Demirbas, 2007; Hoogwijk *et al.*, 2005; Kan *et al.*, 2016; Williams *et al.*, 2012).

There should be efficient utilization of biomass through the adoption of improved energy technologies. There are many existing processes that convert raw biomass to usable forms of energy and chemicals. These include combustion, pyrolysis, gasification, torrefaction, liquefaction, esterification and fermentation (Elliott *et al.*, 1991; Strezov & Evans, 2015). These processes are considered as critical biomass utilization alternatives, offering economic benefits through the production of high value fuel gasses and liquids, char and chemicals (Bulushev & Ross, 2011; Han & Kim, 2008; Rapagnà *et al.*, 1998; Zhang *et al.*, 2016). These processes are highly endothermic requiring large heat input, generally supplied from non-

renewable sources of energy (Morales *et al.*, 2014). Solar energy can be captured and stored in chemicals or fuels, also known as solar fuels, for later use and easy transportation. Utilization of solar energy for assisting the biomass conversion through distillation or thermochemical processing is expected to significantly improve the overall biofuel life cycle performance. Recently biofuel extraction technologies using concentrated solar energy have been tested in solar reactors with real sun (Zeng *et al.*, 2017). Current technologies consist concentrating part with polished aluminium or glass mirror as reflecting surface, biomass reactors mostly made of quartz or borosilicate glasses and different types of metals such as copper and steel, and controllers for temperatures, heating rates, pressure and tracking units (Weldekidan *et al.*, 2017).

The objective of this work is to review solar based technologies and their applications for solar assisted biomass utilization and conversion technologies. The first part of the paper describes the fundamental conversion mechanisms of biomass to biofuels, with emphasis on the thermochemical conversion mechanisms. Different types of solar concentrating technologies with potential to capture the solar heat to drive the thermochemical conversion process are further discussed. Integration of the prospective solar collectors with biomass reactors are additionally elaborated. Finally, review of the solar assisted pyrolysis, gasification and status of solar assisted distillation process, together with characterization of the different product fractions obtained from the processes, are presented.

2.2 Overview of biomass to biofuel conversion mechanisms

Biofuel is a type of energy derived from biomass such as plants, agricultural, animal, domestic, and industrial wastes. Biomass can be converted into higher value biofuels either through biochemical, thermochemical or physico-chemical processes.

Biochemical conversion process involves fermentation of the sugars into alcohols, such as ethanol. This includes biomass pre-treatment followed by fermentation of the sugars to ethanol then separation and purification to produce pure ethanol (Ullah *et al.*, 2015). Fig. 1.1 shows the recent trends for the second generation of biofuel production through biochemical process from lignocellulosic biomass. The efficiency of the biochemical conversion process is between 35 and 50%wt (Singh *et al.*, 2010). This process can also be used to transform biomass into any type of petrochemical product compounds, such as olefins and aromatics which are made from petroleum or fossil fuels.

Distillation is typically used to produce, separate and distil ethanol into usable fuels. The energy is typically supplied through either an external heat source, such as gas or electricity from grid. In both cases, this practice reduces the environmental benefits of the biomass conversion processes on a full life cycle basis.

Thermochemical processes of converting biomass into biofuels involve application of heat energy to treat the biomass in the conversion process with conversion efficiencies in the range between 41–77%wt (Singh *et al.*, 2010). The treatment processes include combustion, gasification and pyrolysis.

Combustion is the direct burning of biomass in the air for the purpose of heating and power generation, initially practiced for long time since mankind has started using fire. Gasification is a process that converts organic or fossil fuel based carbonaceous materials into carbon monoxide, carbon dioxide and hydrogen known as syngas.

The syngas can be processed to produce different types of gaseous biofuels and liquids. Gasification is achieved by reacting the material at high temperatures (>700 °C), without combustion, but with a controlled amount of oxygen and/or steam. Fisher-Tropsch process with chemical catalytic conversion are advanced engineering processes developed to optimize the production of syngas for biofuel production. Gasification is highly endothermic process.

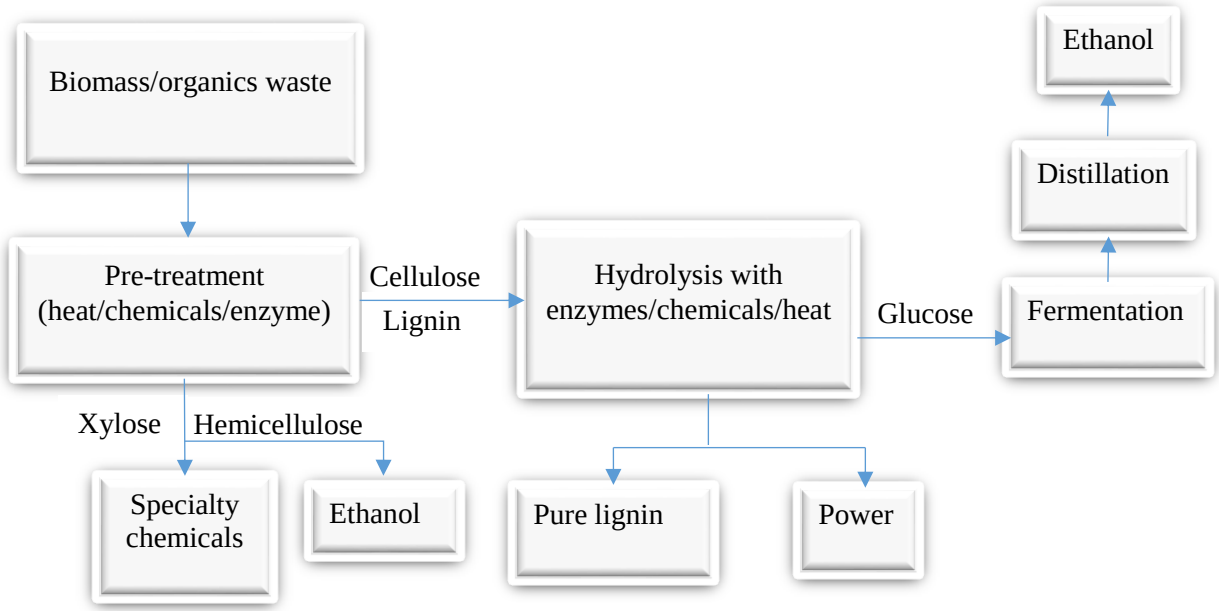

Figure 2-1 Biochemical process of biofuel production

The heat required to maintain this process is supplied from non-renewable sources of energy by burning significant portion (at least 35%) of the feedstock or using the electric grid which lowers the final efficiency of the process (Kenarsari & Zheng, 2014; Piatkowski & Steinfeld, 2008; Pozzobon *et al.*, 2016).

Pyrolysis is another thermochemical process that uses heat in the near absence of oxygen to destruct and distil biomass to produce biofuels, bio-oils (bio-crude), biogas and char. Pyrolysis has high flexibility in that it can be used to produce heavy fuel oil for heat and power applications, upgraded for conventional refinery operations, or it can be gasified for syngas which can be converted to hydrogen. Pyrolysis can convert over 60 wt% of the biomass into liquid bio-oil (Hertwich & Zhang, 2009). Pyrolysis requires moderate temperature in the range of 400 to 600°C to depolymerize biomass to a mixture of oxygenates (or 'bio-oil') that are liquid at room temperature (Mettler *et al.*, 2012). This external heat energy generally comes from burning part of the biomass or fossil fuels or using grid electricity (Morales *et al.*, 2014).

2.3 Energy from the sun

About 885 million terawatt hours reach the earth's surface in a year which is 4,200 times the energy that mankind would consume in 2035 according to the IEA's Current Policies Scenario (Philibert, 2011). In just three hours the Earth collects enough solar radiation to meet world's energy needs for one year. If one-tenth of one percent of the solar energy is captured and distributed, then the energy supply problem disappears (Philibert, 2011).

Biomass captures and converts solar radiation into energy ($C_xH_{2x}O_x$) through photosynthesis (Agrawal & Singh, 2010). Agrawal and Singh (2010) provided a review on the fraction of solar energy which can be recovered as biofuels, mainly liquid fuels for transportation purpose, via the cultivation and then conversion of the biomass using different methods (pyrolysis, gasification, fermentation, H_2bioil B and H_2CAR processes). The highest sunlight conversion efficiency for a full season growing biomass can be achieved up to 3.7% (Zhu *et al.*, 2008). Fast pyrolysis of biomass collected from 1 m^2/year can generate 524–627 litres of liquid fuel per year which corresponds to recovery of 65–77% of the absorbed solar energy by the biomass. Estimates of the solar energy recovery as liquid fuels from fermentation, gasification, H_2bioil-B and H_2CAR processing of biomass were found to be 41–50, 35–50, 59–69% and 58% respectively (Agrawal & Singh, 2010). Using supplementary energy such as H_2 or electricity

that is recovered from solar energy at higher efficiencies than the biomass can increase the fuel yield by a factor of 1.5–3 (Agrawal & Singh, 2010).

These estimates can be considerably improved if the heat energy for biomass conversion can be supplied from the sun using solar concentrating technologies. The following section describes the solar concentrating technologies available to integrate with biomass conversion for production of biofuels from biomass.

2.3.1 Solar concentrating technologies

Solar concentrators are devices which focus the solar energy incident over a large surface onto a smaller surface. There are several types of solar concentrating technologies that can capture the energy from the sun and make it available for application in the biomass to biofuel conversion processes. These are parabolic troughs (Hotz *et al.*, 2010), heliostat fields, linear Fresnel reflectors, parabolic dishes, compound parabolic concentrators, flat plates (Kraemer *et al.*, 2011), box type and linear Fresnel lenses (Baral *et al.*, 2015; Bernardo *et al.*, 2012; Hotz *et al.*, 2010; Kraemer *et al.*, 2011; Lee *et al.*, 2010). Each of these technologies differs in their temperature achievable, focal type, reflective material, operation characteristics, design and application, and therefore each has their own advantages and drawbacks for use in biofuel production. It is important to make appropriate technology choice for use in converting biomass to higher value biofuels.

Flat plate solar collectors are suitable to produce hot water up to 80°C, but flat plate solar collectors integrated with evacuated tubes can reach a temperature of 125°C. The ability to boil water under ambient sunlight without optical concentration was demonstrated by Ni *et al.*, (2016). Ni *et al.* (2016) used graphite as absorber material. To reduce heat losses, bottom of the absorber was insulated using thermal foam and sheet of transparent bubble wrap was placed on top of it. The arrangement was able to generate saturated steam at 100°C at efficiency as high as 64%.

Higher temperatures can be obtained with solar parabolic trough collectors which achieve temperatures greater than 400°C (Morales *et al.*, 2014). This type of arrangement is used to produce steam in industrial operations whereby thermal energy collected in the receiver part is transported by a heat transfer medium to the intended place. Higher temperature can be achieved with central receiver systems or dish concentrators which can achieve temperatures of up to 2000°C.

2.3.2 Parabolic trough concentrator

A parabolic trough is a type of solar thermal device which is straight in one dimension and curved as a parabola (two-dimensional U-shaped symmetrical curve) in the other two. The side that faces the sun is lined with a highly reflective material thus solar radiation is reflected onto a linear receiver placed at the focal line of the parabola (Abid *et al.*, 2016; Blanco *et al.*, 1986; Duffie & Beckman, 2013; Feuermann & Gordon, 1991; Kaygusuz, 2001; Lovejoy *et al.*, 1993; Nixon *et al.*, 2010). The reactor can be placed at this linear focal point of the parabolic trough concentrator. Typically, a reactor made from metal of high thermal conductivity or evacuated glass tube can reach working temperatures of over 400°C and concentration ratio (ratio between the concentrator opening area and the aperture area that receives) of 30-100 (Duffie & Beckman, 2013). Copper or bimetallic copper-steel are good options for this purpose but stratification is unavoidable (Flores & Almanza, 2004). An optical efficiency of 80% has been recorded in California providing 354 W/m^2 and a stagnation temperature of 600°C (Lovejoy *et al.*, 1993). Biomass reactor system, if used with parabolic troughs, can be either heated directly (Alonso & Romero, 2015) in the focal line or use heat transferring medium to heat the reactor placed out of the focal line. There are technical challenges that should be taken into consideration while using parabolic trough for biomass processing including the risk of overheating tubes and instability of the bioreactor. Also, complex control mechanisms are required if an indirect heating system of the bioreactor is to be employed (Nixon *et al.*, 2010).

2.3.3 Linear compound parabolic collector

A linear compound parabolic collector reflector is used as a non-tracking system to concentrate solar energy to a double-sided flat receiver/reactor which is normal to the compound parabolic collector axis (Gu *et al.*, 2014). The common configuration has bottom section resembling a circle while the upper section is a parabola, thus the focus is a line stretching from edge to edge. This is a non-imaging linear concentrator which can also work as a stationary collector without tracking system (Blanco *et al.*, 1986). Maximum achievable temperature is only 200°C for concentration ratio of 3. Thus, unless augmented by additional heat source the compound parabolic collector alone cannot be used for the purpose of biomass thermal processing.

2.3.4 Linear Fresnel reflectors

Linear Fresnel reflectors use long and thin segments of mirrors to focus sunlight onto a fixed absorber/reactor located at a common focal point of the reflectors. The reflectors are made from

cheap flat mirrors and can concentrate sun's rays 30 times. The operation temperature at the focal line is 150°C but, with the use of secondary concentrator, temperatures of up to 300°C can be reached. Additionally, if compound parabolic collector is integrated with linear Fresnels the optical and capture efficiencies can be improved to 60% and 76% respectively (Feuermann & Gordon, 1991; Nixon *et al.*, 2010). The reactor used with linear Fresnel is separated from the reflector field and is stationary. The capital and maintenance cost are much lower than the other types of solar collectors (Feuermann & Gordon, 1991; Nixon *et al.*, 2010).

2.3.5 Parabolic dish reflector

A parabolic dish is a surface generated by a parabola revolving around its axis. It can be used to concentrate the solar rays and achieve reactor temperatures as high as 2000°C. Depending on the size, a solar parabolic dish can have concentration ratio in the range of 500 to 2000 (Tesfay *et al.*, 2014). The parabolic dish is mainly used to concentrate solar radiation for low, medium and high-temperature applications (Abu Bakar *et al.*, 2015; Tsoutsos *et al.*, 2003) but requires two dimensional continuous tracking as the concentrated solar rays should be focused onto a single focal point (Nixon *et al.*, 2010). Parabolic dish has the highest capture of solar energy achieving optical efficiency (ratio of energy reaching the absorber to the irradiance falling on the collector surface) of up to 94%.

With the correct reflective filming of the collector and black reactor coating, a reactor or receiver placed at the focal point can reach a temperature well over 1000°C (Kaygusuz, 2001). For solar thermochemical processes, particularly with solar parabolic dish the best candidate reflective coatings are silver coated glass and silvered polymer films. Polymer reflectors are lighter in weight, offer greater system design flexibility and have the potential for a lower cost than glass reflectors (Kennedy & Terwilliger, 2005; Schissel *et al.*, 1995). The current research trends in the assessment of efficient solar reflective materials for long-term outdoor application range from various silvered glass mirrors, silvered polymer films and anodized sheet aluminum with additional protective polymer coating (Auti *et al.*, 2015; DiGrazia *et al.*, 2009,; Fend *et al.*, 2000). Plain aluminum, with reflectivity of 85%, is the other reflector coating which is of interest for its low cost (Kumar *et al.*, 2015; Nostell *et al.*, 1997).

A number of studies are available on black coatings for solar thermal applications. Black coating materials should be low-cost, easy to manufacture, chemically stable and able to withstand high temperatures (Kennedy, 2002). Moon *et al.* (2015) performed several

experiments on black oxide nanoparticles as solar absorbing material for a high-temperature concentrating solar system. Accordingly, cobalt oxide (Co_3O_4) black coated layer exhibited high-temperature durability and hardly degraded in structure after long working hours. The light absorbing performance of Co_3O_4 was found to be 88.2% making it promising candidate for solar absorption in the next-generation high-temperature solar concentrating systems.

Higher temperature can also be achieved if the receiver or reactor is enveloped in a glass tube. This gives the parabolic dishes the potential to eventually become one of the important devices for solar thermochemical conversion processes. Moreover, parabolic dish systems are typically designed for small-to-moderate capacity applications of the order of ten kilowatts which are suitable for remote power needs in rural areas and the places far away from the national electricity grid. Another advantage of the parabolic dish is unlike other solar thermal systems such as parabolic trough, Fresnel mirrors and compound parabolic, levelled ground is not a requirement for its installation or operation (Nixon *et al.*, 2010). Despite all these benefits, the drawback with the parabolic dish is its high cost and manufacturing difficulties. The reflector, in many cases the mirror, is the major contributor to the high cost although there are alternatives such as stretched aluminium silvered polymer which considerably reduces the cost from \$80–150/m^2 to \$40–80/m^2 and have longer life span than reflective materials used to make mirrors (Nixon *et al.*, 2010). Table 2-1 summarizes potential solar collectors for biomass thermochemical conversion process.

Table 2-1 Solar collectors, focal type, and achievable temperature levels

Type of concentrator	Focus type	Temperature (°C)	Reference
Parabolic dish reflector	Focal point	>1500	(Abu Bakar *et al.*, 2015; Kaygusuz, 2001; Nixon *et al.*, 2010; Tsoutsos *et al.*, 2003)
Parabolic trough	Focal line	400	(Duffie & Beckman, 2013; Lovejoy *et al.*, 1993)
Linear compound parabolic	Focal line	200	(Blanco *et al.*, 1986)
Linear Fresnel	Focal line	300	(Feuermann & Gordon, 1991; Nixon *et al.*, 2010)

2.4 Solar assisted thermochemical conversions

2.4.1 Solar assisted thermochemical reactors

In the solar thermochemical production of biofuels, the feedstock is placed in a reactor and heated by the solar collector either directly or indirectly. In a directly heated reactor, Fig. 2.2 (a), the substrate is exposed to the concentrated solar radiation through a transparent container, made of borosilicate glass or fused quartz providing efficient energy transfer to the reaction site by direct radiation. In the directly heated reactor (Alonso & Romero, 2015), the solar reactor walls should be clean at all times not to hinder the passage of the concentrated rays to the feedstock (Kodama *et al.*, 2010; Melchior *et al.*, 2009; Piatkowski & Steinfeld, 2011). The challenge to keep reactor windows clean can be overcome by using indirectly irradiated reactors but at the expense of heat transfer efficiency. In indirect reactors, Fig. 2.2 (b), the solar energy is first absorbed by opaque wall reactor then transferred to the biomass by conduction (Tesfay *et al.*, 2014) or convection with heat transferring fluid (Asmelash *et al.*, 2014a; Asmelash *et al.*, 2014b). Heat transmission may be limited depending on the absorber and conductive material used. Maximum operating temperature, thermal conductivity, inertness to chemical reaction, resistance to thermal shocks and radiative absorbance are few of the drawbacks (Piatkowski & Steinfeld, 2011). Moreover, packing density of the biomass, ability to move through the reactor, the size of the particles and physical properties of the reactants can affect the heat transfer conditions (Adinberg *et al.*, 2004). Adinberg *et al.* (2004) suggested use of intermediate fluids such as gasses, liquid metals or molten salts to improve the heat transfer conditions from the reactor to the feedstock. Indirect reactors can be made from metals with high thermal conductivity. Assuming thermal conductivity, cost, manufacturing ability, durability and weight of the metals the candidate reactor materials are commercial copper (K = 423 W/m.K), aluminium (K = 215 W/m.K), pure silver (K = 418 W/m.K). Enveloping the reactor by evacuated tube prevents the radiative heat loss and hence improves reactor performance.

2.4.2 Solar assisted pyrolysis

Application of solar energy for biomass thermochemical conversion dates back to the 1980s, starting with solar simulators, called furnace images, as sources of radiation, and parabolic or elliptic mirrors as concentrators (Zeng *et al.*, 2017). Solar simulators were produced from powerful light sources, such as carbon arcs, xenon lamp and mercury-xenon arc lamps. Some of the pioneering works which use solar simulators for biomass pyrolysis were (Authier *et al.*,

2009; Boutin *et al.*, 1998; Olivier Boutin *et al.*, 2002; Hopkins *et al.*, 1984a; Hopkins *et al.*, 1984b; Hunjan *et al.*, 1989; Tabatabaie-Raissi & Antal, 1986).

Solar assisted pyrolysis is currently an emerging technology (Authier *et al.*, 2009; Zeng *et al.*, 2015a) for biomass conversion to biofuels and biochar which is attracting a considerable research interest at present. Table 2-2 summarizes the performance parameters of the solar assisted pyrolysis performed for production of bio-gas, liquid biofuels and bio-char.

Zeng *et al.* (2015a) conducted laboratory scale solar pyrolysis experiment on pellets of wood and investigated the influence of temperature using different flow rates of argon as a sweep gas. The experiments were conducted using down ward facing 1.5 kW parabolic solar dish concentrator focusing the solar rays into a pellet placed at the focus of the parabolic dish inside a transparent and insulated graphite crucible. Series of heliostat mirrors were used to reflect the solar rays and continuously re-direct them to the parabolic dish for exact concentration at the focal point. The temperature and heating rate of the sample were controlled by a shutter which applies a Proportional-Integral-Derivative Controller that modulates the incident radiation. The reactor was made to accommodate gas inlets and outlets to permit entrance and exit of argon gas and reaction products respectively. It was demonstrated that the temperature greatly affects products of pyrolysis compared to the sweep gas. The gas yields (mainly CO and CH_4) were found to increase from 15.3%wt to 37.7%wt when the temperature increased from 600 to 2,000°C at 50°C/s heating rate. The higher the temperature the higher was the gas yield but the liquid yield decreased from 70.7%wt to 51.6%wt with temperature showing most of the tar was decomposed at lower temperature ranges.

Zeng *et al.* (2015b) further performed pyrolysis of wood using solar energy. The solar concentrator was made from downward facing parabolic mirror 2 meters in diameter and 0.85m focal length. It was equipped with a sensor which detects the sun and adjusts the system for maximum concentration at the focal point where the substrate was placed and directly heated by the solar radiation. The maximum power was 1.5 kW and 15000 W/m^2 flux density. A sweeping argon gas was used to wash walls of the transparent Pyrex reactor wall so as to be clean and pass the radiation. The main objective of the experiment was to determine the optimal parameters to maximize lower heating values of wood gas products of pyrolysis during solar pyrolysis processes. Heating rates (5 to 450°C/s) and pressure (0.44 to 1.14 bar) were the investigated parameters in a temperature ranging of 600°C to 2,000°C. 62% of the products were gases (H_2, CH_4, CO and CO_2) and remaining 28 and 10% were liquid bio-oil and char

respectively. The effect of temperature was found to be the most significant parameter in determining the characteristics of solar pyrolysis products and gas composition. More hydrogen and carbon monoxide were obtained at 1200°C, 50°C/s heating rate and atmospheric pressure. The Lower Heating Value (LHV) increased five times when the temperature increased from 600°C to 1,200°C and heating rate increased from 5°C/s to 50°C/s. Moreover, the heating rate had substantial influence but the effect of pressure was not significant on the product distribution of the solar pyrolysis process. The highest lower heating value (LHV), which was 10376 kJ/kg, was found at 1200°C, heating rate 50°C/s and 0.85 bar. Zeng et al. (2015c) performed solar pyrolysis experiment to identify the effects of process parameters (temperature and heating rate) to optimize the solar pyrolysis process to produce combustible gasses from sawdust using solar dish which can generate flux intensity of 15000 kW/m^2 for 1000 W/m^2 of direct normal irradiance. The setup was equipped with solar "blind optical" pyrometer, for measuring the sample temperature and solar tracker for adjusting the system to achieve maximum solar radiation during the day. Sample of wood (diameter 10 mm and height 5 mm) placed in a 6L transparent Pyrex balloon reactor was directly heated from a solar dish with a 1.5 kW power. Temperature 800°C to 2000°C, heating rate 50-450°C/s were the operating variables. Box-Behnken design experiments were performed to optimize the process. It was shown that temperature and heating rate were the most influencing factors for the lower heating value, gas composition and product distributions but the effect of argon flow rate was found to be minimal. The lower heating value of the produced gas (H_2, CO, CO_2, CH_4, and C_2H_6) increased with temperature and heating rates. Particularly, the lower heating value increased four times (from 3527 to 14589 kJ/kg) using solar pyrolysis of the wood.

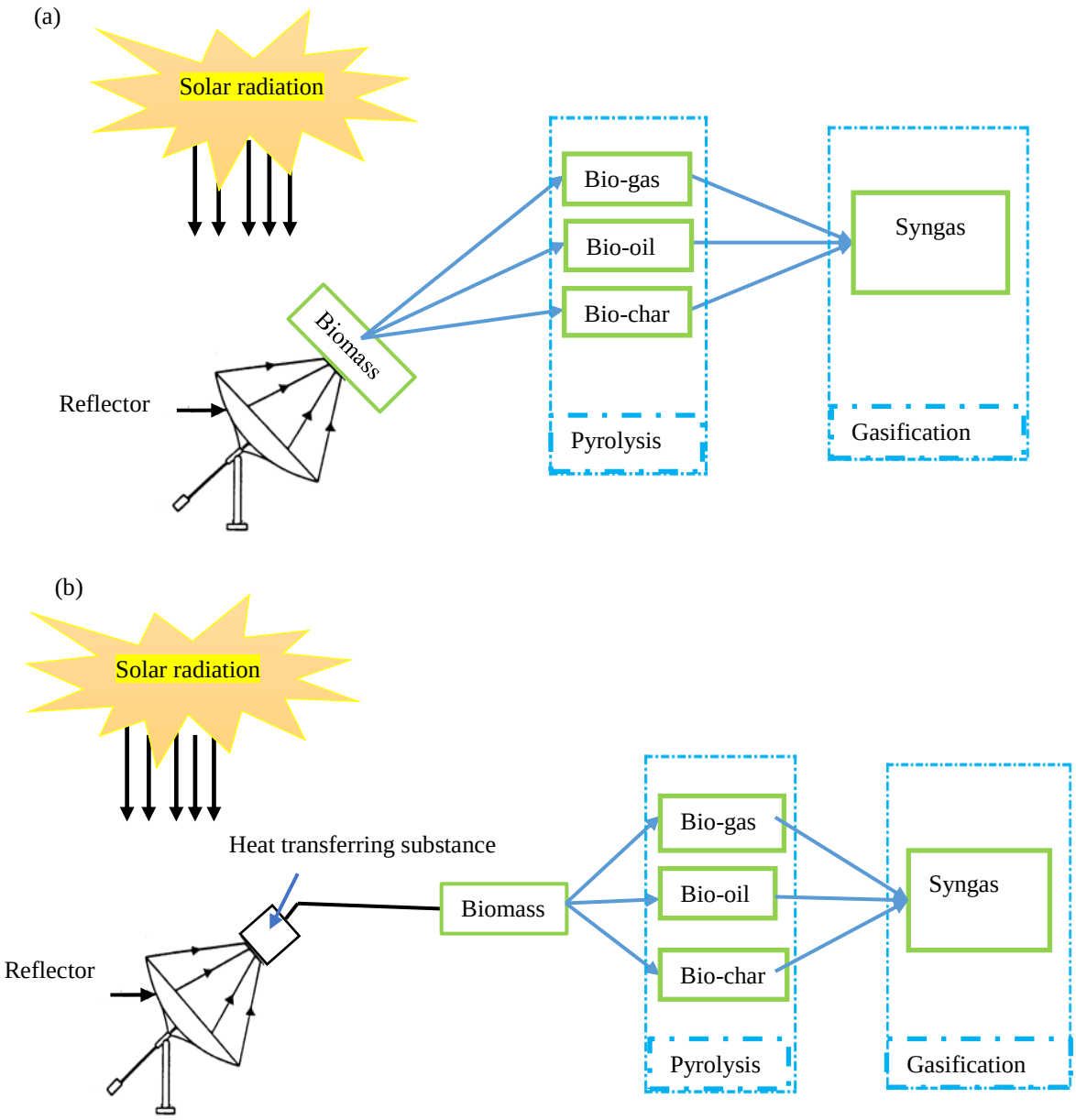

Figure 2-2 Schematic diagram of directly (a) and indirectly (b) irradiated solar reactors

Similar experimental set up was used by Zeng *et al.* (2015d) who conducted solar pyrolysis in a laboratory scale reactor producing char from wood. The biomass samples were prepared into cylinders of size 10 mm in diameter and 5 mm thickness. The char produced increased its surface area and pore volume until the temperature reached 1200˚C then decreased significantly at 2000˚C. In a similar way, the pore volume and surface area increased with the heating rate until 150˚C/s but slightly decreased afterward.

Theoretical and experimental studies of oak wood fast pyrolysis were conducted under controlled heat flux densities (0.3–0.8 MW/m^2) and temperature range of 907–487°C generated from xenon lamp in an elliptical solar mirrors (Authier *et al.*, 2009). The study was conducted to investigate the effect of heat flux density on the pyrolysis zone thickness of the wood. It was shown that the pyrolysis zone thickness of the wood decreased with the increasing flux density and influenced the char yields and gas composition for the lower flux density, the thickness varied from 180×10^{-6} to 750×10^{-6} m but for higher heat flux it was significantly smaller and varied from 100×10^{-6} to 225×10^{-6} m.

Morales *et al.* (2014) investigated orange-peel pyrolysis using solar energy from parabolic trough solar concentrator. The trough was able to generate 27088 W/m^2 which is equivalent to 31 times of the available solar energy in the location. The solar pyrolysis reactor, placed at the focal line of the parabola, reached a peak temperature of 465°C and a total weight loss of 79% was achieved on the orange peel at an average irradiance of 12.55 kW/m^2. In this study it was possible to pyrolyse the orange peel to a liquid (77.64 wt%) and a non-condensable gas (1.43 wt%), leaving 20.93 wt% biochar in the reactor. Furthermore, the work demonstrated the possibility for obtaining valuable chemical and pharmaceutical products such as diisooctyl phthalate, squalene, D-limonene, (Z)-0-octadecenamide and phenol, in addition to the production of combustible gasses such as hydrogen and carbon monoxide, generated through solar radiation augmented by conventional heating sources, including microwave and plasma.

Li *et al.* (2016) conducted solar pyrolysis in a laboratory scale solar reactor to produce fuel gas from pine sawdust, peach pit, grape stalk and grape marc. The solar energy was concentrated to a temperature of 800 to 2000°C using solar dish. The samples were prepared to a cylinder of size 10 mm in diameter by 5 mm height with approximate weight of 0.3 g. For each type of biomass, the influences of final temperature, heating rate and lignocellulose composition were analysed. The results showed increased gas yield and tar decomposition with temperature and heating rates, whereas the liquid yield progressed oppositely. The highest gas yield of 63.5wt% was obtained from pine sawdust at 1200°C and 50°C/s. The remaining 37%wt were tar and char. Higher lignin content promoted char production whereas higher cellulose and hemicellulose contents increased the gas yields. The H_2/CO ratio was always greater than one for both grape by-products, grape marc and grape stalk.

Joardder *et al.* (2014) designed a laboratory scale solar assisted fast pyrolysis reactor where part of the reaction heat came from a solar concentrator. Dried date seeds ground to sizes of

0.2 to 0.6cm^3 in size were used as feedstock. It was found that 50%wt of the liquids were produced at 500°C with a running time of 120 min. It was also found that solar energy would contribute to the reduction of both CO_2 emissions and fuel cost by 32.4%.

A semi-static parabolic solar concentrator with a surface area of 1.37m^2 was tested by Ramos and Perez-Marquez (Ramos & Pérez-Márquez, 2014). During the experiment the temperature in the receiver was above 270^{0}C. The prototype was able to produce 70 g of biochar out of 180 g of wood in five hours in a sunny day, which implies a conversion efficiency of 38%.

In a separate work, solar radiation was concentrated by a Fresnel lens to a maximum temperature of 850°C in a simulated solar radiation intensity of 1500 W/m^2 (Zeaiter *et al.*, 2015). This solar system, integrated with an automated solar tracking electronic system, was able to pyrolyze scrap tyres at a temperature of 550°C. The experiment was carried out in the presence of H-beta, HUSY and TiO_2 catalysts. Pyrolysis with the H-beta catalyst gives high oil and high gas yield of 32.8%. The TiO_2 and non-catalyzed pyrolysis results in gas-like product (isopropane) with a quantity of 76.4 and 88.4wt% respectively. Previous studies on tyre pyrolysis revealed that oil and gas yield increase considerably with temperature but the effect of temperature reduces in a temperature range over 500°C (Laresgoiti *et al.*, 2004; Murillo *et al.*, 2006).

Solar energy, concentrated by Linear Mirrors, was used to drive the pyrolysis of agricultural wastes such as wheat straw (Hans *et al.*, 2015). The system consists of sets of linear mirrors and a rectangular hollow section steel as a reactor placed at 5 m from the mirrors. A maximum temperature of 500°C was reached in about 90 minutes in the reactor which contains the wheat straw. In eight hours of sunshine per day, the system produces solar carbon (charcoal) with an energy density of 24–28 MJ/kg from a biomass of 16.9 MJ/kg. More discussion on the design, construction and concentration principles of solar linear mirrors are presented in Hans *et al.* (2015).

Soria *et al.* (2017) studied beech wood pellet degradation under fast solar pyrolysis with CFD modelling. Simulation results were compared to experimental tests carried out using Zeng *et al.* (2016) solar facility at temperatures ranging from 600 to 2000°C, and heating rates of 10 and 50°C/s. Results indicated that increasing the heating rate improved both uniformity of the char profile and intra-particle tar decomposition, thus producing more volatiles. Moreover, the higher the temperature and heating rate the higher was the gas yield, improving the intra-particle tar decomposition (Zeng *et al.*, 2016). Solar driven pyrolysis and gasification of algae,

wheat straw and sewage sludge were analysed with high flux solar simulator (Arribas *et al.*, 2017). The facility consisted of 7 kW xenon short-arc lamp, flat mirror, tow ellipsoidal mirrors and stainless steel reactor. The arc discharge was located in one of the ellipsoid loci, then emitted radiation was reflected by the flat mirror and concentrated on the second ellipsoid mirror to give maximum flux of 5800 kW/m^2 at the focal plane. Released gases contained syngas in the range of 63–74 vol% for pyrolysis (highest for sludge) and 82–90 vol% for gasification (highest for algae).

2.4.3 Solar assisted gasification processes

There is a limited number of studies with various degrees of success on the integration of concentrated solar radiations with biomass gasification, summarised in Table 2-3. Pozzobon *et al.* (2016) developed a gasification reactor system comprising of artificial sun, xenon arc lamp capable of producing heat fluxes higher than 1000 suns, and new reaction chamber. This system allowed investigation of thermal gasification behavior of thick beech wood when exposed to radiative heat. The impact of moisture content and wood fiber orientation relative to solar flux were tested and showed that increasing sample's moisture content led to direct drying steam gasification of the char. With 50%wt moisture content of the beach wood, the gasification products were H_2 38%vol, 31%vol CO and 13%vol CH_4; while CO_2 was 8.5%vol. Up to 72% of the incident solar power was captured in the chemical form in this work. The wood fibre orientation was found to have no major impact on the production rates and gas composition.

Table 2-2 Summary of solar assisted biomass pyrolysis

Reference	Heat source	Power (KW)	Range of temperature (°C)	Heating rates (°C/s)	Samples studied	Yield summary
Zeng *et al.* (2015a)	Solar simulator	1.5	600–2000	50	Pellet wood	Gases (CO, CH_4) 15.3 – 37.1% and liquids 70.7– 51.6%
Zeng *et al.* (2015b)	Solar dish	1.5	600–2000	5–450	Beech wood	28.% liquid bio oil, 10% char and 62% gas (H_2, CH_4, CO, CO_2 and C_2H_6)
Zeng *et al.* (2015c)	Solar dish	1.5	800–2000	50–450	Beech wood	Gases (H_2, CO, CO_2, CH_4, and C_2H_6) heating value increased about five times (3527 to 14, 589 kJ/kg)
Zeng *et al.* (2015d)	solar simulator	1.5	600–2000	5–450	Wood	Char yield decreased with temperature and heating rate in the temperature range
Authier *et al.* (2009)	Xenon lamp		907–487		Oak wood	Gas and char
Morales *et al.* (2014)	Parabolic trough		465		Orange peel	Liquid (77.64 wt.%), a non-condensable gas (1.43 wt.%) and char 20.93 wt.%
Li *et al.* (2016)	Sun simulator		800–2000	50	Sawdust, peach pit, grape stalk and grape marc	Gas (63%wt), tar and char (37%wt)
Joardder *et al.* (2014)			500	5	Date seed	Liquid (50%wt), solid char and gas (50%)
Ramos and Pérez-Márquez (2014)	Parabolic trough		>270	0.5	Wood	Charcoal (39%)
Zeaiter *et al.* (2015)	Fresnel lens		850		Scrap tyres	Oil and gas
Hans *et al.* (2015)	Linear mirror		500		Agricultural wastes	Charcoal
Soria *et al.* (2017)	Solar dish	1.5–2	600–2000	10 and 50	Beech wood	Char, tar and gases
Arribas *et al.* (2017)	7 Kw xenon short-arc lamp	5800 kW/m^2			Algae, wheat straw and sludge	63–90 vol% Syngas

*Note that empty cells are due to the absence of data.

Ravaghi-Ardebili and Manenti (2015) re-designed gasifier coupled with a low-temperature solar driven steam and investigated the impact of residence time of solid fuel and gas phase, as well as the amount of injected oxygen and steam on the gasification performance. Flavio Manenti and Ravaghi-Ardebili (2013) performed dynamic simulation and control of concentrating solar plants with the aim to define a reasonably simplified layout as well as highlight the main issues for characterization of the process dynamics of these energy systems and their related energy storage capabilities. When operating parameters such as feedstock size, ratio of steam to biomass, type of biomass, geometry of reactors, air and temperature effects are optimized then heat energy collected from a solar concentrator can be stored on a working fluid and therefore generate power for biomass gasification activities.

Bai *et al.*, (2015) proposed solar driven biomass gasification system with the generation of methanol and electricity. The system consisted of three main parts, power generation subsystem (laboratory scale heliostat concentrator), methanol production and gasification subsystems. The endothermic reactions of the fossil fuel gasification were driven by the concentrated solar thermal energy of the heliostat in a range of 1000–1500K, where a syngas from the biomass gasification was used to produce methanol through a synthesis reactor. Results indicated the syngas produced by the solar driven gasification has higher H_2/CO (1.43–1.89) molar ratio which satisfies the requirement for methanol synthesis. Moreover, the produced syngas has better chemical energy quality than the conventional gasification technologies. The energy efficiency of the system was found to be 56.9% which makes it a promising approach for the efficient utilization of the abundant solar and biomass resources.
A novel tri-generation system coupled with biomass gasification and solar thermal system was investigated by Li *et al.* (2016). It comprised of biomass gasification, a steam generation subsystem made of parabolic trough solar collector and an internal combustion engine subsystem. Ground biomass was preheated at 200°C then fed into the gasifier. Steam at 350^{0}C, generated from the solar collector was fed into the gasifier with biomass. After removing the ash, char and certain purification processes the gas was fed to internal combustion engine for electricity generation. In this study, the efficiency of this system was determined to be 19.2%, but introduction of the solar collector reduced the excess consumption of the biomass and improved the efficiency to 29%.

Feasibility of solar steam supplied biomass gasification was demonstrated by Ravaghi-Ardebili and Manenti (2015) and Manenti *et al.* (2014). The study was aimed at storing concentrated

solar energy generated from parabolic troughs for the purpose of steam production to accomplish biomass gasification. The parabolic trough was modelled and simulated to generate steam (approximately 400–410°C) and supplied to produce syngas consisting of H_2 (24.1%), CO (34.2%), CO_2 (33.8%) and CH_4 (7.7%). The syngas was further converted to methanol/dimethyl ether by means of one-step synthesis process.

Solar energy can be stored in chemicals. Hydrogen production driven by solar chemical reaction is one of the ways to store solar energy. Liao and Guo (2015) developed solar receiver integrated with dish concentrator for gasification of ethylene glycol, ethanol, glycerin and glucose in supercritical water. Series of outdoor experiments were conducted at 500–600°C (supercritical water state) and solar power input ranging from 3.1 to 7.2 kW. At 600°C H_2, CH_4 and CO_2; at 41.2%, 15.1% and 34.7% were the generated gases respectively. The gasification efficiency was observed to increase from 48.5 to 105.8% following the radiation increase from 3.1 to 7.2 kW.

Maag and Steinfeld (2010) and Yadav and Banerjee (2016) investigated solar to chemical conversion efficiencies of carbonaceous feedstock. For an optimized reactor geometry and a desired outlet temperature of 1500K, the solar to chemical conversion efficiency was 37% for 1500 suns solar concentration.

Pilot scale solar biomass gasification was demonstrated at the University of Colorado Boulder and Sundrop Fuels (Service, 2009). The demonstration was conducted in tubular solar reactors which can operate at 1 MW and 1473 to 1573K and presented sunlight into hydrogen conversion efficiencies of wood waste at more than 13% efficiency.

Production of synthetic fuels through biomass gasification was studied by Nzihou *et al.* (2012). It was demonstrated that the efficiency of the process can be improved by supplying process heat from concentrated solar systems. Beech-wood cylinders 40 mm in diameter were irradiated using concentrated solar radiation. The production of char fell from 45 to 20% when the irradiation level was increased from 25 to 80 kW/m^2, while the liquid yield increased to 55% and the gas yield increased slowly from 10 to 25%.

Gasification of cellulose particles heated in a molten sodium carbonate and potassium carbonate medium at 800–915°C was investigated in a laboratory scale electrically heated reactor (Adinberg *et al.*, 2004). About 94%wt of the biomass was converted to syngas primarily composed of H_2, CO_2, CH_4 and CO with 26 vol% hydrogen. It was reported that the same

gasification process can be operated using concentrated solar energy supplied from solar collectors. The preliminary assessments of the processes performed for a commercial prototype demonstrated that gasification of biomass particles, dispersed in a molten salt phase and heated by a solar energy is a feasible and promising option for clean production of synthesis gas.

2.4.4 Solar assisted distillation

The initial concentration of ethanol achieved by fermentation is approximately 7–10% v/v (volume/volume), whereas the initial concentration required for use as fuel should be higher than 99.5% v/v (Jareanjit *et al.*, 2014). For this reason, solar distillation can be applied to achieve the ethanol concentration required for achieving the standards. Solar distillation is relatively matured technology used to increase ethanol concentrations to appreciable level. Vorayos *et al.* (2006) performed analysis of solar ethanol distillation using flat plate and evacuated heat pipe solar collectors to generate sufficient heat for ethanol distillation. Accordingly, 4 m^2 evacuated pipe solar collector was able to concentrate solar heat to enhance the ethanol concentration from 10% to 80% (v/v) using solar distillation process. Similarly Jareanjit *et al.* (2015) performed solar distillation experiment to manage ethanol waste from solar distillation process. The system consisted of three solar distillation stages operated in a batch, each contributing to reduce the amount of feed materials (cassava broth) in the system and increase the ethanol concentration from 8% to 80% (v/v).

Table 2-3 Summary of solar-assisted gasification

Reference	Heat source	Power	Range of temperature (˚C)	Samples studied	Yield summary
Pozzobon *et al.* (2016)	Artificial radiation from Xenon arc lamp	1000 suns		Beech wood	H_2 (38% vol), CO (31% vol), CH4 (13% vol) and CO_2 (8.5% vol)
Bai *et al.* (2015)	Laboratory scale Heliostat concentrator		727–1227	Fossil fuel	Syngas and methanol; system efficiency was 56.9%
Liu *et al.* (2016)	Parabolic trough		350	Biomass	Char; system efficiency was 19.2%
F. Manenti *et al.* (2014); Ravaghi-Ardebili and Manenti (2015)	Parabolic trough		400–410	Biomass	H_2 (24.1%), CO (34.2%), CO2 (33.8%) and CH_4 (7.7%)
Liao and Guo (2015)	Dish concentrator	3.7–7.2 kW	500–600	ethylene glycol, ethanol, glycerine and glucose	H_2 (10–26 mol/kg); gasification efficiency ranges 48.5–105.8%
Maag and Steinfeld (2010); Yadav and Banerjee (2016)		1500 suns	1,227	carbonaceous feedstock	37% (solar to chemical conversion efficiency)
Service (2009)		1MW	1200–1300	Wood waste	Hydrogen at 13% conversion efficiency
Nzihou *et al.* (2012)	Concentrate solar system	25–80 kW/m^2		Beechwood	Char (45–20%), liquid (55%) and gas (10–25%)
Adinberg *et al.* (2004)	Electrically heated reactor		800–915	Cellulose	Syngas with 94% conversion efficiency

2.5 Conclusion

Biomass thermochemical processing requires heat which is typically supplied either by combusting part of the biomass or heat from non-renewable energy sources, such as combustion of fossil fuels or using electricity from the grid. This, in turn, decreases the efficiency of the conversion process by about 35% and challenges the sustainability of the biofuel production. Thus, it is important to develop an alternative, clean and environmentally friendly source of energy for production of biofuels. This paper reviewed the current state of research for the use of solar technologies for biomass processing and conversion to biofuels. Parabolic dish has the highest capture of solar energy with optical efficiency reaching 94% followed by parabolic trough. The solar parabolic dish, if integrated with the appropriate receiver/reactor systems selective coatings and reflective structures, can supply the required heat for thermochemical processing of biomass. The paper also reviews the solar assisted pyrolysis, gasification and distillation researches performed to date. Solar assisted pyrolysis was applied to different types of biomass fuels to produce 1.43–63% of bio-gas, 28–77.64% of bio-oils and 21–62% of biochar. The heating rate and the final temperature were identified as the most important parameters which defined the distribution of the biofuel fractions. The solar assisted biomass gasification process has been used to produce several high value fuels, such as hydrogen rich fuel gas and methane at concentrations ranging from 24–38% and 7–13% respectively. The status of solar assisted distillation process is relatively matured technology used to increase the concentration of ethanol to achieve the required level for use as fuel. The solar assisted biofuel extraction is an emerging technology which needs technical breakthrough to overcome the challenges of the process. This implies developing stand-alone solar technologies with efficient concentration and storage capacity for extracting the biofuels. As biomass is low energy density, building small systems which can easily move to biomass available sites can remove transporting bulk biomass and hence maximize the usability and distribution of the solar technologies. After resolving these challenges in the future, the solar extraction of biofuels has the potential to produce high grade energy products that can fully substitute fossil derived fuels and also generate valuable chemicals. This review revealed that solar assisted thermochemical conversion of biomass is a new area of research attracting significant interest for its potential. Especially, most of the research studies on the solar assisted pyrolysis processes were performed in a laboratory environment using artificial sun, which needs to be validated with outdoor research using natural sun to realize possible contribution of solar energy in the process of biofuel extractions. Efficient technologies for extracting

biofuels from biomass using solar energy as process heat need to be further developed and examined.

2.6 References

Abid, M., Ratlamwala, T. A. H., & Atikol, U. (2016). Performance assessment of parabolic dish and parabolic trough solar thermal power plant using nanofluids and molten salts. *International Journal of Energy Research, 40*(4), 550-563.

Abu Bakar, R. b., Froome, C., Sup, B. A., Zainudin, M. F., Ali, T. Z. S., Bakar, R. A., & Ming, G. L. (2015). 2nd International Conference on Sustainable Energy Engineering and Application (ICSEEA) 2014 Sustainable Energy for Green MobilityEffect of Rim Angle to the Flux Distribution Diameter in Solar Parabolic Dish Collector. *Energy Procedia, 68*, 45-52.

Adinberg, R., Epstein, M., & Karni, J. (2004). Solar Gasification of Biomass: A Molten Salt Pyrolysis Study. *Journal of Solar Energy Engineering, 126*(3), 850.

Agrawal, R., & Singh, N. R. (2010). Solar Energy to Biofuels. In J. M. Prausnitz, M. F. Doherty, & R. A. Segalman (Eds.), *Annual Review of Chemical and Biomolecular Engineering, Vol 1* (Vol. 1, pp. 343-364). Palo Alto: Annual Reviews.

Alonso, E., & Romero, M. (2015). Review of experimental investigation on directly irradiated particles solar reactors. *Renewable and Sustainable Energy Reviews, 41*, 53-67.

Arribas, L., Arconada, N., Gonzalez-Fernandez, C., Lohrl, C., Gonzalez-Aguilar, J., Kaltschmitt, M., & Romero, M. (2017). Solar-driven pyrolysis and gasification of low-grade carbonaceous materials. *International Journal of Hydrogen Energy, 42*(19), 13598-13606.

Asmelash, H., Bayray, M., C. Z. M., K., Gebray, P., & Adam, S. (2014a). Performance Test of Parabolic Trough Solar Cooker for Indoor Cooking. *Momona Ethiopian Journal of Science (MEJS), 6*(2), 39-54.

Asmelash, H., Kebedom, A., Bayray, M., & Mustofa, A. (2014b). Performance Investigation of Offset Parabolic Solar Cooker for Rural Applications *International Journal of Engineering Research & Technology (IJERT), 3*(12), 920-923.

Authier, O., Ferrer, M., Mauviel, G., Khalfi, A.-E., & Lédé, J. (2009). Wood Fast Pyrolysis: Comparison of Lagrangian and Eulerian Modeling Approaches with Experimental Measurements. *Industrial & Engineering Chemistry Research, 48*(10), 4796-4809.

Auti, A. B., Pangavane, D. R., Singh, T. P., Sapre, M., & Warke, A. S. (2015). Study on Reflector Material Optimization of a Parabolic Solar Concentrator. In C. Kamalakannan, L. P. Suresh, S. S. Dash, & B. K. Panigrahi (Eds.), *Power Electronics and Renewable Energy Systems* (Vol. 326, pp. 275-284).

Bai, Z., Liu, Q., Lei, J., Li, H., & Jin, H. (2015). A polygeneration system for the methanol production and the power generation with the solar–biomass thermal gasification. *Energy Conversion and Management, 102*, 190-201.

Baral, S., Kim, D., Yun, E., & Kim, K. C. (2015). Experimental and Thermoeconomic Analysis of Small-Scale Solar Organic Rankine Cycle (SORC) System. *Entropy, 17*(4), 2039-2061.

Bernardo, L. R., Davidsson, H., & Karlsson, B. (2012). Retrofitting Domestic Hot Water Heaters for Solar Water Heating Systems in Single-Family Houses in a Cold Climate: A Theoretical Analysis. *Energies, 5*(10), 4110.

Blanco, M. E., Gomez-Leal, E., & Gordon, J. M. (1986). Asymmetric CPC solar collectors with tubular receiver: Geometric characteristics and optimal configurations. *Solar Energy, 37*(1), 49-54.

Boutin, O., Ferrer, M., & Lédé, J. (1998). Radiant flash pyrolysis of cellulose—Evidence for the formation of short life time intermediate liquid species. *Journal of Analytical and Applied Pyrolysis, 47*(1), 13-31.

Boutin, O., Ferrer, M., & Lédé, J. (2002). Flash pyrolysis of cellulose pellets submitted to a concentrated radiation: experiments and modelling. *Chemical Engineering Science, 57*(1), 15-25.

Bulushev, D. A., & Ross, J. R. H. (2011). Catalysis for conversion of biomass to fuels via pyrolysis and gasification: A review. *Catalysis Today, 171*(1), 1-13.

Chen, W.-H., Peng, J., & Bi, X. T. (2015). A state-of-the-art review of biomass torrefaction, densification and applications. *Renewable and Sustainable Energy Reviews, 44*, 847-866.

Cronshaw, I. (2015). World Energy Outlook 2014 projections to 2040: natural gas and coal trade, and the role of China. *Australian Journal of Agricultural and Resource Economics, 59*(4), 571-585.

Demirbas, A. (2007). Progress and recent trends in biofuels. *Progress in Energy and Combustion Science, 33*(1), 1-18.

DiGrazia, M., Gee, R., Jorgensen, G., & Asme. (2009,). *Reflectech (R) mirror film attributes and durability for CSP applications.* Paper presented at the Es2009: Proceedings of the Asme 3rd International Conference on Energy Sustainability, Vol 2, San Francisco, CA.

Duffie, J. A., & Beckman, W. A. (2013). *Solar Engineering of Thermal Processes*: Wiley.

Elliott, D. C., Beckman, D., Bridgwater, A. V., Diebold, J. P., Gevert, S. B., & Solantausta, Y. (1991). Developments in direct thermochemical liquefaction of biomass: 1983-1990. *Energy & Fuels, 5*(3), 399-410.

Fend, T., Jorgensen, G., & Kuster, H. (2000). Applicability of highly reflective aluminium coil for solar concentrators. *Solar Energy, 68*(4), 361-370.

Feuermann, D., & Gordon, J. M. (1991). Analysis of a Two-Stage Linear Fresnel Reflector Solar Concentrator. *Journal of Solar Energy Engineering, 113*(4), 272-279.

Flores, V., & Almanza, R. (2004). Direct steam generation in parabolic trough concentrators with bimetallic receivers. *Energy, 29*(5-6), 645-651.

Gu, X. G., Taylor, R. A., & Rosengarten, G. (2014). Analysis of a New Compound Parabolic Concentrator-Based Solar Collector Designed for Methanol Reforming. *Journal of Solar Energy Engineering-Transactions of the Asme, 136*(4).

Han, J., & Kim, H. (2008). The reduction and control technology of tar during biomass gasification/pyrolysis: An overview. *Renewable and Sustainable Energy Reviews, 12*(2), 397-416.

Hans, G., Marta, B., Marco, C., Marina, C., Enrico, E., Elvis, K., & Andrea, P. (2015). Solar Biomass Pyrolysis with the Linear Mirror II. *Smart Grid and Renewable Energy, 6*, 179-186.

Hertwich, E. G., & Zhang, X. (2009). Concentrating-Solar Biomass Gasification Process for a 3rd Generation Biofuel. *Environmental Science & Technology, 43*(11), 4207-4212.

Hoogwijk, M., Faaij, A., Eickhout, B., de Vries, B., & Turkenburg, W. (2005). Potential of biomass energy out to 2100, for four IPCC SRES land-use scenarios. *Biomass and Bioenergy, 29*(4), 225-257.

Hopkins, M. W., Antal, M. J., & Kay, J. G. (1984a). Radiant flash pyrolysis of biomass using a xenon flashtube. *Journal of Applied Polymer Science, 29*(6), 2163-2175.

Hopkins, M. W., DeJenga, C., & Antal, M. J. (1984b). The flash pyrolysis of cellulosic materials using concentrated visible light. *Solar Energy, 32*(4), 547-551.

Hotz, N., Zimmerman, R., Weinmueller, C., Lee, M.-T., Grigoropoulos, C. P., Rosengarten, G., & Poulikakos, D. (2010). Exergetic analysis and optimization of a solar-powered reformed methanol fuel cell micro-powerplant. *Journal of Power Sources, 195*(6), 1676-1687.

Hunjan, M. S., Mok, W. S. L., & Antal, M. J. (1989). Photolytic formation of free radicals and their effect on hydrocarbon pyrolysis chemistry in a concentrated solar environment. *Industrial & Engineering Chemistry Research, 28*(8), 1140-1146.

Jareanjit, J., Siangsukone, P., Wongwailikhit, K., & Tiansuwan, J. (2014). Development of a mathematical model and simulation of mass transfer of solar ethanol distillation in modified brewery tank. *Applied Thermal Engineering, 73*(1), 723-731.

Jareanjit, J., Siangsukone, P., Wongwailikhit, K., & Tiansuwan, J. (2015). Management of ethanol waste from the solar distillation process: Experimental and theoretical studies. *Energy Conversion and Management, 89*, 330-338.

Joardder, M. U. H., Halder, P. K., Rahim, A., & Paul, N. (2014). Solar Assisted Fast Pyrolysis: A Novel Approach of Renewable Energy Production. *Journal of Engineering, 2014*, 1-9.

Kan, T., Strezov, V., & Evans, T. J. (2016). Lignocellulosic biomass pyrolysis: A review of product properties and effects of pyrolysis parameters. *Renewable and Sustainable Energy Reviews, 57*, 1126-1140.

Kaygusuz, K. (2001). Renewable energy: Power for a sustainable future. *Energy Exploration & Exploitation, 19*(6), 603-626.

Kenarsari, S. D., & Zheng, Y. (2014). CO2 gasification of coal under concentrated thermal radiation: A numerical study. *Fuel Processing Technology, 118*, 218-227.

Kennedy, C. E. (2002). *Review of Mid- to High-Temperature Solar Selective Absorber Materials*. Retrieved from USA: http://www.osti.gov/bridge

Kennedy, C. E., & Terwilliger, K. (2005). Optical durability of candidate solar reflectors. *Journal of Solar Energy Engineering-Transactions of the Asme, 127*(2), 262-269.

Khan, A. A., de Jong, W., Jansens, P. J., & Spliethoff, H. (2009). Biomass combustion in fluidized bed boilers: Potential problems and remedies. *Fuel Processing Technology, 90*(1), 21-50.

Kodama, T., Gokon, N., Enomoto, S.-i., Itoh, S., & Hatamachi, T. (2010). Coal Coke Gasification in a Windowed Solar Chemical Reactor for Beam-Down Optics. *Journal of Solar Energy Engineering, 132*(4), 041004-041004.

Kraemer, D., Poudel, B., Feng, H.-P., Caylor, J. C., Yu, B., Yan, X., . . . Chen, G. (2011). High-performance flat-panel solar thermoelectric generators with high thermal concentration. *Nat Mater, 10*(7), 532-538.

Kumar, A., Pachauri, R. K., Chauhan, Y. K., & Ieee. (2015). Analysis and Performance Improvement of Solar PV System by Solar Irradiation Tracking. *2015 International Conference on Energy Economics and Environment (Iceee)*.

Laresgoiti, M. F., Caballero, B. M., de Marco, I., Torres, A., Cabrero, M. A., & Chomón, M. J. (2004). Characterization of the liquid products obtained in tyre pyrolysis. *Journal of Analytical and Applied Pyrolysis, 71*(2), 917-934.

Lee, M.-T., Werhahn, M., Hwang, D. J., Hotz, N., Greif, R., Poulikakos, D., & Grigoropoulos, C. P. (2010). Hydrogen production with a solar steam–methanol reformer and colloid nanocatalyst. *International Journal of Hydrogen Energy, 35*(1), 118-126.

Li, R., Zeng, K., Soria, J., Mazza, G., Gauthier, D., Rodriguez, R., & Flamant, G. (2016). Product distribution from solar pyrolysis of agricultural and forestry biomass residues. *Renewable Energy, 89*, 27-35.

Liao, B., & Guo, L. J. (2015). Concentrating solar thermochemical hydrogen production by biomass gasification in supercritical water. In Z. Wang (Ed.), *International Conference on Concentrating Solar Power and Chemical Energy Systems, Solarpaces 2014* (Vol. 69, pp. 444-450).

Liu, P., Zhao, Y., Guo, Y., Feng, D., Wu, J., Wang, P., & Sun, S. (2016). Effects of volatile–char interactions on char during pyrolysis of rice husk at mild temperatures. *Bioresource Technology, 219*, 702-709.

Lovejoy, D., Johansson, T., Kelly, H., Reddy, A., & Williams, R. (1993). Renewable energy - sources for fuels and electricity. *Nat Resour Forum, 17*, 244-245.

Maag, G., & Steinfeld, A. (2010). Design of a 10 MW Particle-Flow Reactor for Syngas Production by Steam-Gasification of Carbonaceous Feedstock Using Concentrated Solar Energy. *Energy & Fuels, 24*, 6540-6547.

Manenti, F., Leon-Garzon, A. R., Ravaghi-Ardebili, Z., & Pirola, C. (2014). Assessing thermal energy storage technologies of concentrating solar plants for the direct coupling with chemical processes. The case of solar-driven biomass gasification. *Energy, 75*, 45-52.

Manenti, F., & Ravaghi-Ardebili, Z. (2013). Dynamic simulation of concentrating solar power plant and two-tanks direct thermal energy storage. *Energy, 55*, 89-97.

Melchior, T., Perkins, C., Lichty, P., Weimer, A. W., & Steinfeld, A. (2009). Solar-driven biochar gasification in a particle-flow reactor. *Chemical Engineering and Processing: Process Intensification, 48*(8), 1279-1287.

Mettler, M. S., Vlachos, D. G., & Dauenhauer, P. J. (2012). Top ten fundamental challenges of biomass pyrolysis for biofuels. *Energy & Environmental Science, 5*(7), 7797-7809.

Metzger, J. O., & Hüttermann, A. (2009). Sustainable global energy supply based on lignocellulosic biomass from afforestation of degraded areas. *Naturwissenschaften, 96*(2), 279-288.

Moon, J., Kim, T. K., VanSaders, B., Choi, C., Liu, Z., Jin, S., & Chen, R. (2015). Black oxide nanoparticles as durable solar absorbing material for high-temperature concentrating solar power system. *Solar Energy Materials and Solar Cells, 134*, 417-424.

Morales, S., Miranda, R., Bustos, D., Cazares, T., & Tran, H. (2014). Solar biomass pyrolysis for the production of bio-fuels and chemical commodities. *Journal of Analytical and Applied Pyrolysis, 109*, 65-78.

Murillo, R., Aylón, E., Navarro, M. V., Callén, M. S., Aranda, A., & Mastral, A. M. (2006). The application of thermal processes to valorise waste tyre. *Fuel Processing Technology, 87*(2), 143-147.

Ni, G., Li, G., Boriskina, Svetlana V., Li, H., Yang, W., Zhang, T., & Chen, G. (2016). Steam generation under one sun enabled by a floating structure with thermal concentration. *Nature Energy, 1*, 16126.

Nixon, J. D., Dey, P. K., & Davies, P. A. (2010). Which is the best solar thermal collection technology for electricity generation in north-west India? Evaluation of options using the analytical hierarchy process. *Energy, 35*(12), 5230-5240.

Nostell, P., Roos, A., & Karlsson, B. (1997). *Optical characterisation of solar reflecting surfaces* (Vol. 3138).

Nzihou, A., Flamant, G., & Stanmore, B. (2012). Synthetic fuels from biomass using concentrated solar energy – A review. *Energy, 42*(1), 121-131.

Philibert, C. (2011). *Solar Energy Prespective* (R. J. Paolo Frankl, Didier Houssin Ed.). France International Energy Agency

Piatkowski, N., & Steinfeld, A. (2008). Solar-Driven Coal Gasification in a Thermally Irradiated Packed-Bed Reactor. *Energy & Fuels, 22*(3), 2043-2052.

Piatkowski, N., & Steinfeld, A. (2011). Solar gasification of carbonaceous waste feedstocks in a packed-bed reactor-Dynamic modeling and experimental validation. *AIChE Journal, 57*(12), 3522-3533.

Pozzobon, V., Salvador, S., & Bézian, J. J. (2016). Biomass gasification under high solar heat flux: Experiments on thermally thick samples. *Fuel, 174*, 257-266.

Rahman, M. M., B. Mostafiz, S., Paatero, J. V., & Lahdelma, R. (2014). Extension of energy crops on surplus agricultural lands: A potentially viable option in developing countries while fossil fuel reserves are diminishing. *Renewable and Sustainable Energy Reviews, 29*, 108-119.

Ramos, G., & Pérez-Márquez, D. (2014). Design of Semi-static Solar Concentrator for Charcoal Production. *Energy Procedia, 57*, 2167-2175.

Rapagnà, S., Jand, N., & Foscolo, P. U. (1998). Catalytic gasification of biomass to produce hydrogen rich gas. *International Journal of Hydrogen Energy, 23*(7), 551-557.

Ravaghi-Ardebili, Z., & Manenti, F. (2015). Unified modeling and feasibility study of novel green pathway of biomass to methanol/dimethylether. *Applied Energy, 145*, 278-294.

Schissel, P., Kennedy, C., & Goggin, R. (1995). Role of inorganic oxide interlayers in improving the adhesion of sputtered silver film on PMMA. *Journal of Adhesion Science and Technology, 9*(4), 413-424.

Service, R. F. (2009). Sunlight in Your Tank. *Science, 326*(5959), 1472-1475.

Singh, N. R., Delgass, W. N., Ribeiro, F. H., & Agrawal, R. (2010). Estimation of Liquid Fuel Yields from Biomass. *Environmental Science & Technology, 44*(13), 5298-5305.

Soria, J., Zeng, K., Asensio, D., Gauthier, D., Flamant, G., & Mazza, G. (2017). Comprehensive CFD modelling of solar fast pyrolysis of beech wood pellets. *Fuel Processing Technology, 158*(Supplement C), 226-237.

Strezov, V., & Evans, T. J. (2015). Biomass Processing Technologies [Press release]

Tabatabaie-Raissi, A., & Antal, M. J. (1986). Design and operation of a 30KWe/2KWth downward facing beam ARC image furnace. *Solar Energy, 36*(5), 419-429.

Tesfay, A. H., Kahsay, M. B., & Nydal, O. J. (2014). Design and Development of Solar Thermal Injera Baking: Steam Based Direct Baking. *Energy Procedia, 57*(Supplement C), 2946-2955.

Tsoutsos, T., Gekas, V., & Marketaki, K. (2003). Technical and economical evaluation of solar thermal power generation. *Renewable Energy, 28*(6), 873-886.

Ullah, K., Kumar Sharma, V., Dhingra, S., Braccio, G., Ahmad, M., & Sofia, S. (2015). Assessing the lignocellulosic biomass resources potential in developing countries: A critical review. *Renewable and Sustainable Energy Reviews, 51*, 682-698.

Vorayos, N., Kiatsiriroat, T., & Vorayos, N. (2006). Performance analysis of solar ethanol distillation. *Renewable Energy, 31*(15), 2543-2554.

Weldekidan, H., Strezov, V., & Town, G. (2017). Performance evaluation of absorber reactors for solar fuel production. *Chemical engineering transaction, 61*, 1111-1116.

Williams, A., Jones, J. M., Ma, L., & Pourkashanian, M. (2012). Pollutants from the combustion of solid biomass fuels. *Progress in Energy and Combustion Science, 38*(2), 113-137.

Yadav, D., & Banerjee, R. (2016). A review of solar thermochemical processes. *Renewable & Sustainable Energy Reviews, 54*, 497-532.

Zeaiter, J., Ahmad, M. N., Rooney, D., Samneh, B., & Shammas, E. (2015). Design of an automated solar concentrator for the pyrolysis of scrap rubber. *Energy Conversion and Management, 101*, 118-125.

Zeng, K., Flamant, G., Gauthier, D., & Guillot, E. (2015a). Solar pyrolysis of wood in a lab-scale solar reactor: influence of temperature and sweep gas flow rate on products distribution. In Z. Wang (Ed.), *International Conference on Concentrating Solar Power and Chemical Energy Systems, Solarpaces 2014* (Vol. 69, pp. 1849-1858).

Zeng, K., Gauthier, D., Li, R., & Flamant, G. (2015b). Solar pyrolysis of beech wood: Effects of pyrolysis parameters on the product distribution and gas product composition. *Energy, 93*, 1648-1657.

Zeng, K., Gauthier, D., Lu, J. D., & Flamant, G. (2015c). Parametric study and process optimization for solar pyrolysis of beech wood. *Energy Conversion and Management, 106*, 987-998.

Zeng, K., Gauthier, D., Soria, J., Mazza, G., & Flamant, G. (2017). Solar pyrolysis of carbonaceous feedstocks: A review. *Solar Energy*.

Zeng, K., Minh, D. P., Gauthier, D., Weiss-Hortala, E., Nzihou, A., & Flamant, G. (2015d). The effect of temperature and heating rate on char properties obtained from solar pyrolysis of beech wood. *Bioresource Technology, 182*(Supplement C), 114-119.

Zeng, K., Soria, J., Gauthier, D., Mazza, G., & Flamant, G. (2016). Modeling of beech wood pellet pyrolysis under concentrated solar radiation. *Renewable Energy, 99*(Supplement C), 721-729.

Zhang, Z., Liu, J., Shen, F., Yang, Y., & Liu, F. (2016). On-line measurement and kinetic studies of sodium release during biomass gasification and pyrolysis. *Fuel, 178*, 202-208.

Zhu, X.-G., Long, S. P., & Ort, D. R. (2008). What is the maximum efficiency with which photosynthesis can convert solar energy into biomass? *Current Opinion in Biotechnology*, *19*(2), 153-159.

Chapter 3: Performance evaluation of absorber reactors for solar fuel production

This chapter deals with the design and manufacture of the solar concentrator. Design parameters, such as the average solar irradiance, wind speed and ambient temperature at Macquarie University were considered to design a parabolic dish of 1.8 m aperture diameter and 0.655 m focal length. With this design, it was possible to achieve temperatures as high as 1100°C which is sufficient to pyrolyse organic materials. The design improves limitations of previous solar systems and enables to perform biomass pyrolysis outdoors, using natural sun. Performance evaluation of different types of absorber reactors are presented in this chapter. Additional information on the design parameters, schematic drawing of the reactor and some experimental methods applied for this chapter are given in Appendix 3.

The concept of this paper was developed by myself and my supervisors, Vlad and Graham. I designed the equipment and Macquarie University Technical Services (METS) manufactured with our supervision. Experiments were conducted and first draft outlined by myself while editing and reviewing the manuscript for publication were done by Vlad and Graham.

Authors' contribution summary for this paper

	W. H.	S. V.	G. T.
Design and manufacturing	•	•	
Experiment and data collection	•		
Analysis and manuscript preparation	•	•	•

Publication:

Weldekidan H. (70%), Strezov V. (20%), Town G. (10%). Performance Evaluation of Absorber Reactors for Solar Fuel Production, ***Chemical Engineering Transaction (2017), 66: 1111- 1116, ISBN 978-88-95608-51-8, ISSN 2283-9216.***

Performance evaluation of absorber reactors for solar fuel production

Haftom Weldekidan[a,], Vladimir Strezov[a], Graham Town[b]*

[a] Department of Environmental Sciences, Faculty of Science and Engineering, Macquarie University, Sydney, NSW 2109, Australia

[b] School of Engineering, Faculty of Science and Engineering, Macquarie University, Sydney, NSW Australia

*haftom.weldekidan@hdr.mq.edu.au

Abstract

Waste to energy conversion through thermochemical processing offers a potential option for valorisation of waste biomass, however, it requires external heat supply to process the waste. Solar energy is a promising solution to convert the waste and produce alternative fuels that can replace coal, oil and natural gas for heat and electricity generation. To realize this, the radiation from the sun should be concentrated and converted to thermal energy. Among the solar concentrators, parabolic dish gives the highest concentration ratio per area in converting the solar energy to heat energy and electricity. The absorber is the main part of the dish which is placed at the focal point and converts the concentrated radiation to thermal energy. In this work, experiments were conducted on stainless steel, copper, ceramic and glass reactors as absorber materials of parabolic dish with aperture diameter 1.8 m coated with aluminium pet as reflective material. The objective of this research was to evaluate solar radiation-absorbing performance of the reactor materials and design efficient reactor for solar fuel production. Two sets of experiments were conducted. First, each of the reactors was placed at the focal point then the heating rate and maximum temperatures inside the reactors were recorded as a function of radiation intensity using K-type thermocouples. Secondly, each reactor was coated using carbon soot and then the experiment was repeated. Results showed that the coated glass reactor has the best performance in all the absorbers. Of the uncoated reactors, the stainless steel gave best results with stable and uniform temperature distribution inside the reactor. The results can be used as benchmarks for future design and application of the solar thermal technology.

3.1 Introduction

Fossil fuels as sources of energy have immense social and environmental impacts. The extraction processes generate water and air pollution, and harm local communities. Transporting fuels from the mine site causes air pollution and lead to severe accidents and leaks. Combustion of fossil fuels contributes to toxic and global warming emissions, such as sulphur dioxide, nitrous oxides (NOx), particles and greenhouse gas emissions. Moreover, fossil fuels have limited reserves and once used these resources will deplete. In fact, with the current production pattern of the crude oil, reserves will come to an end at around 2060s (Metzger & Huttermann, 2009). With all these formidable challenges, innovative, environmentally acceptable and feasible alternative energy sources will need to be developed before the fossil fuels are consumed faster than demand.

It is known that biomass is one of the primary sources of renewable energy. Biomass is carbon-dioxide neutral as the amount of carbon dioxide emitted during combustion is equivalent to that consumed during photosynthesis (Han & Kim, 2008). In the last few decades there has been significant increase in the quantity of organic wastes, which is the main source of biomass, mainly due to increased human population and urbanization (Gouda *et al.*, 2017). The annual capacity of biomass can reach 108 Gtoe (Kan *et al.*, 2016). Thus provided this source is sustainably introduced to our energy mix it can contribute 10 to 14 % of the world's energy supply which can reduce global environmental impacts and provide commercially attractive opportunities to meet our energy needs and services (Werle, 2015). Waste to energy conversion through thermochemical processing offers a potential option for valorisation of waste biomass, however, it requires external heat supply to process the waste. Solar energy is a promising solution to extract important fuels and chemicals from organic wastes. In just a year, the earth receives about 885 million terawatt hours (TWh) of energy from the sun. This is equivalent to 4,200 times the energy that mankind would consume in 2035 following the International Energy Agency's Current Policies Scenario (*Solar energy perspective*, 2011). However, the solar energy is diffused and bounded by time and place so it has to be concentrated and stored in the form of chemicals.

This research deals with design, manufacturing and experimental testing of solar concentrator with the aim of producing solar fuels from organic wastes through thermochemical conversion processes. Different sets of tests were conducted to evaluate best performing type of material reactor among stainless steel, copper, glass, aluminium and alumina ceramics.

3.2 Design and construction of the solar concentrator

3.2.1 Dish design and environmental factors

The design of paraboloid concentrator requires the quantity of heat and the maximum solar irradiation level of the experiment. Assuming Macquarie University (33.7738° S, 151.1126° E) as the experimental site, the solar irradiance level can be taken as I_b=1000 W/m^2, though the peak value is 1260 W/m^2. Average ambient temperature and wind speed are 23ºC and 8 to 14 kph m/s respectively (*Geoscience Australia*, 2010).

The heat of reaction was determined to be 80–280 J/g for cellulose and increase with conversion ratios up to 2500–4000 J/g for the forestry and agricultural residues (Chen et al., 2014). These results were used in the design as fundamental data for solving heat energy requirements to pyrolyse 3 g of biomass in a unit time.

The effective energy intercepted by the paraboloid reflector and transmitted to the reactor can be expressed by Eq(1) (Pavlovic & Stefanovic, 2015).

$$Q = I_b A_c \rho \gamma \alpha \qquad (1)$$

Where Q is input heat to the receiver in kW; I_b is irradiance in kW/m^2; A_c is collector (aperture) area in m^2, ρ is reflectance; γ intercepting factor; α is absorptivity (Abid *et al.*, 2016).

3.2.2 Material Property

Dish surface was coated with aluminium polyethylene terephthalate (Al pet) with reflectivity of 0.88 (manufacturers' data), and the absorptivity α of the reactor is assumed as 0.95.

3.2.3 Parameter design

The intercepting factor γ generally depends on the accuracy and precision of the manufacturing processes of the dish and is taken in the range of 0.9 - 0.98.

Substituting 1000 W/m^2 for I_b and values of all the respective constants in Eq(1), the total area of the parabolic dish that can generate the heat of reaction is estimated to be 2.65 m^2. A dish with an aperture diameter of 1.8m and focal length to dimeter ratio (f/d) 0.3788 gives the required area. Focal length located slightly above the centre of gravity reduces the heat losses that may be caused by wind forces (Hijazi *et al.*, 2016). Therefore *f/d* ratio of around 0.3 is selected for the dish used in this study.

The surface of the solar dish is generated by entering x and y coordinates for selected points. Software Parabola Calculator 2.0, as shown in Figure 3.1 was used to determine the necessary locus points that define the parabola. A circular paraboloid, like the one shown in Figure 3.1, is obtained by rotating the parabola segment around its axis. The rim angle, defined by Eq(2) also defines the shape of the paraboloid.

$$\frac{f}{D} = \frac{1}{4\tan(\psi_{rim}/2)} \qquad (2)$$

Since the *f/d* ratio is 0.3788, the rim angle ψ_{rim} becomes 113^0.
Usually paraboloids with large rim angles are most appropriate for external volumetric receivers (Pavlovic & Stefanovic, 2015). Since this design accommodates cylindrical reactor at its focus, the rim angle obtained, in this case, is assumed appropriate.

With the above assumptions the total heat generated from the solar dish is estimated at:

$Q = I_b A_c \rho \gamma \alpha$ = 1000 W/m^2 x 2.65 m^2 x 0.95 x 0.95 x 0.95 = 2,272 W = 2.27 kW

The geometric concentration ratio is defined as the ratio of the area of the optical system (aperture area) to the energy absorbing area of the receiver Eq(3), in this case the reactor.
The geometric concentration ratio is defined as the ratio of the area of the optical system (aperture area) to the energy absorbing area of the receiver Eq(3), in this case the reactor. Thus, the concentration ratio *C* of this design is:

$$C = \frac{A_C}{A_r} = 346.15 \qquad (3)$$

In this work a solar dish with 1.8 m aperture diameter covered with aluminium pet was designed taking into consideration the design parameters from Table 3-1. The aluminium pet was found to be appropriate option as a reflective coating due to its cost, weight, efficiency, it is easy to clean and is resistant to severe weather conditions. Manual tracking system was used for rotation of the disc to ensure the dish always faces the sun for maximum radiation.

Reactor-absorber was placed at the focal region where reflected radiation is concentrated – direct heating. The key point to achieve better performance with the reactor-absorber is to determine the flux distribution at the focal region. To reduce heat losses and cost of the whole system, the absorbing material was made as small as possible (Pavlovic & Stefanovic, 2015); but it should also be large enough to capture as much of the reflected rays as possible (Weldekidan *et al.*, 2014).

In this work SolTrace was used to determine the heat flux distribution around the focal region of the dish through which the optimum size and exact location of the reactor around the focal region were determined.

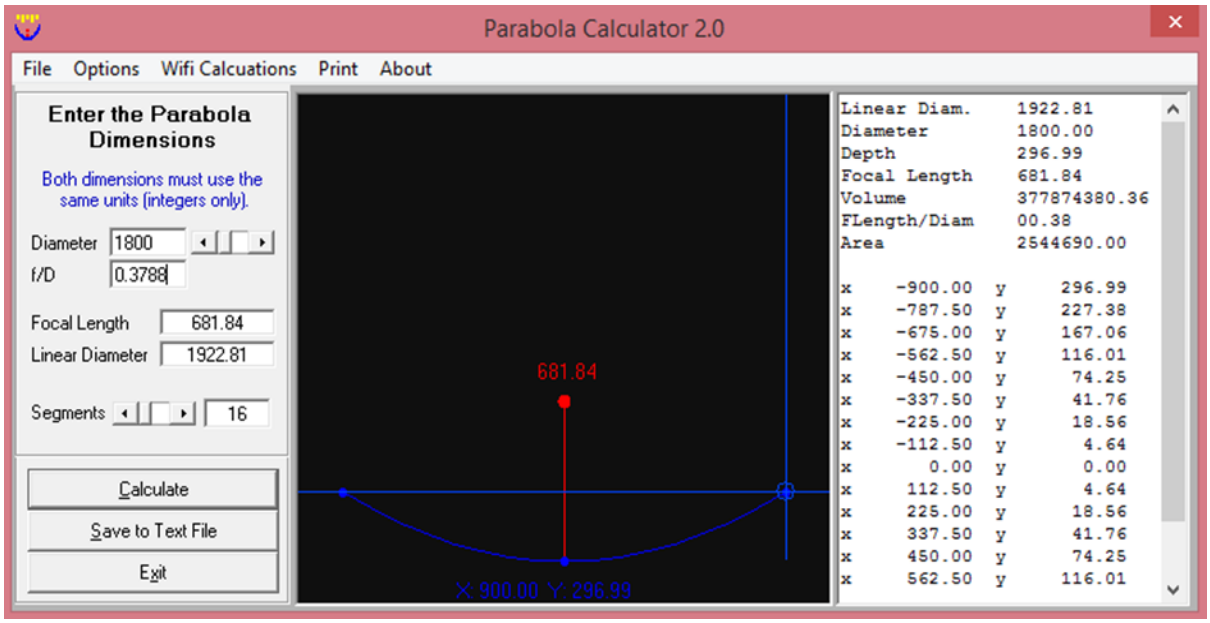

Figure 3-1 Parametric design and locus of points of the solar dish

Table 3-1 Design parameters of solar parabolic dish

Parameters	Numerical value	Unit
Aperture diameter	1.8	[m]
diameter of smaller (bottom) hole	20	[cm]
Gross collector area	2.65	[m^2]
Gross collector volume	~0.65	[m^3]
Cross sectional area of the opening parabola	2.5446	[m^2]
Reactor shape	Directly irradiated	-
Reactor diameters	7-14	[mm]
Reactor height	20	[cm]
Reactor volume	26.546	[cm^3]
Base ring area	$3.623*10^2$	[cm^2]
Effective area of the concentrator	2.61	[m^2]
Reflective material	Al pet	
Concentration ratio	346.15	-
Depth of concentrator	296.99	[mm]
Focal length	682	[mm]
f/d ratio	0.3788	-
Rim angle ψ of paraboloid	113°	-

A theoretical calculation of stagnation temperature based on maximum heat flux value is given by Eq.(4) (Ekman *et al*., 2015). Stagnation temperature is the highest temperature a receiver would achieve when the energy being absorbed is as fast as it is re-radiated.

$$Q = \sigma T^4 \qquad (4)$$

Where Q is the radiated flux per square meter equal to 69,087 W/m^2 (found from SolTrace simulations) and **σ** is the Stefan-Boltzmann constant. The thermal flux in this case would result in a corresponding stagnation temperature of 1,079^{o}C.

3.3 Experiment with the ractor- absrober materials

The experiment was conducted using glass, copper, stainless steel, aluminium and ceramic reactors. The diameter of the reactors ranges from 7 mm to 14 mm but their heights were 35 cm. Table 3-2 shows the dimensions and thermal conductivity of each reactor.

3.3.1 Uncoated reactor-absorber temperature performance

Temperatures in the unloaded (empty) reactors and global net radiations were recorded using K-type thermocouple and pyrometer with Campbell Scientific data logger respectively. The experiments were also repeated using the same reactors coated using carbon soot to create blackbody receiver. All procedures were run in more than three times to obtain the reported results and at all times the tests were run until the stagnation temperatures were reached.

Table 3-3 shows temperature performance of the uncoated reactors and radiation intensity. While running the experiment, the radiation was increasing continuously from 280 to 860 W/m^2. In all the experiments the temperature of the reactors increased with the radiation until the stagnation temperatures were achieved. For most of the tests the rate of temperature increment was fast at the beginning for all reactors and remained constant after some time indicating the thermal energy being absorbed by the reactor is as fast as the energy being dissipated. Maximum temperature of 900^{o}C was recorded with the stainless steel reactor at 744 W/m^2 with an average heating rate of 500^{o}C/min. The effect of radiation on the reactor temperature can be linearly expressed as in Eq.(5).

$$T = 25.274I - 17743; [R^2 = 0.9308] \qquad (5)$$

where T stands for the temperature in ^{o}C and I is radiation in W/m^2.

The second best performing reactor in terms of attaining maximum stagnation temperature was glass reactor. Maximum stagnation temperature of 845^{o}C was recorded for a corresponding radiation of 860 W/m^2. The response in temperature as a result of the changes in radiation was almost similar with the other reactors. Heating rate of the glass at 169^{o}C/min, was lower than stainless steel and copper at the beginning but surpassed the copper reactor after few seconds.

The maximum stagnation temperature in the copper reactor was 749^{o}C, achieved after 6 minutes of the start of the experiment. Corresponding radiation level was 530 W/m^2 and the heating rate was 125^{o}C/min. As with the other reactors the temperature was affected by the radiation which can be expressed using Eq.(6).

$$T = -0.0086I^2 + 9.3821I - 1820.5; [R^2 = 0.906] \quad (6)$$

Copper had lower heating rate, response time and took longer time to reach its maximum stable temperature than the stainless steel. The stagnation temperature for the alumina ceramic reactor was 520^{o}C which started after 6 min of the set-up, when the radiation reached 775 W/m^2. Unlike all other reactors the rise in temperature was not sharp at the beginning. Heating rate of 87^{o}C/min was recorded with the ceramic reactor. The temperature is linearly related to the radiation, as in Eq.(7). The low performance with the ceramic reactor was due to the white colour of the alumina ceramics and its low thermal conductivity relative to the other materials.

$$T = 12.639I - 9268; [R^2 = 0.8278] \quad (7)$$

Table 3-2 Dimensions and thermal property of the reactors

Reactor material	Diameter [mm]	Thermal conductivity [W/m.K] at 298K	Wall thickness [mm]
glass	12	~1	0.8
copper	13	401	0.8
stainless steel	10	16	0.6
aluminium	10	205	1
alumina ceramic	7	16	1

Table 3-3 Temperature performance of the uncoated reactors

Reactor material	Stagnation temperature [^{o}C]	Radiation [W/m^2] at maximum temperature	Heating rate [^{o}C/min]
glass	845±25	860±6	169±5.6
copper	749±15	530±4	125±-5
stainless steel	900±8	744±3	500±3
aluminium	340±10	722±4	57±6.3
alumina ceramic	520±10	775±5	87±3

The stagnation temperature and heating rate with the aluminium reactor were 340^{o}C and 57^{o}C/min respectively with the corresponding heat flux of 722 W/m^{2}. The aluminium reactor was the least performing reactor, mainly because it is a reflective material. The temperature is directly related to the radiation as in Eq.(8).

$$T = 1.8236I - 977.03; [R^2 = 0.8146] \quad (8)$$

It is known that production of solar fuels from pyrolysis of biomass, termed biofuels, requires a temperature as high as 400 to 800°C (Jahirul *et al*., 2012). Thus, the stainless steel reactor at the focal region of the solar dish can generate enough temperature for the thermal treatment of the biomass in the conversion process.

Copper reactor can also generate temperatures that can reach as high as 500 to 700^{o}C which can be used for pyrolysis of biomass. The ceramic reactor can also be used for pyrolysis at lower temperatures, up to 500^{o}C, torrefaction and pre-treatment of the biomass which requires relatively low temperature in the range of 200 to 300^{o}C (Kuzmina *et al*., 2016). Similarly aluminium reactor can be used for torrefaction and pre-treatment of biomass at temperatures lower than 340^{o}C.

3.3.2 Coated reactor-absorber performances

Table 3-4 shows the temperature performance, heating rate and radiations at which the maximum temperature has occurred for the reactors coated with carbon soot produced from combusted acetylene and using the designed solar parabolic dish. As in the previous tests, the temperatures generally increased with the radiation until the stagnation values were reached. The heating rates of all reactors changed considerably comparing to the uncoated reactors. The achieved heating rate using stainless steel tube reduced from 500 to 187^{o}C/min; glass from 169 to 80^{o}C/min; copper from 125 to 83^{o}C/min; but the ceramic and aluminum tube increased the heating rate from 87 to 315^{o}C/min and 57 to 132^{o}C/min, respectively. The concentrated heat oxidized the carbon soot before it reached the walls of the reactors, thus taking longer time than the uncoated reactors. With the aluminum and ceramic reactors the temperature and heating rate showed significant increase with the carbon soot because the reflective property of both reactors was minimized. Except for the glass reactor, the stagnation temperature did not show significant change with the copper and stainless steel reactors. This was because the carbon combusted few seconds after the reactors were placed at the focal point; hence the coating effect on the stainless and copper was minimal. However, with the glass reactor, the carbon

soot combustion increased the temperature reaching and maintaining maximum stagnant temperature of 1040^{o}C.

This experiment has also proved that the carbon coated stainless steel, glass, copper, aluminum and ceramic reactors, if integrated with the solar dish can increase the maximum temperatures to drive the pyrolysis, torrefaction and pre-treatment of the biomass in the course of extracting the bio-fuels, such as bio-oil, char and gases.

Table 3-4 Temperature performance of carbon soot coated reactor-absorbers

Type of reactor	Stagnation temperature [^{o}C]	Radiation [W/m^2] at maximum temperature	Heating rate [^{o}C/min]
glass	1040±28	964±5	80±6
copper	748±15	885±4	83±4.5
stainless steel	936±12	1003±4	187±5
aluminium	>660±8	936±5	132±5
alumina ceramic	630±8	950±4	315±5

3.4 Conclusion

In this work solar parabolic dish with 1.8 m aperture diameter was designed and manufactured with the aim of producing solar fuels from organic wastes through thermochemical conversion processes. The dish was covered with 88% reflective aluminium pet and integrated manual tracking system to ensure maximum concentrations. Two sets of experiments, 1) carbon soot coated and 2) uncoated, glass, copper, stainless-steel, aluminium and ceramic reactors were conducted to evaluate best performing reactor-absorber material to design solar assisted biomass pyrolyser to extract biofuel chemicals. Maximum temperature of 1040^{o}C was recorded with the coated glass reactor at a radiation of 964 W/m^2. Whereas of all the uncoated reactors, 900^{o}C was the maximum temperature recorded with the stainless steel at a radiation of 744 W/m^2. In most of the experiments the temperature was directly related with the radiations. Considering biofuel extraction from biomass through pyrolysis processing requires temperatures in the range of 400 to 800^{o}C, all the coated reactors can generate sufficient temperatures to carry out the pyrolysis with the solar dish, while of all the uncoated reactors glass, copper, steel and aluminium can achieve the pyrolysis temperatures. The aluminium reactor can only be used for torrefaction and pre-treatment processes.

3.5 References

Abid, M., Ratlamwala, T. A. H., & Atikol, U. (2016). Performance assessment of parabolic dish and parabolic trough solar thermal power plant using nanofluids and molten salts. *International Journal of Energy Research*, *40*(4), 550-563.

Chen, Q., Yang, R. M., Zhao, B., Li, Y., Wang, S. J., Wu, H. W., . . . Chen, C. H. (2014). Investigation of heat of biomass pyrolysis and secondary reactions by simultaneous thermogravimetry and differential scanning calorimetry. *Fuel*, *134*, 467-476.

Ekman, B. M., Brooks, G., & Rhamdhani, M. A. (2015). Development of high flux solar simulators for solar thermal research. *Solar Energy Materials and Solar Cells, 141*, 436-446.

Geoscience Australia. (2010). Retrieved from Australian energy resource assessment, Canberra: ISBN: 978-1 921672-58-3.

Gouda, N., Singh, R. K., Meher, S. N., & Panda, A. K. (2017). Production and characterization of bio oil and bio char from flax seed residue obtained from supercritical fluid extraction industry. *Journal of the Energy Institute, 90*(2), 265-275.

Han, J., & Kim, H. (2008). The reduction and control technology of tar during biomass gasification/pyrolysis: An overview. *Renewable & Sustainable Energy Reviews, 12*(2), 397-416.

Hijazi, H., Mokhiamar, O., & Elsamni, O. (2016). Mechanical design of a low cost parabolic solar dish concentrator. *Alexandria Engineering Journal, 55*(1), 1-11.

Jahirul, M. I., Rasul, M. G., Chowdhury, A. A., & Ashwath, N. (2012). Biofuels Production through Biomass Pyrolysis-A Technological Review. *Energies, 5*(12), 4952-5001.

Kan, T., Strezov, V., & Evans, T. J. (2016). Lignocellulosic biomass pyrolysis: A review of product properties and effects of pyrolysis parameters. *Renewable & Sustainable Energy Reviews, 57*, 1126-1140.

Kuzmina, J. S., Sytchev, G. A., & Zaychenko, V. M. (2016). Torrefaction. Prospects and Application. In K. KohseHoinghaus & E. Ranzi (Eds.), *2nd International Conference on Biomass* (Vol. 50, pp. 265-270).

Metzger, J. O., & Huttermann, A. (2009). Sustainable global energy supply based on lignocellulosic biomass from afforestation of degraded areas. *Naturwissenschaften, 96*(2), 279-288.

Pavlovic, S. R., & Stefanovic, V. P. (2015). Ray Tracing Study of Optical Characteristics of the Solar Image in the Receiver for a Thermal Solar Parabolic Dish Collector. *Journal of Solar Energy, 2015*, 10.

Solar energy perspective. (2011). Retrieved from International Energy Agency, France,: ISBN: 978-92-64-12457-8

Weldekidan, H. A., Bayray, M., Kimambo., C. Z. M., Gebray, P., & Sebit., A. M. (2014). Performance test of parabolic trough solar cooker for indoor cooking. *Momona Ethiopian Journal of Science (MEJS), 6*, 39-54.

Werle, S. (2015). Influence of the Waste Biomass Gasification Gas Composition on the Laminar Flame Speed Values. In P. S. Varbanov, J. J. Klemes, S. R. W. Alwi, J. Y. Yong, & X. Liu (Eds.), *Pres15: Process Integration, Modelling and Optimisation for Energy Saving and Pollution Reduction* (Vol. 45, pp. 781-786)

Chapter 4: Waste to energy conversion of chicken litter through solar-driven pyrolysis process

The study in Chapter 4 characterizes pyrolysis products obtained from chicken-litter waste at different temperatures using the solar concentrator designed in Chapter 3. The feedstock was collected from Sydney then dried in a vacuum oven and pulverized to a size that can fit in the solar reactor. Yields and composition of the pyrolysis gases, bio-oil and char were intensively studied. A wide range of instruments such as gas chromatograph mass spectrometry, scanning electron microscope and others have been applied to investigate the property of the solar pyrolysis products. Possible areas of applications of each product are briefly discussed.

The concept of this paper was developed by Vlad. I together with Tao designed the experiment, prepared the sample and analysed the data. The manuscript was written by myself, then Vlad, Tao and Graham have edited and made it for publication.

Authors' contribution summary for this paper

	W. H.	S. V.	T. G.	K. T.
Experiment Design	•			
Sample Preparation	•	•		•
Data Collection	•			
Analysis	•			•
Manuscript	•	•	•	•

Publication**:**

Weldekidan H. (65%), Strezov V. (10%), Kan T. (15%), and Town G. (10%). Waste to energy conversion of chicken litter through a solar-driven pyrolysis process, ***Energy & fuels (2018), 32: 4341-4349.***

Adopted with permission from Energy & Fuels, Energy Waste to Energy Conversion of Chicken Litter through a Solar-Driven Pyrolysis Process, Haftom Weldekidan, Vladimir Strezov, Tao Kan, publication date April 1, 2018 American Chemical Society. Permission letter is appended in Appendix IV.

Waste to Energy Conversion of Chicken Litter through Solar-Driven Pyrolysis Process

Haftom Weldekidan[1], Vladimir Strezov[1], Tao Kan[1], and Graham Town[2]*

[1] Department of Environmental Sciences, Macquarie University, Sydney, NSW 2109, Australia

[2] Department of Engineering, Macquarie University, Sydney, NSW2109, Australia

* Email: tao.kan@mq.edu.au

Abstract

Application of solar energy for biomass pyrolysis is a promising technology for converting biomass to energy, fuels and other chemical substances with neutral CO2 emissions. Compared to the conventional pyrolysis process, the biomass conversion efficiency can be greatly improved if the pyrolysis heat is supplied from a concentrated solar system which can be achieved at reasonably moderate solar radiations. This paper discusses fast pyrolysis of chicken litter at different temperatures (560, 760, 860 and 900°C) supplied from a solar dish of maximum flux-density 69,087 W/m^2 under 1000 W/m^2 of net (all wave) solar radiation. Yields of the different product fractions (gas, liquid bio-oil and solid bio-char) were assessed using different techniques. The gas yield increased with temperature from 45.3 wt% at 560°C to its maximum value of 58.6 wt% at 860°C. Gas chromatograph results showed CO2, CO and CH4 as the dominant gases with contents of 30.2, 22.4 and 2.4 wt% respectively. When the temperature increased to 900°C lower gas yields of 48 wt% were produced. The gas chromatography–mass spectrometry analysis showed that the generated bio-oils (14–36 wt%) mainly contained fatty acids, phenols, sterols and nitrogen containing compounds. Scanning electron microscopic images of evolved bio-chars showed increasing porous structure with temperature, while the Fourier transform infrared spectroscopy of the bio-chars showed presence of –OH, aliphatic C-H and other functional groups in the bio-char which gradually disappeared with temperature. The obtained results revealed the potential use of solar energy in the waste to energy valorization of organic chicken litter waste.

Key words: Solar pyrolysis, chicken litter, bio-oil, gas yield, solar radiation, waste

4.1 Introduction

The growing demand for alternative energy sources is driving not only investigation of new and renewable alternative feedstocks but also clean production mechanisms. Biomass resources, such as municipal wastes, forest residues, agricultural waste, aquatic plants, energy crops and animal manures are recognized as the major sources of renewable energy (Sawin *et al.*, 2016). Chicken litter is a potential biomass fuel of animal origin produced in poultry farming. It consists manure, feathers, spilled food, chip woods and straw. Chicken farming is one of the largest industries and continuously growing due to the population increase (Bolan *et al.*, 2010). From 2013 to 2014, the world production of broiler and poultry meat increased to 95.8 million tonnes (Benchmark Holdings Ltd, 2014) resulting in more production of chicken manure and litter. In the US about 35 million tonnes of dry chicken litter is generated per annum (Ma & Agblevor, 2014) and Brazil, the second largest producer of broiler chickens in the world, generates around 8-10 million tonnes of litter per year (Dalolio *et al.*, 2017).Total chicken litter production in Australia is estimated to be over 1 million tonnes (1.6 million m^3) per annum (Wiedemann, 2015).

Traditionally, chicken litter has been applied as a fertiliser and soil conditioner which still remains the most important and largest end use of poultry litter. However, land application only is not a sufficient solution to the growing volume of chicken litter waste, as its excessive land use adversely impacts surface and ground water (Lori *et al.*, 2009) degrades water quality (Moore & Edwards, 2007) and contributes to toxic concentrations of ammonia nitrates (Edwards & Daniel, 1992). Chicken litter as ruminant feed supplement is also under pressure because of cattle health threats (Putun *et al.*, 2002). Alternative mechanisms are increasingly required to address the disposal challenges of chicken litter. One potential means is to use more efficient energy conversion methods to generate energy-dense alternative fuels. Pyrolysis is one of the most attractive alternative options to obtain fuels and value added products from organic wastes, such as chicken litter.

Pyrolysis is a thermochemical process which applies heat in the partial or total absence of an oxidizing agent to convert biomass and other organic materials to more stable, high-energy-density solid material called bio-char, high-energy-density liquid product termed bio-oil, and relatively low energy density biogas (Azargohar *et al.*, 2013). Gas products can be used for power generation, heating applications and production of chemicals (Zeng *et al.*, 2017). The bio-oils can be used in boilers and engines for energy and heat generation whereas the bio-char

may be used as solid fuels or as soil conditioners, such as soil stabilization and for retention of nutrients and water (Bruun *et al.*, 2012; Wang & Li, 2017; Zhang *et al.*, 2015).

Yields of 60.1% bio-char with 38% organic carbon, 41.7g/kg nitrogen and 36.3 $cmol_c/kg$ maximum cation exchange capacity was found at 300°C (Song & Guo, 2012). Chicken litter pyrolysis at 450 to 550°C produced 40% of bio-char with high ash content (24-54 wt%) and rich in potassium and phosphorus components. The process was also observed to generate bio-oils (36-25 wt%) with relatively high nitrogen content (4 to 8 wt%), very low sulfur (<1%), and gases such as CO_2, CO and low weight hydrocarbon in the range of 13 to 24 wt% (Agblevor *et al.*, 2010). Lima *et al.* (2009) pyrolysed chicken litter at 700 to 800°C and produced 33.5% of bio-char (maximum yield). Gas production was found to decrease with temperature from 40 to 31%. Another chicken litter pyrolysis performed by Baniasadi *et al.* (2016) from 400 to 800°C at heating rates of 0.5 to 2°C/s, generated 48 wt% of gases (CO_2, CO and CH_4) and condensable compounds such as palmitic and oleic (18.8–35%), nitrogen containing compounds (6.3–10.2%), phenols (5.8–13.2%) and sterols (0.9–2.3%). Four fraction of bio-oils, namely hexane (46 g), Toluene (29 g), chloroform (48g) and methanol (14 g) were achieved from the pyrolysis of 140 g of chicken litter at 450°C, fed to the reactor at 50 kg per hour (Ma & Agblevor, 2014).

The effect of wood-shaving on the pyrolysis products of chicken litter was studied at 450°C by Mante and Agblevor Mante and Agblevor (2010). It was found that increasing the wood proportion increased bio-oil yields from 43.3 to 53.5 wt% when the mixture had 75 wt % wood and the char yield had decreased from 43.1 to 29.5 wt%.

Although pyrolysis is prominent candidate for processing of biomass materials for renewable energy production, it has limitations as the driving heat is supplied from either external non-renewable sources or through consumption of the produced biofuel products, pyrolysis gas or bio-oils. Extensive heat energy is consumed to heat the biomass in the reactor from external biomass or electrical heater. These reduce the available biomass for pyrolysis and in the same time generate greenhouse gases. One way to overcome these problems is by using solar energy to drive the biomass pyrolysis process. There are different types of solar collectors that can easily achieve pyrolysis temperatures. Operating temperatures as high as 1,050°C was achieved with solar dish on carbon-soot coated stainless-steel reactor at 964 W/m^2 (Weldekidan *et al.*, 2017). Parabolic trough can also be used for biomass pyrolysis at lower temperatures ranging up to 300°C (Morales *et al.*, 2014). Low pyrolysis temperature, <400°C, favors conversion of

char whereas syngas and bi-oil are favorably generated at high pyrolysis temperatures (>600°C) (Hanif *et al.*, 2016).

While solar energy has been used for cooking, space heating and power generation applications, its application to drive the thermochemical processing of organic wastes is at a very early technology readiness level. Integration of solar energy with biomass pyrolysis would not only solve the waste disposal and environmental challenges of the pyrolysis process, but also convert the waste to valuable products such as biofuels, pharmaceutical commodities, cosmetics and dehydrants more efficiently with improved environmental performance.

The objective of the present study is to develop and perform a study on a solar driven pyrolysis process for extraction of biofuels from chicken-litter waste and investigate the effects of solar insolation on the pyrolysis temperatures as well as pyrolysis gases, bio-oil and bio-char pyrolysis products.

4.2 Experimental section

4.2.1 Feedstock preparation and analysis

The sample material used in this study was chicken litter collected from a local chicken farm (Carlingford Produce, Sydney, Australia). Prior to the experiments, the biomass was dried in a vacuum oven for 2 hours at 70°C and 80 KPa then ground and sieved by 0.28 mm sieve.

The proximate and ultimate analyses of the chicken litter used in this study, reported in Table 4-1, show higher contents of ash (27.1%) and nitrogen (5.36%) compared to the other biomass materials, such as forest residue (0.4–1.2 wt% ash and 0.9–1.2 wt% nitrogen) (Amutio *et al.*, 2013), sawdust (0.4–0.7 wt% ash and 0.6–0.65 wt% nitrogen), demolition wood (1.7 wt% ash and 0.9 wt% nitrogen) and olive cake pellets (8.2 wt% ash and 1.3 wt% nitrogen) (Mahmoudi *et al.*, 2010). The source of nitrogen is mainly due to the protein content of the chicken litter.

Table 4-1 Proximate and ultimate analysis of chicken-litter waste

Proximate analysis				Ultimate analysis				
Ash	Volatile matter	Fixed carbon	Moisture	C	H	O	N	S
%mass, dry basis			%mass	%mass, dry and ash free				
27.1	62.6	10.3	9.9	46.9	5.4	42	5.36	0.32

The large amount of ash, relatively high volatile matter (62.6%) and fixed carbon contents (10.3%) indicate that chicken litter is not suitable for production of porous value-added products, such as activated carbon and carbon sorbents (Azargohar *et al.*, 2013). The higher heating value (*HHV*) was calculated to be 17.85 MJ/kg according to the following formula:

$$HHV = 349.1 \times C + 1178.3 \times H + 100.5 \times S - 103.4 \times O - 15.1 \times N - 21.1 \times Ash \text{ (kJ/kg)}$$

(Channiwala & Parikh, 2002)

4.2.2 Solar experimental setup

A solar dish (1.8 m aperture diameter, 0.655 m focal length) with integrated biomass reactor system at its focal place was designed and constructed. It was laminated using aluminum polyethylene terephthalate (Al pet) with 88% reflective material. Various reactor tubes were tested for their temperature performances and applications (Weldekidan *et al.*, 2017). Accordingly, stainless steel and silica glass tube reactors with 35 cm length by 13 mm diameter were found to give the best performance, hence the silica glass reactor was employed in this pyrolysis experiment. Repetitive experiments on the performance of the reactors indicated that there was not significant temperature difference across 25mm spot size in the reactors which was thus considered as constant temperature zone.

One end of the reactor tube was attached to a two-inlet pipe with one inlet used to direct an argon carrier gas at flow rates of 100 mL/min while the other adjacent inlet was used to insert a K-type thermocouple to measure the pyrolysis temperature of the sample. TC-08 type of data logger with USB serial interface and PicoLog data logging software were applied to log and display the recorded temperatures in a computer. Shadow of a stick attached to the periphery of the dish was calibrated (marked) with the temperature in the reactor. Each time the experiment was conducted, the shadow of the stick had to be tracked to lay on the correct mark as per the final temperature requirement.

The pyrolysis experiments were carried out in a batch. In each run maximum of 100 mg sample was loaded at the center of the reactor tube. The remaining part of the reactor was filled with quartz wool, which was used to trap heavy organics (tars) generated during the pyrolysis process, and at the same time the wool was used to hold the sample in place as in Fig. 4.1. The reactor's outlet side was connected to coiled copper pipe immersed in an ice cooling chamber to condense heavy tars of the pyrolysis gases. The pyrolysis gases were then collected in a Tedlar bag for analysis by a micro-GC.

The reactor tube was purged with argon gas at 100 mL/min for about 15 min. Finally, the reactor was tuned to the maximum irradiance and continuously tracked to face the sun such that its reflected beam illuminated the reactor to achieve the required pyrolysis temperatures.

To analyze heat flux distribution of the reflected rays around the focal spot, ray tracing calculations were performed using SolTrace software (Wendelin, 2013) at different aim points. Assumed parameters for SolTrace were insolation (1,000 W/m^2 equal to 1 sun), aperture diameter (1.8 m), surface reflectivity (88%), glass reactor diameter (25mm), range of focal lengths (0.6–0.75 m) and specularity standard deviation of 0.5 mrad. With these assumptions, the maximum heat flux generated by the solar dish at 0.655 m focal length and over a size of 25 mm diameter spot was 69,087 W/m^2, which represents a concentration of 70 times the available solar energy. Fig. 4.2 (a) shows the flux distributions of the solar dish at different focal lengths. A theoretical calculation of temperature based on the maximum heat flux value gave an equivalent temperature of 1,051°C. To validate this, experiment was conducted to measure temperature performance of different reactors at 0.655 m focal length. Fig. 4.2 (b) is the average temperature performance of glass tube reactor at different irradiance levels for 3 runs. The temperature sharply increased up to 745°C at 3°C/(W/m^2); followed by slow raise up to its maximum value of 1,060°C at 1,020 W/m^2, which agreed well with the SolTrace results.

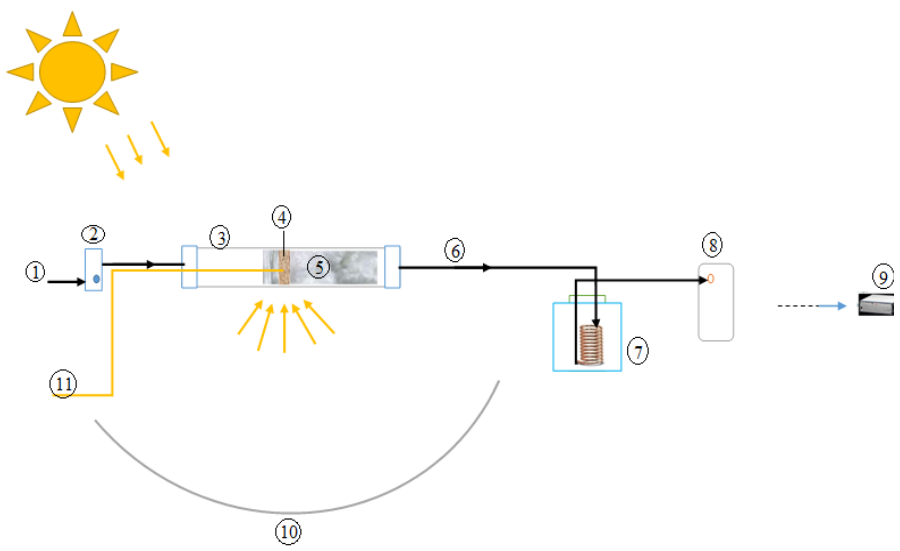

Figure 4-1 Schematic of the experimental set-up

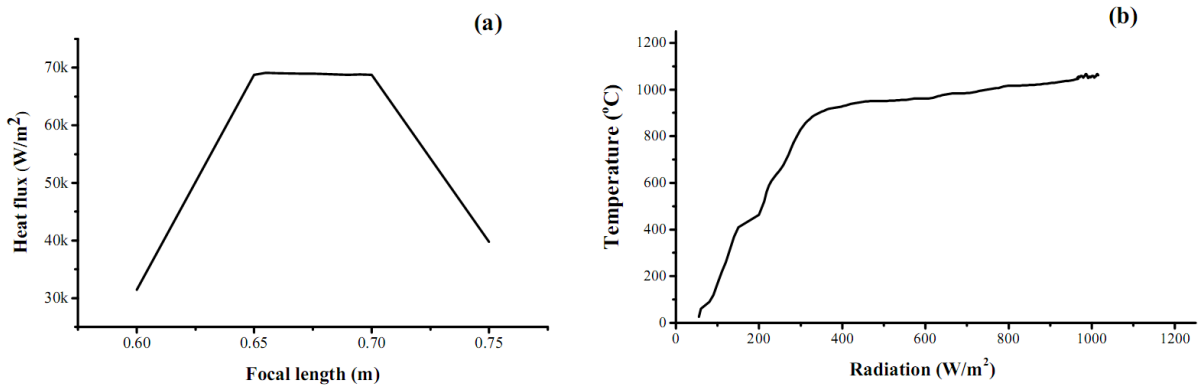

Figure 4-2 Solar assisted pyrolyser performance, (a) heat flux distribution at different focal lengths; (b) reactor temperature performance at 0.655 m focal length (note 5% error in each graph)

4.2.3 Pyrolysis product recovery

4.2.3.1 Pyrolysis gases

The sample loaded reactor was heated by the reflected solar radiations up to the maximum temperatures of 560, 760, 860 and 900°C respectively. These temperatures were selected based on the tracking simplicity of the solar device. Tracking the device to these range of temperatures could be done with relatively better accuracy than other ranges of temperatures. Fig. 4. 3 shows variation of temperature with time during the experiments. Based on this graph the average heating rate achieved was calculated to be 190 $\pm$ 6°C/min. Produced gases, collected in the Tedlar gas bags, were subjected to M200 micro-gas chromatograph (micro-GC) with ultra-high purity helium (at 50 mL/min) as the carrier gas. A U column polymer Paraplot, 8 m long and 0.32 mm in diameter kept at 40°C was employed to determine CO_2, CH_4, C_2H_4 and C_2H_6 while H_2 and CO were analyzed by a 5A molecular sieve (10 m long and 0.32 mm in diameter) at 60°C. Chromatograms were obtained every 100 s using thermal conductivity detector (TCD). More details on the apparatus and calibration procedures employed in this experiment were discussed by Kan, *et al*. (2014a); Opatokun *et al*. (2016) and Strezov *et al*. (2012).

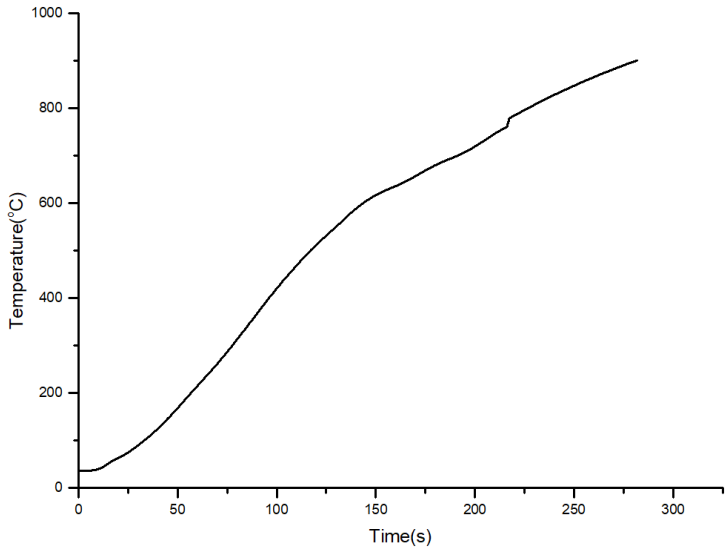

Figure 4-3 Temperature variation of the reactor as a function of time

4.2.3.2 Liquid bio-oils

The bio-oils trapped by the glass wool and cooled by ambient air at room temperature were collected for each experiment (560, 760, 860 and 900°C) and then dissolved in a dichloromethane (DCM) solvent. N, O-bis(trimethylsilyl) trifluoroacetamide and 1% trimethylchlorosilane (BSTFA + 1% TMCS) was added to the solution, to improve separation and thermal stability of the compounds in the GC-MS analysis (Kan *et al.*, 2014b) The bio-oil solution was then analysed by Agilent 7890B gas chromatography coupled with 5977A mass spectrometry (GC-MS) equipped with an HP-5MS capillary column (60 mx 0.25 µm). The gas flow rate through the column was 1.2324 ml/min. The GC oven was firstly heated to 40°C and kept for 2 min, then increased to 310°C at 2°C/min and kept for 30 min. The injector and Mass Spectrometer Detector (MSD) transfer line temperatures were 310°C, while quadrupole mass spectrometer (MS Quad) temperature was set at 150°C. Compounds were analysed using the MassHunter software. The match factor with the NIST database was set over 80. The product yield of the bio-oils was calculated from the mass difference between the total sample weight and the mass sum of the produced chars and evolved pyrolysis gas.

4.2.3.3 Solid bio-chars

In each experiment, the solid residue (bio-char) was analysed using Fourier Transform Infrared Spectroscopy (FT-IR) and Scanning Electron Microscopy (SEM). FT-IR spectra of raw chicken litter and produced bio-chars at different temperatures were recorded by Nicolet 6700

FTIR spectrometer using an attenuated total reflectance method with a crystal diamond. The experiments were accomplished through 32 total number of scans with 4 cm^{-1} spectral resolution.

The variable pressure SEM system (JEOL JSM- 6480 LA) equipped with Energy Dispersive Spectroscopy (EDS) was employed to observe the morphological differences of the raw chicken litter and produced bio-chars at different temperatures. Images of the different samples ranging in size from 0.28 to 0.1 mm were produced at a maximum resolutions of 4 nm. In this experiment, an accelerating voltage of 15 KV with energy dispersion ranges between 0-20 KeV was applied at the working distance of 10 ± 2 mm.

4.3 Result

4.3.1 Product distribution

Bio-char, bio-oil and pyrolysis gas yields obtained from the solar pyrolysis of chicken litter at the final temperatures of 560, 760, 860 and 900°C are shown in Fig. 4.4. The values reported in the figure are obtained as the average value of at least three experiments with relative errors less than 5%. The gas and liquid yields increased with the pyrolysis temperature, whereas the bio-char yield decreased. At 560°C, 40.4 wt% bio-char and 45.3 wt% pyrolysis gas yields were produced. When the temperature raised to 760°C, the bio-char yield decreased to 24.5 wt%, whereas the pyrolysis gas yield slightly increased to 48.9 wt%. This was primarily due to the char decomposition mechanism at this temperature range, which was also reported previously (Uzun et al., 2006; Yang et al., 2014). The liquid yield was found to increase from 14.4 wt% at 560°C to 24.5 wt% at 760°C. The maximum gas yield of 58.6 wt% was obtained at 860°C indicating most of the tar decomposition occurred at this temperature range which can be confirmed by the decrease in the liquid and bio-char contents at 15.3 and 26.1 wt% respectively. As the pyrolysis temperature further increased to 900°C, the pyrolysis gas and bio-char yields reduced substantially to 47.8 and 16.1 wt% respectively, while the liquid yield increased to 35.9 wt%. The decrease in the pyrolysis gas and increase in bio-oil yield at 900°C could be due to hydrocarbon polymerization in the high-temperature zone and at high heating rate, resulting in increased liquid yields. Similar yield patterns were observed with Zeng et al. (2015) and Septien et al. (2012) at higher temperatures. This result could also come due to inconsistencies such as packing density of the biomass and errors in the manual tracking of the solar device which causes variations in the heating rate.

The relatively high content of inorganic compounds present in the sample in the form of ash (Table 4-1) can hinder further formation of gases (Pattiya, 2011) resulting for the gas yield to be almost the same throughout the process.

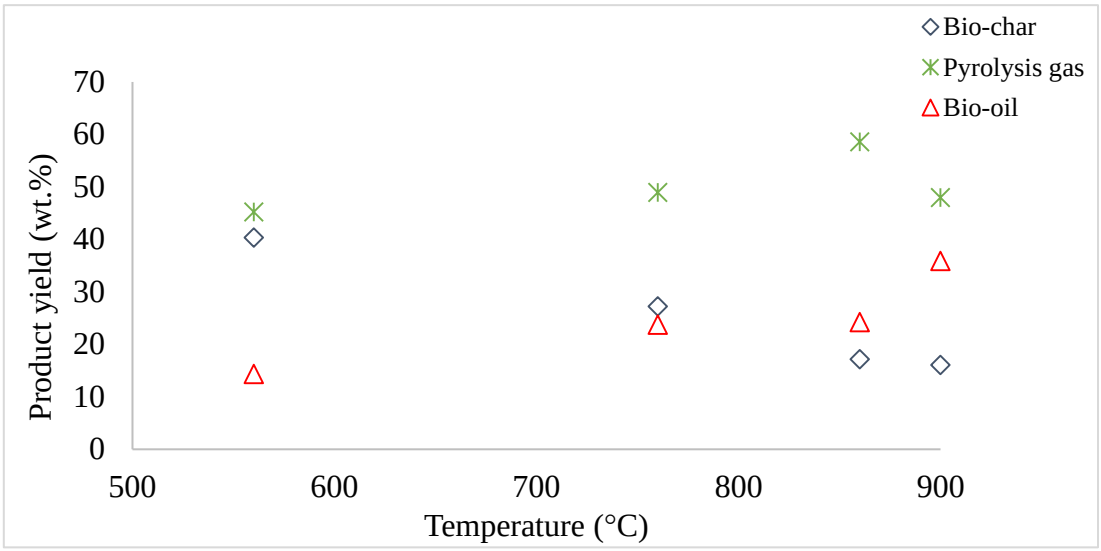

Figure 4-4 Solar pyrolysis product distribution of chicken-litter waste as function of the temperature (the relative standard deviation for the experiments was 5%).

4.3.2 Pyrolysis gases

The non-condensable gases were composed of lower molecular weight gas products as shown in Fig. 4.5. The main gas products were CO_2, CO, CH_4, C_2H_4, C_2H_6 and H_2, where CO_2, CO and CH_4 were the dominant gas products. The yields of CO_2 and CO significantly increased from 21 to 30.2 wt% and 19 to 22.4 wt%, respectively, as the temperature increased from 560 to 860°C. The rapid increase in CO_2 production at this temperature interval could be due to protein and fat decomposition which favors formation of CO_2 and CO. As discussed by Kim *et al.* (2009), the raise in CO production may also be associated with secondary tar reactions at higher temperatures.

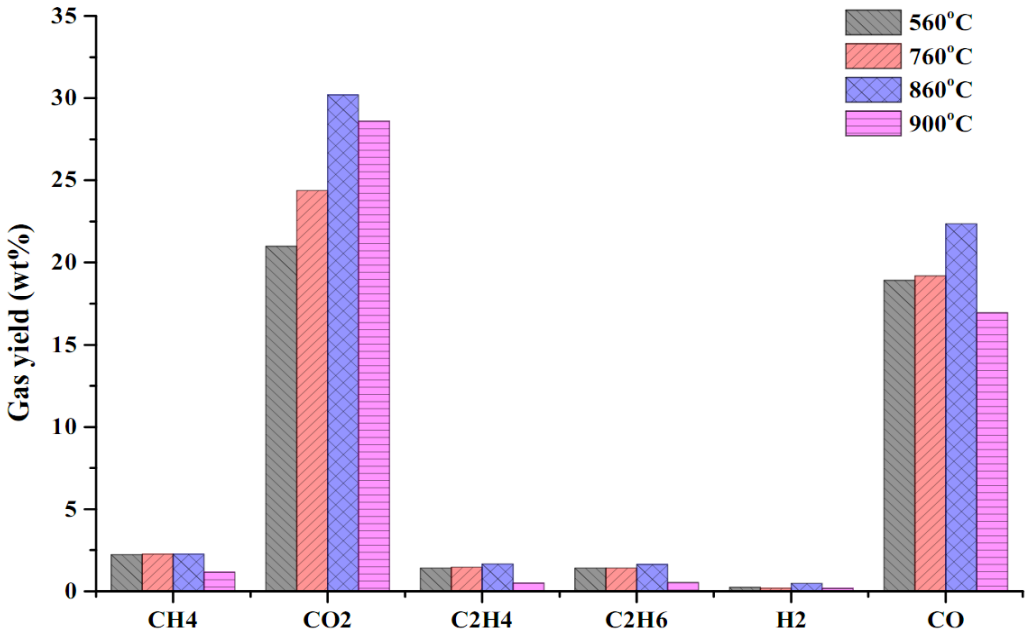

Figure 4-5 Solar pyrolysis Chicken-litter waste gas composition at different temperatures (Note: relative error was 5%)

However, when the temperature further increased to 900°C, CO_2 and CO yields were reduced to 28.6 and 17 wt% respectively. There were no significant differences with temperature with the rest of the gases species. CH_4 and C_2H_4 yields first slightly raised from 2.25 and 1.42 wt% at 560°C to 2.27 and 1.7 wt% at 860°C then decreased to 1.2 for CH_4 and 0.53 for C_2H_4 at 900°C. Hydrogen was the gas with the lowest yield achieving maximum of 0.5 wt% at 860°C.

4.3.3 GC-MS characterization of bio-oil

Fig. 4.6 shows the GC-MS spectra of the bio-oils produced at 560, 760, 860 and 900°C by solar pyrolysis of chicken litter. The area percentage of each identified compound was based on the proportion of each gas chromatograph peak area to the total peak area, as suggested by Tsai *et al.* (2009) and Cao *et al.* (2015). Generated bio-oils were found to be oxygen-rich components due to the high content of oxygen (42%, Table 4-1) with small traces of nitrogen, as shown in Table 4-2. Nitrogen containing bio-oils, such as C_2H_5NO (maximum 3.16%), $C_4H_9NO_2$ (1.25%), C_5H_5NO (3.67%), $C_7H_4N_2S$ (2.82%), $C_4H_6N_2O_2$ (1.7%), $C_{14}H_{27}NO_2$ (4.18%) etc were attributed to the nitrogen/protein in the chicken litter.

The liquid products obtained at each pyrolysis temperature were analyzed to compare the trend of the compounds. Despite the difference in the pyrolysis temperature, Phenols (3-Ethylphenol; o-Cresol; m-Cresol; p-Cresol), fatty acids (palmitic acid; stearic acid; Octanoic acid; 9-

Octadecenoic acid; 9,12-Octadecadienoic acid, Butyric Acid, etc), sterols, such as cholesterol, N-compounds (acetamide, 3-Pyridinol; 6-Isopropyl-benzothiazol-2-ylamine, 2-[3,4-hydroxyl-phenyl] ethanamine, etc) and other compounds were identified with varying concentrations. The prominent compounds at 560°C were triethylene glycol (6.18%), palmitic acid (5.19%), phenol (4.7%), 9-Octadecenoic acid, (E)- (3.8%) and acetamide (3.16%). Except for palmitic acid and 9-Octadecenoic acid, (E)-, their concentration decreased with temperature at 760°C, indicating they were decomposed to gas and other products. Triethylene glycol is used by the oil and gas industry to dehydrate natural gas and other oxygenated gases, such as CO_2 and H_2S. It is also a mild disinfectant used to target a variety of bacteria and the influenza virus. Palmitic acid, on the other hand, is mainly used to produce soaps, cosmetic and release agents. Phenol is one of the main ingredients in the synthesis of dyes, aspirin, and plastics.

Two of the dominant compounds produced at 860°C were palmitic acid (5.27%) and 9-Octadecenoic acid, (E)- (3.93), while at 900°C butyric acid (4.52%), 4-Pyridinol (3.67%), 2-[3,4-hydroxyl-phenyl] ethanamine (4.18%), pentadecanoic acid (5.65%) and 9,12-Octadecadienoic acid (Z,Z)-(3.82%) are the dominant compounds.

Overall, the produced bio-oil has acidic and unstable properties hence it needs further treatment, such as hydrothermal upgrading for use as liquid fuels (Strezov & Evans, 2009) or direct combustion in engines may provide alternative application of the pyrolysis oils as a fuel (Strezov *et al.*, 2012).

The hydrogen to carbon (H/C) and oxygen to carbon (O/C) ration are the simple and overall characterisation parameters for hydrocarbon fuels. For the solar generated bio-oils the H/C ratio was found to be 1.61 which is quite comparable with kerosene based hydrocarbon fuels (H/C = 1.6–2.3) (Yue *et al.*, 2016). But the O/C ratio was 0.78 which is higher than the conventional heavy oil of around 0.18 (Bridgwater & Peacocke, 2000; Hassan *et al.*, 2016).

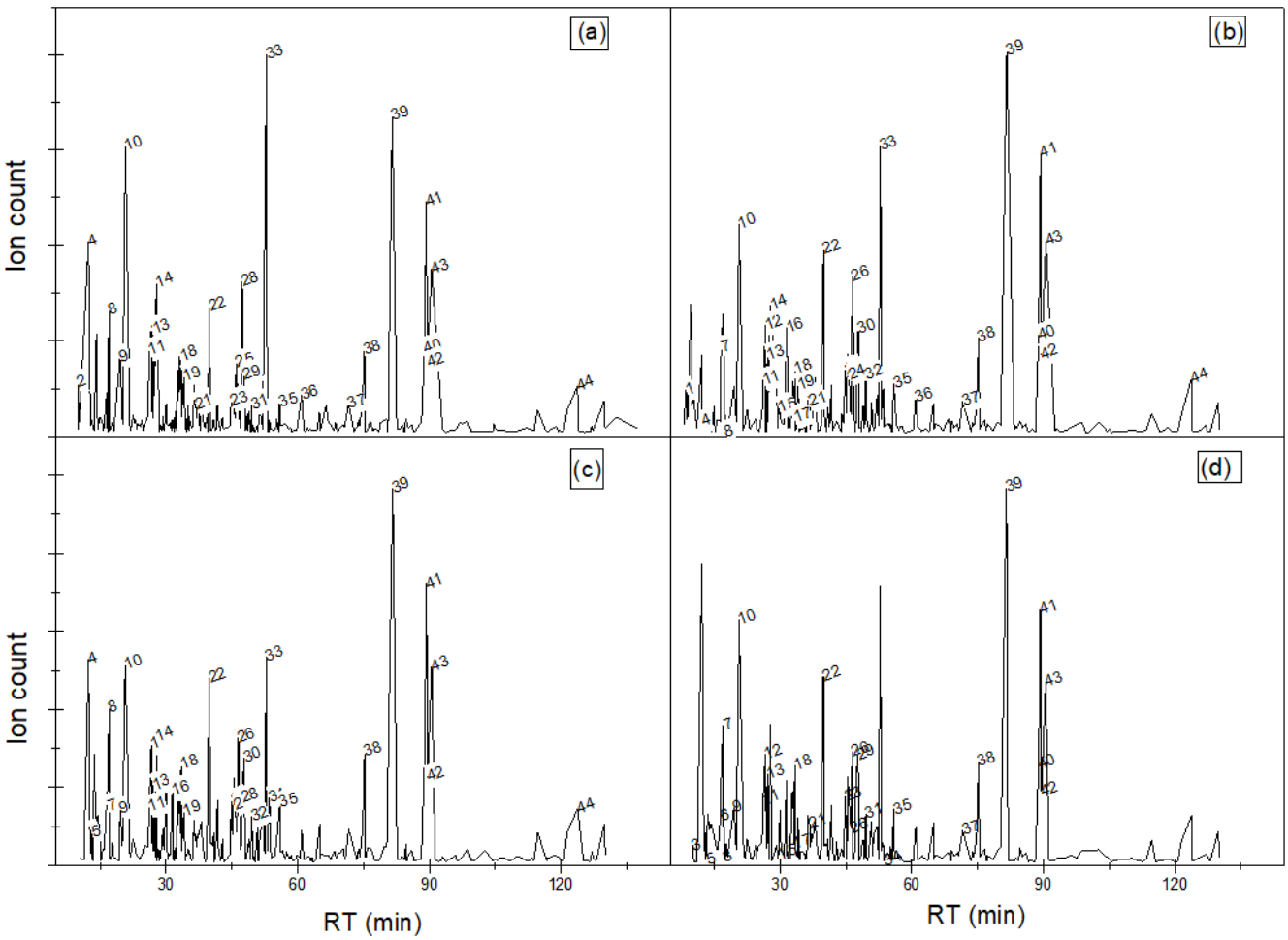

Figure 4-6 GC-MS spectra of bio-oils from chicken litter solar pyrolysis at (a) 560°C, (b) 760°C, (c) 860°C, and (d) 900°C

Table 4-2 GC-MS identification of compounds from solar pyrolysis of chicken litter waste

Peak no	RT (min)	Formula	Compound Name	Area Percent, %			
				560°C	760°C	860°C	900°C
1	8.58	$C_6H_{10}O_4$	Ethyl hydrogen succinate		0.76		
2	9.86	$C_4H_{10}O$	Isobutanol	0.87			
3	10.09	$C_4H_8O_2$	Butyric Acid				4.52
4	12.33	C_2H_5NO	Acetamide	3.16	1.33	1.17	
5	13.02	$C_5H_{10}O_2$	3-Methylbutanoic acid			0.47	0.73
6	16.37	$C_4H_9NO_2$	2-Aminobutanoic acid				1.25
7	16.6	$C_2H_6O_2$	Ethylene glycol		1.45	0.83	2.09
8	17.04	$C_5H_6O_2$	Furfuryl alcohoe	2.05	2	2.2	0.87
9	19.5	C_5H_5NO	4-Pyridinol	1.27		0.78	3.67
10	20.72	C_6H_6O	Phenol	4.7	3.49	2.81	0.98
11	26.17	C_7H_8O	o-Cresol	1.39	0.92	0.82	1.66
12	26.65	C_5H_5NO	3-Pyridinol	1.73	1.82	1.69	1.37
13	27.13	C_7H_8O	m-Cresol	1.74	1.33	1.13	2.11
14	27.84	C_7H_8O	p-Cresol	2.5	2.16	1.8	
15	29.66	$C_4H_{10}O_2$	Isobutylene glycol		0.47		1.27
16	31.47	$C_{10}H_{18}O$	exo-Norborneol		1.78	1.04	
17	33.04	$C_8H_{10}O$	3,5-Dimethylphenol	1.29	0.9		1.51
18	33.39	$C_7H_8O_2$	Guaiacol	1.3	1.1	1.41	0.71
19	34.08	$C_8H_{10}O$	3-Ethylphenol	0.97	0.83	0.76	
20	36.32	$C_8H_{16}O_2$	Octanoic acid		0.58		
21	36.78	$C_7H_4N_2S$	6-Isopropyl-benzothiazol-2-ylamine	0.51	0.57		2.82
22	39.86	$C_6H_6O_2$	Catechol	2.1	3.07	2.62	1.03
23	44.89	$C_7H_8O_2$	4-Methylcatechol	0.57	1.09	0.9	1.02
24	45.75	C6H6O2	Hydroquinone		1.01	0.84	
25	46.03	$C_4H_6N_2O_2$	Dihydrouracil	1.19			1.7
26	46.51	$C_{17}H_{42}O_5$	A-Arabinofuranose		2.63	1.78	1.31
27	47.27	$C_{12}H_{15}NO$	3-Buten-2-one, 4-[4-(dimethylamino)phenyl]-				
28	47.33	$C_{12}H_{15}NO$	2,3-2H-Quinolin-2-one, 3,3,4,7-tetramethyl-	2.51		0.94	
29	47.75	$C_{12}H_{17}NO_2$	(+)-Salsolidine	0.98			1.65

30	47.85	$C_{20}H_{25}NO_4$	Reticuline, 6'-methyl		1.76	1.51	
31	49.52	$C_{13}H_{26}$	1,3-Butadiene, (Z,E)-2,3-dipropyl-	0.51			0.77
32	49.56	$C_{14}H_{27}NO_2$	2-{3,4-hydroxyl-phenyl}ethanamine		1.01	0.68	4.18
33	52.9	$C_6H_{14}O_4$	Triethylene glycol	6.18	4.76	2.92	
34	53.56	$C_{11}H_{26}O_4$	1-butoxypropan-2-ol;1,2-dimethoxyethane			0.95	0.83
35	55.91	$C_{10}H_{12}O_2$	Eugenol	0.54	0.87	0.87	0.58
36	60.93	$C_{12}H_{24}O_2$	Dodecanoic acid	0.66	0.63		
37	71.61	$C_{14}H_{28}O_2$	Myristic acid	0.53	0.57		1.55
38	75.22	$C_{15}H_{30}O_2$	Pentadecanoic acid	1.39	1.63	1.59	5.65
39	81.62	$C_{16}H_{32}O_2$	Palmitic Acid	5.19	6.33	5.27	1.51
40	88.96	$C_{18}H_{32}O_2$	9,12-Octadecadienoic acid (Z,Z)-	1.41	1.65	1.59	3.82
41	89.34	$C_{18}H_{34}O_2$	9-Octadecenoic acid, (E)-	3.8	4.65	3.93	1.1
42	89.58	$C_{18}H_{34}O_2$	11-Octadecenoic acid, (E)-	1.19	1.34	1.24	2.74
43	90.57	$C_{18}H_{36}O_2$	Stearic acid	2.71	3.21	2.78	0.74
44	123.76	$C_{27}H_{46}O$	Cholesterol	0.82	0.94	0.8	

4.3.4 FT-IR spectra and SEM analysis of bio-chars

The Fourier Transform Infrared spectroscopy of the chicken litter chars evolved at the different temperatures are shown in Fig. 4.7. Raw chicken litter exhibited broad banding at 3300 cm^{-1} related to the OH vibration of the hydroxyl groups (Robert *et al.*, 2005). Smaller bands at 2930 and 2850 cm^{-1} of raw chicken litter, assigned as aliphatic C–H stretching of CH_3 and CH_2 groups respectively indicating aliphatic chains in the lipids (Cao *et al.*, 2016). The peaks shown at 1630 cm^{-1} for the raw chicken litter retained C=O stretch of CO_2H and C=O of primary amides revealing the presence of proteins, while the peaks at 1550 cm^{-1} was related to N–H bending vibrations in secondary amides (Robert *et al.*, 2005). The weak bands at around 1420 cm^{-1} observed in the raw chicken litter and the evolved bio-chars at 560, 760 and slightly at 860°C were related to saturated fatty acids and cellulose (CH_2 deformation) (Robert *et al.*, 2005). The peak at 1030 cm^{-1}, observed in all samples, was due to C–O stretching of carbohydrates, while the peaks observed between 500 and 900 cm^{-1} were most likely associated with inorganic fractions of the samples such as sulfate leachates (Smidt & Meissl, 2007). The strong peak at

876 cm^{-1} for the char sample evolved at 560°C was assigned to the C–O carbonate groups, while 733 cm^{-1} showed formation of aromatic C–H structure during the process.

Chars samples produced at 560°C showed slight peak at 3640 cm^{-1} which continued growing with temperature, maximum at 900°C, in all char samples which was assigned to O–H stretching of non-bonded hydroxyl groups (Kan *et al.*, 2017).
The spectra of each solid product diminished with temperature confirming dissolution of the carbohydrates. The band at 3300 cm^{-1} decreased significantly at 560°C and completely disappeared at 860°C indicating that the carboxyl acid dissolved as the temperature increased. The aliphatic C–H stretching of CH_3 and CH_2 observed at 2930 and 2850 cm^{-1} also disappeared due to the hydrolysis and dissolution of the aliphatic chain. All C=O groups assigned to the primary amides and stretches of CO_2H observed at 1630 cm^{-1} vanished in all char samples when the temperature was increased to 560°C.

A study by Cao *et al.* (2016) reported that most of the main components (proteins, lipids and carbohydrates) in the raw chicken litter are almost fully dissolved at temperatures greater than 500°C, and new C–O stretching and aromatic structure is formed due to polymerization and Diels-Alder reactions.

The SEM images of the surface morphologies of raw chicken litter and its evolved chars at different temperatures are demonstrated in Fig. 4.8. Compared to the raw chicken litter, the morphology of the char at 560°C was modified with obvious porous structures being observed. The bio-chars' structure consisted of complex network of small pores and long channels. Distinct morphologies of increasing porous structure with irregular surfaces can be seen in each evolved bio-chars. When increasing the temperature from 560 to 760°C, larger pores in the substrate could be identified. Further increase in temperature did not result in obvious morphological change of chars; especially, the SEM images did not show significant difference between the bio-chars produced at 860 and 900°C.

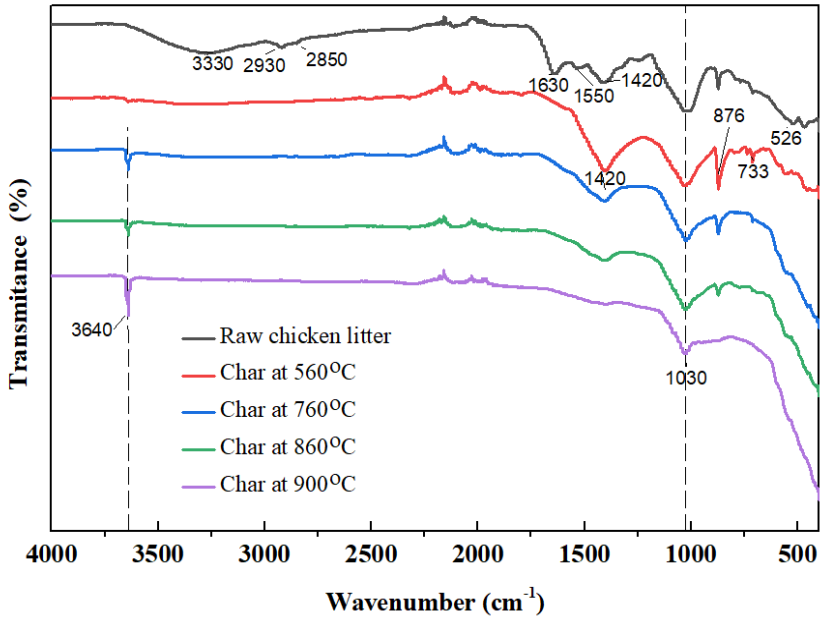

Figure 4-7 FT-IR spectra of raw chicken litter and bio-chars obtained at different temperatures

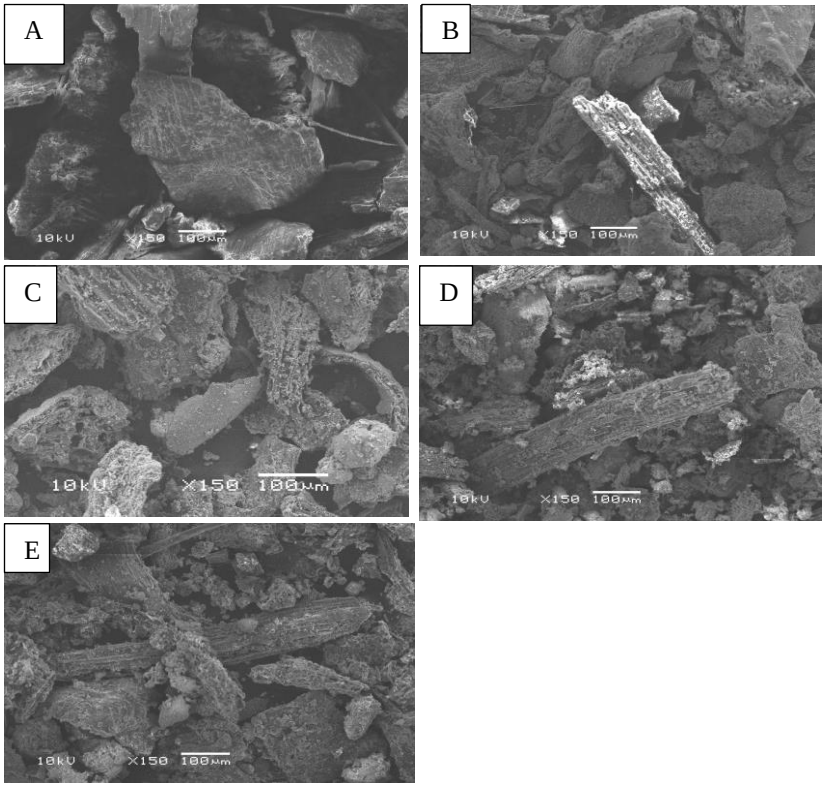

Figure 4-8 SEM images of surface morphologies of raw chicken litter and bio-chars produced at different temperatures (A) raw chicken litter, (B) 560°C, (C) 760°C, (D) 860°C, and (E) 900°C

4.4 Conclusion

Solar energy from solar-dish concentrator was employed to pyrolyse chicken litter waste at four different temperatures. Maximum solar flux density of 69,087 W/m^2, equivalent to 70 times of the available solar energy, was achieved to concentrate at the focal spot. Pyrolysis of chicken litter under the concentrated solar radiation generated bio-char, bio-oil and pyrolysis gases of different chemical composition at each pyrolysis temperature. The highest gas yield of 58.6 wt% was obtained at 860°C with CO_2, CO, and CH_4 as the main gas products. The char yield continuously decreased with temperature from 40.4 wt% at 560°C to 16.1 wt% at 900°C. Identified components of the liquid fraction were acids, phenols, nitrogen containing compounds and sterols. The FT-IR spectra of the produced bio-chars diminished with temperature indicating dissolution of carboxylic acids and long aliphatic chains. Char morphology was significantly modified at 760°C with large pores and long channel structures. The product characterization showed that solar driven pyrolysis fractions are not any different from traditional pyrolysis processes, hence solar energy can become viable potential for converting organic waste into fuels and important chemicals such as dehydrants, cosmetics and pharmaceutical commodities.

4.5 References

Agblevor, F. A., Beis, S., Kim, S. S., Tarrant, R., & Mante, N. O. (2010). Biocrude oils from the fast pyrolysis of poultry litter and hardwood. *Waste Management, 30*(2), 298-307.

Amutio, M., Lopez, G., Alvarez, J., Moreira, R., Duarte, G., Nunes, J., . . . Bilbao, J. (2013). Flash pyrolysis of forestry residues from the Portuguese Central Inland Region within the framework of the BioREFINA-Ter project. *Bioresource Technology, 129*, 512-518.

Azargohar, R., Jacobson, K. L., Powell, E. E., & Dalai, A. K. (2013). Evaluation of properties of fast pyrolysis products obtained, from Canadian waste biomass. *Journal of Analytical and Applied Pyrolysis, 104*, 330-340.

Baniasadi, M., Tugnoli, A., Conti, R., Torri, C., Fabbri, D., & Cozzani, V. (2016). Waste to energy valorization of poultry litter by slow pyrolysis. *Renewable Energy, 90*, 458-468.

Benchmark Holdings Ltd. (2014). Global poultry trends 2014: Steady Rise in Chicken Meat Output for Africa and Oceania. Retrieved from http://www.thepoultrysite.com/articles/3289/global-poultry-trends-2014-steady-rise-in-chicken-meat-output-for-africa-and-oceania/

Bolan, N. S., Szogi, A. A., Chuasavathi, T., Seshadri, B., Rothrock, M. J., & Panneerselvam, P. (2010). Uses and management of poultry litter. *Worlds Poultry Science Journal, 66*(4), 673-698.

Bridgwater, A. V., & Peacocke, G. V. C. (2000). Fast pyrolysis processes for biomass. *Renewable & Sustainable Energy Reviews, 4*(1), 1-73.

Bruun, E. W., Ambus, P., Egsgaard, H., & Hauggaard-Nielsen, H. (2012). Effects of slow and fast pyrolysis biochar on soil C and N turnover dynamics. *Soil Biology & Biochemistry, 46*, 73-79.

Cao, C. Q., Guo, L. J., Yin, J. R., Jin, H., Cao, W., Jia, Y., & Yao, X. D. (2015). Supercritical Water Gasification of Coal with Waste Black Liquor as Inexpensive Additives. *Energy & Fuels, 29*(1), 384-391.

Cao, W., Cao, C. Q., Guo, L. J., Jin, H., Dargusch, M., Bernhardt, D., & Yao, X. D. (2016). Hydrogen production from supercritical water gasification of chicken manure. *International Journal of Hydrogen Energy, 41*(48), 22722-22731.

Channiwala, S. A., & Parikh, P. P. (2002). A unified correlation for estimating HHV of solid, liquid and gaseous fuels. *Fuel, 81*(8), 1051-1063.

Dalolio, F. S., da Silva, J. N., de Oliveira, A. C. C., Tinoco, I. D. F., Barbosa, R. C., Resende, M. D., Coelho, S. T. (2017). Poultry litter as biomass energy: A review and future perspectives. *Renewable & Sustainable Energy Reviews, 76*, 941-949.

Edwards, D. R., & Daniel, T. C. (1992). Environmental impacts of on-farm poultry waste-disposal - a review *Bioresource Technology, 41*(1), 9-33.

Hanif, M. U., Capareda, S. C., Iqbal, H., Arazo, R. O., & Baig, M. A. (2016). Effects of Pyrolysis Temperature on Product Yields and Energy Recovery from Co-Feeding of Cotton Gin Trash, Cow Manure, and Microalgae: A Simulation Study. *PLOS ONE, 11*(4).

Hassan, E. B., Abou-Yousef, H., Steele, P., & El-Giar, E. (2016). Characterization of bio-oils from the fast pyrolysis of white oak and sweetgum. *Energy Sources, Part A: Recovery, Utilization, and Environmental Effects, 38*(1), 43-50.

Kan, T., Grierson, S., de Nys, R., & Strezov, V. (2014a). Comparative Assessment of the Thermochemical Conversion of Freshwater and Marine Micro- and Macroalgae. *Energy & Fuels, 28*(1), 104-114.

Kan, T., Strezov, V., & Evans, T. (2014b). Catalytic Pyrolysis of Coffee Grounds Using NiCu-Impregnated Catalysts. *Energy & Fuels, 28*(1), 228-235.

Kan, T., Strezov, V., & Evans, T. (2017). Fuel production from pyrolysis of natural and synthetic rubbers. *Fuel, 191*, 403-410.

Kim, S.-S., Agblevor, F. A., & Lim, J. (2009). Fast pyrolysis of chicken litter and turkey litter in a fluidized bed reactor. *Journal of Industrial and Engineering Chemistry, 15*(2), 247-252.

Lima, I. M., Boateng, A. A., & Klasson, K. T. (2009). Pyrolysis of Broiler Manure: Char and Product Gas Characterization. *Industrial & Engineering Chemistry Research, 48*(3), 1292-1297.

Lori, M., Greg, M., Matt, H., & Eldridge R., C. (2009). Land Application of Broiler and Turkey Litter for Farming Operations Without a DEQ Permit. *Virginia Cooperative Extension*, Publication number 442-052.

Ma, B., & Agblevor, F. A. (2014). Polarity-based separation and chemical characterization of fast pyrolysis bio-oil from poultry litter. *Biomass and Bioenergy, 64*, 337-347.

Mahmoudi, S., Baeyens, J., & Seville, J. P. K. (2010). NOx formation and selective non-catalytic reduction (SNCR) in a fluidized bed combustor of biomass. *Biomass and Bioenergy, 34*(9), 1393-1409.

Mante, O. D., & Agblevor, F. A. (2010). Influence of pine wood shavings on the pyrolysis of poultry litter. *Waste Management, 30*(12), 2537-2547.

Moore, P. A., & Edwards, D. R. (2007). Long-term effects of poultry litter, alum-treated litter, and ammonium nitrate on phosphorus availability in soils. *Journal of Environmental Quality, 36*(1), 163-174.

Morales, S., Miranda, R., Bustos, D., Cazares, T., & Tran, H. (2014). Solar biomass pyrolysis for the production of bio-fuels and chemical commodities. *Journal of Analytical and Applied Pyrolysis, 109*, 65-78.

Opatokun, S. A., Kan, T., Al Shoaibi, A., Srinivasakannan, C., & Strezov, V. (2016). Characterization of Food Waste and Its Digestate as Feedstock for Thermochemical Processing. *Energy & Fuels, 30*(3), 1589-1597.

Pattiya, A. (2011). Bio-oil production via fast pyrolysis of biomass residues from cassava plants in a fluidised-bed reactor. *Bioresource Technology, 102*(2), 1959-1967.

Putun, A. E., Apaydin, E., & Putun, E. (2002). Bio-oil production from pyrolysis and steam pyrolysis of soybean-cake: product yields and composition. *Energy, 27*(7), 703-713.

Robert, S., Francis, W., & David, K. (2005). *Spectrometric identification of organic compounds*. New York, USA: John Wiley & Sons.

Sawin, J. L., Seyboth, K., & Sverrisson, F. (2016). *RENEWABLES 2016: GLOBAL STATUS REPORT*. Retrieved from Retrived from Paris, France www.fs-unep-centre.org

Septien, S., Valin, S., Dupont, C., Peyrot, M., & Salvador, S. (2012). Effect of particle size and temperature on woody biomass fast pyrolysis at high temperature (1000-1400 degrees C). *Fuel, 97*, 202-210.

Smidt, E., & Meissl, K. (2007). The applicability of Fourier transform infrared (FT-IR) spectroscopy in waste management. *Waste Management, 27*(2), 268-276.

Song, W., & Guo, M. (2012). Quality variations of poultry litter biochar generated at different pyrolysis temperatures. *Journal of Analytical and Applied Pyrolysis, 94*, 138-145.

Strezov, V., & Evans, T. J. (2009). Thermal processing of paper sludge and characterisation of its pyrolysis products. *Waste Manag, 29*(5), 1644-1648.

Strezov, V., Popovic, E., Filkoski, R. V., Shah, P., & Evans, T. (2012). Assessment of the Thermal Processing Behavior of Tobacco Waste. *Energy & Fuels, 26*(9), 5930-5935.

Tsai, W. T., Lee, M. K., Chang, J. H., Su, T. Y., & Chang, Y. M. (2009). Characterization of bio-oil from induction-heating pyrolysis of food-processing sewage sludges using chromatographic analysis. *Bioresource Technology, 100*(9), 2650-2654.

Uzun, B. B., Pütün, A. E., & Pütün, E. (2006). Fast pyrolysis of soybean cake: Product yields and compositions. *Bioresource Technology, 97*(4), 569-576.

Wang, H., & Li, C. (2017). Hydroprocessing of Coal Tar to Prepare Clean Fuel Oil *Encyclopedia of Sustainable Technologies* (pp. 411-422). Oxford: Elsevier.

Weldekidan, H., Strezov, V., & Town, G. (2017). Performance evaluation of absorber reactors for solar fuel production. *Chemical engineering transaction, 61*, 1111-1116.

Wendelin, T. (2013). *SolTrace: A Ray-Tracing Code for Complex Solar Optical Systems*. Retrieved from Colorado, U.S.: http://www.osti.gov/bridge

Wiedemann, S. G. (2015). *Land Application of Chicken Litter: A Guide for Users* (14/094). Retrieved from Canberra-Australia www.rirdc.gov.au

Yang, S. I., Wu, M. S., & Wu, C. Y. (2014). Application of biomass fast pyrolysis part I: Pyrolysis characteristics and products. *Energy, 66*, 162-171.

Yue, L., Li, G., He, G., Guo, Y., Xu, L., & Fang, W. (2016). Impacts of hydrogen to carbon ratio (H/C) on fundamental properties and supercritical cracking performance of hydrocarbon fuels. *Chemical Engineering Journal, 283*(Supplement C), 1216-1223.

Zeng, K., Gauthier, D., Li, R., & Flamant, G. (2015). Solar pyrolysis of beech wood: Effects of pyrolysis parameters on the product distribution and gas product composition. *Energy, 93*, 1648-1657.

Zeng, K., Gauthier, D., Minh, D. P., Weiss-Hortala, E., Nzihou, A., & Flamant, G. (2017). Characterization of solar fuels obtained from beech wood solar pyrolysis. *Fuel, 188*, 285-293.

Zhang, Y., Bi, P., Wang, J., Jiang, P., Wu, X., Xue, H., Li, Q. (2015). Production of jet and diesel biofuels from renewable lignocellulosic biomass. *Applied Energy, 150*(Supplement C), 128-137.

Chapter 5: Production and analysis of fuels and chemicals obtained from rice husk pyrolysis with concentrated solar radiation

In Chapter 4 the pyrolysis products of chicken litter, which is protein and lipids based feedstock are investigated, whereas in this chapter the pyrolysis of rice husk, which is lignin and carbohydrate containing biomass is dealt. With these investigations we can have complete understanding of pyrolytic product behaviour of range of feedstocks under the solar pyrolysis conditions.

This project was initiated by Vlad. I designed and conducted the experiments including sample preparation, data collection and analysis, and manuscript preparation. Vlad, Tao and Graham have reviewed and edited the manuscript for publication.

Authors' contribution summary for this paper

	W. H.	S. V.	T. G.	K. T.
Experiment Design	•			
Sample Preparation	•			
Data Collection	•			
Analysis	•	•		
Manuscript	•	•	•	•

Publication:

Weldekidan H. (70%), Strezov V. (10%), Kan T. (10%), and Town G. (10%). Production and analysis of fuels and chemicals obtained from rice husk pyrolysis with concentrated solar radiation, ***Fuel (2018), 233: 396-403***.

Adopted for this thesis with the exclusive rights from Elsevier.

Production and analysis of fuels and chemicals obtained from rice husk pyrolysis with concentrated solar radiation

Haftom Weldekidan[1], Vladimir Strezov[1], Graham Town[2], and Tao Kan[1]*

[1] Department of Environmental Sciences, Macquarie University, Sydney, NSW 2109, Australia

[2] School of Engineering, Macquarie University, Sydney, NSW 2109, Australia

* Email: tao.kan@mq.edu.au

Abstract

Solar energy is the greatest source of renewable energy which can be applied for biomass thermochemical conversion processes. In this study, pyrolysis of rice husk was performed at different temperatures obtained from concentrated solar radiation. The solar pyrolysis of rice husk mainly produced bio-oils (20.6–43.13 wt. %), followed by bio-char and pyrolysis gases. The pyrolysis gas was observed to increase with temperature from 14 wt.% at 500°C to its maximum yield of 25.48 wt. % at 800°C. The highest bio-char yield was found to be 43 wt.% at 500°C. As observed by the FTIR spectrometer, functional groups of the raw rice husk changed with pyrolysis temperature. SEM images showed large glass-like holes in the chars produced at 500°C while EDS analysis revealed highest silica concentrations of 12.3% at 700°C. Acids, alcohols and phenols as well as trace amounts of ester and aldehydes were the GC-MS identified bio-oil compounds. Solar pyrolysis of rice husk could be a promising and energy-saving technology for fuel and chemical production

Key words: Solar fuels, pyrolysis gases, bio-char, product yields, GC-MS analysis, biomass

5.1 Introduction

Fossil derived fuels have become a limited resource and emissions of greenhouse gases are impacting the environment and climate (Ciampi *et al.*, 2018; Li *et al.*, 2017; Zhao *et al.*, 2015). Considerable research has been performed to look for alternative fuels and energy sources which can reduce dependency on fossil fuels and CO_2 emissions (Kumar & Kumar, 2017; Kumar *et al.*, 2016; Martinopoulos & Tsalikis, 2018). Biomass, being a renewable and carbon

neutral source of energy, is widely and readily available in almost all parts of the world. It is a natural resource which can be converted into gaseous, liquid and solid fuels the properties and yields of which depend on the thermal, biological or physical conversion mechanisms (Ahmad *et al.*, 2016; Kirkels, 2012; Pottmaier *et al.*, 2013).

The large quantities of residue and leftovers from maize, wheat and rice, which constitute world's top three agricultural by-products, can be sought as a strategic source of renewable energy (Pottmaier *et al.*, 2013). After the harvest season, open field burning or decaying of the residues in the field is the common disposal practice in many countries, creating health and environmental concerns (Lim *et al.*, 2012).

Rice husk, which accounts for 20-25% of the total paddy weight, has an annual global capacity of 700.7 million tonnes (Liu *et al.*, 2016). It is produced in the first step of milling when the husk is separated from the grain and ends up as a leftover in the open air in most countries (Suzana Y. *et al.*, 2016). Rice husk contains lignin (up to 10%), cellulose (20-35%), hemicellulose (15-30%) and some other materials. Generally, it is characterized by high ash content and low bulk density (Naqvi *et al.*, 2014).

Rice husk can be converted to different types of fuels using thermochemical processes. Direct combustion, pyrolysis, gasification and liquefaction are among the available thermochemical conversion mechanisms which are considered as critical biomass utilization alternatives, offering economic benefits through the production of high value fuel gasses, liquids and chars (Zhang *et al.*, 2016a). Pyrolysis of biomass is one of the most efficient technologies for bio-char, bio-oil and bio-gas production (Zhou *et al.*, 2013). It involves moisture evaporation at around 100°C, followed by biomass cracking and devolatilization when the temperature reaches around 300°C, releasing pyrolysis gases such as CO_2, CO, H_2, light weight hydrocarbons and tars (Zhang *et al.*, 2016b).

Many studies have investigated rice husk pyrolysis in reactors heated by products of pyrolysis. Some of the recent studies on traditional rice husk pyrolysis can be seen in the literatures (Dunnigan *et al.*, 2018; Qiyuan Li *et al.*, 2016; Li *et al.*, 2017; Tsai *et al.*, 2007; Yue *et al.*, 2016). Li *et al.* (2017) used rice husk pyrolysis products, mainly bio-oil, as raw material to produce synthesis gas (H_2 and CO). The rice husk fed to quartz tube reactor at a rate of 0.29 g/min, was pyrolysed at temperatures ranging from 500 to 800°C. H_2 and CO produced from the pyrolysis of the bio-oil were found to reach 56 and 18%, respectively, 37% and 36% from

the volatiles, respectively. Pyrolysis temperatures ranging from 400 to 800°C and feeding rate of 1.3 g/min were used to generate raw pyrolysis volatiles with different bio-oil to syngas ratios (Dunnigan *et al.*, 2018). Maximum gas, bio-oil and bio-char yields were found to be 45%, 38% and 43% recepectively. The maximum uncondensable pyrolysis gases, containing mainly CO, H_2, CO_2 and CH_4 were obtained at 800°C. Bio-oil and bio-char yeilds were investigated from fast pyrolysis experiments of rice husk conducted in a fix-bed induction heating system at 400 to 800°C and 200°C /min (Tsai *et al.*, 2007). The oil yield was observed to increase from 10 to 37% over the entire range of the pyrolysis temperatures while the bio-char was found to decrease with temperature from 84.22 to 30.7%. Characterization of bio-char, bio-oil and gas produced from the pyrolysis of rice husk at various temperatures (350 to 600°C) and feeding rate of 2 g/min were performed by Yu *et al.* (2016). Maximum gas yield (78 wt.%) was obtained at 600°C while the maximum yields of char (45 wt.%) and liquids (47 wt%) were obtained at 350 and 500°C, respectively.

The above conventional pyrolysis processes require partial combustion and use of the pyrolysis products to maintain the pyrolysis temperature, which compromises the quality and amount of the pyrolysis products. Solar energy if coupled with pyrolysis has vast potential to overcome these shortcoming, as it can provide the required heat to carry out the pyrolysis and enable full recovery of the pyrolysis products (Bait & Si-Ameur, 2017; Weldekidan *et al.*, 2018a). Australia receives an average of $58x10^{21}$ Joules of solar energy in a year which positions the country as one of the best solar energy receivers in the world (Lohmann *et al.*, 2006). Integrating solar technology for biomass pyrolysis in Australia has substantial advantages and can bring significant contribution for the future development of the solar energy technology. Rice husk as well as other lignocellulosic biomass materials can be processed using integrated solar pyrolysis method, however its behaviors under the solar pyrolysis conditions has never been investigated to this date. In this study, rice husk as an abundant agricultural waste was selected as the feedstock. In addition, the higher ash content of rick husk than most of the other lignocellulosic materials, was an additional important parameter for selection of this feedstock for solar pyrolysis. Although high ash content biomass was studied previously by Weldekidan *et al.* (2018b), however, the biomass used was chicken litter, which is primarly lipid anc protein based biomass feedstock. In the current work, the high ash lignocellulosic feedstock was selected with a focus to pyrolyse rice husk at different temperatures and evaluate the different pyrolysis products obtained from the solar pyrolysis. The aim of this work was to investigate

properties of pyrolysis gases, bio-char (including the contained ash) and bio-oils through rice husk pyrolysis induced by concentrated solar radiation at different temperatures.

5.2 Materials and methods

5.2.1 Materials

Sample rice husk from Carlingford Produce, Sydney, Australia was dried in a vacuum oven for 2 hours at 70°C and 80 kPa then ground and sieved by a 280 µm sieve. ASTM D7582 test method was applied to determine the proximate analysis of the sample while the ultimate analysis was determined with CHNS analyser using Vario MICRO cube elemental analyser (Elementar Analysensysteme GmbH, Germany) with PC based data system Windows^{TM} and electronic micro balance).

It contained 25.32% ash, 14.14% fixed carbon, 54.51% volatile matters and the moisture content was found to be 6.03%.

The elemental analysis of the rice husk shows 34.33 % C, 4.98 % H, 0.38 % N, 0.19 % S and on ash free basis the O (by difference) was 60.12 %.

5.2.2 Solar pyrolysis reactor

The solar pyrolysis system, with design reported in a previous study (Weldekidan *et al.*, 2017), was employed to pyrolyze the sample. The system contains 1.8 m aperture diameter parabolic dish coated with an 88% reflective aluminum material. The reactor, which was silica glass tube with 13 mm in diameter and 35 cm length was loaded with 100 mg of sample and placed at the focal region of the dish which is at 0.655 m from the bottom edge of the dish. Samples were positioned in the middle of the reactor and held in place by glass wool. The parabolic dish has maximum heat flux concentrating capacity of 70 kW/m^2 for one sun (1000 W/m^2), which generates the pyrolysis temperatures. Table 5-1 is the optical characteristics of the parabolic dish obtained from SolTrace (Wendelin, 2013) simulations.

Based on the heat flux distribution, theoretical calculation of the highest temperature ***(T)*** on a blackbody is given by equation (1) (Ekman *et al.*, 2015; Weldekidan *et al.*, 2017):

$$\boldsymbol{Q = \sigma T^4} \qquad (1)$$

Where $\boldsymbol{Q}$ is the radiated flux per square meter (70 kW/m^2) and $\boldsymbol{\sigma}$ is the Stefan-Boltzmann constant. Accordingly, the concentrated radiation in this case would result in a corresponding highest temperature of 1,060°C.

The parabolic dish was calibrated for its maximum temperature using K-type thermocouple with USB serial interface, PicoLog software and stick-road which was bolted to the surface of the dish. The dish was first set to its maximum performance position, then corresponding length and position of the shadow of the stick-road, which lie on the dish surface, was marked for reference. To control the temperature during the pyrolysis process, the dish was tracked for the shadow of the stick-road to lie on the reference mark always. When the target temperature was reached, for instance 500°C, the dish could be rotated to its offset position easily then sample temperature instantly started to drop to ambient value. To maintain constant heating rate, all the experiments were conducted at the same radiation levels, 700 to 720 W/m^2. Fig. 5.1 shows variation of the temperature with time during the pyrolysis experiment.

Table 5-1 Optical characteristics of dish

Parameters	Dimensions
Aperture diameter	1.8 m
Surface reflectivity	88 %
Focal length	0.655 m
Reactor tube diameter	13 mm
Power per ray	0.25641 W
Generated heat per area	70 kW/m^2
Sun ray count	12,636
Highest temperature	1,060°C

Semi rigid nylon tube (1/4" outer diameter) was connected to the reactor inlet to pass argon gas (at a flow rate of 85 mL/min) to purge the reactor and as a carrier gas for the pyrolysis gases. Another nylon tube was connected to the reactor outlet to collect the gases in a Tdlar® gas bag for further analysis by the GC machine. Fig. 5. 2 shows schematic of the experimental set-up. Samples were heated up to the maximum temperatures of 500, 600, 700 and 800°C at a heating rate of 160 ± 6°C/min. These temperatures have been selected as most of the pyrolysis products can sufficiently be produced in the range of temperatures (Li *et al*., 2017). However, the heating rate depend on the available solar radiation in the area during the solar pyrolysis process. A TC-08 type of data logger from PICO TECHNOLOGY with USB serial interface and PicoLog data logging software was applied to log and display the recorded temperatures in a computer. Each experiment was repeated for at least 3 times until the average error was less than 5%.

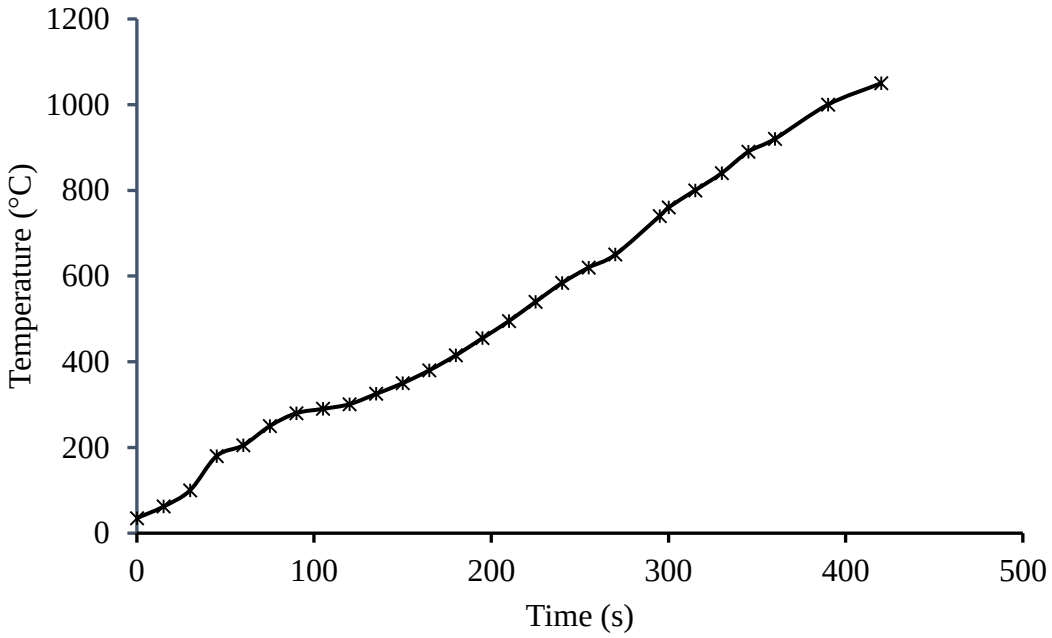

Figure 5-1 Temperature variation of the reactor as a function of time (relative error was 5%)

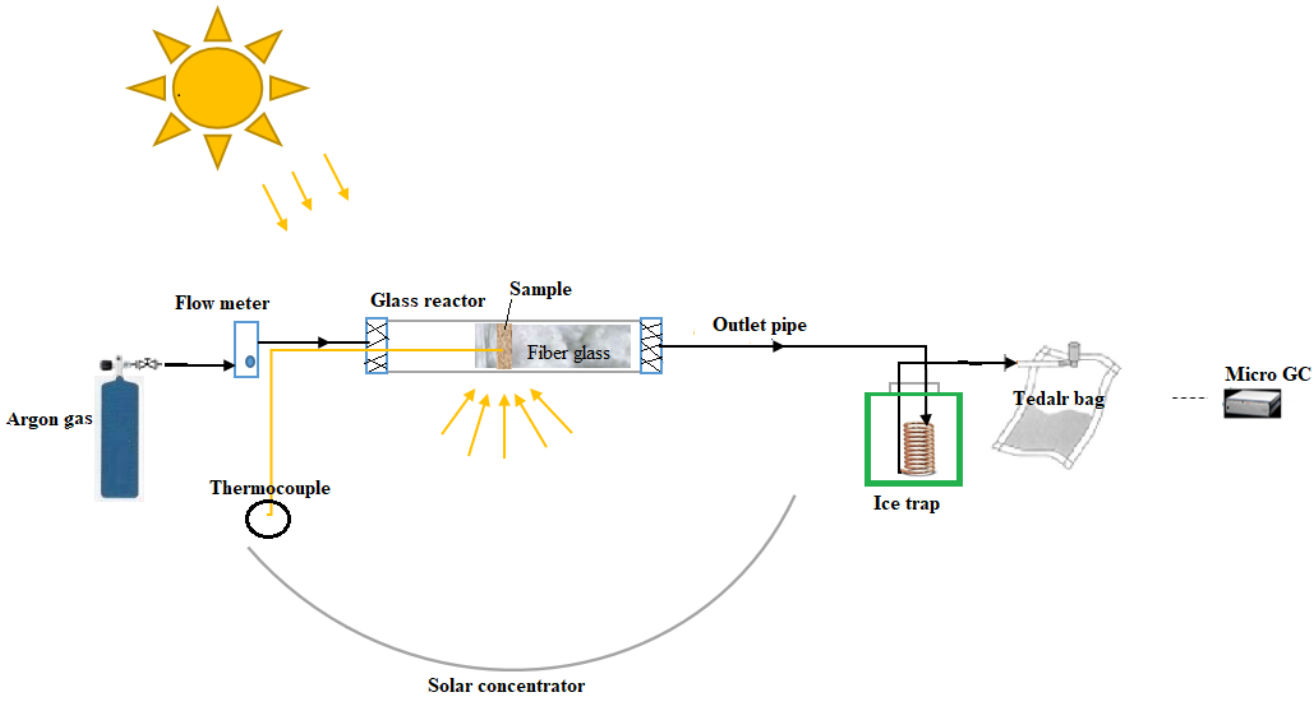

Figure 5-2 Experimental set-up (Weldekidan., et al., 2018b)

5.2.3 Product recovery

5.2.3.1 Pyrolysis gases

Pyrolysis gases collected in the gas bag at each targeted temperature were analyzed with M200 micro-gas chromatograph. CO_2, CH_4, C_2H_4 and C_2H_6 were analyzed by a polymer Paraplot U column kept at 40°C while another column with molecular sieve 5A maintained at 60°C was selected to separate and analyze H_2 and CO. Chromatograms were recorded every 100 s using thermal conductivity detector (TCD). More details on the apparatus and calibration procedures can be obtained from the previous works (Kan *et al.*, 2017; Strezov *et al.*, 2012; Weldekidan *et al.*, 2018b).

Volumes of each pyrolysis gases were quantified from standard mix gases with known concentrations, then the weight percentages of each gases were calculated based on the ideal gas equation.

The higher heating values (HHVs) of the gas products were calculated based on the heating values and molar yields of the combustible gas components using equations (2) (Yu *et al.*, 2016).

$$HHV_{gas} = x_{co}HHV_{CO} + x_{CH4}HHV_{CH4} + x_{H2}HHV_{H2} + \cdots \sum(x_{CnHn}HHV_{CnHm}) \qquad (2)$$

Where *HHV*x (x=CO, CH4, H2 and other gases) are the higher heating constants of individual gases obtained from Lars and Nilsson (2001) and ***X***s (s= CO, CH_4, H_2 and other gases) are the molar fractions of each gases.

5.2.3.2 Liquids

Solar pyrolysis oils condensed on the glass wool at each temperature were extracted using dichloromethane (DCM) solvent then derivatized by N,O-bis(trimethylsilyl) trifluoroacetamide with 1% trimethylchlorosilane (BSTFA + 1% TMCS) which improved separation and thermal stability of the compounds in the gas chromatography-mass spectrometry (GC-MS) analysis. The difference between the mass of the original rice husk and, gas and char yields was assumed as the liquid yield. Agilent 7890B gas chromatography coupled with 5977A mass spectrometry system equipped with an HP-5MS column (60 m x 0.25 µm) was employed to analyze components of the solar pyrolysis oils. The GC oven temperature was maintained at 40°C for 2 min then increased to 310°C at 2°C/min. The injector and mass spectrometer detector (MSD) line temperatures were set to 310°C, while the quadruple mass spectrometer (MS Quad) temperature was at 150°C. MassHunter software was applied to analyze the compounds with the match factor database set over 80.

5.2.3.3 Bio-char

The solid residue left in the reactor after each pyrolysis procedure was considered as bio-char. Functional groups of the raw rice husk and bio-chars produced at each targeted temperature were acquired by a Fourier transform-infrared spectrometer (Nicolet 6700 maFT-IR) which applies attenuation of total reflectance method with crystal diamond. Total number of scans with 4 cm^{-1} spectral resolution were 32.

Desktop PhenomWorld SEM linked with Energy-Dispersive Spectroscopy (EDS) was used to study the morphology and quantitatively analyze the elemental composition of the raw rice husk and bio-chars evolved at each pyrolysis temperature. Samples were mounted on aluminum film and positioned at 2.5 mm below the holder surface for both SEM images and EDS analysis. Images of different samples with magnitudes ranging from 280 µm to 100 µm were produced. Morphologies of high resolution SEM images were produced at 10 kV imaging-mode and the

elemental concentrations were analyzed with EDS-Mode of 15 kV using point for point analysis method.

5.3 Result and discussion

5.3.1 Product yields

The product yields from the solar pyrolysis of rice husk at various temperatures are presented in Fig. 5.3. It can be observed that the gas yield substantially increased with temperature from 13.9 wt.% at 500°C to its maximum value of 25.5 wt.% at 800°C. Generally, higher temperature favors production of gas due to secondary tar cracking (Yu *et al.*, 2016). The liquid yield showed peak value of 43.1 wt.% at 700°C and decreased to its minimum value of 38.7 wt.% at 800°C, while the bio-char yield was maximum (43 wt.%) at 500°C and minimum (35.8 wt.%) at 800°C. The high bio-char yield is largely due to the high ash content and low volatile matter of the feedstock. The inherent high lignin content of rice husk could also contribute to the relatively higher char yields (Gani & Naruse, 2007). The high heating rate, which was achieved at moderate solar radiation in this experiment, was observed to produce relatively higher liquid yields than conventional rice husk pyrolysis with lower heating rates (Williams & Nugranad, 2000). Solar is inherently better for providing high temperature and fast heating rates in the solar pyrolysis process (Zeng *et al.*, 2015, 2017). The Solar pyrolysis products are similar to the conventional pyrolysis processes. The main difference is that the high bio-oil yields from the solar pyrolysis could be more easily achieved than conventional electricity or heat driven pyrolysis processes due to the utilization of renewable solar energy. In addition, the solar beams can heat the biomass particle through direct radiation on biomass surface as well as in an indirect way by heating up surrounding atmosphere and then convection.

5.3.2 Pyrolysis gas products

Fig. 5.4 shows the gas yields for the different pyrolysis temperatures. Pyrolysis gases produced during the solar pyrolysis process were CO_2, CO, CH_4, C_2H_4, C_2H_6 and H_2, of which CO_2, CO, CH_4 and, at higher temperatures H_2, were the dominantly evolved gases. CO_2 and CO had the highest yields at 500°C (5 wt.% and 3.5 wt.% respectively) and substantially decreased with temperature which was due to the primary decomposition of the biomass, significantly producing CO_2 and CO at lower temperatures. CO content increased from 2.13 wt% at 700 to 2.7 wt% at 800°C. On the contrary the CO_2 yield continuously decreased over the entire range of the pyrolysis temperatures. CO_2 reduction by carbon to CO at higher temperatures was the

main reason for increasing the CO yield. At higher pyrolysis temperatures carbonylation to CO is favoured over decarboxylation to CO_2. CH_4 yield was observed to slightly increase from 1.1 wt.% at 500°C to 1.53 wt.% at 600°C mainly due to depolymerization (Opatokun *et al.*, 2016) then decreased with temperature. It is known that CH_4 is unstable at higher temperatures (Khan & Crynes, 1970). H_2 showed its highest yield (1.54 wt.%) at 800°C. The increase in H_2 was due to secondary tar and light hydrocarbons cracking (Kan *et al.*, 2014). As can be seen in Fig. 5.4, CH_4 and H_2 have inverse yield patterns. As observed from Fig. 5.5, the total heating value of the pyrolysis gases increased with temperature, particularly sharp increase was observed from 700 to 800°C (197 kJ/kg) which is almost twice the heating value obtained at 700°C (107 kJ/kg). This was mainly due to the highest H_2 production at 800°C which contributed largely to the HHV of the gas mixture. Therefore the optimum operating temperature to produce valuable combustible pyrolysis gases in this range of pyrolysis temperature was at 800°C. These higher heating values of the pyrolysis gases can make it suitable candidate for heat and power generation in gas turbines.

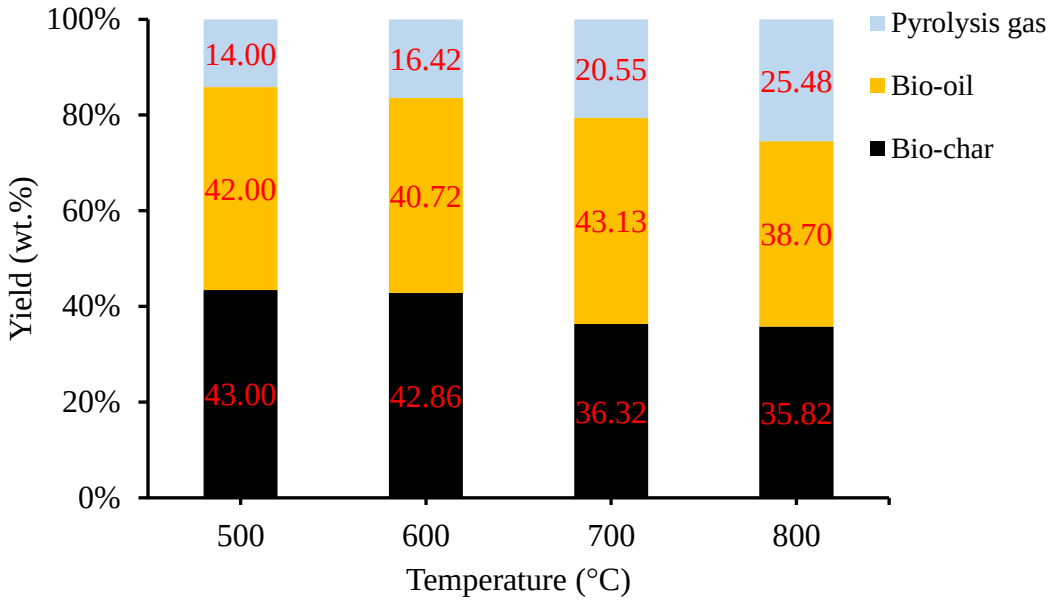

Figure 5-3 Mass yield of pyrolysis gas, bio-liquid and bio-char from solar pyrolysis of rice husk (relative error 5%)

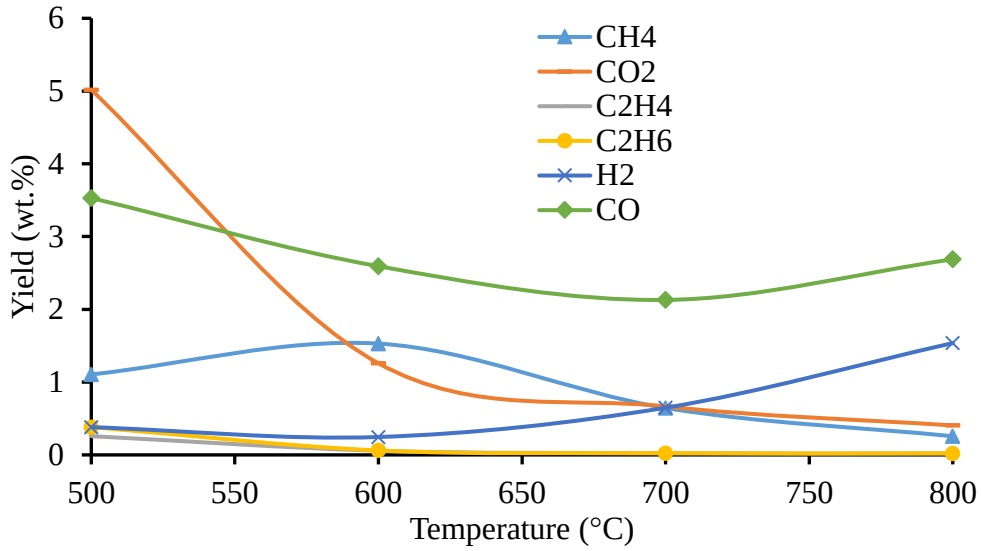

Figure 5-4 Yields of pyrolysis gas species from solar pyrolysis of rice husk (relative error 5%)

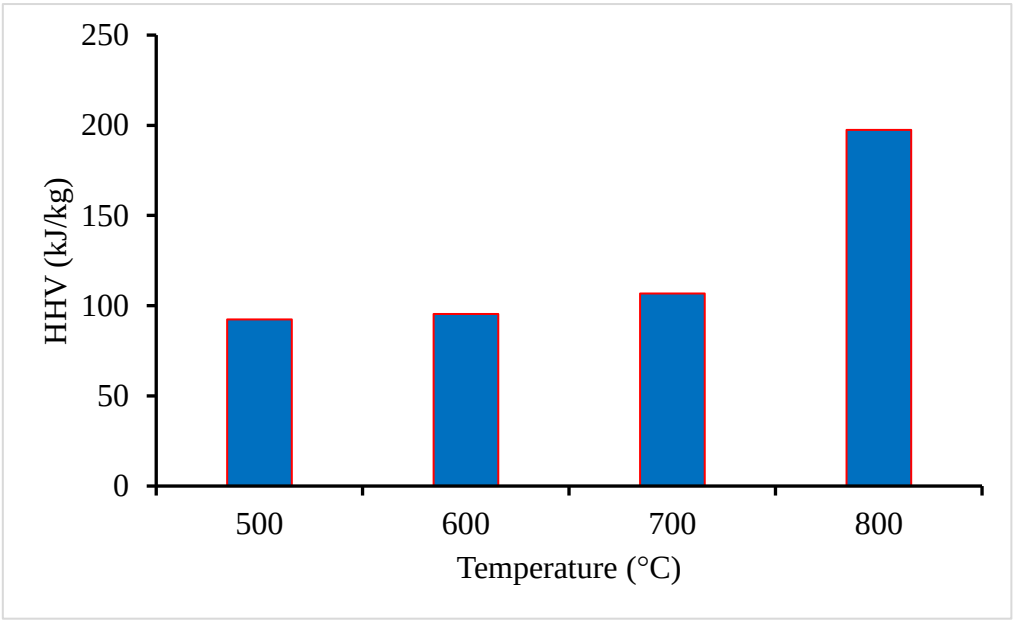

Figure 5-5 Higher heating values of pyrolysis gases from rice husk pyrolysis at various temperatures (relative error 5%)

5.3.3 Pyrolysis liquids

GC-MS spectra of the bio-oils obtained from the solar pyrolysis of rice husk at 500, 600, 700 and 800°C are shown in Fig. 5.6, while Table 5-2 represents the major 30 compounds identified

in the pyrolysis liquids with the GC-MS. The compounds were listed based on the area percentage, starting from the largest % down to the lowest %. The detected products could be classified into acids (sorbic, hexanoic, palmitic, dodecanoic etc), alcohols (isobutanol, 2-Methyl-1-butanol, furfuryl, guaiacol etc), phenols (3-ethylphenol, 4-methylcatechol, catechol, cresols etc) and small amounts of esters, ketones as well as aldehydes such as 1-dimethylvinylsilyloxy-3-methylbenzene and vanillin. Despite the difference in temperature, most of the bio-oils produced at all pyrolysis temperatures were similar but the area percentages of most compounds decreased with temperature which was attributed to the decomposition of the compounds to gaseous products. Oxygen rich bio-oils were formed due to the high oxygen content of cellulose and hemicellulose in the rice husk. The bio-oil compounds have also acidic property hence they cannot be directly used as transportation fuels. Further hydrothermal or catalytic upgrading can transform them into more stable compounds (Weldekidan *et al.*, 2018b). Isobutanol (7.2%), 1-dimethylvinylsilyloxy-3-methylbenzene (6.42%) and heptaethylene glycol (5.66%) were the prominent compounds produced at 500°C. As the temperature increased to 600°C, isobutanol decreased to 5.4%. Pentaethylene glycol (6.8%) was the other dominant compound at 600°C. High concentrations of isobutanol (5.73%), 1-dimethylvinylsilyloxy-3-methylbenzene (5.45%) and heptaethylene glycol (5.04%) were detected at 700°C. As the temperature further increased to 800°C, the ketone compound 1-dimethylvinylsilyloxy-3-methylbenzene (6.18%) was found to be the highest bio-oil yield.

The bio-oils obtained at 500 and 700°C can be excellent precursors for solvent production. Isobutanol with its highest concentrations of 7.2% and 5.73% at 500 and 700°C respectively, is an important industrial solvent and found in many domestic cleaning agents and paint removers. Pentaethylene glycol (6.8%) produced at 600°C can be used for detergent production while bio-oils obtained at 800°C are used by the oil and gas industry to dehydrate natural gas. As the temperature increased from 600 to 800°C lighter and less oxygenated bio-oil compounds were produced in large quantities, due to oil cracking at a higher temperature. Compounds such as triethylene glycol (6.01%) produced in large quantity at 800°C were less oxygenated than those produced at 600°C and are commonly used to dehydrate natural gas (Zeng et al., 2017) and other oxygenated compounds which need less oxygenated bio-oil compounds. For example, triethylene glycol (6.01%) produced in large quantity at 800°C is used to dehydrate gases including CO_2, H_2S and other oxygenated gases.

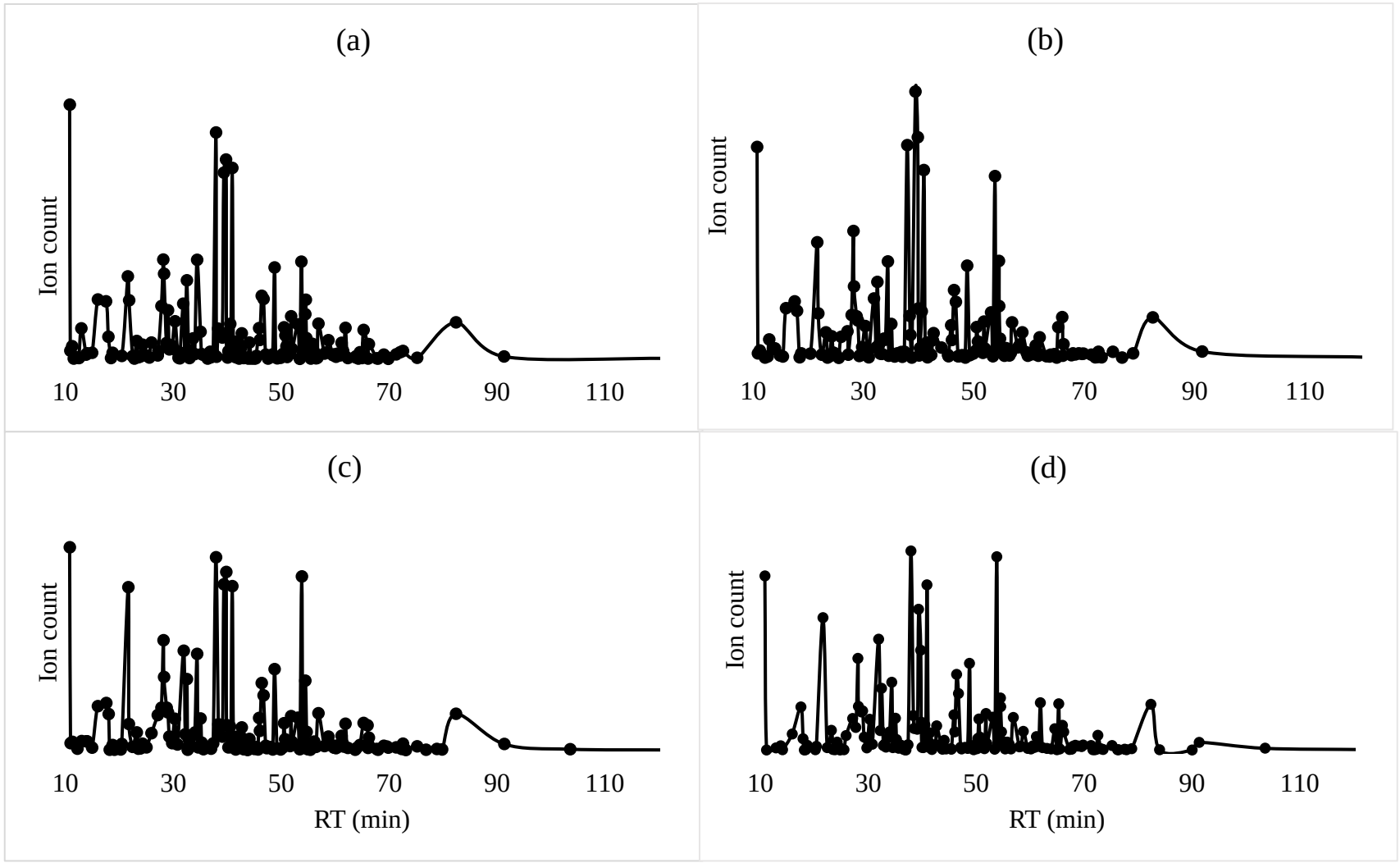

Figure 5-6 GC-MS spectra of the bio-oils from the solar pyrolysis of rice husk at (a) 500°C, (b) 600°C, (c) 700°C and (d) 800°C

Table 5-2 Major bio-oil compounds

500°C			600°C			700°C			800°C		
compound name	Formula	area%	compound name	Formula	area%	compound name	formula	area%	Compound name	Formula	area %
Isobutanol	$C_4H_{10}O$	7.2	Pentaethylene glycol	$C_{10}H_{22}O_6$	6.8	Isobutanol	$C_4H_{10}O$	5.73	1-Dimethylvinylsilyloxy-3-methylbenzene	C_8H_8O	6.18
1-Dimethylvinylsilyloxy-3-methylbenzene	C_8H_8O	6.42	Heptaethylene glycol	$C_{14}H_{30}O_8$	5.64	1-Dimethylvinylsilyloxy-3-methylbenzene	C_8H_8O	5.45	Triethylene glycol	$C_6H_{14}O_4$	6.01
Heptaethylene glycol	$C_{14}H_{30}O_8$	5.66	1-Dimethylvinylsilyloxy-3-methylbenzene	C_8H_8O	5.45	Heptaethylene glycol	$C_{14}H_{30}O_8$	5.04	Catechol	$C_6H_6O_2$	5.15
Catechol	$C_6H_6O_2$	5.42	Isobutanol	$C_4H_{10}O$	5.4	Triethylene glycol	$C_6H_{14}O_4$	4.92	Phenol	C_6H_6O	4.13
Pentaethylene glycol	$C_{10}H_{22}O_6$	5.29	Triethylene glycol	$C_6H_{14}O_4$	4.66	Pentaethylene glycol	$C_{10}H_{22}O_6$	4.69	Heptaethylene glycol	$C_{10}H_{22}O_6$	3.13
Guaiacol	$C_7H_8O_2$	2.85	Phenol	C_6H_6O	2.99	Catechol	$C_6H_6O_2$	4.64	Isobutanol	$C_4H_{10}O$	3.01
Triethylene glycol	$C_6H_{14}O_4$	2.8	Guaiacol	$C_7H_8O_2$	2.5	Phenol	C_6H_6O	4.61	Syringol	$C_8H_{10}O3$	2.39
Furfuryl alcohol	$C_5H_6O_2$	2.45	Sorbic acid	$C_6H_{14}O_2$	1.99	Guaiacol	$C_7H_8O_2$	2.75	Guaiacol	$C_7H_8O_2$	2.14
Phenol	C_6H_6O	2.38	Ethylene glycol	$C_2H_6O_2$	1.5	Sorbic acid	$C_6H_{14}O_2$	2.04	Sorbic acid	$C_6H_{14}O_2$	1.96
Levoglucosan	$C_{15}H_{18}O_5$	2.32	Hydroquinone	$C_6H_6O_2$	1.48	Syringol	$C_8H_{10}O3$	1.93	Hydroquinone	$C_6H_6O_2$	1.8
Sorbic acid	$C_6H_{14}O_2$	2.28	Vanillin	$C_8H_8O_3$	1.38	Hydroquinone	$C_6H_6O_2$	1.59	Dodecanoic acid	$C_{12}H_{24}O_2$	1.51
p-Cresol	C_7H_8O	2.11	2-Methyl-1-butanol	$C_5H_{12}O$	1.32	Ethylene glycol	$C_2H_6O_2$	1.37	Palmitic Acid	$C_{16}H_{33}O_2$	1.47
Syringol	$C_8H_{10}O3$	1.84	Furfuryl alcohol	$C_5H_6O_2$	1.26	Levoglucosan	$C_{15}H_{18}O_5$	1.32	(2,3-Dimethylbutan-2-yloxy) trimethylsilane	$C_6H_{14}O$	1.4
Hydroquinone	$C_6H_6O_2$	1.75	Hexanoic acid	$C_6H_{12}O_2$	1.13	2-Methyl-1-butanol	$C_5H_{12}O$	1.28	Ethylene glycol	$C_2H_6O_2$	1.39
2-Methyl-1-butano	$C_5H_{12}O$	1.73	p-Cresol	C_7H_8O	1.12	p-Cresol	C_7H_8O	1.24	p-Cresol	C_7H_8O	1.23
Ethylene glycol	$C_2H_6O_2$	1.69	Levoglucosan	$C_{15}H_{18}O_5$	1.1	Eugenol	$C_{10}H_{12}O$	1.08	4-Methylcatechol	$C_7H_8O_2$	1.14

(2,3-Dimethylbutan-2-yloxy) trimethylsilane	$C_6H_{14}O$	1.13	Palmitic Acid	$C_{16}H_{33}O_2$	1.09	Palmitic Acid	$C_{16}H_{33}O_2$	1.07	Eugenol	$C_{10}H_{12}O$	1.06
Palmitic Acid	$C_{16}H_{33}O_2$	1.09	Eugenol	$C_{10}H_{12}O$	0.97	Furfuryl alcohol	$C_5H_6O_2$	1.06	3-Ethylphenol	$C_8H_{10}O$	1.04
Eugenol	$C_{10}H_{12}O$	1.06	3-Ethylphenol	$C_8H_{10}O$	0.92	o-Cresol	C_7H_8O	1.03	o-Cresol	C_7H_8O	1.03
4-Hydroxybutanoic acid	$C_4H_8O_3$	1.03	4-Methylcatechol	$C_7H_8O_2$	0.89	4-Methylcatechol	$C_7H_8O_2$	0.96	2-Methylresorcinol	$C_7H_8O_2$	1.01
o-Cresol	C_7H_8O	0.98	2-Methylresorcinol	$C_7H_8O_2$	0.85	(2,3-Dimethylbutan-2-yloxy) trimethylsilane	$C_6H_{14}O$	0.93	Levoglucosan	$C_{15}H_{18}O_5$	0.89
2-Methylresorcinol	$C_7H_8O_2$	0.96	Dodecanoic acid	$C_{12}H_{24}O_2$	0.85	3-Ethylphenol	$C_8H_{10}O$	0.93	Octaethylene glycol	$C_{14}H_{30}O_8$	0.84
Dodecanoic acid,	$C_{12}H_{24}O_2$	0.94	o-Cresol	C_7H_8O	0.74	2-Methylresorcinol	$C_7H_8O_2$	0.8	Maltol	$C_6H_6O_3$	0.72
4-Methylcatechol	$C_7H_8O_2$	0.93	D-(-)-Lactic acid	$C_3H_6O_3$	0.71	Dodecanoic acid	$C_{12}H_{24}O_2$	0.79	D-(-)-Lactic acid	$C_3H_6O_3$	0.67
Hexanoic acid	$C_6H_{12}O_2$	0.92	Syringol	$C_8H_{10}O3$	0.7	Hexanoic acid	$C_6H_{12}O_2$	0.77	2-Methyl-1-butanol	$C_5H_{12}O$	0.56
3-Ethylphenol	$C_8H_{10}O$	0.83	Glycolic acid	$C_2H_4O_3$	0.62	Octaethylene glycol	$C_{14}H_{34}O_9$	0.72			
Octaethylene glycol	$C_{14}H_{34}O_9$	0.8				D-(-)-Lactic acid	$C_3H_6O_3$	0.55			
Maltol	$C_6H_6O_3$	0.71									
Vanillin	$C_8H_8O_3$	0.65									
D-(-)-Lactic acid	$C_3H_6O_3$	0.57									

5.3.4 Bio-char

5.3.4.1 SEM analysis

Fig. 5.7 Shows comparison of the SEM images of the raw husk and its bio-chars produced at different pyrolysis temperatures. As can be seen from Fig. 5.7, SEM image of the parent material (Fig. 5.7a) is composed of solid cells in a manner of plates with no visible pores, resulting in low surface area but pores of varying size and structure were generated with temperature. Large glass-like cylindrical holes were produced at 500°C (Fig. 5.7b), which indicated a large amount of organic compounds might be driven off in some particles at this temperature. For the biochar at 600°C (Fig. 5.7c) many fine pores arranged in an orderly fashion were formed. The char structure at 700°C (Fig. 5.7d) had loose and porous shape. Fine materials around the outer surface of the pores could be observed falling down and closing the pores. These materials were mainly silicon, potassium and calcium minerals as evidenced with sharp peaks in the EDS spectrum shown in Fig. 5.7. The pore structures produced at 800°C (Fig. 5.7e) were almost fused and destroyed with the minerals (silicon, potassium and calcium) which started to massively emerge at 700°C.

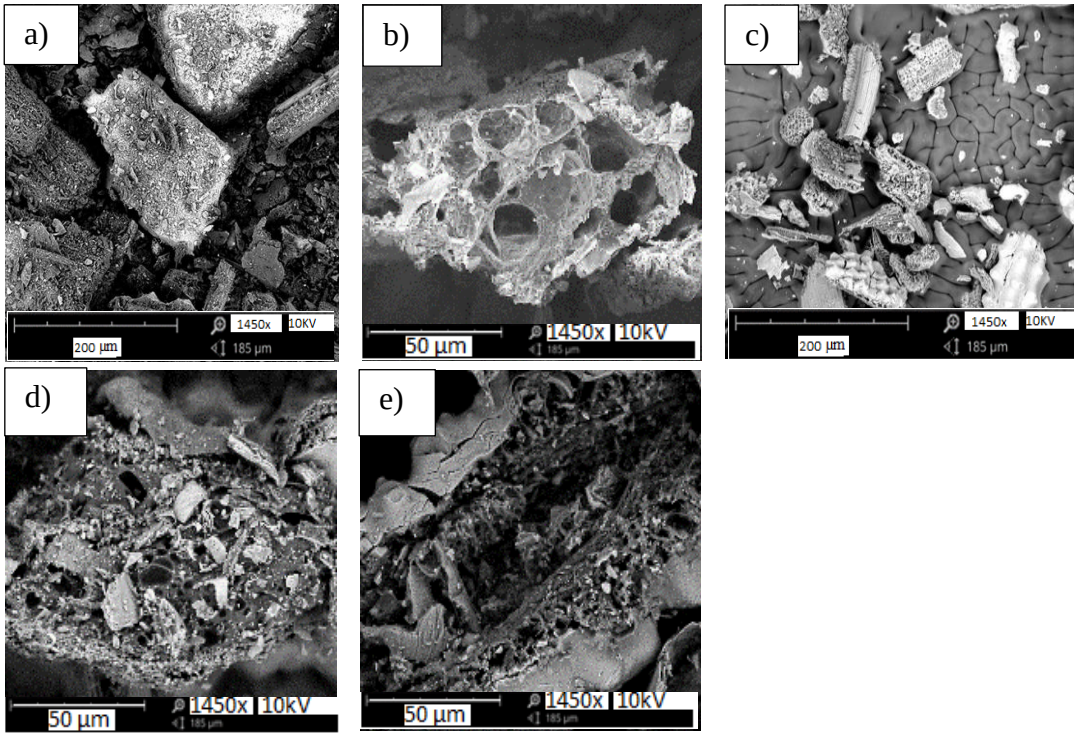

Figure 5-7 SEM images of (a) raw rice husk, (b) bio-char at 500°C, (c) bio-char at 600°C, (d) bio-char at 700°C and (e) bio-char at 800°C

5.3.4.2 EDS analysis

The EDS spectra of each bio-char are shown in Fig. 5.8. Next to carbon and oxygen, silicon was the major element in all the bio-chars with small amounts of potassium, calcium and magnesium. The highest Si concentration (12.32%) was obtained in the bio-char produced at 700°C, then with increasing the temperature spectra of metals (potassium, magnesium, calcium etc.) were observed to emerge showing enrichment of inorganic constituents in the biochar with temperature. Maximum calcium concentration (1.98%) was recorded in the 800°C bio-char, while the highest potassium concentration (2.51%) was obtained at 600°C. Overall, presence of alkali metals in the bio-chars can confirm high salt intake capacity of rice husk as compared to plant biomass which typically contains negligible amount of siliceous compounds (Muradov *et al.*, 2012).

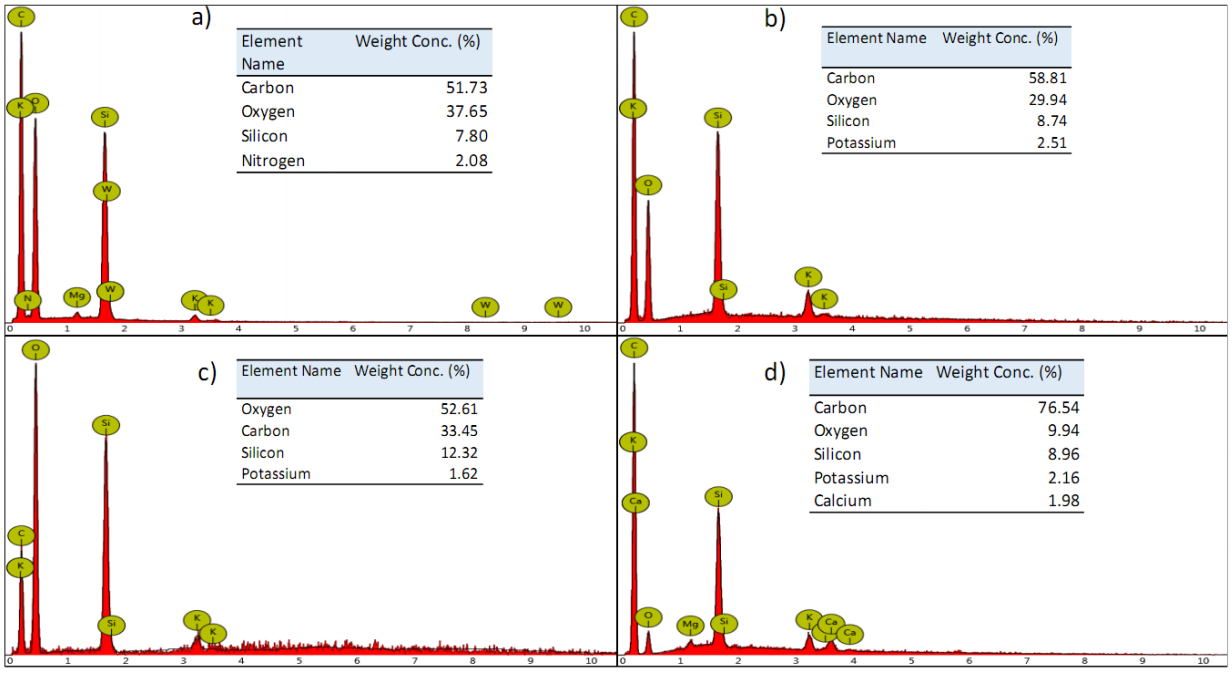

Figure 5-8 EDS analysis of bio-chars produced at (a) 500°C, (b) 600°C, (c) 700°C and (d) 800°C

5.3.4.3 FTIR analysis

The FTIR spectra of rice husk and its bio-chars generated at different pyrolysis temperature are shown in Fig. 5.9. Pyrolysis at 500°C changed many functional groups of the raw rice husk. For example, the broad band at 3324 cm^{-1} of the raw rice husk assigned to the stretching of hydrogen-bonded hydroxyl groups which indicate presence of phenols and alcohols (Claoston *et al.*, 2014) was observed to diminish with temperature and completely disappear after 600°C.

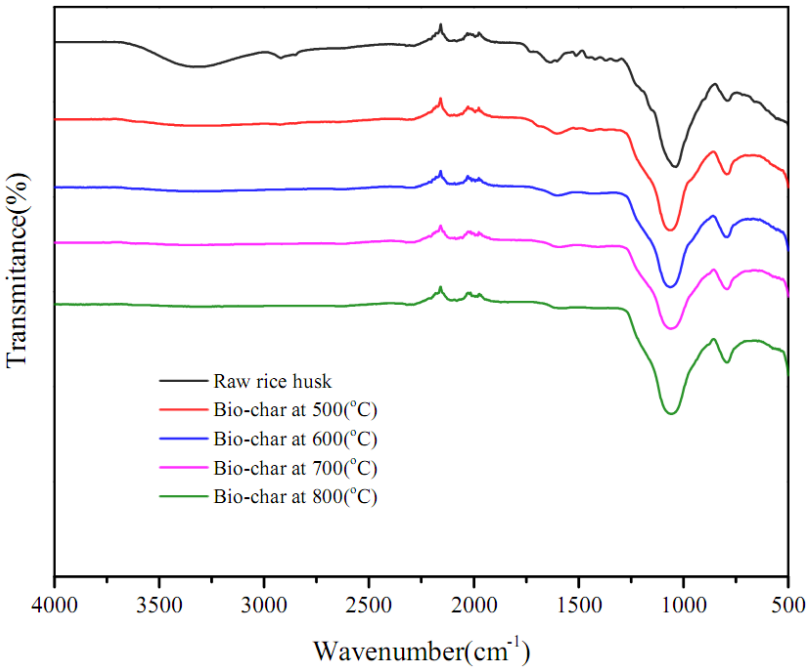

Figure 5-9 FTIR spectra of raw rice husk and bio-chars produced at different temperatures

Two of the small peaks identified at 2900 and 2845 cm^{-1} of the rice husk spectra were related to weak aliphatic C-H stretching of CH_3 and CH_2 groups respectively (Biswas *et al.*, 2017; Chintala *et al.*, 2017). Also the weak band at 1727 cm^{-1} was due to symmetric vibration of C=O from –COOH group (Umair *et al.*, 2016). The peaks shown at 1629 cm^{-1} for the raw rice husk retained C=O stretch of CO_2H and C=O primary amides (Robert *et al.*, 2005). All these peaks were removed during pyrolysis in all the bio-chars. A very sharp peak at 1051 cm^{-1} was observed in all samples. This corresponds to the stretching vibration of Si-O-Si bridges in SiO_x and the relatively weak band at 784 cm^{-1} observed in all samples is related to inorganic species and silica (Muradov *et al.*, 2012; Vasquez-A *et al.*, 2007). The results observed with the FTIR analysis are consistent with the results from the EDS analysis. As observed from the FTIR spectra, the bio-chars produced at 600, 700 and 800°C have the same functional groups.

5.4 Conclusion

A parabolic dish with maximum heat flux concentrating capacity of 70 kW/m^2, was used to generate pyrolysis temperatures of 500, 600, 700 and 800°C on biomass loaded reactor. The highest gas, bio-oil and bio-char yields were found to be 25.48 wt.% at 800°C, 43.13 wt. % at 700°C and 43 wt.% at 500°C, respectively. CO_2, CO, CH_4 and H_2 were the dominant gas species evolved at higher contents at each pyrolysis temperature. HHV of the evolved pyrolysis gas was above 197 kJ/kg which makes it suitable candidate for heat and power generation in gas turbines while generated bio-oils were found to be excellent precursors for solvent and

detergent productions. Presence of calcium (1.98 %, maximum) and potassium (2.51 %, maximum) metals in the bio-chars confirm high salt intake capacity of rice husk.

5.5 References

Ahmad, A. A., Zawawi, N. A., Kasim, F. H., Inayat, A., & Khasri, A. (2016). Assessing the gasification performance of biomass: A review on biomass gasification process conditions, optimization and economic evaluation. *Renewable & Sustainable Energy Reviews, 53*, 1333-1347.

Bait, O., & Si-Ameur, M. (2017). Tubular solar-energy collector integration: Performance enhancement of classical distillation unit. *Energy, 141*, 818-838.

Biswas, B., Pandey, N., Bisht, Y., Singh, R., Kumar, J., & Bhaskar, T. (2017). Pyrolysis of agricultural biomass residues: Comparative study of corn cob, wheat straw, rice straw and rice husk. *Bioresource Technology, 237*, 57-63.

Chintala, V., Kumar, S., Pandey, J. K., Sharma, A. K., & Kumar, S. (2017). Solar thermal pyrolysis of non-edible seeds to biofuels and their feasibility assessment. *Energy Conversion and Management, 153*, 482-492.

Ciampi, G., Rosato, A., & Sibilio, S. (2018). Thermo-economic sensitivity analysis by dynamic simulations of a small Italian solar district heating system with a seasonal borehole thermal energy storage. *Energy, 143*, 757-771.

Claoston, N., Samsuri, A. W., Husni, M. H. A., & Amran, M. S. M. (2014). Effects of pyrolysis temperature on the physicochemical properties of empty fruit bunch and rice husk biochars. *Waste Management & Research, 32*(4), 331-339.

Dunnigan, L., Ashman, P. J., Zhang, X., & Kwong, C. W. (2018). Production of biochar from rice husk: Particulate emissions from the combustion of raw pyrolysis volatiles. *Journal of Cleaner Production, 172*, 1639-1645.

Ekman, B. M., Brooks, G., & Rhamdhani, M. A. (2015). Development of high flux solar simulators for solar thermal research. *Solar Energy Materials and Solar Cells, 141*, 436-446.

Gani, A., & Naruse, I. (2007). Effect of cellulose and lignin content on pyrolysis and combustion characteristics for several types of biomass. *Renewable Energy, 32*(4), 649-661.

Kan, T., Grierson, S., de Nys, R., & Strezov, V. (2014). Comparative Assessment of the Thermochemical Conversion of Freshwater and Marine Micro- and Macroalgae. *Energy & Fuels, 28*(1), 104-114.

Kan, T., Strezov, V., & Evans, T. (2017). Fuel production from pyrolysis of natural and synthetic rubbers. *Fuel, 191*, 403-410.

Khan, M. S., & Crynes, B. L. (1970). Survey of Recent Methane Pyrolysis Literature. *Industrial & Engineering Chemistry, 62*(10), 54-59.

Kirkels, A. F. (2012). Discursive shifts in energy from biomass: A 30 year European overview. *Renewable & Sustainable Energy Reviews, 16*(6), 4105-4115.

Kumar, R., & Kumar, P. (2017). Future Microbial Applications for Bioenergy Production: A Perspective. *Frontiers in Microbiology, 8*(450).

Kumar, R., Singh, L., & Zularisam, A. W. (2016). Exoelectrogens: Recent advances in molecular drivers involved in extracellular electron transfer and strategies used to improve it for microbial fuel cell applications. *Renewable and Sustainable Energy Reviews, 56*, 1322-1336.

Lars, W., & Nilsson, T. (2001). *Heating value of gases from biomass gasification. A report prepared for: IEA Bioenergy Agreement, Task 20 - Thermal Gasification of Biomass, Nyköping, Sweden*. Retrieved from www.ieatask33.org/app/webroot/files/file/publications/HeatingValue.pdf+&cd=1&hl=en&ct=clnk&gl=au

Li, Q., Zheng, C., Mesgari, S., Hewkuruppu, Y. L., Hjerrild, N., Crisostomo, F., . . . Taylor, R. A. (2016). Experimental and numerical investigation of volumetric versus surface solar absorbers for a concentrated solar thermal collector. *Solar Energy, 136*, 349-364.

Li, Z. Y., Jiang, E. C., Xu, X. W., Sun, Y., & Wu, Z. X. (2017). The complete utilization of rice husk for production of synthesis gas. *Rsc Advances, 7*(53), 33532-33543.

Lim, J. S., Manan, Z. A., Alwi, S. R. W., & Hashim, H. (2012). A review on utilisation of biomass from rice industry as a source of renewable energy. *Renewable & Sustainable Energy Reviews, 16*(5), 3084-3094.

Liu, P., Zhao, Y., Guo, Y., Feng, D., Wu, J., Wang, P., & Sun, S. (2016). Effects of volatile–char interactions on char during pyrolysis of rice husk at mild temperatures. *Bioresource Technology, 219*, 702-709.

Lohmann, S., Schillings, C., Mayer, B., & Meyer, R. (2006). Long-term variability of solar direct and global radiation derived from ISCCP data and comparison with reanalysis data. *Solar Energy, 80*(11), 1390-1401.

Martinopoulos, G., & Tsalikis, G. (2018). Diffusion and adoption of solar energy conversion systems - The case of Greece. *Energy, 144*, 800-807.

Muradov, N., Fidalgo, B., Gujar, A. C., Garceau, N., & T-Raissi, A. (2012). Production and characterization of Lemna minor bio-char and its catalytic application for biogas reforming. *Biomass and Bioenergy, 42*, 123-131.

Naqvi, S. R., Uemura, Y., & Yusup, S. B. (2014). Catalytic pyrolysis of paddy husk in a drop type pyrolyzer for bio-oil production: The role of temperature and catalyst. *Journal of Analytical and Applied Pyrolysis, 106*, 57-62.

Opatokun, S. A., Kan, T., Al Shoaibi, A., Srinivasakannan, C., & Strezov, V. (2016). Characterization of Food Waste and Its Digestate as Feedstock for Thermochemical Processing. *Energy & Fuels, 30*(3), 1589-1597.

Pottmaier, D., Costa, M., Farrow, T., Oliveira, A. A. M., Alarcon, O., & Snape, C. (2013). Comparison of Rice Husk and Wheat Straw: From Slow and Fast Pyrolysis to Char Combustion. *Energy & Fuels, 27*(11), 7115-7125.

Robert, S., Francis, W., & David, K. (2005). *Spectrometric identification of organic compounds*. New York, USA: John Wiley & Sons.

Strezov, V., Popovic, E., Filkoski, R. V., Shah, P., & Evans, T. (2012). Assessment of the Thermal Processing Behavior of Tobacco Waste. *Energy & Fuels, 26*(9), 5930-5935.

Suzana Y., Yiin C. L, Tan C. J., & Bawadi A. (2016). Determination of optimum condition for the production of rice husk-derived bio-oil by slow pyrolysis process *Process Design Strategies for Biomass Conversion Systems* (First ed., pp. 329-340). Tronoh, Malaysia: John Wiley & Sons, Ltd.

Tsai, W. T., Lee, M. K., & Chang, Y. M. (2007). Fast pyrolysis of rice husk: Product yields and compositions. *Bioresource Technology, 98*(1), 22-28.

Umair, M. M., Jiang, Z. M., Ullah, N., Safdar, W., Xie, Z. W., & Ren, X. H. (2016). Development and characterisation of antibacterial suture functionalised with N-halamines. *Journal of Industrial Textiles, 46*(1), 59-74.

Vasquez-A, M. A., Rodriguez, G. A., Garcia-Salgado, G., Romero-Paredes, G., & Pena-Sierra, R. (2007). FTIR and photoluminescence studies of porous silicon layers oxidized in controlled water vapor conditions. *Revista Mexicana De Fisica, 53*(6), 431-435.

Weldekidan, H., Strezov, V., & Town, G. (2018a). Review of solar energy for biofuel extraction. *Renewable and Sustainable Energy Reviews, 88*, 184-192.

Weldekidan, H., Strezov, V., Kan, T., & Town, G. (2018b). Waste to Energy Conversion of Chicken Litter through a Solar-Driven Pyrolysis Process. *Energy & Fuels, 32*(4), 4341-4349.

Weldekidan, H., Strezov, V., & Town, G. (2017). Performance evaluation of absorber reactors for solar fuel production. *Chemical engineering transaction, 61*, 1111-1116.

Wendelin, T. (2013). *SolTrace: A Ray-Tracing Code for Complex Solar Optical Systems*. Retrieved from Colorado, U.S.: http://www.osti.gov/bridge

Williams, P. T., & Nugranad, N. (2000). Comparison of products from the pyrolysis and catalytic pyrolysis of rice husks. *Energy, 25*(6), 493-513.

Yu, Y., Yang, Y., Cheng, Z. C., Blanco, P. H., Liu, R. H., Bridgwater, A. V., & Cai, J. M. (2016). Pyrolysis of Rice Husk and Corn Stalk in Auger Reactor. 1. Characterization of Char and Gas at Various Temperatures. *Energy & Fuels, 30*(12), 10568-10574.

Yue, L., Li, G., He, G., Guo, Y., Xu, L., & Fang, W. (2016). Impacts of hydrogen to carbon ratio (H/C) on fundamental properties and supercritical cracking performance of hydrocarbon fuels. *Chemical Engineering Journal, 283*(Supplement C), 1216-1223.

Zeng, K., Gauthier, D., Li, R., & Flamant, G. (2015). Solar pyrolysis of beech wood: Effects of pyrolysis parameters on the product distribution and gas product composition. *Energy, 93*, 1648-1657.

Zeng, K., Gauthier, D., Li, R., & Flamant, G. (2017). Combined effects of initial water content and heating parameters on solar pyrolysis of beech wood. *Energy, 125*, 552-561.

Zhang, Z., Liu, J., Shen, F. H., Yang, Y. J., & Liu, F. (2016a). On-line measurement and kinetic studies of sodium release during biomass gasification and pyrolysis. Fuel, 178, 202-208.

Zhang, S., Dong, Q., Zhang, L., & Xiong, Y. (2016b). Effects of water washing and torrefaction on the pyrolysis behavior and kinetics of rice husk through TGA and Py-GC/MS. *Bioresource Technology, 199*, 352-361.

Zhao, Y., Kamiya, K., Hashimoto, K., & Nakanishi, S. (2015). In Situ CO2-Emission Assisted Synthesis of Molybdenum Carbonitride Nanomaterial as Hydrogen Evolution Electrocatalyst. *Journal of the American Chemical Society, 137*(1), 110-113.

Zhou, L. Y., Yang, H. M., Wu, H., Wang, M., & Cheng, D. Q. (2013). Catalytic pyrolysis of rice husk by mixing with zinc oxide: Characterization of bio-oil and its rheological behavior. *Fuel Processing Technology*, *106*, 385-391.

Chapter 6: Solar assisted catalytic pyrolysis of chicken-litter waste with in-situ and ex-situ loading of CaO and char

It was observed that biomass pyrolysis with concentrated solar radiation produces pyrolytic gas highly concentrated with CO_2. The bio-oil compounds were also oxygenated and were acidic property hence they cannot be directly used as transportation fuels. This chapter presents ways of improving quality of pyrolysis gas and bio-oil compounds achieved from the solar pyrolysis of chicken-litter waste. Experiments were designed and conduct to assess the effects of char and CaO catalysts on the yield and composition of pyrolysis products. The catalysts are loaded with the biomass in the solar reactor in different ratio and modes.

This project has been primarily initiated by myself. I together with Vlad designed the experiments. All experiments and data collection were performed by myself. My colleague Ravi has participated in analysing the bio-oil data and Vlad, Tao, Graham and Jing reviewed and edited the manuscript for publication.

Authors' contribution summary for this paper

	W. H.	S. V.	T. G.	K. T.	K. R.	H. G.
Experiment Design	•					
Sample Preparation	•					
Data Collection	•					
Analysis	•	•			•	
Manuscript	•	•	•	•	•	•

Publication:

Weldekidan, H. (70%), Strezov, V. (5%), Kan, T. (5%), Kumar, R. (15%), He, J. (2.5%) and Town, G. (2.5%). "Solar assisted catalytic pyrolysis of chicken-litter waste with in-situ and ex-situ loading of CaO and char", ***Fuel (2019), 246: 408-416.***

Adopted for this thesis with the exclusive rights from Elsevier.

Solar assisted catalytic pyrolysis of chicken-litter waste with *in-situ* and *ex-situ* loading of CaO and char

Haftom Weldekidan[1], Vladimir Strezov[1], Tao Kan[1]*, Ravinder Kumar[1], Jing He[1] and Graham Town[2]*

[1] Department of Environmental Sciences, Macquarie University, Sydney, NSW 2109, Australia

[2] School of Engineering, Macquarie University, Sydney, NSW 2109, Australia

* To whom correspondence should be addressed:

Tel: +612-9850-6959

Fax: +612-9850-7972

E-mail address: vladimir.strezov@mq.edu.au; tao.kan@mq.edu.au

Abstract

Utilisation of solar energy for thermochemical conversion of biomass can facilitate sustainable development of society by reducing greenhouse gas (GHG) emissions which originate from excessive use of conventional sources of energy. In this work, gas and liquid fuels obtained from solar assisted pyrolysis of chicken-litter waste were upgraded using CaO and char catalysts. The catalysts were loaded in the solar reactor in an *in-situ* and *ex-situ* modes at different catalyst to biomass ratios. In both cases there was substantial decrease in CO_2 accompanied by an increase in the formation of CO and H_2 with temperature and catalyst to biomass ratio. The *in-situ* pyrolysis with 50% CaO loading exhibited maximum CO (63 wt. %) and H_2 (15 wt. %) yields at 800°C. Similarly, the *in-situ* pyrolysis with 50% char catalyst produced 60 wt. % CO and 5 wt. % H_2. The addition of CaO exhibited considerable deoxygenation performance for the fatty acids. Minimum concentration of fatty acids in the liquid product achieved with 50% CaO in the *in-situ* and *ex-situ* pyrolysis were 8% and 3%, respectively. On the other hand, the addition of char did not show significant deoxygenation difference for either the alcohols or fatty acids of the bio-oil compounds.

Keywords: solar fuels, deoxygenation, catalytic pyrolysis, CO_2 capture, solar radiation

6.1 Introduction

Biomass has been recognized as one of the most suitable substitutes of fossil fuels for its carbon neutrality, low cost, high availability and renewability. Every year significant amounts of biomass are produced from agricultural, municipal and forest residues, most of which are only burned or left over in an open field. Valorisation of biomass through energy recovery processes provides advanced solutions by generating useful energy, while sustainably solving the disposal and environmental management challenges (Weldekidan *et al.*, 2018a).

Pyrolysis, a process where the biomass is exposed to temperatures generally ranging from 300 to 900°C in an inert gas, has been considered as one of the most economical pathways to produce chemicals and fuels (Hallenbeck *et al.*, 2016; Wan *et al.*, 2013). Depending on the operating conditions and source of heat supply, the pyrolysis process can generally be categorised into conventional pyrolysis and solar assisted pyrolysis. In the conventional pyrolysis, the heat is supplied from fossil derived sources or from combusting the biomass itself, whereas in the solar assisted pyrolysis the heat is supplied from concentrated solar radiation which reduces pollution discharge to the environment (Bai *et al.*, 2017). Besides, compared with conventional pyrolysis, the solar assisted pyrolysis can provide several other benefits. Products obtained from solar pyrolysis are not contaminated with pyrolysis by-products (Nzihou *et al.*, 2012). High temperatures and fast heating rates are typically achieved with solar pyrolysis, which enable production of pyrolysis gas products with higher caloric value than from conventional pyrolysis (Tanaka *et al.*, 2015; Zeng *et al.*, 2017).

Bio-gas is one of the important products of solar pyrolysis of chicken litter which can be further utilised for heat supply and power generation (Weldekidan *et al.*, 2018b). However, the process was found to generate significant CO_2 yields and contributes to formation of oxygenated liquid bio-fuels. Catalytic pyrolysis can improve the quality of pyrolysis products and the overall energy efficiency of the solar pyrolysis system (Udomsirichakorn *et al.*, 2014). Catalysts and/or absorbents can be directly added to biomass (*in-situ*) in the solar reactor, or downstream of the biomass (*ex-situ*) to minimise the CO_2 production and also deoxygenate the bio-oils, eventually upgrading the quality of pyrolysis products (Liu *et al.*, 2014). Loading catalyst with the biomass can catalyze the pyrolysis oil vapors and gas shortly after their generation from the biomass. In addition, catalyst loading with biomass offers solution to upgrade pyrolysis products by reducing the oxygen content during pyrolysis, which contributes to lower cost during subsequent bio-oil improvement (Zhang *et al.*, 2016). In-situ catalytic pyrolysis can generate

more aromatic hydrocarbons than ex-situ, producing higher olefin content, which is a preferred product (Kaige Wang *et al.*, 2014). High oxygen content leads to decreased energy density and catalytic deoxygenation is the most effective way to reduce oxygen content of the pyrolysis products (Muley *et al.*, 2016).

Application of CaO as a catalyst or CO_2 sorbent has currently gained significant attention for its abundance and low cost (Udomsirichakorn *et al.*, 2014). CaO can be extracted from naturally occurring substances, such as dolomite, limestone and calcium hydroxide at low cost. CaO has the capacity to scavenge CO_2 to very low concentrations at moderate pyrolysis temperatures (450–750°C) (Florin & Harris, 2008). Evolved CO_2 from biomass pyrolysis could be captured with CaO to form stable solid species of $CaCO_3$ following the carbonation reaction equation (1) (Florin & Harris, 2008).

$$CaO\ (s) + CO_2 \rightarrow CaCO_3\ (s), \quad \Delta H^{\circ}_{923} = -170.5\ kJ \qquad \text{(exothermic)} \qquad (1)$$

Equation (1) is a reversible reaction hence when CaO reaches its ultimate conversion capacity, it can be regenerated by heating $CaCO_3$ at 700-950°C. The reverse reaction, called calcination, is an endothermic reaction but the carbonation is exothermic reaction which can compensate the heat energy consumed in the calcination of $CaCO_3$ (Florin & Harris, 2008). CaO can play vital role of not only producing the CO_2 sorbent, but also acting as a tar reforming catalyst which enhances total gas and hydrogen yields (Han *et al.*, 2011). The main function of CaO is to deoxygenate the bio-oil by extracting or fixing the active compounds similar to CO_2 or also termed as active quasi-CO_2 intermediates by liquid-solid contact during pyrolysis of biomass, rather than gas-solid reaction and promote dehydration reactions during the pyrolysis process. Previous studies have successfully shown decreased cumulative amount of CO_2 in the presence of CaO (Wang *et al.*, 2010). These studies also reported significant decrease in the content of carboxylic acids, which was attributed to the reaction of the acid compounds or their precursors with CaO (Lin *et al.*, 2010).

Another important material considered as an alternative to remove tar and also CO_2 from pyrolysis gases is bio-char. Bio-chars are derived from biomass pyrolysis at selected temperatures and can act as a catalyst or support structure due to their highly porous structure. They can be applied for tar conversion and CO_2 reduction in biomass pyrolysis (Shen, 2015). Besides, bio-chars typically contain metals, such as calcium, potassium, iron, magnesium and

other, which may increase the rate of deoxygenation reactions of biomass degradation during pyrolysis (Shen, 2015).

The use of char as catalyst in biomass pyrolysis has been investigated by different authors. Pine wood sample pyrolysed with its own char at 700°C was found to improve the yields of H_2 by 3.9 and CO by 1.2 times as high as those obtained without the char (Sun *et al.*, 2011). Al-Rahbi *et al.* (2016) applied tyre derived char catalyst in the pyrolysis of waste wood at 600–800°C and increasing the percentage of the char from 50 to 75 % increased the content of CO from 27 to 35 vol. % while decreased the CO_2 yield from 27 to 22 vol. %. Another study conducted on the gasification of different types of biomass at 600 to 900°C using cotton char as a catalyst produced 81.9 wt. % H_2 and it was suggested that the highest catalytic effect of the char was due to the presence of alkali and alkaline earth metals in the char (Yao *et al.*, 2016).

The effects of different types of catalysts on the conventional pyrolysis have been extensively investigated in the past. However, only limited studies investigated the adsorption and catalytic behavior of CaO and bio-chars in the solar assisted pyrolysis processes (Hu *et al.*, 2015). Solar energy is used to heat the sample in the pyrolysis process and its photocatalytic role in pyrolysis is yet to be testified, but CaO based catalysts have visible light driven photocatalytic activity and property for degradation and reduction of dyes and organic compounds (Kornprobst & Plank, 2012; Song & Zhang, 2010). CaO was found to be more effective than NiO-CaO in degrading organic materials when exposed to light (Song *et al.*, 2009). Similarly, studies are indicating that bio-chars can promote photocatalytic activity of elements found in biomass during pyrolysis. A recent study by Mian and Liu (2018) reviewed progress of bio-char supported photocatalysts and revealed that incorporation of bio-chars in biomass pyrolysis is an effective way to produce high grade products. Overall, the mechanisms of CaO and bio-char as catalysts and the application of their photocatalytic attributes in the complex system of biomass pyrolysis are under investigation. However, the combination of biomass pyrolysis in the presence of CaO and bio-char with concentrated light irradiation could bring about strong research interests.

In this work chicken-litter waste was pyrolysed in a reactor heated by solar radiation to temperatures between 500 and 800°C. The paper aims to enhance the quality of pyrolysis gases by removing produced CO_2 during the process using CaO and bio-char respectively as *in-situ* and *ex-situ* catalysts. The bio-char used in this research was residual char from pyrolysis of chicken-litter waste where the char properties were determined by the pyrolysis conditions.

The effect of biomass to catalyst ratio on the pyrolysis gas composition and bio-oil products are studied to understand the performance of the catalysts under concentrated solar radiation. Pyrolysis of chicken-litter waste and rice husk were studied without any catalyst previously by the same authors; while the current paper aimed at reducing concentration of CO_2 from the pyrolysis gases and deoxygenation of the bio-oil compounds, applied different types of catalyst in different arrangements. Moreover, performance the catalysts under the solar conditions was thoroughly investigated in this paper.

6.2 Materials and methods

6.2.1 Sample preparation

Chicken-litter waste was collected from Sydney, Australia, dried in a vacuum oven for 2 hours at 70°C, 80 kPa, then pulverized and sieved with 280 µm sieve. Proximate and ultimate analyses of the chicken-litter waste, determined according to Weldekidan *et al.*, (2018c), are shown in Table 6-1.

6.2.2 Catalyst preparation and characterization

Pure CaO powder with particle size less than 160 nm and average density 3.3 g/mL was purchased from Sigma-Aldrich and used as received while the bio-char was prepared by pyrolysis of chicken-litter at 80°C/min to the maximum temperature of 500°C.

X-ray diffraction (XRD) (PANalytical X'Pert Pro MPD X-ray diffractometer, Netherlands) analysis was employed to study the fresh and used CaO and char. The radiation source used was CuKα with X-ray generator tube operating at 45 kV and 40 mA. Samples were scanned in the Bragg angle (2θ) range of 10 to 90° with a scanning rate of 25 s per step. The char catalyst and its parental feedstock (chicken litter) were further studied for their metallic concentration using a handheld X-ray fluorescence (XRF) analyser (Olympus Delta Pro, Japan) with tantalum anode X-ray tube and results are presented in Table 6-2.

Table 6-1 Proximate and ultimate analysis of chicken-litter waste.

Proximate analysis				Ultimate analysis				
Ash	Volatile matter	Fixed carbon	Moisture	C	H	O*	N	S
% mass, dry basis			%mass	% mass, ash free				
27.1	62.6	10.3	9.9	46.9	5.4	42.02	5.36	0.32

* By difference

Table 6-2 Concentrations of elements in the raw biomass and char measured with XRF

Feedstock	Element concentrations (mg/kg)									
	P	S	K	Ca	Cr	Mn	Fe	Cu	Zn	Pb
Raw chicken litter	17185	1155	24033	83045	8	430	2345	49	361	7
Catalytic char	73289	1496	62642	197425	20	813	5176	217	765	16

For the *in-situ* pyrolysis, samples were prepared by mechanically mixing each catalyst with the chicken-litter at 15%, 25% and 50 wt.% ratios. In the *ex-situ* pyrolysis the same catalyst and ratios were used. The catalyst to biomass ratios were selected to understand the catalytic performance of the catalysts at these three ranges of catalyst to biomass ratio. Selection of catalyst to biomass ratio was based on previous literatures. For example Balasundram *et al.* (2018); Hernando *et al.* (2016); Imran *et al.* (2016); and Paasikallio *et al.* (2017) applied catalyst to biomass ratios greater than 50% and found significant improvements in the quality of their pyrolysis products. Hence, the experiments at 50% catalyst loading, were conducted to investigate the effect of high catalyst to biomass ratio to the products of biomass pyrolysis under the solar conditions.

Although char and CaO catalyst are known to improve the formation of CO and different hydrocarbons through decarbonylation reaction, the optimum ratio by which these catalysts perform under the solar pyrolysis process has not been investigated in the past. The optimum catalytic activity of the two catalysts between these three ratios has not been studied yet in the solar assisted pyrolysis process. The catalyst was positioned downstream of the biomass and was separated from the biomass by a thin layer of quartz wool. The produced volatiles passed through the catalyst to reduce the oxygenated compounds.

6.2.3 Solar setup and analytical instruments

6.2.3.1 Solar setup

Parabolic dish with aperture diameter and focal length at 1.8 m and 0.655 m respectively was used to concentrate the solar radiation. The dish was laminated with 88% reflective aluminum polyethylene terephthalate. A silica glass reactor tube with 35 cm in length and 13 mm in diameter was loaded with around 100 mg of sample and placed at the focal region of the dish. The sample was packed in the center of the reactor and positioned with quartz wool at both

ends. One end of the reactor was connected to an argon carrier gas, flowing at 85 mL/min, while the other end to an ice chamber which was used to trap the water, tar and other heavy organics. The ice chamber was attached to Tedlar® gas bag where the pyrolysis gases were collected, and the bio-oils were captured by glass wool and then collected by washing with dichloromethane (DCM) solvent. Sample temperature was measured with K-type thermocouple attached to TC-08 data logger with USB serial interface and PicoLog logging software installed in a computer. Fig. 6.1 shows schematic presentation of the solar experimental setup.

6.2.3.2 Temperature control

The dish was mounted on a rotating structure used for adjusting the height and azimuth angles of the sun. A thin stick-road was welded to the dish to make a shadow falling on the dish surface, which was used to control the temperature. The collector was first calibrated for its maximum performing position with length and direction of the stick shadow marked for reference. To control the temperature during the pyrolysis process, the dish was adjusted so that the shadow of the stick could always fall at the marked reference. When the sample temperature reached the target value, the dish could be rotated to offset the sun, which instantly dropped sample temperature to the ambient. To maintain constant heating rate, all experiments were conducted at the same radiation (700–720 W/m^2) levels. Fig. 6.2 shows variation of the temperature with time during the experiments. Samples were heated to final temperatures of 500, 600, 700 and 800°C with an average heating rate of 160 $\pm$ 6°C/min and kept at each final temperature for a maximum of 4 min to complete the reaction.

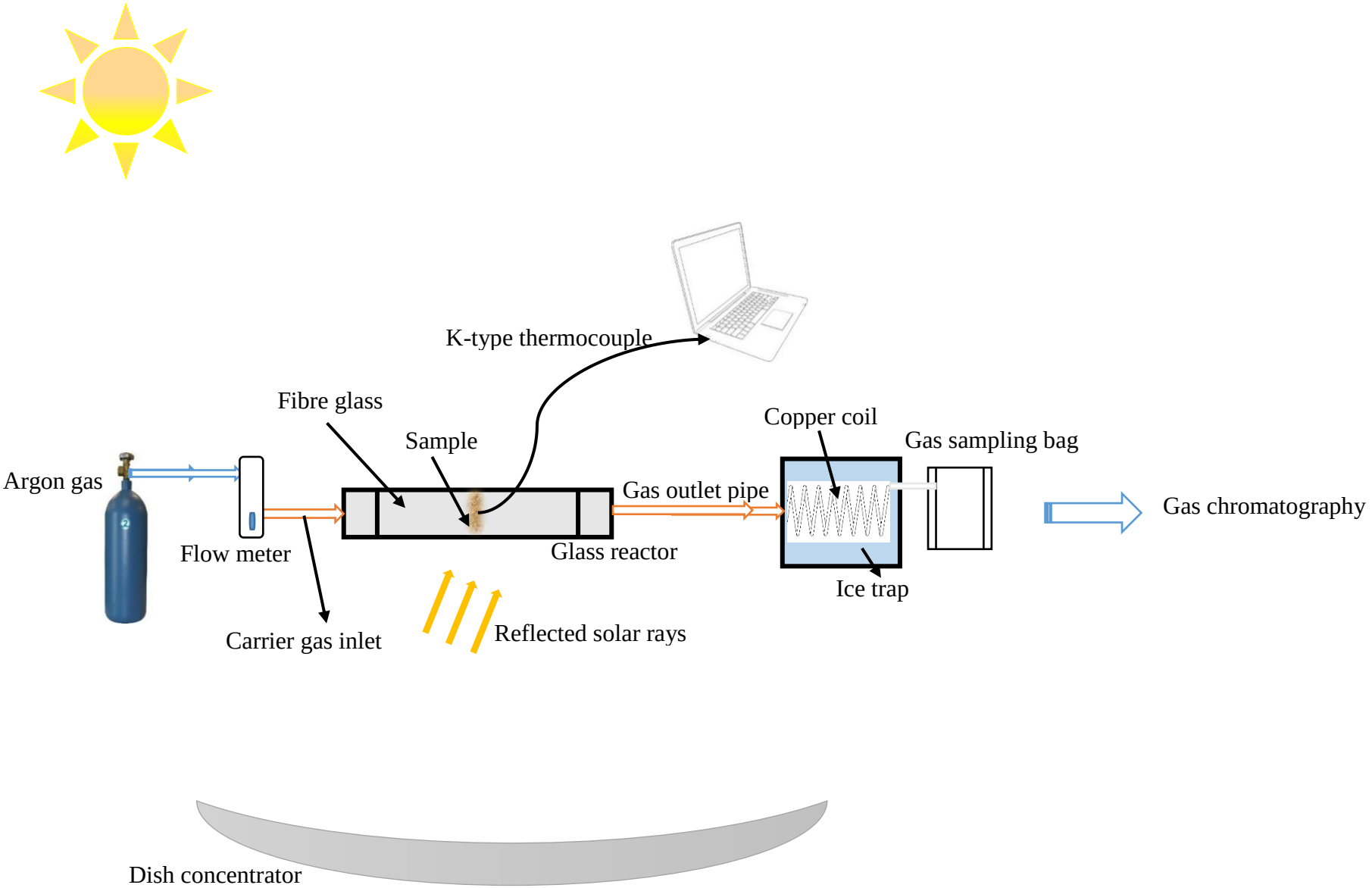

Figure 6-1 Schematic of the experimental setup (Weldekidan *et al.*, 2018c)

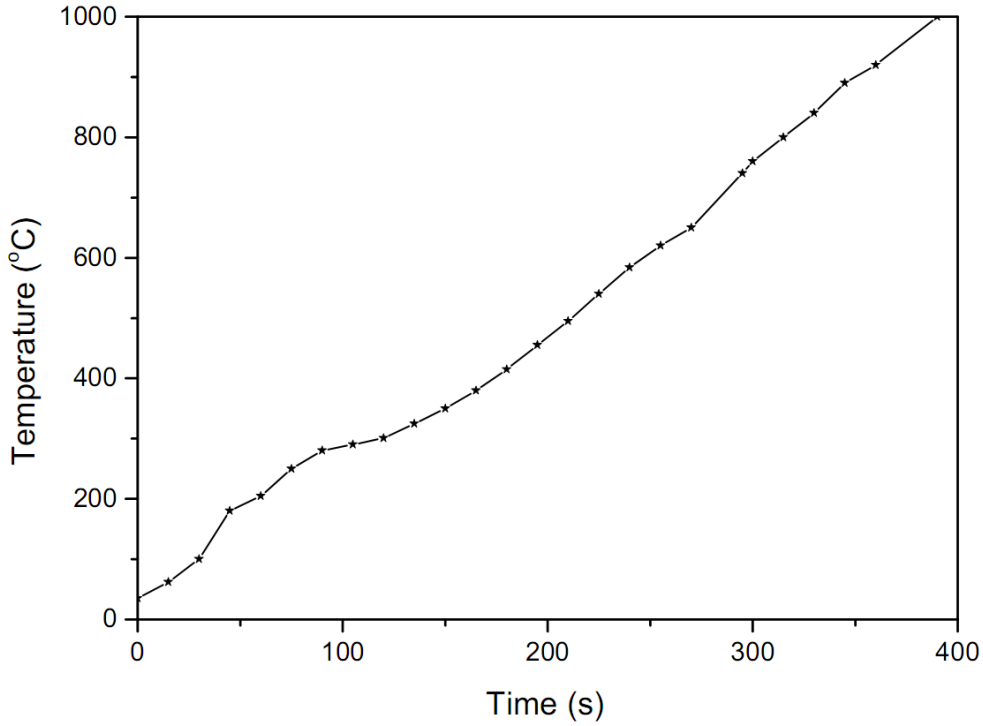

Figure 6-2 Temperature variation of the reactor as a function of time

6.2.3.3 Gas analysis

Pyrolysis gases from different pyrolysis temperatures were analysed by M200 micro-gas chromatograph. The micro-GC has two channels: Channel A, a polymer paraplot U column maintained at 40°C to analyse CO_2, CH_4, C_2H_4 and C_2H_6, and Channel B, column molecular sieve of 5A kept at 60°C, to separate H_2 and CO products. Chromatograms were recorded every 100 s using thermal conductivity detector (TCD). Volumes of each pyrolysis gases were quantified from standard mix gases of known concentrations and then converted to weight percent of the initial sample mass based on the ideal gas low. More details on the gas analysis can be found in a previous work at (Strezov *et al.*, 2012).

6.2.3.4 Bio-oil analysis

Bio-oils produced from the *in-situ* and *ex-situ* catalytic pyrolysis at 800°C were washed with dichloromethane (DCM) solvent, filtered with glass wool for removal of impurities and dehydrated with Na_2SO_4. To improve separation and thermal stability during analysis, the solution was derivatised by N,O-bis(trimethylsilyl) trifluoroacetamide with 1% trimethylchlorosilane (BSTFA + 1% TMCS) before injecting into the GC-MS. Agilent 7890B gas chromatography equipped with HP-5MS column (60 m × 0.25 µm) connected to 5977A mass spectrometry system was employed to analyse the bio-oil compounds. Oven temperature

of the GC stayed initially at 40°C for 2 min then increased to 310°C at 2°C/min. The quadruple mass spectrometer temperature was kept at 150°C while temperatures of the transfer line and mass spectrometer detector were set to 310°C. MassHunter software was applied to analyse the compounds with match factor for the database set to over 80. The peak area of each identified compound was calculated and presented in the results.

6.3 Result and discussion

6.3.1 Catalyst properties

The XRD analysis of spent and fresh catalysts of CaO and char are shown in Fig. 6.3. No significant changes were observed in the XRD patterns of the fresh and spent catalysts, revealing retention of framework structure throughout the reaction. The XRD results of the fresh and used CaO showed peaks at 32.1°, 37.6°, 59.9°, 64.2° and 674° with lattice parameters agreeing well with the corresponding standard values given in JCPDS PDF# 82-121690 (CaO). All spent CaO catalysts have small diffraction peaks around 29° due to the leftover $CaCO_3$ compounds produced during the endothermic forward reactions. Similarly, the XRD patterns of the fresh and used char catalysts were similar to each other. It can be seen that the intensive peak at $2\theta = 29.62°$ indicated presence of calcite/limestone ($CaCO_3$, ASTM 46-1045). Calcium was the highest detected element in the chicken litter derived bio-char, hence the presence of $CaCO_3$ in the XRD result is consistent with the XRF result shown in Table 6-2. The spent and fresh char catalysts have a number of peaks at 26.6° and from 32 to 62° which belong to potassium chloride and calcium magnesium iron hydrogen phosphate, respectively.

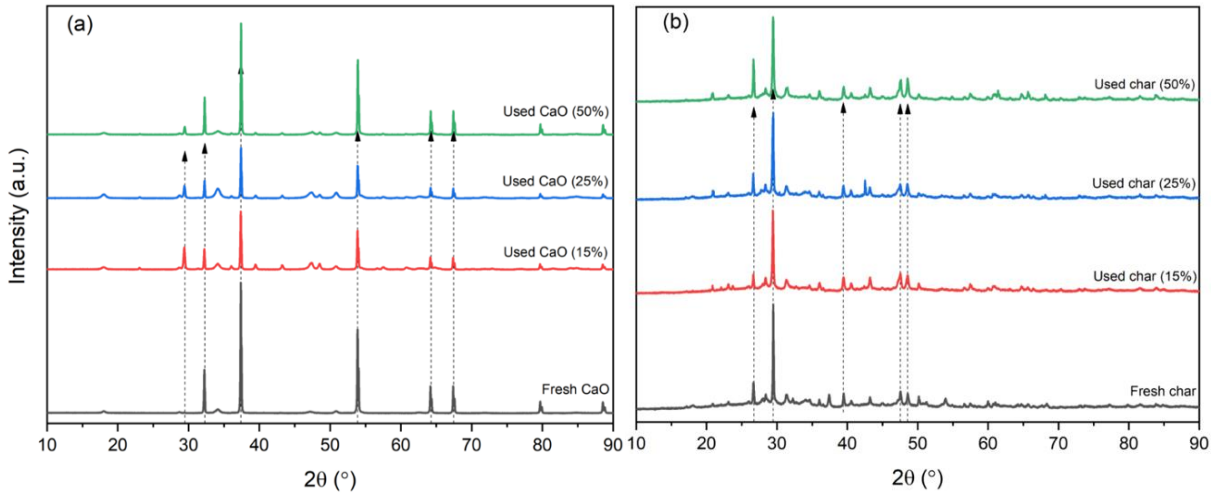

Figure 6-3 XRD pattern of (a) fresh and spent CaO catalyst and (b) fresh and spent char catalyst

6.3.2 Analysis of pyrolysis gases

6.3.2.1 Effect of in-situ and ex-situ catalyst loading to the product yields

The influence of the char and CaO catalysts on the yields of pyrolysis products at 800°C was further investigated. The gas, bio-oil and char yields of the non-catalytic pyrolysis were 46, 24 and 30 wt.%, respectively. In this work, the yields of the pyrolysis products (gas, liquid and char) and composition of the volatiles are reported in wt. %, expressed based on the feedstock mass.

As shown in Fig. 6.4, there is a noticeable effect of the catalyst mass loading on the yields of the pyrolysis products. A higher bio-oil yield was observed with the 15% char and CaO catalyst (both in-situ and ex-situ) than non-catalytic pyrolysis (Fig. 6.4 a and b). Addition of the alkaline based metal catalyst (Ca) could greatly enhance the production of bio-oil compounds in the process. Similarly, the presence of potassium, phosphorous, calcium, copper and iron metals in the char catalyst can improve the bio-oil yield. Menendez *et al.*, (2007) reported that metal catalysts and their supports can strongly promote acid-catalysis of the biomass components into a higher yield of pyrolysis oil. Bio-oil yields with the use of CaO and char catalysts first increased, followed by significant decrease to a range of 9–11 wt.% with the CaO and 7–11 wt.% with the char, respectively, at 50% catalyst loading, for both in-situ and ex-situ modes. On the other hand the gas yield was observed to increase up to 68 wt.%. These could be due to the higher catalyst mass loading that attributed to the secondary cracking of the bio-oil compounds into gas products over the specified catalysts ratio (Paasikallio *et al.*, 2017).

6.3.2.2 Gas composition without catalyst

Produced gases without catalyst were composed of CO_2, CO, CH_4, C_2H_4, C_2H_6 and H_2. CO_2 was the dominant product throughout the pyrolysis process with a maximum yield of 32 wt. % at 500^{o}C which decreased to 23 wt. % when the temperature further increased to 700°C. The CO yield was generally observed to increase from 10 wt. % at 500°C to its highest yield (12 wt. %) at 800°C. The changes could be explained by the primary stages of pyrolysis which produce more CO_2, which can be converted to CO with temperature through a gasification reaction with produced char (Menéndez *et al.*, 2007; Palumbo *et al.*, 2015). Similar to previous study (Weldekidan *et al.*, 2018a), an increase in temperature from 700 to 800°C, favored formation of CO_2 and slightly increased its yield from 23 to 29 wt. %. It can be observed in

Fig. 6.5 that for the experiment without any catalyst the amount of H_2, CH_4 and the other light gases were low with a maximum yield of 1 wt. % for H_2 and 2 wt. % for CH_4 at 700°C.

Similar to previous study (Weldekidan *et al.*, 2018a), an increase in temperature from 700 to 800°C, favored formation of CO_2 and slightly increased its yield from 23 to 29 wt. %. It can be observed in Fig. 6.5 that for the experiment without any catalyst the amount of H_2, CH_4 and the other light gases were low with a maximum yield of 1 wt. % for H_2 and 2 wt. % for CH_4 at 700°C.

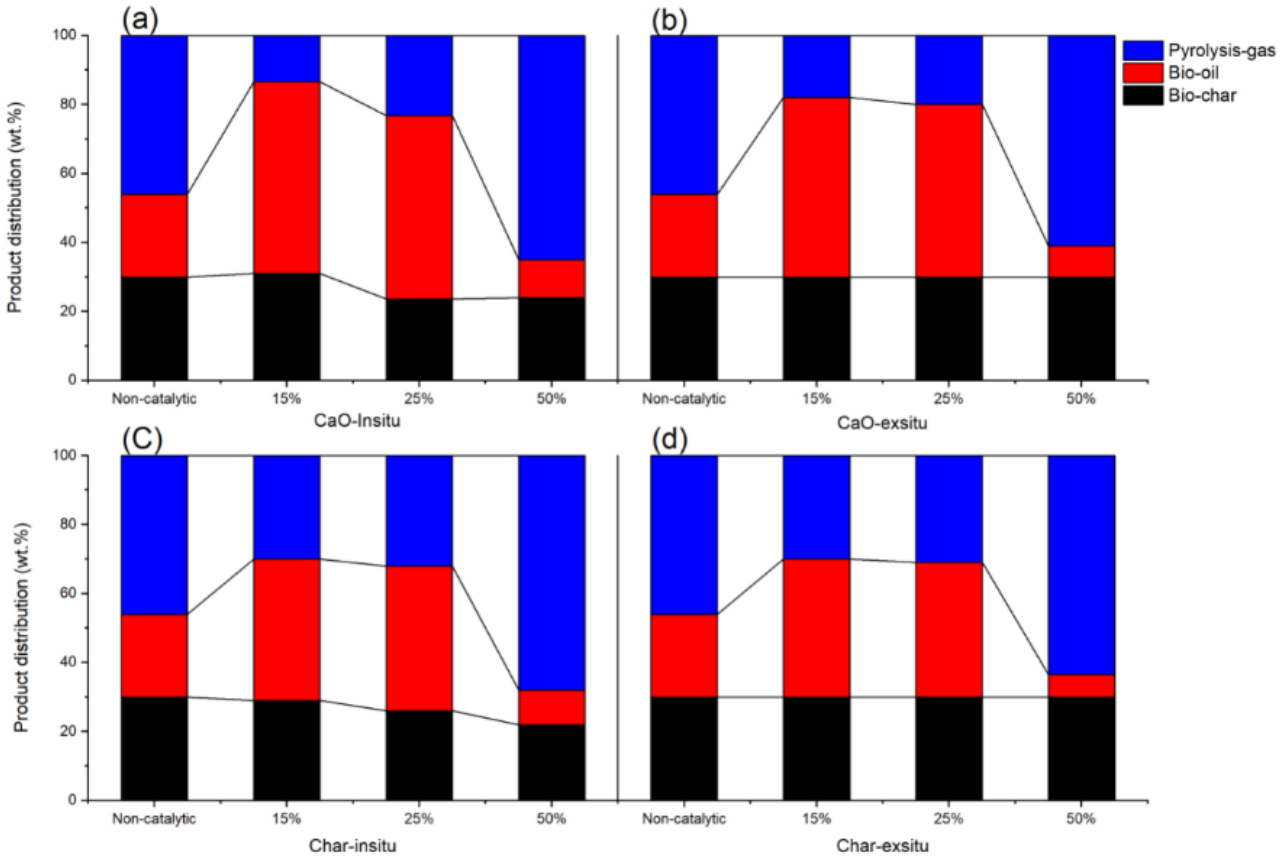

Figure 6-4 Pyrolysis product distribution of CaO loading during (a) in-situ, ex-situ (b); and char loading during in-situ (c), ex-situ (d)

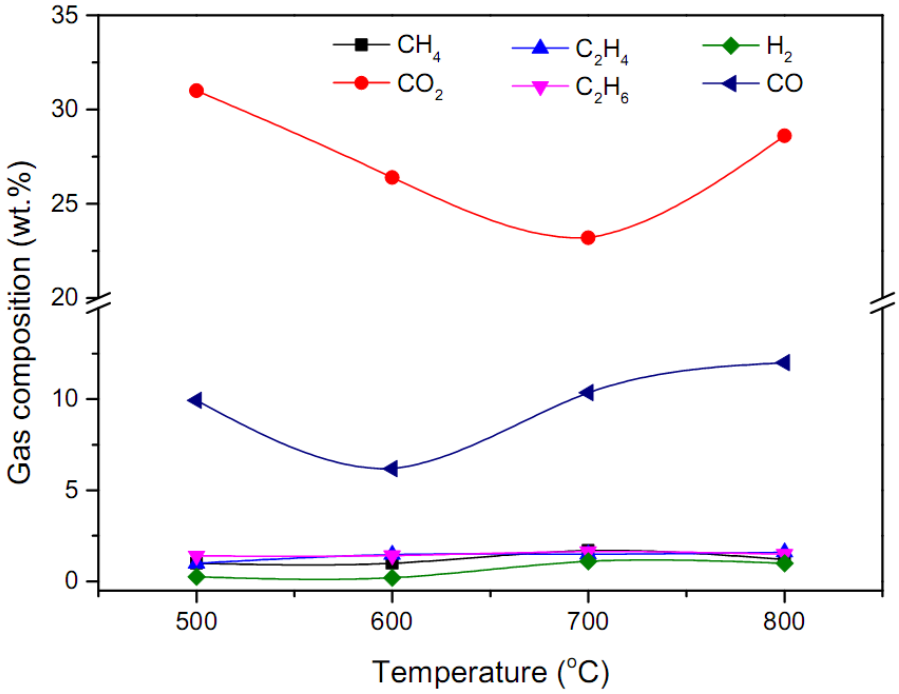

Figure 6-5 Gas composition without catalyst (relative error 5%)

6.3.2.3 Effect of *in-situ* CaO loading to the gas composition

Pyrolysis gas composition of chicken litter for different *in-stu* CaO loadings are summarised in Fig. 6 6 (**a–c**). For all the pyrolysis temperatures, the CO_2 content was observed to sharply decrease with increasing the catalyst loading. The highest CO_2 yield (23 wt. %) was obtained at 500°C with 15% CaO and continuously decreased with temperature to 4 wt. % at 800°C. The highest CO yield for the 15% CaO loading was 8 wt. % at 800°C. There was no significant difference in the CO_2 and other gas species with increasing the CaO loading to 25%, except for the CO which substantially increased from 6 wt. % at 500°C to 18 wt. % at 800°C. The 50% CaO loading showed the highest reduction in CO_2 from the produced syngas. The CO_2 yield decreased to 13 wt. % at 500°C and seriously decreased with temperature to ca 2 wt. % at 800°C. The highest CO yield (63 wt. %) was also obtained with 50% catalyst loading at 800°C.

6.3.2.4 Effect of *ex-situ* CaO loading

Gas composition of the chicken-litter waste pyrolysis at different temperatures in the presence of *ex-situ* CaO loaded at different ratios are illustrated in Fig. 6.7 (**a–c**). The plots for the *ex-situ* pyrolysis have similar patterns as those of *in-situ* pyrolysis. Dominant gas products were CO, CO_2 and H_2 with traces of CH_4, C_2H_4 and C_2H_6. For all the pyrolysis processes increasing the CaO % generally decreased the CO_2 yield and improved production of CO and H_2.

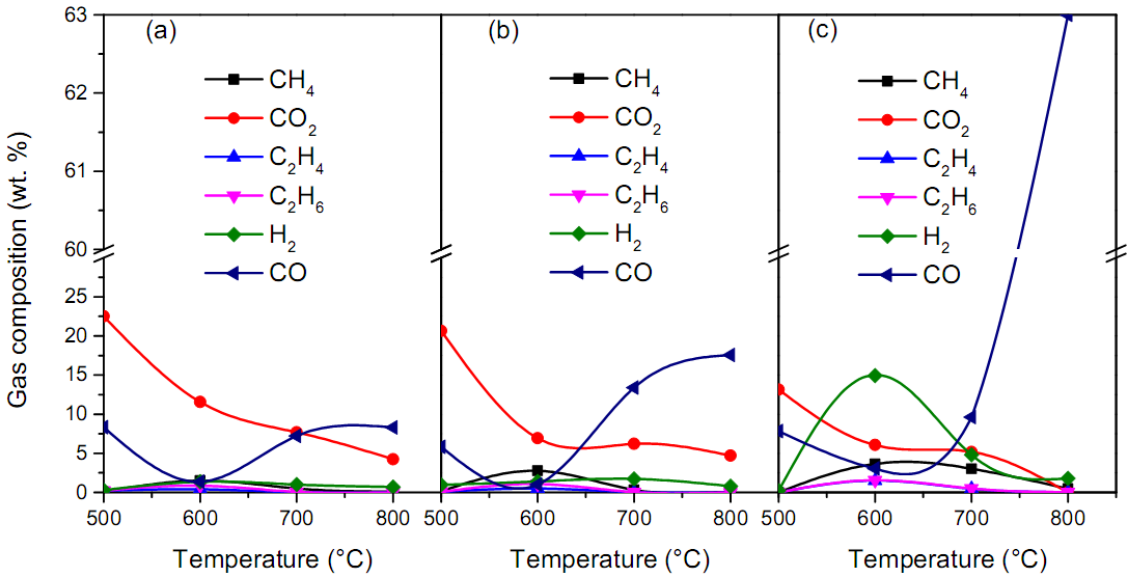

Figure 6-6 Effect of 15% (a), 25% (b) and 50% (c) in-situ CaO loadings on the gas composition (relative error 5%)

The 50% CaO loading at 800°C reduced the CO_2 yield from 21 wt. % (at 500°C and 15% CaO) to its minimum value of 2 wt. % and increasing the yield of CO to its highest yield of 59 wt% (Fig. 6.7, **c**). Typically, CaO carbonation reaction which captures most of the produced CO_2 occurs at 800°C (Wei *et al.*, 2008). As shown in Fig. 6.7, the CO content decreased up to 550–600°C and then showed sharp raise up to 800°C in all experiments. This was due to the secondary cracking of volatiles and CO_2 reduction which normally occurred at higher temperatures contributing to the raise of CO yield (Heidari *et al.*, 2014). These results are consistent with the previous study on catalytic pyrolysis of biomass under similar reaction conditions (Wang *et al.*, 2017).

H2 content was observed to increase with temperature up to 700°C (maximum 9 wt. % at 50% CaO) and decreased when the temperature further increased to 800°C. Higher temperatures do not facilitate CaO carbonation reaction with the produced CO2 and consequently increase the percentage concentration of hydrogen but favors the decomposition of CaCO3 into CaO (Wei et al., 2008). The amounts of other pyrolysis gas species were small and did not change when increasing the catalyst ratio and temperature. Overall, *in-situ* catalytic pyrolysis generated more CO, H2 and significantly reduced CO2 than the *ex-situ* pyrolysis.

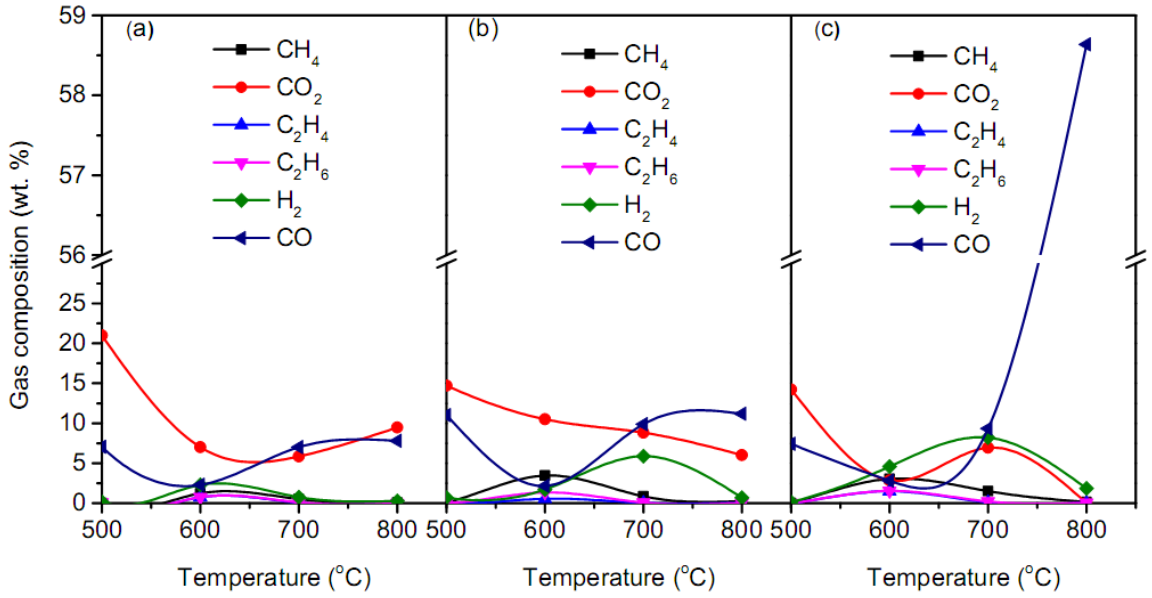

Figure 6-7 Effect of 15% (a), 25% (b) and 50% (c) ex-situ CaO loadings on the gas composition (relative error 5%)

6.3.2.5 Effect of *in-situ* char loading

Previous studies demonstrated that char can catalyse tar cracking and CH_4 reforming (Ren *et al.*, 2014; Shen, 2015). One of the main benefits of using char instead of commercial catalysts is that the char catalyst can be replaced by fresh char after it has been deactivated. Three chicken-litter waste samples mixed with 15, 25 and 50 wt. % char were pyrolysed at temperatures ranging from 500 to 800°C. The gas composition after *in-situ* pyrolysis in presence of char catalyst is shown in Fig. 6.8 (**a–c**). Similar to the CaO loading experiments, CO_2 was the main product at 500°C and continuously decreased with temperature and char ratio, whereas CO was observed to dominate at higher temperature ranges and char ratios. H_2 was the other gas which increased with the percentage of char loading and temperature, reaching the highest concentration at 700°C. The concentration of CH_4 in all char to biomass ratios were observed to peak at 600°C and decrease afterwards, which may be attributed to methane cracking reactions at higher temperatures (Song *et al.*, 2008).

The highest CO_2 yield (55 wt. %) was obtained for the 15% char (Fig. 6.8-**a**) and sharply decreased with temperature to 13 wt. % at 800°C for this sample. The CO, on the other hand, started to increase after 600°C and reached its maximum yield of 14 wt. % at 700°C. This was due to CO_2 reduction to CO which commonly occurs at higher biomass pyrolysis temperatures even without any catalyst (Menendez *et al.*, 2007). H_2 and CH_4 were the other products observed in minor yields for this sample at higher temperatures, owing to the tar cracking

reactions. Increasing the ratio of char to 25% in the sample slightly improved the CO to 21 wt. % at 800°C but did not bring significant difference to the rest of the products.

CO (60 wt. %) was the prominent product obtained at 800°C for the *in-situ* 50% char loaded sample and CO_2 sufficiently decreased from 42 wt. % to 7 wt. % at 800°C for this sample. With a higher char amount, the pyrolysis vapour has a high chance of interaction with the char, resulting in cracking of the tar compounds to gaseous species, particularly in case of CO and H_2 (Al-Rahbi *et al.*, 2016). In addition, at higher temperatures, the Boudouard reaction ($C + CO_2 \rightarrow 2CO$) was suggested to be enhanced, where the char acts as expendable reactant to promote further increase of CO production (Yao *et al.*, 2016). The increase in the CO could also be due to the alkali, alkaline earth and transition metal species (Na, Ca, K, Fe, Cu) present in the char (Table 6-2) which improved the catalytic performance of the char in reducing the CO_2 concentration (Hanaoka & Okumura, 2014). Methane reforming reaction, which is responsible for increasing the CO and H_2 content, was also improved by the catalytic activity of the char (Ren et *al.*, 2014). The observed reduction in methane with the increase in catalyst ratio in this study confirmed the occurrence of CH_4 reforming. The highest H_2 (5 wt. %) and CH_4 (5 wt. %) were produced with the *in-situ* 50% char loading, due to the enhanced catalytic conversion of the tar at higher temperatures (El-rub *et al.*, 2008).

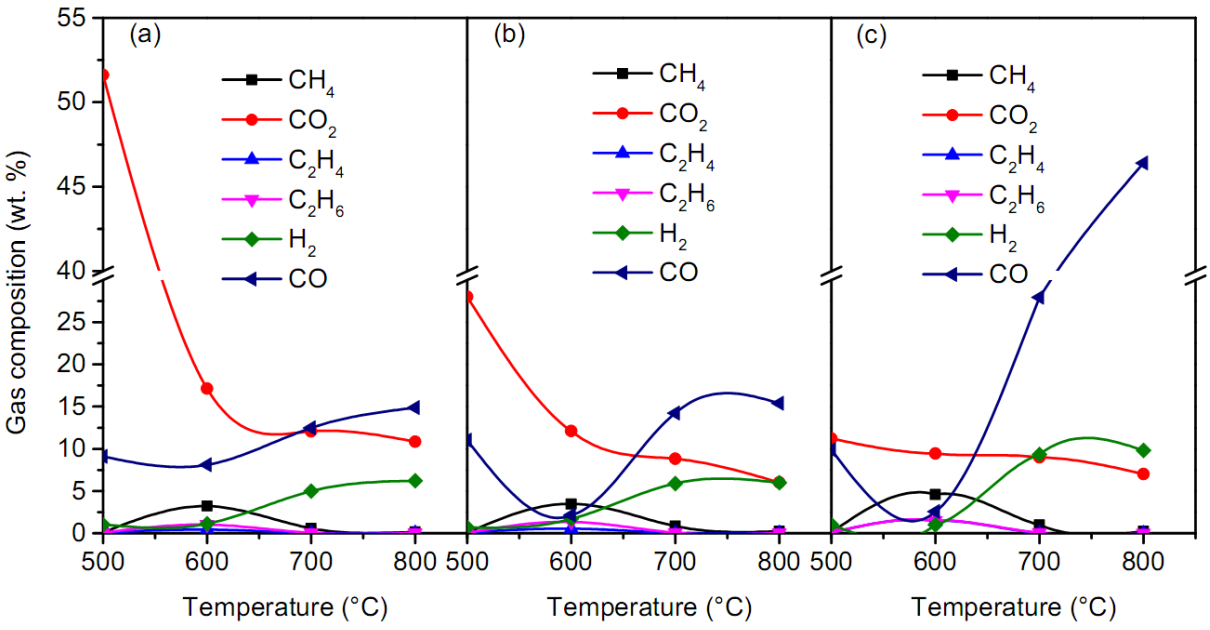

Figure 6-8 Effect of 15% (a), 25% (b) and 50% (c) in-situ char loading on the gas composition (relative error 5%)

6.3.2.6 Effect of *ex-situ* char loading

The gas composition profiles for the pyrolysis with *ex-situ* char loadings (15, 25 and 50 %) are shown in Fig. 6.9 (**a–c**). Overall, the profiles are similar to the pyrolysis experiments shown in Fig. 6.8. In general, as the temperature increased, there was a substantial decrease in CO_2 accompanied by an increase in formation of CO and H_2. The CO_2 yield was high at 500°C and continuously decreased throughout with *ex-situ* char loading. The highest CO_2 yield of 52 wt. % and CO yield of 46 wt. % were obtained with 15% char (T = 500°C) and 50% char (T = 800°C), respectively. As discussed previously the reason for this was the Boudouard reaction which was dominant at higher temperatures and char ratio, resulting in more CO generation. The highest yields for H_2 (10 wt. %) at 800°C and CH_4 (5 wt. %) were achieved for the 50% catalyst loading.

6.3.3 Bio-oil analysis

6.3.3.1 Effect of CaO on bio-oil composition

Fig. 6.10 shows GC-MS results of bio-oil composition after *in-situ* and *ex-situ* pyrolysis of chicken litter at 800°C with different CaO loadings. Approximately forty compounds with the highest peak area percentages were selected from each spectrum for further analysis. The detected compounds were further classified according to their functional groups i.e. alcohols, acids, hydrocarbons and nitrogenous compounds while the remaining compounds were named as others.

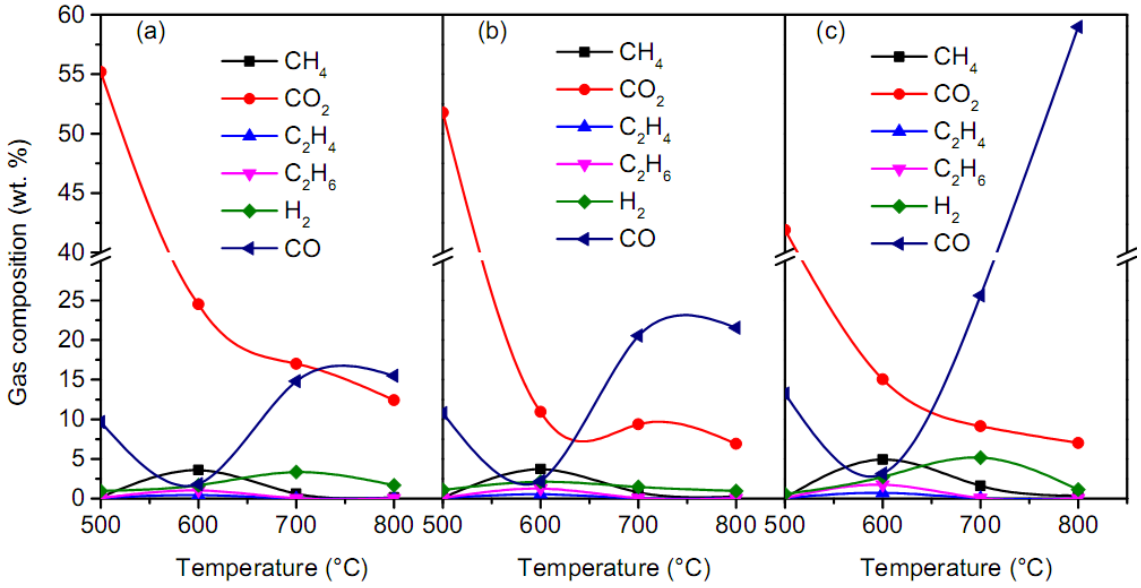

Figure 6-9 Effect of 15% (a), 25% (b) and 50% (c) ex-situ char loading on the gas composition (relative error 5%)

Fractional compositions of each of these compounds were determined based on the peak area percentage of their GC-MS spectrum. The results revealed that all the bio-oil samples mainly contained oxygenated compounds, dominantly alcohols, e.g. cresol, triethylene glycerol etc., and acids, such as palmitic acid, sorbic acid and dodecanoic acid. Besides, some nitrogenous compounds, such as acetamide, 3-pyridinol, and reticuline were also present in the bio-oils. These results were well consistent with the previous studies, which also showed nearly similar bio-oil composition after pyrolysis of chicken litter (Weldekidan *et al.*, 2018b). The results showed that different compositions of bio-oils were obtained between the *in-situ* and *ex-situ* pyrolysis. Evidently, the *in-situ* pyrolysis resulted in alcohols with a GC-MS spectrum of peak area percentges in the range of (20-84%), acids (8-11%), while the nitrogen containing compounds were in the range of (2-7%).

The results showed that different compositions of bio-oils were obtained between the *in-situ* and *ex-situ* pyrolysis. Evidently, the *in-situ* pyrolysis resulted in alcohols with a GC-MS spectrum of peak area percentges in the range of (20-84%), acids (8-11%), while the nitrogen containing compounds were in the range of (2-7%). On the other hand, *ex-situ* pyrolysis resulted in bio-oil enriched with (40-44%) alcohols, (2-8%) acids and (8-14%) nitrogen containing compounds. The addition of CaO did not show effective deoxygenation performance to produce bio-oils containing more hydrocarbon compounds either during *in-situ* or *ex-situ* pyrolysis. For example, pyrolysis with no catalyst produced bio-oils with a GC-MS spectrum of peak area percentage for alcohols (29%) and fatty acids (3 to 29%) but the introduction of CaO at 15% increased the alcohol content to 58% in the *in-situ* and 53% in *ex-situ* experiments, respectively. The alcohols are believed to be formed by the dehydration reactions of proteins and lipids present in the feedstock. Previous studies have demonstrated that CaO greatly promotes the dehydration reactions during pyrolysis (Ding *et al.*, 2018; Lin *et al.*, 2010). Therefore, it can be suggested that CaO contributed to the dehydration of proteins and lipids during the pyrolysis of chicken-litter waste, and resulted in increased production of alcohol compounds. These results also support the findings of Lin *et al.* (2010) that demonstrated an increase in alcohol content during catalytic pyrolysis of biomass with CaO. However, CaO showed a substantial decrease in fatty acids in the bio-oil during the *ex-situ* pyrolysis. The minimum concentration of fatty acids achieved with 50% CaO in the *in-situ* and *ex-situ* pyrolysis was 8 and 3% (GC-MS peak area percentage) respectively. This obeservation can be further supported with the gas analysis results where higher concentration of CO gas was achieved with increased CaO addtion. Moreover, it has also been suggested that CaO

particles can deoxygenate the bio-oil by directly reacting with acid compounds or their precursors to form organic or inorganic calcium salts (Lin *et al.*, 2010). It could be suggested that CaO deoxygenated the fatty acids mainly through decarboxylation (removal of oxygen as CO_2) and decarbonylation reaction (removal of oxygen as CO) (Ranganathan & Gu, 2018).

6.3.3.2 Effect of char on bio-oil composition

Fig. 6.11 shows GC-MS results of bio-oil composition after *in-situ* and *ex-situ* pyrolysis of chicken litter at 800°C under different char loadings. Noticeably, the addition of char regardless of its concentration or type of pyrolysis (*in-situ* or *ex-situ*) did not change the bio-oil composition effectively as approximately similar compounds were detected in all samples. However, a significant variation in concentration of these compounds was observed in the bio-oil. For example, *in-situ* pyrolysis with char-15% produced ca. 19% triethylene glycerol, which decreased to 16% with char-50%. The overall GC-MS spectrum peak area percentage of alcohols, acids and nitrogenous compounds were (30-41%), (18-31%), (4-8%), respectively in the bio-oil samples obtained with different concentrations of char, either from *in-situ* or *ex-situ* pyrolysis. On the other hand, one aliphatic hydrocarbon i.e. propane was detected in pyrolytic oil with char-15% and char-50% (*in-situ*) at a concentration of 0.6% and 0.7% (peak area percentages), respectively, but it was not observed in the *ex-situ* pyrolytic oils. Overall, it can be concluded that bio-oil samples obtained in this study were highly oxygenated and further downstream treatment is required to upgrade the bio-oil. Noticeably, the addition of char did not show deoxygenation activity for either alcohols or fatty acids to as nearly similar composition of compounds was obtained in all the bio-oil samples. This could probably be due to the depletion of the CaO present in the char to reduce the CO_2 in the pyrolysis gases to CO. This converts all the CaO to $CaCO_3$ which is a stable compound and cannot deoxygenate the bio-oil compounds. On the other hand, addtion of 50% CaO achieved a considerable deoxygenation activity of the fatty acids.

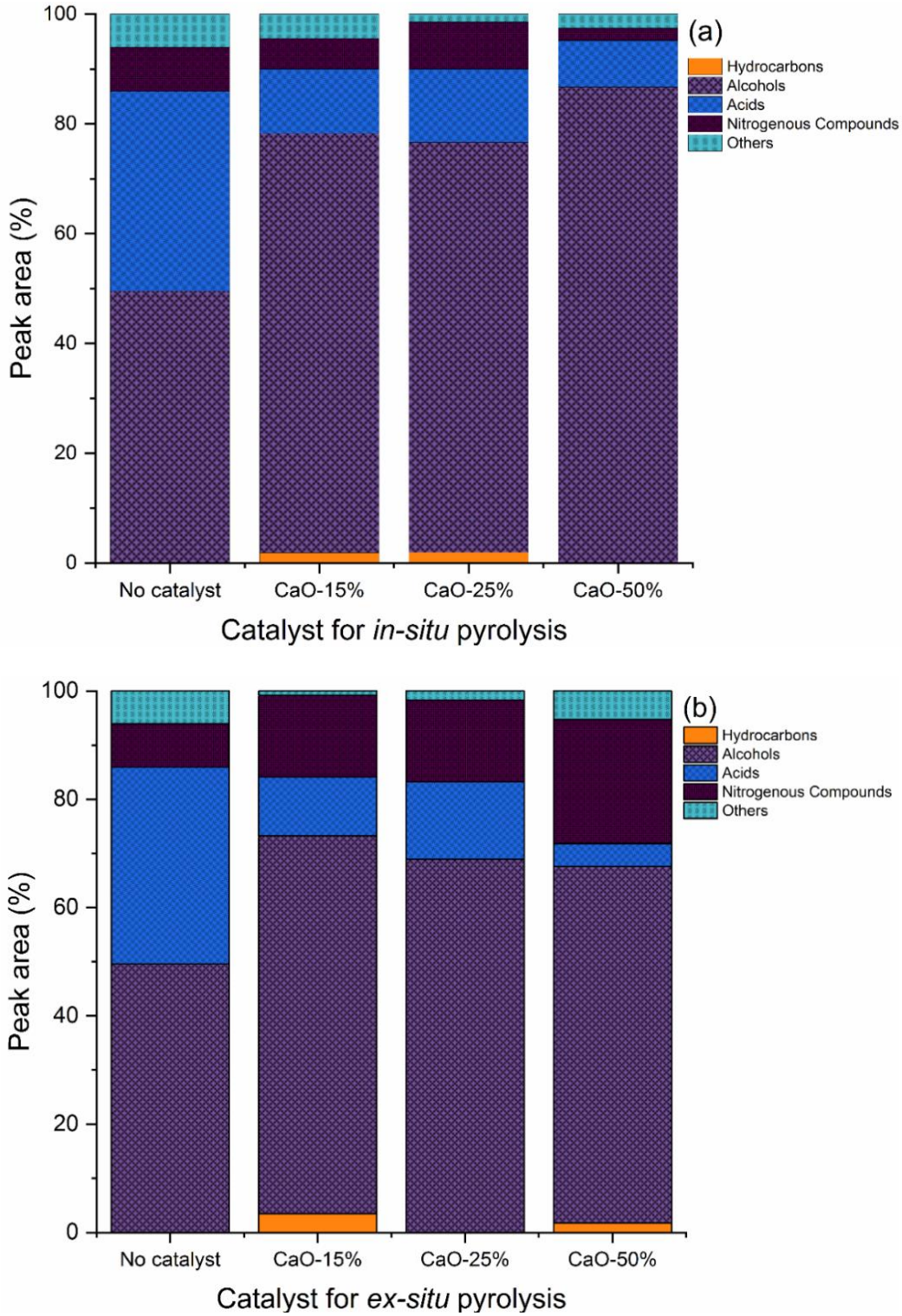

Figure 6-10 GC-MS results for bio-oil composition with different ratio of CaO loading during (a) in-situ and (b) ex-situ pyrolysis of chicken litter at 800°C (relative error 5%).

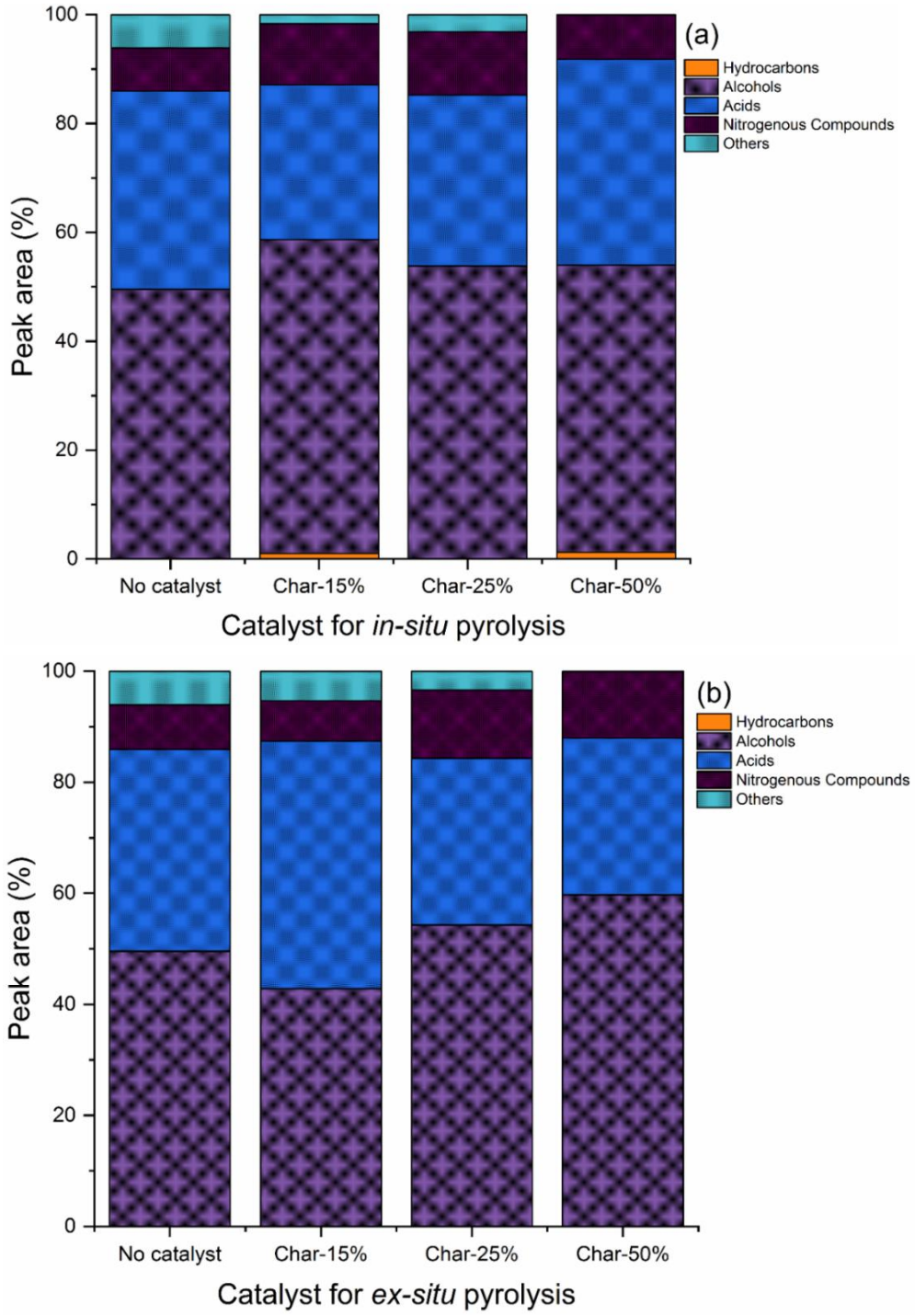

Figure 6-11 GC-MS results for bio-oil composition with different compositions of char during (a) in-situ and (b) ex-situ pyrolysis of chicken litter at 800°C (relative error 5 %).

6.4 Conclusion

The effects of CaO and char catalysts on the pyrolysis products of chicken-litter waste were studied in *in-situ* and *ex-situ* modes under concentrated solar radiation. In both cases the highest catalytic performance on reduction of CO_2 and improving CO and H_2 yields in the pyrolytic gas was achieved with 50% catalyst loading at 800°C. The highest CO and H_2 yields were 63 wt. % and 15 wt. %, respectively, obtained with the 50% CaO *in-situ* loading at 800°C. Both catalysts were efficient in reducing the CO_2 concentrations at higher temperatures. CO_2 content was substantially reduced ca 2 % with 50% CaO loading at 800°C while the minimum CO_2 yield with the char catalyst was around 7 wt. % for both *in-situ* and *ex-situ* pyrolysis. Pyrolysis of chicken litter with addition of CaO also produced bio-oil compounds having more alcohols with peak area percentages of up to 84% and substantially reduced the fatty acids to 3%, whereas pyrolysis with addition of char did not show significant deoxygenation activities for the bio-oils, but was comparable with CaO in absorbing the CO_2 and producing CO, H_2 and CH_4 in the pyrolysis gases.

6.5 Reference

Al-Rahbi, A. S., Onwudili, J. A., & Williams, P. T. (2016). Thermal decomposition and gasification of biomass pyrolysis gases using a hot bed of waste derived pyrolysis char. *Bioresource Technology, 204*, 71-79.

Bai, Z., Liu, Q. B., Lei, J., Hong, H., & Jin, H. G. (2017). New solar-biomass power generation system integrated a two-stage gasifier. *Applied Energy, 194*, 310-319.

Balasundram, V., Ibrahim, N., Kasmani, R. M., Isha, R., Hamid, M. K. A., Hasbullah, H., & Ali, R. R. (2018). Catalytic upgrading of sugarcane bagasse pyrolysis vapours over rare earth metal (Ce) loaded HZSM-5: Effect of catalyst to biomass ratio on the organic compounds in pyrolysis oil. *Applied Energy, 220*, 787-799.

Ding, K., Zhong, Z., Wang, J., Zhang, B., Fan, L., Liu, S., . . . Ruan, R. (2018). Improving hydrocarbon yield from catalytic fast co-pyrolysis of hemicellulose and plastic in the dual-catalyst bed of CaO and HZSM-5. *Bioresource Technology, 261*, 86-92.

El-Rub, Z. A., Bramer, E. A., & Brem, G. (2008). Experimental comparison of biomass chars with other catalysts for tar reduction. *Fuel, 87*(10-11), 2243-2252.

Florin, N. H., & Harris, A. T. (2008). Enhanced hydrogen production from biomass with in situ carbon dioxide capture using calcium oxide sorbents. *Chemical Engineering Science, 63*(2), 287-316.

Hallenbeck, P. C., Grogger, M., Mraz, M., & Veverka, D. (2016). Solar biofuels production with microalgae. *Applied Energy, 179*, 136-145.

Han, L., Wang, Q. H., Yang, Y. K., Yu, C. J., Fang, M. X., & Luo, Z. Y. (2011). Hydrogen production via CaO sorption enhanced anaerobic gasification of sawdust in a bubbling fluidized bed. *International Journal of Hydrogen Energy, 36*(8), 4820-4829.

Hanaoka, T., & Okumura, Y. (2014). Effect of metal content on CO2 gasification behavior of K- and Fe-loaded bio-chars. *Journal of Thermal Science and Technology, 9*(2).

Heidari, A., Stahl, R., Younesi, H., Rashidi, A., Troeger, N., & Ghoreyshi, A. A. (2014). Effect of process conditions on product yield and composition of fast pyrolysis of Eucalyptus grandis in fluidized bed reactor. *Journal of Industrial and Engineering Chemistry, 20*(4), 2594-2602.

Hernando, H., Jimenez-Sanchez, S., Fermoso, J., Pizarro, P., Coronado, J. M., & Serrano, D. P. (2016). Assessing biomass catalytic pyrolysis in terms of deoxygenation pathways and energy yields for the efficient production of advanced biofuels. *Catalysis Science & Technology, 6*(8), 2829-2843.

Hu, M., Guo, D. B., Ma, C. F., Hu, Z. Q., Zhang, B. P., Xiao, B., . . . Wang, J. B. (2015). Hydrogen-rich gas production by the gasification of wet MSW (municipal solid waste) coupled with carbon dioxide capture. *Energy, 90*, 857-863.

Imran, A., Bramer, E. A., Seshan, K., & Brem, G. (2016). Catalytic Flash Pyrolysis of Biomass Using Different Types of Zeolite and Online Vapor Fractionation. *Energies, 9*(3).

Kornprobst, T., & Plank, J. (2012). Photodegradation of Rhodamine B in Presence of CaO and NiO-CaO Catalysts. *International Journal of Photoenergy, 2012*, 6.

Lin, Y., Zhang, C., Zhang, M., & Zhang, J. (2010). Deoxygenation of Bio-oil during Pyrolysis of Biomass in the Presence of CaO in a Fluidized-Bed Reactor. *Energy & Fuels, 24*(10), 5686-5695.

Liu, C., Wang, H., Karim, A. M., Sun, J., & Wang, Y. (2014). Catalytic fast pyrolysis of lignocellulosic biomass. *Chemical Society Reviews, 43*(22), 7594-7623.

Menendez, J. A., Dominguez, A., Fernandez, Y., & Pis, J. J. (2007). Evidence of self-gasification during the microwave-induced pyrolysis of coffee hulls. *Energy & Fuels, 21*(1), 373-378.

Menéndez, J. A., Domínguez, A., Fernández, Y., & Pis, J. J. (2007). Evidence of Self-Gasification during the Microwave-Induced Pyrolysis of Coffee Hulls. *Energy & Fuels, 21*(1), 373-378.

Mian, M. M., & Liu, G. J. (2018). Recent progress in biochar-supported photocatalysts: synthesis, role of biochar, and applications. *Rsc Advances, 8*(26), 14237-14248.

Muley, P. D., Henkel, C. E., Aguilar, G., Klasson, K. T., & Boldor, D. (2016). Ex situ thermo-catalytic upgrading of biomass pyrolysis vapors using a traveling wave microwave reactor. *Applied Energy, 183*, 995-1004.

Nzihou, A., Flamant, G., & Stanmore, B. (2012). Synthetic fuels from biomass using concentrated solar energy - A review. *Energy, 42*(1), 121-131.

Paasikallio, V., Kalogiannis, K., Lappas, A., Lehto, J., & Lehtonen, J. (2017). Catalytic Fast Pyrolysis: Influencing Bio-Oil Quality with the Catalyst-to-Biomass Ratio. *Energy Technology, 5*(1), 94-103.

Palumbo, A. W., Sorli, J. C., & Weimer, A. W. (2015). High temperature thermochemical processing of biomass and methane for high conversion and selectivity to H2-enriched syngas. *Applied Energy, 157*, 13-24.

Ranganathan, P., & Gu, S. (2018). Numerical simulation of catalytic upgrading of biomass pyrolysis vapours in a FCC riser. *Fuel Processing Technology, 171*, 162-172.

Ren, S. J., Lei, H. W., Wang, L., Bu, Q., Chen, S. L., & Wu, J. (2014). Hydrocarbon and hydrogen-rich syngas production by biomass catalytic pyrolysis and bio-oil upgrading over biochar catalysts. *Rsc Advances, 4*(21), 10731-10737.

Shen, Y. F. (2015). Chars as carbonaceous adsorbents/catalysts for tar elimination during biomass pyrolysis or gasification. *Renewable & Sustainable Energy Reviews, 43*, 281-295.

Song, L., & Zhang, S. (2010). Preparation and visible light photocatalytic activity of Bi2O3/CaO photocatalysts. *Reaction Kinetics, Mechanisms and Catalysis, 99*(1), 235-241.

Song, L., Zhang, S., Chen, B., & Sun, D. (2009). Highly active NiO–CaO photocatalyst for degrading organic contaminants under visible-light irradiation. *Catalysis Communications, 10*(5), 421-423.

Song, Q. L., Xiao, R., Li, Y. B., & Shen, L. H. (2008). Catalytic carbon dioxide reforming of methane to synthesis gas over activated carbon catalyst. *Industrial & Engineering Chemistry Research, 47*(13), 4349-4357.

Strezov, V., Popovic, E., Filkoski, R. V., Shah, P., & Evans, T. (2012). Assessment of the Thermal Processing Behavior of Tobacco Waste. *Energy & Fuels, 26*(9), 5930-5935.

Sun, Q., Yu, S., Wang, F., & Wang, J. (2011). Decomposition and gasification of pyrolysis volatiles from pine wood through a bed of hot char. *Fuel, 90*(3), 1041-1048.

Tanaka, Y., Mesfun, S., Umeki, K., Toffolo, A., Tamaura, Y., & Yoshikawa, K. (2015). Thermodynamic performance of a hybrid power generation system using biomass gasification and concentrated solar thermal processes. *Applied Energy, 160*, 664-672.

Udomsirichakorn, J., Basu, P., Salam, P. A., & Acharya, B. (2014). CaO-based chemical looping gasification of biomass for hydrogen-enriched gas production with in situ CO2 capture and tar reduction. *Fuel Processing Technology, 127*, 7-12.

Wan, S. L., Pham, T., Zhang, S., Lobban, L., Resasco, D., & Mallinson, R. (2013). Direct catalytic upgrading of biomass pyrolysis vapors by a dual function Ru/TiO2 catalyst. *Aiche Journal, 59*(7), 2275-2285.

Wang, K., Johnston, P. A., & Brown, R. C. (2014). Comparison of in-situ and ex-situ catalytic pyrolysis in a micro-reactor system. *Bioresource Technology, 173*, 124-131.

Wang, K. G., Zheng, Y., Zhu, X. F., Brewer, C. E., & Brown, R. C. (2017). Ex-situ catalytic pyrolysis of wastewater sewage sludge - A micro-pyrolysis study. *Bioresource Technology, 232*, 229-234.

Wang, Z., Wang, F., Cao, J., & Wang, J. (2010). Pyrolysis of pine wood in a slowly heating fixed-bed reactor: Potassium carbonate versus calcium hydroxide as a catalyst. *Fuel Processing Technology, 91*(8), 942-950.

Wei, L., Xu, S., Liu, J., Liu, C., & Liu, S. (2008). Hydrogen Production in Steam Gasification of Biomass with CaO as a CO2 Absorbent. *Energy & Fuels, 22*(3), 1997-2004.

Weldekidan, H., Strezov, V., & Town, G. (2018a). Review of solar energy for biofuel extraction. *Renewable and Sustainable Energy Reviews, 88*, 184-192.

Weldekidan, H., Strezov, V., Kan, T., & Town, G. (2018b). Waste to Energy Conversion of Chicken Litter through a Solar-Driven Pyrolysis Process. *Energy & Fuels, 32*(4), 4341-4349.

Weldekidan, H., Strezov, V., Town, G., & Kan, T. (2018c). Production and analysis of fuels and chemicals obtained from rice husk pyrolysis with concentrated solar radiation. *Fuel, 233*, 396-403.

Yao, D., Hu, Q., Wang, D., Yang, H., Wu, C., Wang, X., & Chen, H. (2016). Hydrogen production from biomass gasification using biochar as a catalyst/support. *Bioresource Technology, 216*, 159-164.

Zeng, K., Gauthier, D., Minh, D. P., Weiss-Hortala, E., Nzihou, A., & Flamant, G. (2017). Characterization of solar fuels obtained from beech wood solar pyrolysis. *Fuel, 188*, 285-293.

Zhang, Y., Chen, P., & Lou, H. (2016). In situ catalytic conversion of biomass fast pyrolysis vapors on HZSM-5. *Journal of Energy Chemistry*, *25*(3), 427-433.

Chapter 7: Distribution of solar pyrolysis products and product gas composition produced from agricultural residues at different operating parameters

In this chapter the influence of process parameters on the pyrolysis of agricultural residues with concentrated solar radiation is presented. Experimental results of pyrolysis of chicken litter and rice husk are investigated at different temperatures, heating rate and particle sizes. The experiments were performed in PROMES-CNRS, which is one of the biggest solar energy laboratories in the world. High heating rate and relatively higher pyrolysis temperatures have been considered. Energy content of the combustible pyrolysis gases produced at different operating conditions are determined in this chapter.

I together with Prof G. Flamant and Rui developed the concept and designed the experiments. Rui and Prof Gilles Flamant gave me the induction training to the solar laboratories in PROMES-CNRS; then Rui and I conducted the experiments. Data analysis and write-ups were done by myself while Gilles Flamant, Vlad, Rui, Ravinder, Jing, Tao and Prof. Graham were involved in editing and reviewing the manuscript.

Authors' contribution summary for this paper

	W. H.	S. V.	T. G.	K. T.	K. R.	H. J.	R. L.	G. F.
Experiment Design	•							
Sample Preparation	•							
Data Collection	•							
Analysis	•	•						
Manuscript	•	•	•	•	•	•	•	•

Results have been compiled and submitted to the ***Renewable Energy*** journal for publication, which is now under review, as:

Weldekidan, H. (80%), Strezov, V. (3%), Li, R. (6%), Kan, T. (1%), Town, T. (1%), Kumar, R. (1%), He, J. (1%) and Flamant, G. (6%). "Distribution of solar pyrolysis products and product gas composition produced from agricultural residues at different operating parameters", ***Renewable Energy (submitted on the 23rd of January 2019).***

Distribution of solar pyrolysis products and product gas composition produced from agricultural residues at different operating parameters

Haftom Weldekidan[a], Vladimir Strezov[a], Rui Li[b], Tao Kan[a], Graham Town[c], Ravinder Kumar[a], Jing He[a], Gilles Flamant[b]*

[a] Department of Environmental Sciences, Faculty of Science Engineering, Macquarie University, Sydney, NSW 2109, Australia

[b] Processes, Materials and Solar Energy Laboratory (PROMES-CNRS), 7 Rue du Four Solaire, Odeillo 66120 Font-Romeu, France

[c] School of Engineering, Faculty of Science and Engineering, Macquarie University, Sydney, NSW 2109, Australia

*Gilles.Flamant@promes.cnrs.fr

Abstract

Solar energy and biomass are the two major sources of renewable energy, which can be integrated to produce heat, power and transportation fuels, chemicals and biomaterials using pyrolysis. In this work, separate samples of chicken-litter waste and rice husk of different particle sizes (280 and 500 µm) were pyrolysed with a concentrated solar radiation to produce pyrolysis gases of high calorific value. Different operating parameters were investigated under the solar pyrolysis conditions. Heating rates from 10 to 500°/s and temperatures in the range of 800 to 1600°C, generated from a lab-scale solar furnace with maximum power capacity of 1.5 kW, were applied. Temperature was found to have the highest effect, changing the gas yield from 10 to 39 wt.%; decreasing the bio-oil and char yields from 48 to 41 wt. % and 42 to 18 wt.%, respectively as the temperature increased from 800 to 1600°C. The highest higher heating value (HHV) of the gas (7255 ± 566 kJ/kg) was obtained with the 280 µm particle size chicken litter at 1600°C. Overall, gases produced from solar assisted biomass pyrolysis have a high concentration of combustible products that can be directly used as fuels in engines or power plants.

Key words: solar pyrolysis, combustible gases, renewable energy, biomass, solar fuels

7.1 Introduction

Due to the depletion of fossil fuels and high concern for environmental protection from the conventional sources of energy, the alternative and renewable energy sources are attracting increased attention. Biomass is one of the renewable energy sources that can directly replace fossil fuels in many applications, such as the production of heat, chemicals and biomaterials, power and transportation fuels through the pyrolysis process (Arribas *et al.*, 2017). Biomass pyrolysis involves extremely complex chemical and physical processes, such as heat transfer, mass transfer, thermal dynamics and their interactions influenced by temperature, heating rate, biomass particle size and density, physical and chemical pretreatments of the process and others (Gómez *et al.*, 2018; Zhai *et al.*, 2015). Numerous studies have investigated the effects of different process parameters on the yield and composition of the pyrolysis products. Recently, Guedes *et al.* (2018) reviewed the pyrolysis parameters and their effects on the properties and yields of pyrolysis products and Zeng *et al.* (2017a) reviewed solar pyrolysis of carbonaceous feedstock. In the former paper, temperatures in the range of 400 to 650°C at different heating rates (5 to 700°C/min) were investigated for different types of biomass. Bio-oil yields from rice husk and waste palms were found to increase with temperature and reached maximum values of 70 % at 450 °C and 72.4% at 500°C respectively. However, as shown in the latter paper, a further increase in the temperature and the heating rate favors formation of gas. According to Morf *et al.* (2002) lower ranges of pyrolysis temperatures (>500°C) for processing of wood chip produces CO_2, CO and small amount of CH_4 from primary decomposition, and at temperatures higher than 650°C the CO, CH_4 and H_2 concentrations increase due to secondary tar cracking.

The heating rate is another important parameter in biomass pyrolysis. Heating rates up to 100°C/s can create heat and mass transfer limitations in samples during pyrolysis, hence bringing substantial variations to the yield and composition of pyrolysis gases, possibly due to non-homogenous heating of the samples. An increase in the heating rate from 100 to 300°C/min in the pyrolysis of rapeseed at 500°C increased the bio-oil yield to 58 % (Ateş *et al.*, 2004). Yields of CO, H_2, CH_4 and C_2H_6 were observed to increase with increasing the heating rate from 5 to 50°C/s in the solar pyrolysis of beech wood (Zeng *et al.*, 2015).

Biomass feedstock differ considerably in their lignin, cellulose and hemicellulose contents. The volatile matter, ash and moisture contents are also some of the typical variations in biomass,

which can affect the distribution of pyrolysis products (Guedes *et al.*, 2018). Biomass with a higher lignin content tends to produce more char than cellulose and hemicellulose, which favor production of tar and non-condensable volatiles (Akhtar & Saidina Amin, 2012). The amount of volatile matter in feedstock also has a significant role in determining the quantity of each pyrolysis product. A higher tar yield can be obtained from feedstock with higher content of volatile matter due to improved volatility and reactivity advantages (Omar *et al.*, 2011).

Particle size is another factor that affects the yield and composition of the pyrolysis products (Luo *et al.*, 2010). Shen *et al.* (2009) investigated the effects of different particle sizes (0.18 to 5.6 mm) of mallee wood on pyrolysis at 500°C and found the liquid yield to decrease by 12 to 14 %, while the gas and char yields increased by around 14 and 4 % when the particle size increased from 0.3 to 1.5 mm, respectively. However, a further increase in size up to 5.6 mm could not bring any significant variations to the results. Small particle sizes enhance the formation of H_2 and CO contents. The increments of 18.3 and 17 % were recorded in the H_2 and CO yields, respectively as the particle sizes changed from 10 to 5 mm in the pyrolysis of municipal solid waste at 900°C. As biomass has low thermal conductivity, very large particle size can limit heat transfer to adjacent particles, resulting in an inefficient pyrolysis process.

As discussed, biomass is one of the most important sources of renewable energy that can be converted to various gaseous, liquid and solid fuels (variable in product distribution and composition) using thermochemical conversion processes. This process, however, requires heat to carry out the pyrolysis, which can be supplied by partially combusting some of the evolved volatiles, thereby reducing the overall amount of produced pyrolysis products, or through external solar heat, which can significantly improve the efficiency of the pyrolysis process, and the cleaning and separation of the gas produced. Integration of solar energy to drive the thermochemical processing of biomass offers opportunities for developing new and sustainable biomass-solar technologies and storage of solar energy in the products (Bashir *et al.*, 2017; Chintala, 2018; Wu *et al.*, 2018; Zeng *et al.*, 2017b).

There have been intensive research studies that have investigated the effects of different operating parameters on the pyrolysis product distribution in the traditional/conventional pyrolysis, which is commonly held below 1000°C at relatively lower heating rates. Solar assisted biomass pyrolysis is currently an emerging technology attracting considerable research interest at present (Weldekidan *et al.*, 2018b; Yadav & Banerjee, 2016; Zeng *et al.*, 2017a). Fuels with higher calorific values and chemicals of different quality and quantity can be

produced from the solar pyrolysis of biomass by varying the operating parameters. Solar pyrolysis is different from conventional pyrolysis by providing fast heating rate and achieving flexible temperatures that can range up to 2000°C. With only limited studies investigating solar assisted biomass pyrolysis, the distribution of solar pyrolysis products as a function of biomass composition and origin, at different solar conditions are still not sufficiently investigated.

This work investigates the effects of different heating rates (10 to 500°C/s), temperature in the rages of 800 to 1600°C, biomass (agriculture residues) type and particle size to the pyrolysis product distribution and gas composition in the solar pyrolysis process. Product yields, gas composition and the higher heating values (HHVs) of the product gases are studied thoroughly with respect to each pyrolysis parameter.

7.2 Experimental

7.2.1 Sample

The biomass materials used in this study were chicken-litter waste and rice husk separately. Samples of chicken-litter waste had mean particle sizes of 280 µm while the rice husk had two different samples prepared from 280 µm and 500 µm particle sizes, separately. The results of proximate and ultimate analysis of the two biomass samples are summarized in Table 7-1.

Table 7-1 Proximate and ultimate analysis of chicken-litter and rice husk.

Biomass	Proximate analysis				Ultimate analysis				
	Ash	Volatile matter	Fixed carbon	Moisture	C	H	O*	N	S
	%mass, dry basis			%mass	%mass, ash free				
Chicken-litter	27.1	62.6	10.3	9.9	46.9	5.4	42	5.38	0.32
Rice husk	28	58	15	6.03	34.3	5	60.1	0.38	0.19

*By difference

7.2.2 Solar experimental setup

Solar experiments were carried out with one of the PROMES-CNRS small solar furnaces (vertical axis, beam down type). The setup applied in this research is shown in Fig 7.1. The solar concentrating system was composed of a 25 m^2 flat heliostat and a downward facing parabolic mirror (2 m in diameter and 0.85 m focal length). The heliostat tracked the sun continuously and reflected vertical and parallel rays to the optical axis of the parabolic dish that in turn concentrated the parallel rays onto the focus situated 0.85 m below the vertex of

the dish. The maximum power and flux density of this configuration was 1.5 kW and 12,000 kW/m^2, respectively. A shutter placed in the optical path between the heliostat and the parabola allowed control the solar power with time (heating rate) and the plateau temperature. The shutter was monitored with a PID controller. Compressed pellets of the biomass were placed in a graphite crucible (10 mm i.d) located at the focus of the parabola. The reactor is composed of a metallic base, a water-cooled moving sample holder and a transparent Pyrex dome that closes the vessel.

Sample temperature was measured with an optical pyrometer (KLEIBER monochromatic operating at 5.2 µm), and the pyrolysis gases mixed with argon (sweeping gas) were pumped out with a vacuum pump and passed through a condensation train for trapping bio-oil and other heavy organics. Finally, the volatiles were collected in a Tedlar bag and then injected to GC (SRA Instruments MicroGC 3000) for further analysis.

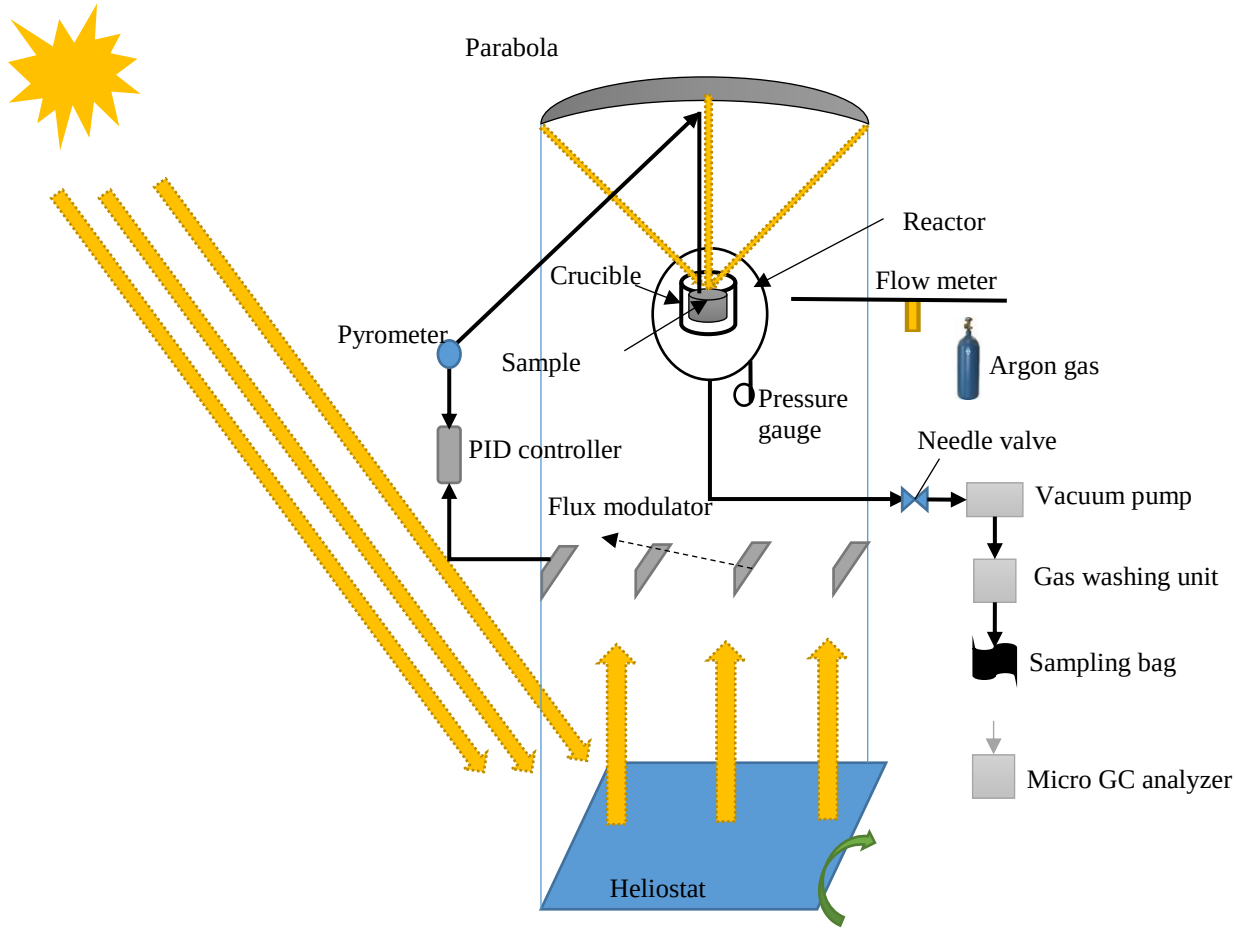

Figure 7-1 Schematic of the solar setup

7.2.3 Experimental procedures

A range of experiments were conducted to assess the influence of process parameters on the gas products of the solar-assisted pyrolysis. In each experiment, 0.33 g of the sample was first compressed into cylinders of 10 mm diameter and 5 mm height and placed in a graphite crucible. Before each experiment, the argon gas was purged at 9 NL/min (controlled by Bronkhorst, EL-FLOW® flowmeter) into the reactor, and the oxygen concentration inside the reactor was completely pumped out with the vacuum pump. A 3100 SYNGAS analyzer was employed to on-line monitor the oxygen content in the reactor.

The first set of experiments was performed to determine the effect of heating rate on the product yield and gas composition. For this, the chicken litter samples were pyrolyzed at heating rates of 10, 50, 100, 200 and 500°C/s to the final temperature of 1200°C. The next set of experiments was performed to investigate the effect of final pyrolysis temperatures in the ranges of 800 to 1600°C, during which the heating rate was fixed at 50°C/s. To examine the effect of biomass particle size, experiments were conducted with two different sizes (280 and 500 µm) of rice husk at 800 to 1600°C and 50°C/s. In each experiment, reactions were held at the final temperatures for a maximum of 5 min. The yields and gas compositions obtained from the pyrolysis of chicken litter and rice husk at the same operating parameters were compared to assess the effect of biomass composition.

The solid mass that remained in the crucible at the end of each experiment was assumed as the char yield, and the gas yield was calculated form the ideal gas equation using argon as a tracer while the bio-oil yield was calculated from the mass difference between the total sample mass and the mass sum of the chars and pyrolysis gases. Then the wt.% of each product was found by dividing these quantities by the original sample mass.

Finally, the total higher heating value (HHV) of the pyrolysis gases was determined from the yield and heating value of individual combustible gas components (H_2, CO, CH_4 and C_2H_6) as reported in (Lars & Nilsson, 2001; Wang *et al.*, 2016; Weldekidan *et al.*, 2018c).

7.3 Result and discussion

7.3.1 Influence of heating rate on product distribution and gas composition

Fig. 7.2 shows the product distribution obtained from the pyrolysis of chicken-litter waste (280 µm particle size) at final temperature of 1200°C and heating rates of 10, 50, 200 and 500°C/s.

An increase of heating rate from 10 to 50°C/s resulted in slight decrease of the bio-oil yield from 53 to 47 wt. % whilst the gas yield was increased significantly from 18 to 25 wt. %. The possible reason is that increasing the heating rate enhanced the secondary cracking reactions and increased the rate of depolymerization of the bio-oil to primary volatiles (Chen *et al.*, 1997). Increasing the heating rate to 200°C/s slightly reduced the char and bio-oil yields to 45 and 28 wt. %, respectively, whilst the gas yield increased to 27 wt. %. Further increase in the heating rate to 500°C/s slowly decreased the liquid yield to 40 wt. % and increased the gas yield to 34 wt. %. These changes could be attributed to the heat and mass transfer limitation caused by the fast heating rates (Soria *et al.*, 2017; Uzun *et al.*, 2010). The pyrolysis gas composition of the chicken-litter waste at the different heating rates are depicted in Fig. 7.3. The results demonstrated that CO, H2 and CH4 were the main gas components throughout the process. As shown in Fig. 7.3, CO and H2 substantially increased from 32 to 42 %, and from 29 to 38 %, respectively, when the heating rate increased from 10 to 50°C/s. On the contrary, the CH4 production remarkably decreased from 24 to 9 %. At the same time C2H6 contents slightly decreased from 5 to 2 %. The substantial increase in CO and H2 with rise in the heating rate from 10 to 50°C/s suggested that a rapid heating during the pyrolysis process enhanced the secondary cracking of oxygenates and promoted the decarbonylation reactions to release CO gas. Higher concentration of CH4 at 10°C/s, which decreased to its minimum value of 6 % at 500°C/s, was caused by the water shift and steam reforming reactions.

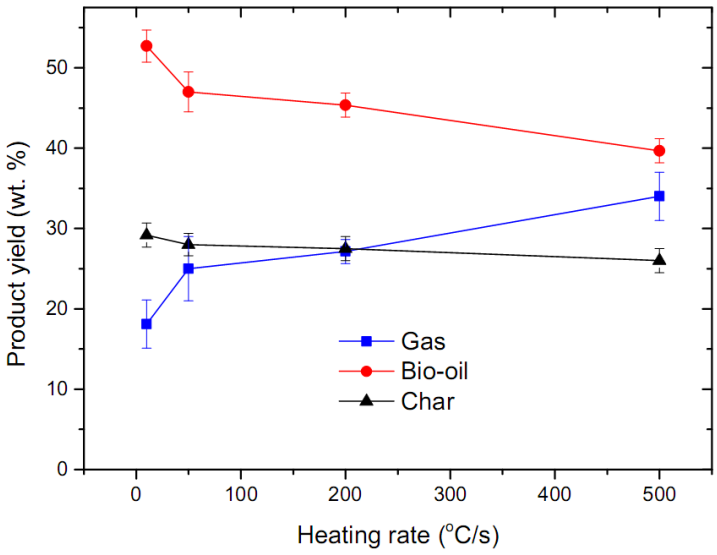

Figure 7-2 Product yields of chicken-litter waste pyrolysis formed at different heating rates to plateau temperature of 1200°C (error bars indicate standard deviation of 3 repeated experiments)

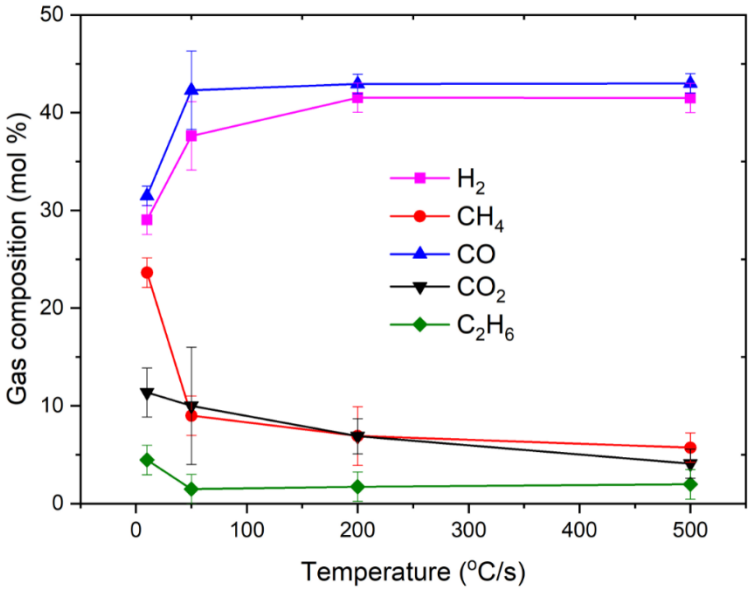

Figure 7-3 Gas composition of chicken-litter waste pyrolysis formed at different heating rates to plateau temperature of 1200°C (error bars indicate standard deviation of 3 repeated experiments)

As reported by Newalkar *et al.* (2014), these types of reactions reach equilibrium at 800 to 1200°C pyrolysis temperatures if the heating rate is low or at longer residence time. A further increase in the heating rate to 200 and 500°C/s did not bring significant difference to the gas composition. These results agree with the reports by Li *et al.* (2016), who demonstrated that the most significant influence of heating rate on the gas composition occurs in heating rates between 10 and 50°C/s.

Table 7-2 shows the higher heating values of the total and individual gas components. The HHVs of the individual gases revealed remarkable changes as the heating rate increased from 10 to 50°C/s. Specifically, the HHVs of H_2 and CO increased by more than two-fold, from 764 ± 31 kJ/kg to 1641 ± 166 kJ/kg and from 827 ± 26 to 1840 ± 188 kJ/kg, respectively. Whereas the HHVs of CH_4 and C_2H_6 substantially decreased from 1948 ± 97 to 742 ± 212 kJ/kg and from 644 ± 26 to 361 ± 52 kJ/kg as the heating rate increased from 10 to 50°C/s. However, a further increase in the heating rate slightly increased the HHVs but was not significant. The highest total gas HHV (6402 ± 810 kJ/kg) was achieved at 500°C/s. The H_2 to CO ratio, which was almost unity for all heating rates, confirms that the pyrolysis gases produced in this form can have better performance in engines but at the expense of higher NO_x emissions (Sahoo *et al.*, 2012).

Table 7-2 Higher heating values and H2 to CO ratio of the pyrolysis gases at 1200°C final pyrolysis temperature, expressed based on the biomass weight (the uncertainties represent standard deviation of the mean value of 3 repeated experiments)

Heating rates (°C/s)	HHV (kJ/kg)					H_2/CO
	(H_2)	(CH_4)	(CO)	(C_2H_6)	Total	
10	764 ± 31	1948 ± 97	827 ± 26	644 ± 161	4182 ± 315	0.92
50	1641 ± 166	742 ± 212	1840 ± 188	361 ± 52	4585 ± 618	0.9
200	1828 ± 52	953 ± 491	1885 ± 45	418 ± 104	5083 ± 692	0.97
500	2328 ± 67	983 ± 218	2499 ± 58	592 ± 467	6402 ± 810	0.97

7.3.2 Influence of plateau temperature on the product yield and gas composition

Fig. 7.4 shows the measured product yields as a function of plateau pyrolysis temperature at 50°C/s. Chicken-litter waste with 280 µm particles size, packed into cylindrical pellets of 10 mm in diameter and 5 mm length was used as biomass feedstock. As shown in Fig. 7.4, 800°C produced a maximum bio-oil yield of 48 wt. %, which continuously decreased with further increase in temperature, producing a minimum yield of 41 wt. % at 1600°C. Similarly, the char yield was sharply reduced from 42 wt. % at 800°C to 18 wt. % at 1600°C. This is attributed to the greater primary decomposition of the biomass or secondary decomposition of the char residue with increasing temperatures. On the other hand, the gas yield was constantly increased from its minimum yield of 10 wt. % at 800°C to its maximum yield of 39 wt. % at 1600°C. The trend is consistent with the results obtained from the solar pyrolysis of beech wood pellets in the same range of temperatures (Zeng *et al.*, 2015). Upon increasing the temperature, the reaction between the vapor and char phase was dominant. Moreover, secondary reactions of heavy molecular weight compounds were high which can cause the char and bio-oil yields to decrease, while increasing the gas yield (Salehi *et al.*, 2011). Gas composition of the chicken litter waste pyrolysis at temperature ranges between 800 to 1600°C and heating rate of 50°C/s is shown in Fig. 7.5. The effect of temperature was mainly observed in the evolution of CO, H_2 and CO_2. CO and H_2 were the dominant products with maximum molar yields of 46 and 48 % at 1600°C, respectively.

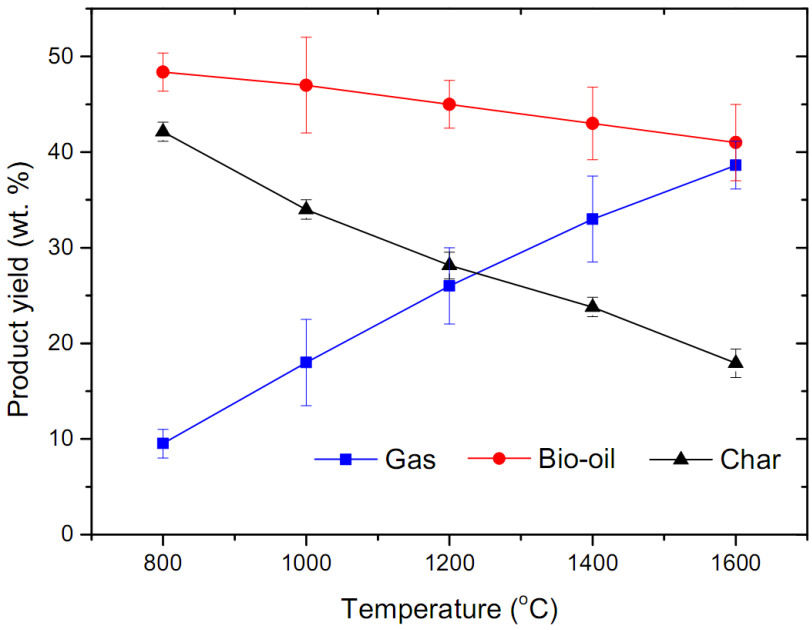

Figure 7-4 Product yield of chicken-litter waste pyrolysis formed at different final temperatures and 50°C/s heating rate (error bars indicate standard deviation of 3 repeated experiments)

The increase in H_2 with temperatures can be associated to the cracking of all condensable and non-condensable products at higher temperatures (Zhao *et al.*, 2010), while the increase in CO content was due to the reverse Boudouard reaction at higher temperatures (Becidan *et al.*, 2007) which was also responsible for substantially depleting the CO_2 content from 38 to 2 %, as shown in Fig. 7.5. There were no appreciable changes to the contents of CH_4 and C_2H_6.

Table 7-3 shows the higher heating values (HHVs), expressed based on the biomass weight, and H_2 to CO ratio of the pyrolysis gases obtained from chicken litter at temperatures ranging from 800 to 1600°C and 50°C/s. The HHVs of most gases and hence the total gas heating values increased with rise in temperature. The higher heating values of H_2 and CO at the lowest temperature (800°C) were 305 ± 11 and 262 ± 102 kJ/kg and continuously increased with temperature to the maximum values of 2798 ± 140 and 3066 ± 153 kJ/kg respectively at 1600°C. Similarly, the highest HHV of the total gas increased linearly from 838 ± 48 at 800°C to 7255 ± 566 kJ/kg at 1600°C, due to the increased yield of H_2 and CO with temperature. The highest HHV of CH_4 (916 ± 458 kJ/kg) was obtained at 1400°C and decreased to 865 ± 247 kJ/kg at 1600 °C which was attributed to the cracking of CH_4 to H_2. The H_2/CO ratio was also affected by temperature. Except at 1200 and 1400°C, this ratio was either equal to one or greater than one (1.1).

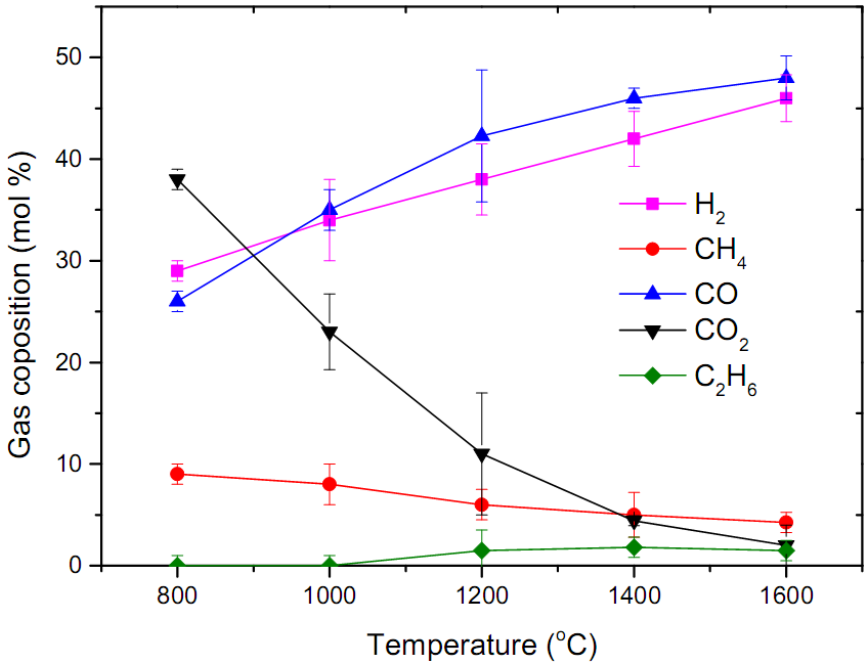

Figure 7-5 Gas composition of chicken-litter waste pyrolysis produced at different final temperatures and 50°C/s (error bars indicate standard deviation of 3 repeated experiments)

Table 7-3 Higher heating values and H2 to CO ratio of the pyrolysis gases formed from chicken litter at different final temperatures and 50°C/s (the uncertainties represent standard deviation of the mean value of 3 repeated experiments)

Temperature (°c)	H_2	CH_4	CO	C_2H_6	total	H_2/CO
	Higher heating value (kJ/kg)					
800	305 ± 11	271 ± 27	262 ± 10	0	838 ± 48	1.1
1000	852 ± 95	698 ± 174	840 ± 49	0	2390 ± 318	1
1200	1641 ± 149	742 ± 247	1841 ± 263	361 ± 5	4585 ± 665	0.9
1400	2283 ± 126	916 ± 458	2561 ± 100	511 ± 26	6272 ± 611	0.9
1600	2798 ± 140	865 ± 247	3066 ± 153	526 ± 26	7255 ± 566	1.1

7.3.3 Influence of biomass type on the yield and gas composition

Chicken-litter waste and rice husk samples with 280 µm particle sizes were pyrolysed in the temperature ranges 800–1600°C at 50°C/s to determine the influence of biomass type on the yield and composition of the evolved volatiles. The product yields of pyrolysis of these two biomass samples under the concentrated solar radiation are shown in Fig. 7.6. The results demonstrated that variations to the product yields with respect to biomass type were insignificant. It can be seen that the lowest gas yields, 12 wt. % for chicken litter and 10 wt. % for rice husk, were obtained at 800°C and increased to 39 and 39 wt. %, respectively at 1600°C. However, a remarkable difference was observed in the char and bio-oil yields, especially at high pyrolysis temperatures. It was further noticed that bio-oil yields produced from the chicken litter sample were higher than those of the rice husk at all pyrolysis temperatures (maximum difference being 5 wt. % at 1400°C). Contrary to the bio-oil, the char yields from the rice husk pyrolysis were higher than the chars from the chicken litter pyrolysis at almost all temperatures. The highest variation between the char yields produced from rice husk and chicken litter was 7 wt. %, recorded at 1400°C.

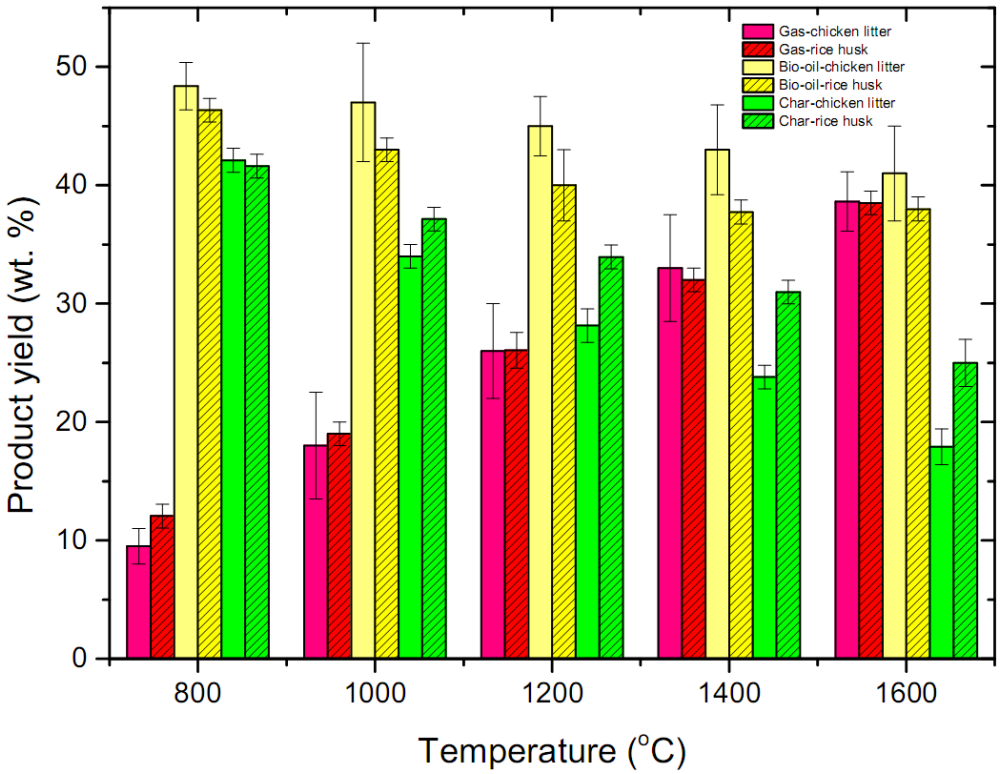

Figure 7-6 Product distribution from the pyrolysis of chicken litter and rice husk (280 µm sizes) at 50°C/s and different temperatures (error bars indicate standard deviation of 3 repeated experiments)

The opposite trends of the bio-oil and char yields from the two samples can be related to the volatile content of the feedstock, which was 63 % in the chicken litter sample and 55 % in the rice husk (Table 7-1). Feedstock with high volatile contents have higher volatility and reactivity advantages which favor bio-oil production. The higher char yield produced from the rice husk pyrolysis is linked to the higher lignin content of the rice husk (Wang *et al.*, 2016) compared to the chicken-litter waste. A high lignin content contributes to production of higher char yields (Guedes *et al.*, 2018). Table 7-4 shows the composition of pyrolysis gases obtained with the 280 µm particle size of rice husk and chicken litter. There were significant differences in H_2, CO and CO_2 production at the lower ranges of pyrolysis temperatures (800 and 1000°C) with differences decreasing as the temperature increased and there were almost the same molar yields at 1600°C for both biomass samples. The H_2, CO and CO_2 productions from the rice husk sample at 800°C were 13 ± 1.5 %, 49 ± 1.5 % and 25 ± 1.5 %, respectively. The H_2 and CO_2 productions from chicken litter sample were 29 ± 1 % and 38 ± 1, respectively, while the CO production (26 ± 1 wt. %) was smaller than the rice husk. As the temperature increased to 1000°C, these differences were observed to reduce and with further increase in the pyrolysis temperature the gas compositions were almost the same for both biomass samples. The difference in the gas composition could arise from the proteins, fats and carbohydrates components of the biomasses. It is known that chicken litter has higher content of proteins and fats (Weldekidan *et al.*, 2018a). Pyrolysis of these materials can produce significant amount of CO_2 as compared to the pyrolysis of rice husk, which has higher lignin content than chicken litter (Azargohar *et al.*, 2013). The higher H_2 production with the rice husk at 800 and 1000°C could also be explained by the higher lignin content of the biomass; it is known that lignin produces more H_2 (Li *et al.*, 2016).

Table 7-4 Gas composition from rice husk and chicken litter pyrolysis at 800 to 1600°C and 50°/s heating rate (the uncertainties represent standard deviation of the mean value of 3 repeated experiments)

Temperature (°C)	(H_2) [mol %]		(CH_4) [mol %]		(CO) [mol %]		(CO_2) [mol %]		(C_2H_6) [mol %]	
	Rice husk	Chicken litter	Rice husk	Chicken litter	Rice husk	Chicken litter	Rice husk	Chicken litter	Rice husk	Chicken litter
800	13 ±1.5	29 ±1	12 ±1.5	9 ±1	49 ±1.5	26 ±1	25 ±1.5	38 ±1	0	0
1000	24±1.5	34 ±4	10 ±1.5	8 ±2	44 ±1.5	35 ±2	15 ±1.5	23 ±3.7	0	0
1200	33 ±1.5	38 ±3.5	8 ±1.5	6 ±1.5	44 ±1.5	42 ±3.5	8 ±2	11 ±3	1 ±1	2 ±1.5
1400	42 ±2.5	42 ±2.7	6 ±1.5	5 ±2.2	46 ±1.5	46 ±1	6 ±1.6	4 ±0.5	1 ±1	2 ±1
1600	50 ±2	46 ±2.3	5 ±1.5	4 ±1	49 ±1.5	48 ±2.1	4 ±1.5	2 ±2	2 ±0.5	2 ±1

Table 7-5 shows the higher heating value and H_2 to CO ratio of the pyrolysis gases formed from the pyrolysis of rice husk at 800 to 1600°C and 50°C/s heating rates. Compared to the HHVs of the pyrolysis gases from chicken-litter waste under similar operating parameters (Table 7-3), the total gas HHVs slowly increased with temperature. For example, the total gas HHV from the rice husk at 800 °C was 1271 ± 140 kJ/kg and slightly increased to its highest value of 7198 ± 531 kJ/kg at 1600 °C; whereas the total gas HHV from the chicken litter at 800 °C was 838 ± 48 kJ/kg and sharply increased to 7255 ± 566 kJ/kg at 1600 °C. The changes in CO production from rice husk at higher ranges of temperature were not considerable (Table 7-4), hence the changes in the HHVs of the gas from rice husk were also not as significant as the HHVs of the gas obtained from the chicken litter. The H_2 to CO ratio showed significant variation with temperature from 0.3 at 800°C to 1 at 1600°C. This was due to the higher rate of H_2 production with temperature.

Table 7-5 Higher heating values and H2 to CO ratio of the pyrolysis gases formed from rice husk at different final pyrolysis temperatures and 50°C/s heating rate (the uncertainties represent standard deviation of the mean value of 3 repeated experiments)

Temperature (°c)	H_2	CH_4	CO	C_2H_6	total	H_2/CO ratio
	Higher heating value (kJ/kg)					
800	166 ± 18	490 ± 54	615 ± 15	0	1271 ± 140	0.3
1000	768 ± 38	927 ± 116	1109 ± 28	0	2805 ± 183	0.5
1200	1628 ± 54	1065 ± 213	1797 ± 47	597 ± 52	5087 ± 366	0.8
1400	2107 ± 105	1018 ± 255	2325 ± 58	298 ± 50	5748 ± 423	0.9
1600	2602 ± 104	916 ± 305	3150 ± 75	531 ± 47	7198 ± 531	1

7.3.4 Influence of particle size on the yield and composition of pyrolysis products

Table 7-6 shows product yields for the pyrolysis of rice husk at the plateau temperatures of 800, 1200 and 1600°C, respectively and at a heating rate of 50°C/s for the rice husk particle sizes of 280 and 500 µm. Smaller biomass particles exhibit higher surface to volume ratio, which favors the fast rate of heat transfer than the larger particles. Higher gas and bio-oil yields can be expected from the biomass with smaller particle sizes in fast pyrolysis processes (Sensoz *et al.*, 2006). In this work, the bio-oil yield slightly increased from 44 to 46 wt. % with decreasing the particle size. In contrast, an increasing trend of gaseous yields from 12 to 20 wt. %, and a decreasing char yield from 41.6 to 36.59 wt. % was noticed as the particle size

increased from 280 to 500 µm. These changes could be explained by the low bulk density and wider intra particle voids of the larger particles and associated heat transfer advantages which could facilitate the diffusion of gaseous products and thermal cracking of the chars into small molecule gases. Pyrolysis of both biomass samples at 1200 and 1600°C did not bring any significant difference to the gas, bio-oil and char yields. This observation is in broad agreement with the findings reported in literature (Kang *et al.*, 2006; Kersten *et al.*, 2005; Shen *et al.*, 2009).

Table 7-7 presents the influence of rice husk particle size on the distribution of pyrolysis gases. The experiment was conducted at three temperatures (800, 1200 and 1600°C) at a heating rate of 50°C/s with 280 and 500 µm particle sizes. It is shown that the biomass particle size had little effect on the distribution of the pyrolysis gases. The highest effect was observed on the H_2 content at 1600 °C. The 280 and 500 µm rice husk produced about 50 % and 41 % H_2, respectively. Similarly, with increasing the particle size from 280 to 500 µm, the CO_2 content decreased from 25 to 17 % but the H_2 was observed to increase from 13 to 19 % at the 800°C.

Table 7-6 Product yields from the pyrolysis of rice husk with 280 and 500 µm particle sizes at 800 to1600°C pyrolysis temperatures and 50°C/s heating rate (error was less than 5 %)

Temperature (°C)	Particle size (µm)					
	280	500	280	500	280	500
	Pyrolysis gas (wt.%)		Bio-oil (wt.%)		Bio-char (wt.%)	
800	12	20	46	44	42	37
1200	26	26	40	41	34	32
1600	39	37	38	38	25	25

Table 7-7 Influence of particle size on the pyrolysis gas composition (the uncertainties represent standard deviation of the mean value of 3 repeated experiments)

Temperature (°C)	Particle sizes (µm)									
	280	500	280	500	280	500	280	500	280	500
	Gas composition [mol %]									
	(H_2)		(CH_4)		(CO)		(CO_2)		(C_2H_6)	
800	13 ±1.5	19 ±1.5	12 ±1.5	14 ±1.5	50 ±1.5	50 ±1	25 ±1.5	17 ±1.5	0	0
1200	33 ±1.5	28 ±1.5	8 ±1.5	12 ±1.5	44 ±1.5	43 ±0.5	8 ±2	14 ±1.5	1±0.5	4 ±1
1600	50 ±2	41 ±1.5	5 ±1.5	4 ±1.5	49 ±1.5	46 ±1	4 ±1.5	6 ±1.5	2 ±0.5	1 ±1.5

Table 7-8 shows the HHVs and H_2 to CO ratio of the pyrolysis gases from the 280 and 500 µm rice husk sample. There was relatively sharp rise with temperature in the HHVs of individual and the total gases from the pyrolysis of the 280 µm size sample as compared to the HHVs of the gases from the rice husk with 500 µm size. The highest total gas heating value from the 280 µm particles substantially increased from 1271 ± 140 kJ/kg at 800°C to 7198 ± 531 at 1600°C. Whereas the lowest and highest HHVs of total gas produced at the same pyrolysis conditions from the 500 µm sample were 2663 ± 141 and 6617 ± 656 kJ/kg, respectively. These differences were due to the combined effects of H_2 and CO produced from the pyrolysis of the 280 µm particle size which have higher production rate at each of the pyrolysis temperatures. The H_2 to CO ratio of the gases from both particle sizes were almost same in all pyrolysis temperatures. Overall, the effect of the feedstock size difference could not affect the HHVs and H_2 to CO ratio of the gas in this study.

Table 7-8 Higher heating values and H2 to CO ratio of the pyrolysis gases formed from rice husk at different final pyrolysis temperatures and 50°C/s heating rate (the uncertainties represent standard deviation of the mean value of 3 repeated experiments)

Temperature (°C)	Particle sizes (µm)											
	280	500	280	500	280	500	280	500	280	500	280	500
	Higher heating values (HHVs) (kJ/kg)										H_2/CO	
	H_2		CH_4		CO		C_2H_6		total			
800	166± 18	457±30	490 ± 54	1041±87	615±15	1165±24	0	0	1271±140	2663±141	0.3	0.4
1200	1628± 4	852±34	1065±213	1118±140	1797±47	1336±17	597±52	577±115	5087±366	3883±306	0.8	0.6
1600	2602±99	2640±76	916±305	721±288	3150±75	2788±62	531±47	460±230	7198±531	6617±656	1	0.9

7.4 Conclusion

Solar pyrolysis of chicken-litter waste and rice husk of different particel sizes was performed at different heating rates and temperatures. Temperature and lower ranges of heating rates (10 to 50°C/s) were found to have significant influence on the yield and composition of pyrolysis products. The highest bio-oil yield of 53 wt. % was achieved from the pyrolysis of 280 µm particle size chicken-litter waste at 1200 °C and at a heating rate of 10 °C/s; whereas maximum yields of bio-oil (39 wt. %) and char (42 wt. %) were obtained at 1600°C and 800°C, respectively at a heating rate of 50°C/s. It was further noticed that the contents of CO and H_2 increased with rise in temperature for both biomass types and particle sizes. Similarly, the HHVs of the total gases increased with temperature in all pyrolysis conditions. Bio-oil yields

produced from chicken litter were greater than the bio-oils from the rice husk through out the pyrolysis temperature; whereas char yields obtained from rice husk were greater than the chicken litter by a maximum of 7 wt.%. Variations in gas yield and compositon with respect to particle sizes were insignficant in this study. The highest H_2/CO ratio of mostly produced gases were around 1, which confirms that the pyrolysis gases produced in this work can be utilized to run engines or power plants.

Acknowledgements

This work was supported by the French "Investments for the future" programme managed by the National Agency for Research under contracts ANR-10-LABX-22-01-SOLSTICE and ANR-10-EQPX-49-SOCRATE.

7.5 References

Akhtar, J., & Saidina Amin, N. (2012). A review on operating parameters for optimum liquid oil yield in biomass pyrolysis. *Renewable and Sustainable Energy Reviews, 16*(7), 5101-5109.

Arribas, L., Arconada, N., González-Fernández, C., Löhrl, C., González-Aguilar, J., Kaltschmitt, M., & Romero, M. (2017). Solar-driven pyrolysis and gasification of low-grade carbonaceous materials. *International Journal of Hydrogen Energy, 42*(19), 13598-13606.

Ateş, F., Pütün, E., & Pütün, A. E. (2004). Fast pyrolysis of sesame stalk: yields and structural analysis of bio-oil. *Journal of Analytical and Applied Pyrolysis, 71*(2), 779-790.

Azargohar, R., Jacobson, K. L., Powell, E. E., & Dalai, A. K. (2013). Evaluation of properties of fast pyrolysis products obtained, from Canadian waste biomass. *Journal of Analytical and Applied Pyrolysis, 104*, 330-340.

Bashir, M., Yu, X., Hassan, M., & Makkawi, Y. (2017). Modeling and Performance Analysis of Biomass Fast Pyrolysis in a Solar-Thermal Reactor. *ACS Sustainable Chemistry & Engineering, 5*(5), 3795-3807.

Becidan, M., Skreiberg, Ø., & Hustad, J. E. (2007). Products distribution and gas release in pyrolysis of thermally thick biomass residues samples. *Journal of Analytical and Applied Pyrolysis, 78*(1), 207-213.

Chen, G., Yu, Q., & Sjöström, K. (1997). Reactivity of char from pyrolysis of birch wood. *Journal of Analytical and Applied Pyrolysis, 40-41*, 491-499.

Chintala, V. (2018). Production, upgradation and utilization of solar assisted pyrolysis fuels from biomass – A technical review. *Renewable and Sustainable Energy Reviews, 90*, 120-130.

Gómez, N., Banks, S. W., Nowakowski, D. J., Rosas, J. G., Cara, J., Sánchez, M. E., & Bridgwater, A. V. (2018). Effect of temperature on product performance of a high ash biomass during fast pyrolysis and its bio-oil storage evaluation. *Fuel Processing Technology, 172*, 97-105.

Guedes, R. E., Luna, A. S., & Torres, A. R. (2018). Operating parameters for bio-oil production in biomass pyrolysis: A review. *Journal of Analytical and Applied Pyrolysis, 129*, 134-149.

Kang, B.-S., Lee, K. H., Park, H. J., Park, Y.-K., & Kim, J.-S. (2006). Fast pyrolysis of radiata pine in a bench scale plant with a fluidized bed: Influence of a char separation system and reaction conditions on the production of bio-oil. *Journal of Analytical and Applied Pyrolysis, 76*(1), 32-37.

Kersten, S. R. A., Wang, X., Prins, W., & van Swaaij, W. P. M. (2005). Biomass Pyrolysis in a Fluidized Bed Reactor. Part 1: Literature Review and Model Simulations. *Industrial & Engineering Chemistry Research, 44*(23), 8773-8785.

Lars, W., & Nilsson, T. (2001). *Heating value of gases from biomass gasification. A report prepared for: IEA Bioenergy Agreement, Task 20 - Thermal Gasification of Biomass, Nyköping, Sweden*. Retrieved from www.ieatask33.org/app/webroot/files/file/publications/HeatingValue.pdf+&cd=1&hl=en&ct=clnk&gl=au

Li, R., Zeng, K., Soria, J., Mazza, G., Gauthier, D., Rodriguez, R., & Flamant, G. (2016). Product distribution from solar pyrolysis of agricultural and forestry biomass residues. *Renewable Energy, 89*, 27-35.

Luo, S., Xiao, B., Hu, Z., & Liu, S. (2010). Effect of particle size on pyrolysis of single-component municipal solid waste in fixed bed reactor. *International Journal of Hydrogen Energy, 35*(1), 93-97.

Morf, P., Hasler, P., & Nussbaumer, T. (2002). Mechanisms and kinetics of homogeneous secondary reactions of tar from continuous pyrolysis of wood chips. *Fuel, 81*(7), 843-853.

Newalkar, G., Iisa, K., D'Amico, A. D., Sievers, C., & Agrawal, P. (2014). Effect of Temperature, Pressure, and Residence Time on Pyrolysis of Pine in an Entrained Flow Reactor. *Energy & Fuels, 28*(8), 5144-5157.

Omar, R., Idris, A., Yunus, R., Khalid, K., & Aida Isma, M. I. (2011). Characterization of empty fruit bunch for microwave-assisted pyrolysis. *Fuel, 90*(4), 1536-1544.

Sahoo, B. B., Sahoo, N., & Saha, U. K. (2012). Effect of H2:CO ratio in syngas on the performance of a dual fuel diesel engine operation. *Applied Thermal Engineering, 49*, 139-146.

Salehi, E., Abedi, J., & Harding, T. (2011). Bio-oil from Sawdust: Effect of Operating Parameters on the Yield and Quality of Pyrolysis Products. *Energy & Fuels, 25*(9), 4145-4154.

Sensoz, S., Demiral, I., & Ferdi Gercel, H. (2006). Olive bagasse (Olea europea L.) pyrolysis. *Bioresour Technol, 97*(3), 429-436.

Shen, J., Wang, X.-S., Garcia-Perez, M., Mourant, D., Rhodes, M. J., & Li, C.-Z. (2009). Effects of particle size on the fast pyrolysis of oil mallee woody biomass. *Fuel, 88*(10), 1810-1817.

Soria, J., Zeng, K., Asensio, D., Gauthier, D., Flamant, G., & Mazza, G. (2017). Comprehensive CFD modelling of solar fast pyrolysis of beech wood pellets. *Fuel Processing Technology, 158*, 226-237.

Uzun, B. B., Apaydin-Varol, E., Ateş, F., Özbay, N., & Pütün, A. E. (2010). Synthetic fuel production from tea waste: Characterisation of bio-oil and bio-char. *Fuel, 89*(1), 176-184.

Wang, X., Lv, W., Guo, L., Zhai, M., Dong, P., & Qi, G. (2016). Energy and exergy analysis of rice husk high-temperature pyrolysis. *International Journal of Hydrogen Energy, 41*(46), 21121-21130.

Weldekidan, H., Strezov, V., Kan, T., & Town, G. (2018a). Waste to Energy Conversion of Chicken Litter through a Solar-Driven Pyrolysis Process. *Energy & Fuels, 32*(4), 4341-4349.

Weldekidan, H., Strezov, V., & Town, G. (2018b). Review of solar energy for biofuel extraction. *Renewable and Sustainable Energy Reviews, 88*, 184-192.

Weldekidan, H., Strezov, V., Town, G., & Kan, T. (2018c). Production and analysis of fuels and chemicals obtained from rice husk pyrolysis with concentrated solar radiation. *Fuel, 233*, 396-403.

Wu, H., Gauthier, D., Yu, Y., Gao, X., & Flamant, G. (2018). Solar-Thermal Pyrolysis of Mallee Wood at High Temperatures. *Energy & Fuels, 32*(4), 4350-4356.

Yadav, D., & Banerjee, R. (2016). A review of solar thermochemical processes. *Renewable and Sustainable Energy Reviews, 54*, 497-532.

Zeng, K., Gauthier, D., Li, R., & Flamant, G. (2015). Solar pyrolysis of beech wood: Effects of pyrolysis parameters on the product distribution and gas product composition. *Energy, 93*, 1648-1657.

Zeng, K., Gauthier, D., Minh, D. P., Weiss-Hortala, E., Nzihou, A., & Flamant, G. (2017a). Characterization of solar fuels obtained from beech wood solar pyrolysis. *Fuel, 188*, 285-293.

Zeng, K., Gauthier, D., Soria, J., Mazza, G., & Flamant, G. (2017b). Solar pyrolysis of carbonaceous feedstocks: A review. *Solar Energy, 156*, 73-92.

Zhai, M., Wang, X., Zhang, Y., Dong, P., & Qi, G. (2015). Characteristics of rice husk tar pyrolysis by external flue gas. *International Journal of Hydrogen Energy, 40*(34), 10780-10787.

Zhao, B., Zhang, X., Sun, L., Meng, G., Chen, L., & Xiaolu, Y. (2010). Hydrogen production from biomass combining pyrolysis and the secondary decomposition. *International Journal of Hydrogen Energy, 35*(7), 2606-2611.

Chapter 8: Energy conversion efficiency of pyrolysis of chicken litter and rice husk biomass

In this chapter energy conversion potential of the pyrolysis of chicken-litter waste and rice husk using the conventional pyrolysis methods is assessed. The energy balance which is the difference between energy recovered in the pyrolysis products and the energy needed to run the pyrolysis process was determined. The obtained information was applied to determine the general efficiency of a solar-assisted pyrolysis process.

The idea of this work was initiated by Prof Vlad then designed and developed by Prof. Graham and myself. Experiments were performed by myself and Jing, while Ravinder, Samuel, Israel, Sayka and Tao have participated in editing and reviewing the manuscript for publication. Results have been compiled and published in Energy and fuels journal.

Author contribution summary for this paper

	W.H	S.V	T.G	K.T	K.R	H.J	R.L	G.F
Experiment Design	•							
Sample Preparation	•							
Data Collection	•							
Analysis	•	•						
Manuscript	•	•	•	•	•	•	•	•

Publication:

Weldekidan, H. (70%), Strezov, V. (10%), He, J. (2.5%), Kumar, R. (2.5%), Asumadu-Sarkodie, S. (2.5), Doyi, I. (1.5%), Jahan, S. (1%), Kan, T. (2.5%), Town, G. (7.5%). "Energy conversion efficiency of pyrolysis of chicken litter and rice husk biomass", ***Energy & fuels (2019),*** *https://doi.org/10.1021/acs.energyfuels.9b01264.*

Adopted with permission from Energy & Fuels, Energy Conversion efficiency of pyrolysis of chicken litter and rice husk biomass, Haftom Weldekidian, Vladimir Strezov, Jing He, Ravinder Kumar, Samuel Asumadu-Sarkodie, Israel Doyi, Sayka Jahan, Tao kan and Graham Town, publication date May 1, 2019 American Chemical Society. Copyright permission letter is included in appendix IV.

Energy conversion efficiency of pyrolysis of chicken litter and rice husk biomass

Haftom Weldekidan[1], Vladimir Strezov[1*], Jing He[1], Ravinder Kumar[1], Samuel Asumadu Sarkodie[1], Israel Doyi[1], Sayka Jahan[1], Tao Kan[1], Graham Town[2]*

[1] Department of Environmental Sciences, Faculty of Science & Engineering, Macquarie University, Sydney, NSW 2109, Australia

[2] School of Engineering, Faculty of Science & Engineering, Macquarie University, Sydney, NSW 2109, Australia

*Email: haftom.weldekidan@hdr.mq.edu.au; Phone: +61 452 363828

*Email: vladimir.strezov@hdr.mq.edu.au

Abstract

Pyrolysis is a well-established method of converting biomass to different types of value-added products, such as high energy density biofuels and chemicals. In this work, chicken-litter waste and rice husk were pyrolysed at different temperatures with the aim of investigating the thermal behaviour and energy recovery potential of the feedstocks. Computer-aided thermal analysis and thermogravimetric analysis were employed to study the pyrolysis properties of each biomass in a temperature-controlled regime. The specific heats of chicken litter and rice husk samples during their pyrolysis and the energy content of their pyrolysis products were investigated to determine the energy required to complete the pyrolysis of each sample and the energy recovery potential of each pyrolytic product. Most of the volatile products were evolved at 350 to 450°C with CO_2, CO and CH_4 being the dominant gas products from both samples throughout the pyrolysis process. At 500°C and at a heating rate of 10°C/min, the gas, bio-oil and char yields from chicken litter and rice husk were in the ranges of 18 to 19, 35 to 39 and 42 to 47 wt %, respectively, with a total recoverable energy value of 12.7 MJ/kg from chicken litter and 13.9 MJ/kg from rice husk. The energy consumed to heat the samples to the final pyrolysis temperature of 500°C was also estimated to be 1.2 and 0.8 MJ per kilogram of chicken litter and rice husk, respectively. With the measured values, the efficiency of the pyrolysis of chicken litter and rice husk samples is estimated to be 84% and 89%, respectively,

assuming the heat required to carry out the pyrolysis process is supplied by combustion of the evolved pyrolytic gas products. If the pyrolysis is instead driven by solar thermal energy, the overall efficiency will increase to 92% for the chicken litter and 94% for the rice husk pyrolysis.

Keywords: biomass energy, pyrolysis products, biofuels, thermochemical conversion, specific heat

8.1 Introduction

Global climate change and associated environmental concerns have triggered ongoing research to produce clean and renewable sources of energy. Biomass is an attractive source of renewable energy which can be converted to bio-fuels (gas, bio-oil, and bio-char) through the thermochemical conversion process. Bio-fuels offer many advantages over fossil-based fuels, including reliability of supply, fuel diversity, greenhouse gas (GHG) reduction, carbon sequestration and increased investment in plant and equipment (Balat, 2011). Similarly, solar energy is another attractive and unlimited source of renewable energy with a potential net zero carbon footprint (Bashir *et al*., 2017; Weldekidan *et al*., 2019). Clearly, integration of these two most abundant and renewable sources of energy could bring significant solutions to the ongoing energy crisis and increasing concern over global warming (Chintala, 2018; Weldekidan *et al*., 2018b). One of the basic paths of technologies that can combine biomass with solar energy is the thermochemical conversion process, such as pyrolysis. Fuels of high heating values can be sufficiently produced from biomass pyrolysis (Kumar *et al*., 2016). Pyrolysis is one of the most developed technologies that can be applied to achieve the thermal decomposition of biomass without oxygen and produce pyrolysis gas, bio-oil, and bio-char of high energy value (Chen et al., 2019; Karaca *et al*., 2018; Li *et al*., 2014; Strezov *et al*., 2003b). Pyrolysis gases are valuable products for power and heat generation in engines and power plants and the bio-char can be used for the preparation of activated carbon and as a soil amendment due to its high surface area (Auta *et al*., 2014). Bio-char is also resistant to decomposition and mineralization and thus can lock carbon in a stable form (He et al., 2019; Kumar *et al*., 2019b; Vardon *et al*., 2013). The bio-oil is a dark brown liquid which is viscous, highly corrosive and oxygenated compound and can be used to produce energy by direct combustion or can be treated thermally to produce high calorific value synthetic fuels (Abu Bakar & Titiloye, 2013; Kumar *et al*., 2019a). With simple downstream treatments, the bio-oil can be used as an additive for refined petroleum feedstocks, gas turbines and can also be applied to produce useful chemicals (Abu Bakar *et al*., 2013).

Biomass can also be directly combusted in conventional stoves to generate heat and power, but the efficiency of these systems is very low. Depending on the type of feedstock and stoves used, the combustion efficiency can reach a maximum of 20% (Li *et al*., 2014). Similarly, the efficiency of electricity production from stationary power plants with direct combustion of biomass is only 30% (Viana *et al*., 2010). Energy generation from biomass with the conventional pyrolysis processes has limitations. For example, part of the biomass or its pyrolysis products should be combusted to generate process heat, thus reducing the available energy efficiency. Li *et al*., (2014) performed pyrolysis of spent coffee at 500°C and 10°C/min using an electric furnace and the maximum pyrolysis efficiency of 83.4% was found. The authors further reported that the increased heating rate to 60°C/min slightly increased the efficiency to 84.8%. However, the pyrolysis efficiency can be improved by integrating solar-assisted pyrolysis processes during which time the energy required to pyrolyse the biomass is supplied from a solar source (Weldekidan *et al*., 2018a; Werder & Steinfeld, 2000)

It is evident from the previous studies that a conventional and solar-assisted pyrolysis process can be applied to generate different energy carrier products from various biomass feedstocks, which can be further used as fuels for potential applications. However, insufficient information is currently available for comparative assessments of the efficiency of conventional and solar-assisted pyrolysis processes.

Pyrolysis efficiency is the thermal efficiency obtained as the ratio of the difference between the total heating values of the pyrolytic products and the thermal energy required to heat the sample, to the energy contained in the feedstock material measured as higher heating values.

In this work, chicken-litter waste and rice husk samples were pyrolysed at different pyrolysis temperatures using conventional pyrolysis methods and the energy required to heat and pyrolyse the biomass was quantified. The energy contents of the pyrolysis products of these two different types of biomasses were analysed to estimate the total energy generating potential of each feedstock at a specified pyrolysis conditions. The approach was applied to determine and compare efficiencies of conventional and solar-assisted pyrolysis processes under the assumption that solar pyrolysis products are not different to conventional pyrolysis products (Tuller, 2017; Weldekidan *et al*., 2018c) if the same operating conditions are maintained.

8.2 Material and methods

8.2.1 Biomass properties

Chicken litter and rice husk were selected biomass feedstocks for this study. These two feedstock were chosen because chicken litter is a protein and lipid containing waste which is continuously increasing as a result of population increase, while rice husk is a lignocellulosic or carbohydrate based biomass of agricultural byproducts with an annual global capacity of more than 800 million tonnes (Dunnigan *et al*., 2018a). Thus, studying the pyrolysis properties of the feedstocks, besides the energy recovery potentials, could be an interesting approach to waste valorisation and minimization techniques. Samples of these two different types of biomass were prepared by heating the feedstocks in a vacuum oven at 70°C for 2 h and then sieved with a 280 µm sieve size. The proximate analysis of each sample was determined according to the ASTM D7582 test methods whereas the ultimate analysis was performed with a CHNS analyser using Vario MICRO cube elemental analyser (Elementar Analysensysteme GmbH, Germany) with a Windows PC-based data system and an electronic micro balance. Table 8-1 shows the results of the proximate and ultimate analyses of the samples. The nitrogen content of the chicken litter (5.38%) was significantly high compared to the rice husk (0.38%). This was due to the amount of proteins in the chicken litter. The volatile and carbon contents of the chicken litter sample were also higher than in the rice husk sample.

Table 8-1 Proximate and ultimate analysis of chicken-litter and rice husk samples

Proximate analysis %	Chicken-litter waste	Rice husk
Moisture	9.9	6.03
Fixed carbon	10.3	14.1
Volatile matter	62.6	54.5
Ash	27.1	25.3
Ultimate analysis (%) (ash-free)		
Carbon	46.9	34.3
Hydrogen	5.4	5
Nitrogen	5.38	0.38
Sulphur	0.32	0.19
Oxygen (by difference)	42	60.1
Calorific value (MJ/kg)	13.7	14.7

8.2.2 Computer Aided Thermal Analysis (CATA)

Computer Aided Thermal Analysis (CATA) technique was used to determine the specific heat of the samples. The instrument consists of an infrared gold coated furnace and heating elements for heating a packed bed sample of 2.4 cm^3 volume. The sample was placed at the centre of a silica glass tube and supported with glass wool on the sides. Two chromel-alumel (K-type) thermocouples, one at the centre (T1) and the other on the surface (T2) of the sample were used to measure the temperatures of the sample during the heating process. The whole assembly was then inserted into a graphite tube which acts as a heating element to the sample glass tube. Another thermocouple (T3) was embedded in the graphite tube which controlled the heating rate of the process. Figure 8-1 shows the CATA apparatus used for this technique. Heating from the graphite to the sample was predominantly achieved by radiation. To ensure uniform thermal emissivity to the sample, the surface of the glass tube was coated with carbon soot from combusted acetylene. The heating process was set to start from ambient temperature and raise to a maximum temperature of 700°C at a heating rate of 10°C/min. Produced volatiles in the glass tube were continuously removed with argon gas flowing at 5 mL/min. The graphite tube was protected and kept inert with argon gas flowing at 50 mL/min through the sealed section of the furnace. Temperature data obtained from the centre and surface of the sample were applied in an inverse numerical technique to determine the specific heat of the sample. For endothermic reactions, the specific heat had increasing values and in the case of exothermic reactions, the specific heat values decreased. A more detailed explanation on the methods and evaluation techniques of the process can be found in (Strezov *et al.*, 2003a; Strezov *et al.*, 2003b, 2004).

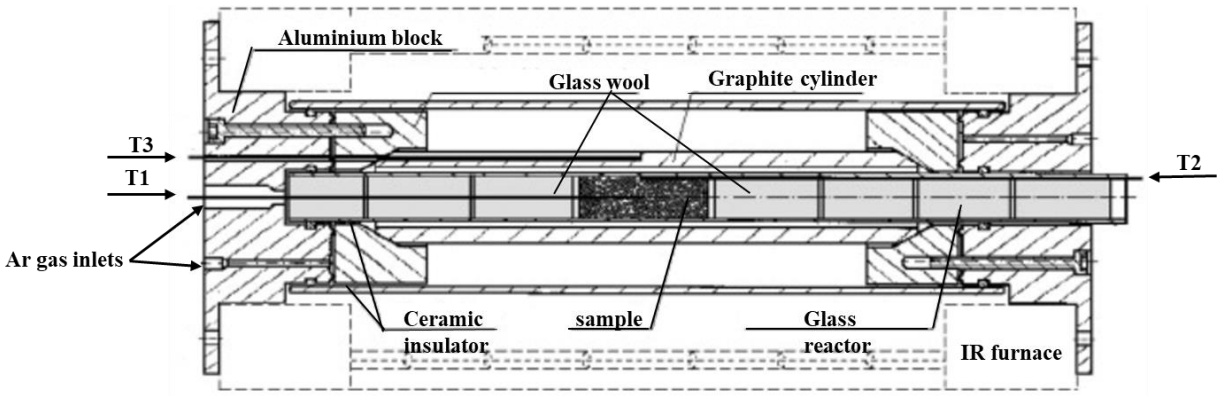

Figure 8-1 Schematic diagram of the CATA apparatus

8.2.3 Thermogravimetric analysis (TGA)

A TGA/DSC 1 STAR^e instrument from Mettler Toledo, Ltd., USA, was employed to analyse the mass loss of the sample during the heating process. Approximately 10 mg of the sample was heated from ambient temperature to 1000°C at 10°C/min under nitrogen gas with a flow rate of 50 mL/min. Each experiment was purged for 20 min before starting the heating process. TGA data were differentiated with respect to temperature to calculate the differential thermogravimetric curves of the samples.

8.2.4 Gas chromatographic (GC) analysis

Pyrolysis gases mainly containing CO_2, CO, H_2, CH_4 as well as other lightweight hydrocarbons were produced with the infrared furnace from 80 mg of sample packed in a similar manner as in the CATA experiment. Ultrahigh purity helium carrier gas flowing at 50 mL/min was passed through the sample bed while heating at 10°C/min to a final temperature of 700°C. Moisture and condensable materials were first removed from the gas using an ice trap, and then the gases were injected to an MTI Activon M200 model micro GC which was equipped with a thermal conductivity detector and two columns. H_2 and CO were separated with a molecular sieve 5A column, heated to 60°C, while a Paraplot U-shaped column at 40°C was used to analyse the CO_2, CH_4, C_2H_4, and C_2H_6 gas components. GC spectra were collected every 1.5 min and converted into a gas evolution rate (in wt. %/min) following the Ideal Gas Law. The total gas yield and individual gas components were determined as a progressive integral of the measured gas evolution rates.

8.2.5 Char and liquid recovery

The char yield at each pyrolysis temperature was estimated from the TGA mass loss while the liquid fraction was obtained by subtracting the initial mass of the feedstock from total char and pyrolysis gas yields obtained at each temperature. The variation in the solid, liquid and gas yields is shown in Table 8-2.

8.2.6 Energy recovery potentials of the pyrolysis products

The energy that can be recovered from all pyrolysis products (solid, liquid and gas) produced at 500°C was further determined. The calorific values of the biomass and bio-char were determined with a IKA C 1 static jacket oxygen bomb calorimeter which operates according to DIN 51900 and ISO 1928 standards. The calorimeter was coupled with a IKA RC 2

recirculating chiller which was set to a working temperature of 21°C and targeted speed pump of 2000 rpm. Both the calorimeter and chiller were from Staufen, Germany. The equipment was first calibrated using benzoic acid with a gross calorific value of 26461 J/g and a 50 J ignition string in excess oxygen under 30 bar. Then around 300 mg of the sample was placed in a crucible in the decomposition vessel (bomb) and connected to the ignition electrode with the 50 J thread. Finally, the lid was screwed on, and the oxygen was injected into the bomb to combust the sample. The resulting amount of the heat, measured in the previously calibrated system, allows the determination of the calorific value of the samples.

The heating value (HHV) of the liquid products produced at 500°C was determined as:

$$HHV_x = 0.35 \times u_C + 1.18 \times u_H - 0.1u_O - 0.02u_N + 0.1 \times u_S - 0.02u_A \qquad (1)$$

where u_s (s = C, H, N, S) are mass fractions (dry basis) of the individual elements obtained from the elemental analysis of the pyrolysis liquid and u_A is the ash content of the samples at 500°C. Equation (1) is a standard formula used to relate the heating values of biomass and pyrolysis products with their elemental analysis. It is a verified and widely applied equation to determine the energy contents of any type of organic material (Bychkov *et al.*, 2017; Pérez-Arévalo *et al.*, 2015). The C, H, N and S contents of the liquid products were analysed with CHNS analyser as described in section 8.2.1. The bio-oil sample for the CHNS analysis was produced using the infrared furnace from 500 mg of sample packed in a similar manner as in the CATA experiment. When the biomass sample was heated at the specified temperature in the reactor, the bio-oil was produced. Produced bio-oil was then carried to the reactor outlet by the pressure of the argon gas and then collected with crucibles for the CHNS analysis. Around 5 mg of the generated bio-oil was filled into a lightweight oxidisable metal container and dropped into a vertical quartz tube of the Vario MICRO cube analyser which was heated to 970°C at a constant flow of pure oxygen. The sample was then passed over several oxidative reagents and catalyst producing CO_2, H_2O, N_2 and sulfur from the elemental carbon, hydrogen, nitrogen, and sulfur of the sample. A standard sample of known elemental composition was used to analyse the CHNS contents of the bio-oil samples.

Similarly, the heating value of the combustible gas was calculated as described by Zhang *et al.* (2011):

$$HHVs = \sum n_i HHV_i \qquad (2)$$

Where n_i is the yield in wt. % and HHV_i is the higher heating values of the combustible gases at standard conditions. The heating value constants of the pyrolysis gases used in the calculation are shown in Table 8-2.

Table 8-2 HHVs constants of pyrolysis gases (Zhang *et al.*, 2011)

Gas	HHV (MJ/kg)
H_2	141
CO	10
CO_2	-
CH_4	56
C_2H_4	50
C_2H_6	52

The overall maximum efficiency of the pyrolysis process of each feedstock at 500°C was determined as:

$$\eta = \frac{Q_{recovered} - Q_{pyrolysis}}{Q_{biomass}} \times 100\% \quad (3)$$

Where

$$Q_{recovered} = HHV_{gas} \times mass_{gas} + HHV_{liquid} \times mass_{liquid} + HHV_{char} \times mass_{char} \quad (4)$$

(Cong *et al.*, 2018), (Piatkowski *et al.*, 2011).

8.3 Results and discussion

8.3.1 Specific heat and pyrolysis gas analysis

The apparent specific heat of the two samples as a function of temperature is represented in Figure 8-2. At room temperature, specific heats of the chicken-litter and rice husk samples were found to be 1.12 and 1 MJ/m^3.K, respectively. Considering the packing densities of the samples, these initial specific heats are equivalent to 2.23 and 1.6 kJ/kg.K, respectively. Both samples have sharp endothermic peaks around 130°C associated with the release of strongly bonded water molecules which remained stable in the sample after drying (Strezov & Evans, 2009). A small peak can be seen between 310 to 334°C followed by relatively sharp exothermic trough around 352°C for both samples. The peak in the chicken litter sample was attributed to the conversion of NH_3 and other N-containing heterocycles to N_2O during pyrolysis (Whitely *et al.*, 2006) while the peak in the rice husk sample was due to the decomposition of hemicellulose and cellulose constituents of the sample. A similar observation was reported by

Strezov *et al*. (2003b) at 330 to 390°C. The specific heat for the rice husk sample was almost stable around 0.8 MJ/m^3.K (1.2 kJ/kg.K) after 400°C, whereas the chicken litter sample showed fluctuations from 1.2 to 1.4 MJ/m^3.K (2.2 to 2.6 kJ/kg.K) at 368 and 465°C but stabilised at ~ 1.2 MJ/m^3.K for higher temperatures. The main endothermic peak at ~ 360°C for the chicken litter sample was mainly due to the degradation of proteins (Chen *et al.*, 2018) while the peaks shown at temperatures > 460°C were entirely from the decomposition of lipids (Bach & Chen, 2017; Bui *et al*., 2016).

Pyrolysis product yields and gas composition of the chicken litter and rice husk samples as a function of temperature are shown in Table 8-3 and Figure 8-3, respectively. The bio-char was continuously decomposed with temperature, generating gas and bio-oil products. The highest bio-oil yields, 39 wt.% from chicken litter and 35 wt.% from the rice husk were achieved at 500°C. At 700°C, the total bio-char yields from the chicken-litter and rice husk samples were 40 and 45 wt.%, and the gas contents were observed to increase with temperature and achieved maximum yields of 22 and 21 wt.%, respectively. This was due to the higher conversion rate of the organic fractions into gas at higher pyrolysis temperatures (Wu *et al*., 2018; Gopu *et al*., 2018). A similar gas production pattern was observed by Dunnigan *et al*., (2018b) during the pyrolysis of agricultural waste at 400°C to 800°C. The dominant volatile species from both samples were CO_2 followed by CO and CH_4. The highest CO_2 and CO evolutions from rice husk occurred at around 350°C which coincided with the exothermic trough of the CATA results. Similarly, CO_2 from the chicken litter peaked at ~ 350°C but the evolution of CO was mostly dominant after 460°C which can be explained by the decomposition of lipids at this temperature range. Generation of hydrocarbons (CH_4, H_2, C_2H_4, and C_2H_6) started after 350°C. As corroborated by Grierson *et al*. (2009); Kan *et al*., (2014); Zhong *et al*., (2012) these compounds are results of secondary cracking of oxygenated compounds including phenolic and oxygenous heterocyclic compounds from the bio-oils.

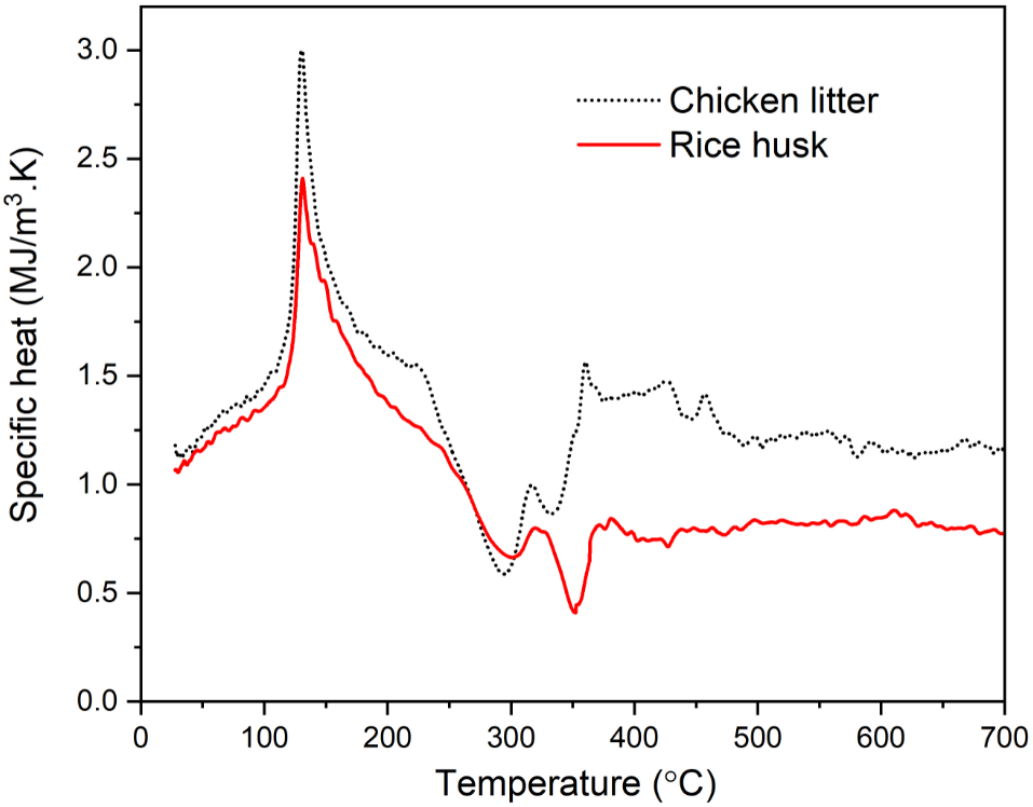

Figure 8-2 Specific heats of chicken litter and rice husk as a function of temperature.

Table 8-3 Solid, liquid and gas fractions with temperature

Temperature	Chicken litter (wt. %)			Rice husk (wt. %)		
(°C)	Solid	Liquid	Gas	Solid	Liquid	Gas
22	100	0	0	100	0	0
100	97	3	0	98	2	0
200	95	5	0	97	3	0
300	76	22	2	84	15	1
400	54	37	9	52	35	13
500	42	39	19	47	35	18
600	42	38	20	46	34	20
700	40	38	22	45	34	21

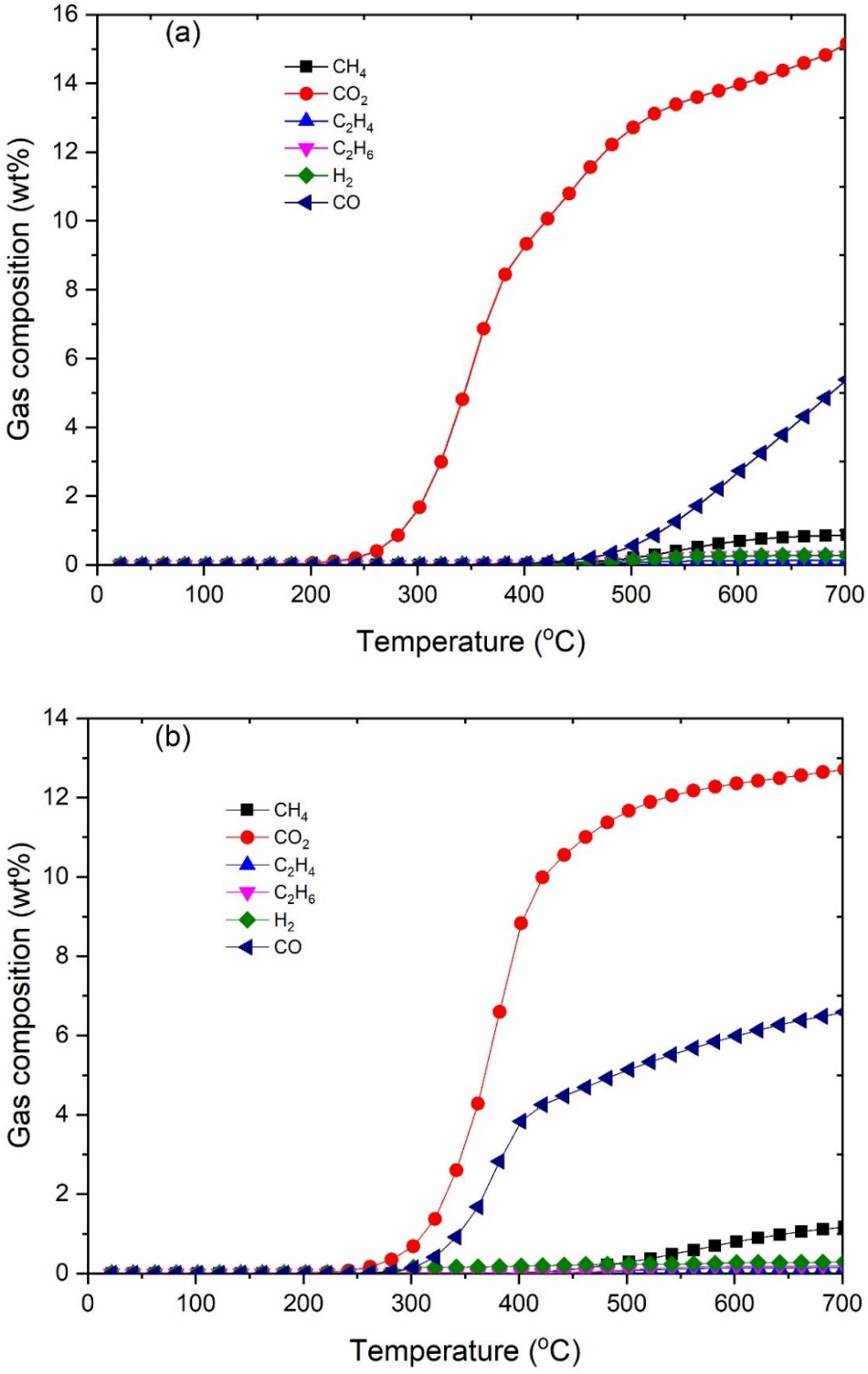

Figure 8-3 Pyrolysis gas composition of the chicken-litter waste (a) and rice husk (b) at different pyrolysis temperatures.

8.3.2 TGA and DTG results

Thermogravimetric (TG) and differential thermogravimetric (DTG) analysis, Figure 8-4, were applied to further investigate the thermal decomposition behaviour of the chicken litter and rice husk samples. The DTG curves of both samples have small peaks between 50 to 150°C, revealing the release of water from the samples (Jayaraman *et al.*, 2018). Their largest peaks, corresponding to the main devolatilization process, occurred between 250 and 450°C. At this stage, the different constituents of the samples (carbohydrate, proteins, and lipids from the chicken litter; and cellulose and hemicellulose from the rice husk) were significantly degraded, contributing approximately to 60 wt.% of the sample mass loss. The chicken litter sample has another small peak at ~ 700°C which was due to the decomposition of lipids and other minor components of the sample (López-González *et al.*, 2015).

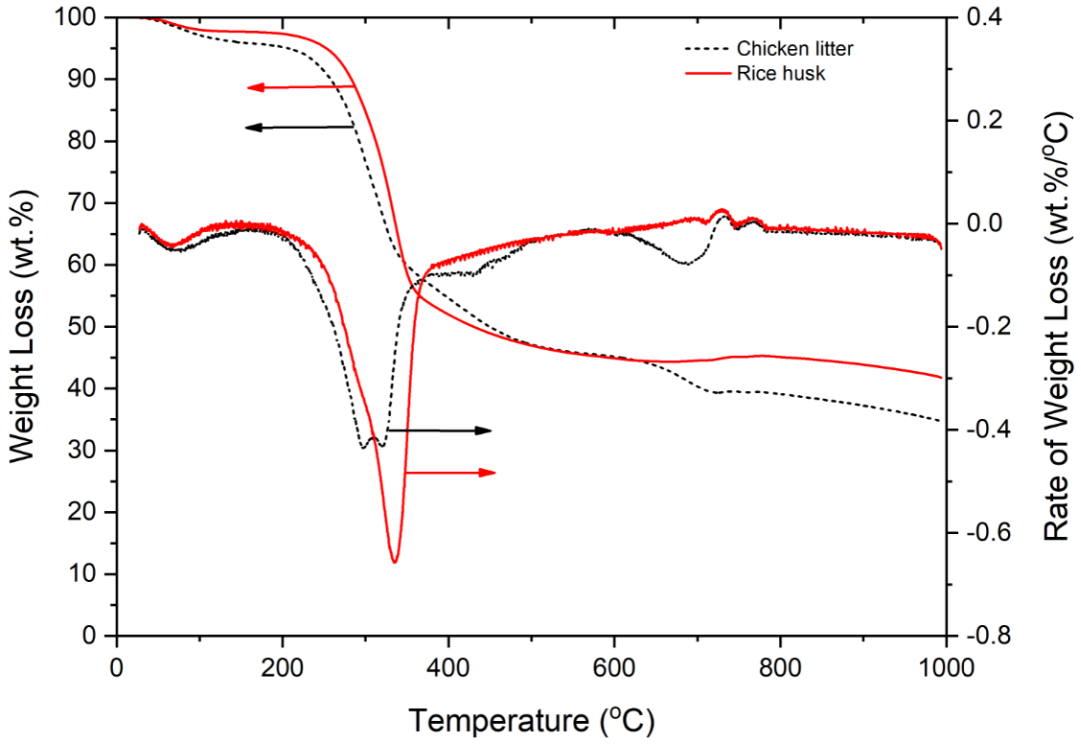

Figure 8-4 TGA and DTG curves of chicken-litter waste and rice husk.

8.3.3 Energy conversion potentials of chicken-litter waste and rice husk with conventional pyrolysis process

Analysis of the measured specific heat of each feedstock and energy contents of their pyrolysis products at different temperatures were applied to determine the potential energy contribution of the pyrolysis process, assuming the energy required for pyrolysis can be carried out by combustion of the evolved pyrolytic gas product. For this purpose, the energy contents of the combustible pyrolysis gases were empirically calculated for each temperature region, while the energy required to carry out the pyrolysis process was determined by integrating the specific heat data shown in Figure 8-2. A positive difference between these values is the possible energy contribution of the pyrolysis gas.

The energy balance for the chicken litter and the rice husk samples, represented in Figure 8-5, shows a positive difference between the recovered HHV in the pyrolysis gases and the energy required to heat the sample at temperatures greater than 490°C for the chicken litter and 400°C for the rice husk. This means at pyrolysis temperatures greater than 490°C, the heat of combustion of the evolved volatiles from the chicken litter is sufficient to carry out the pyrolysis process of the chicken litter (Strezov *et al.*, 2009). As the pyrolysis temperature further increased to 700°C, the recoverable energy from the pyrolysis gases alone can compensate the process heat through internal combustion and contribute an additional 736 kJ/kg of energy. Similarly, the energy value of the pyrolysis gases of the rice husk produced at temperatures > 400°C can compensate the pyrolysis heat of the rice husk.

The ultimate analysis and recovered energy ($Q_{recovery}$) in the pyrolysis products at 500°C are given in Tables 8-4 and 8-5, respectively. These ultimate analysis data were used to determine the energy content of the bio-oils.

The total recoverable potential energy from the solid, liquid and gaseous pyrolysis products of the chicken litter and rice husk samples at 500°C was estimated as: 12.7 and 13.9 MJ/kg, respectively, while the amount of heat energy consumed to heat the samples to 500°C was estimated at 1.2 MJ/kg for the chicken litter and 0.8 MJ/kg for the rice husk. Therefore, the net energy balances that can be obtained from the pyrolysis of the chicken litter and rice husk biomass at the prescribed conditions were 11.5 MJ/kg and 13.1 MJ/kg. The heating values of the chicken litter and rice husk feedstocks determined with the IKA C 1 bomb calorimeter were 13.7 MJ/kg and 14.7 MJ/kg, respectively (Table 8-1). Similarly, the heating value of the bio-

chars generated at 500°C was determined to be 15 MJ/kg for the chicken litter and 16 MJ/kg for the rice husk.

Table 8-4 Ultimate analysis of rice husk and chicken-litter waste pyrolysis products at 500°C

Ultimate analysis (%)	Chicken litter		Rice husk	
	Bio-char	Bio-oil	Bio-char	Bio-oil
C	46	56.3	42	59.3
H	3	6.6	2.6	6.0
N	4.4	1.3	//	//
S	0.2	//	//	//
O (by difference)	46.4	35.8	55.4	34.7

Table 8-5 Energy recovery potentials of pyrolytic products of chicken litter and rice husk at 500°C

Product	Chicken litter			Rice husk		
	Mass (%)	Heating value (MJ/kg)	$Q_{recovered}$ (MJ/kg)	Mass (%)	Heating value (MJ/kg)	$Q_{recovered}$ (MJ/kg)
Solid	42	15	6.3	47	16	7.52
Liquid	39	16	6.24	35	17	5.95
Gas	19	1	0.19	18	2.3	0.414
Total $Q_{recovered}$			12.73			13.884

Accordingly, the overall maximum efficiencies of the pyrolysis processes at 500°C and 10°C/min were calculated to be 84.2% for the chicken litter and 89% for the rice husk. In case when the pyrolysis heat is supplied from solar energy, the ($Q_{pyrolysis}$) component of equation 3 becomes zero as the heat energy needed to perform the pyrolysis is freely supplied from the sun; thus, the efficiency can further increase to 92% for the chicken litter and 94% for the rice husk in the case of solar-assisted pyrolysis.

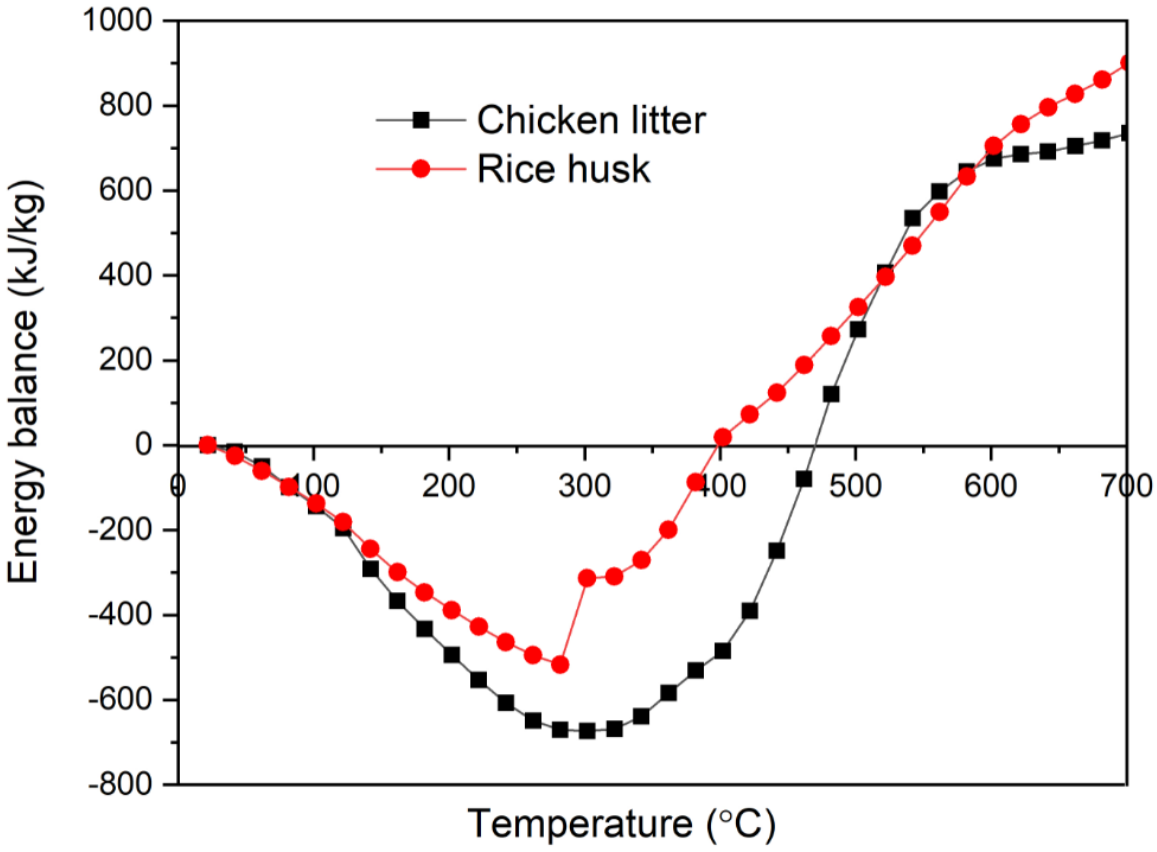

Figure 8-5 Pyrolysis gas energy balance of the chicken-litter waste and rice husk; calculated as a difference between the calorific value of the volatiles and the energy required to heat the sample to each temperature.

8.4 Conclusion

Thermal analysis of chicken-litter waste and rice husk samples were studied with the objective of estimating heat energy required to perform the pyrolysis and quantify recoverable energy from the samples heated at different pyrolysis temperatures. Bio-char yields of the chicken litter and rice husk samples were observed to continuously decrease to 40 and 45 wt.%, respectively, with temperature, while the gas yields of both samples increased to around 21 wt.% at 700°C. The highest bio-oil yield, which was in the range of 35 to 39 wt.%, was achieved at 500°C for both samples. The energy balance of the process was further studied and found a positive balance from the recovered energy of the chicken litter and rice husk pyrolysis gas after 490°C and 400°C, respectively. Under the prescribed pyrolysis conditions, a total net energy balance of 11.5 MJ/kg and 13.1 MJ/kg can be obtained from the pyrolysis of chicken-litter waste and rice husk feedstock, respectively, corresponding to efficiencies of 84.2% and 89%. These efficiencies can be further increased to 92% for the chicken litter and 94% for the

rice husk by integrating solar energy for pyrolysis of biomass and full recovery and utilisation of the evolved pyrolytic gas products.

8.5 References

Abu Bakar, M. S., & Titiloye, J. O. (2013). Catalytic pyrolysis of rice husk for bio-oil production. *Journal of Analytical and Applied Pyrolysis, 103*, 362-368.

Auta, M., Ern, L. M., & Hameed, B. H. (2014). Fixed-bed catalytic and non-catalytic empty fruit bunch biomass pyrolysis. *Journal of Analytical and Applied Pyrolysis, 107*, 67-72.

Bach, Q.-V., & Chen, W.-H. (2017). Pyrolysis characteristics and kinetics of microalgae via thermogravimetric analysis (TGA): A state-of-the-art review. *Bioresource Technology, 246*, 88-100.

Balat, M. (2011). Production of bioethanol from lignocellulosic materials via the biochemical pathway: A review. *Energy Conversion and Management, 52*(2), 858-875.

Bashir, M., Yu, X., Hassan, M., & Makkawi, Y. (2017). Modeling and Performance Analysis of Biomass Fast Pyrolysis in a Solar-Thermal Reactor. *ACS Sustainable Chemistry & Engineering*, *5*(5), 3795-3807.

Bui, H.-H., Tran, K.-Q., & Chen, W.-H. (2016). Pyrolysis of microalgae residues – A kinetic study. *Bioresource Technology, 199*, 362-366.

Bychkov, A. L., Denkin, A. I., Tikhova, V. D., & Lomovsky, O. I. (2017). Prediction of higher heating values of plant biomass from ultimate analysis data. *Journal of Thermal Analysis and Calorimetry, 130*(3), 1399-1405.

Chen, J., Zhao, K., Zhao, Z., He, F., Huang, Z., & Wei, G. (2019). Identifying the roles of MFe2O4 (M=Cu, Ba, Ni, and Co) in the chemical looping reforming of char, pyrolysis gas and tar resulting from biomass pyrolysis. *International Journal of Hydrogen Energy, 44*(10), 4674-4687.

Chen, W.-H., Chu, Y.-S., Liu, J.-L., & Chang, J.-S. (2018). Thermal degradation of carbohydrates, proteins and lipids in microalgae analyzed by evolutionary computation. *Energy Conversion and Management, 160*, 209-219.

Chintala, V. (2018). Production, upgradation and utilization of solar assisted pyrolysis fuels from biomass – A technical review. *Renewable and Sustainable Energy Reviews, 90*, 120-130.

Cong, H., Mašek, O., Zhao, L., Yao, Z., Meng, H., Hu, E., & Ma, T. (2018). Slow Pyrolysis Performance and Energy Balance of Corn Stover in Continuous Pyrolysis-Based Poly-Generation Systems. *Energy & Fuels, 32*(3), 3743-3750.

Dunnigan, L., Ashman, P. J., Zhang, X., & Kwong, C. W. (2018a). Production of biochar from rice husk: Particulate emissions from the combustion of raw pyrolysis volatiles. *Journal of Cleaner Production, 172*, 1639-1645.

Dunnigan, L., Morton, B. J., Ashman, P. J., Zhang, X. P., & Kwong, C. W. (2018b). Emission characteristics of a pyrolysis-combustion system for the co-production of biochar and bioenergy from agricultural wastes. *Waste Management, 77*, 59-66.

Gopu, C., Gao, L. H., Volpe, M., Fiori, L., & Goldfarb, J. L. (2018). Valorizing municipal solid waste: Waste to energy and activated carbons for water treatment via pyrolysis. *Journal of Analytical and Applied Pyrolysis, 133*, 48-58.

Grierson, S., Strezov, V., Ellem, G., McGregor, R., & Herbertson, J. (2009). Thermal characterisation of microalgae under slow pyrolysis conditions. *Journal of Analytical and Applied Pyrolysis, 85*(1), 118-123.

He, J., Strezov, V., Kan, T., Weldekidan, H., Asumadu-Sarkodie, S., & Kumar, R. (2019). Effect of temperature on heavy metal(loid) deportment during pyrolysis of Avicennia marina biomass obtained from phytoremediation. *Bioresource Technology, 278*, 214-222.

Jayaraman, K., Gokalp, I., Petrus, S., Belandria, V., & Bostyn, S. (2018). Energy recovery analysis from sugar cane bagasse pyrolysis and gasification using thermogravimetry, mass spectrometry and kinetic models. *Journal of Analytical and Applied Pyrolysis, 132*, 225-236.

Kan, T., Grierson, S., de Nys, R., & Strezov, V. (2014). Comparative Assessment of the Thermochemical Conversion of Freshwater and Marine Micro- and Macroalgae. *Energy & Fuels, 28*(1), 104-114.

Karaca, C., Sozen, S., Orhon, D., & Okutan, H. (2018). High temperature pyrolysis of sewage sludge as a sustainable process for energy recovery. *Waste Management, 78*, 217-226.

Kumar, R., Singh, L., & Zularisam, A. W. (2016). Exoelectrogens: Recent advances in molecular drivers involved in extracellular electron transfer and strategies used to improve it for microbial fuel cell applications. *Renewable and Sustainable Energy Reviews, 56*, 1322-1336.

Kumar, R., Strezov, V., Lovell, E., Kan, T., Weldekidan, H., He, J., . . . Scott, J. (2019a). Bio-oil upgrading with catalytic pyrolysis of biomass using Copper/zeolite-Nickel/zeolite and Copper-Nickel/zeolite catalysts. *Bioresource Technology, 279*, 404-409.

Kumar, R., Strezov, V., Lovell, E., Kan, T., Weldekidan, H., He, J., . . . Scott, J. (2019b). Enhanced bio-oil deoxygenation activity by Cu/zeolite and Ni/zeolite catalysts in combined in-situ and ex-situ biomass pyrolysis. *Journal of Analytical and Applied Pyrolysis, 140*, 148-160.

Li, X., Strezov, V., & Kan, T. (2014). Energy recovery potential analysis of spent coffee grounds pyrolysis products. *Journal of Analytical and Applied Pyrolysis, 110*, 79-87.

López-González, D., Puig-Gamero, M., Acién, F. G., García-Cuadra, F., Valverde, J. L., & Sanchez-Silva, L. (2015). Energetic, economic and environmental assessment of the pyrolysis and combustion of microalgae and their oils. *Renewable and Sustainable Energy Reviews, 51*, 1752-1770.

Pérez-Arévalo, J. J., Callejón-Ferre, A. J., Velázquez-Martí, B., & Suárez-Medina, M. D. (2015). Prediction models based on higher heating value from the elemental analysis of neem, mango, avocado, banana, and carob trees in Guayas (Ecuador). *Journal of Renewable and Sustainable Energy, 7*(5), 053122.

Piatkowski, N., Wieckert, C., Weimer, A. W., & Steinfeld, A. (2011). Solar-driven gasification of carbonaceous feedstock—a review. *Energy & Environmental Science, 4*(1), 73-82.

Strezov, V., & Evans, T. J. (2009). Thermal processing of paper sludge and characterisation of its pyrolysis products. *Waste Management, 29*(5), 1644-1648.

Strezov, V., Lucas, J. A., & Strezov, L. (2003a). Computer aided thermal analysis. *Journal of Thermal Analysis and Calorimetry, 72*(3), 907-918.

Strezov, V., Moghtaderi, B., & Lucas, J. A. (2003b). Thermal study of decomposition of selected biomass samples. *Journal of Thermal Analysis and Calorimetry, 72*(3), 1041-1048.

Strezov, V., Moghtaderi, B., & Lucas, J. A. (2004). Computational calorimetric investigation of the reactions during thermal conversion of wood biomass. *Biomass & Bioenergy, 27*(5), 459-465.

Tuller, H. L. (2017). Solar to fuels conversion technologies: a perspective. *Materials for Renewable and Sustainable Energy, 6*(1), 3.

Vardon, D. R., Moser, B. R., Zheng, W., Witkin, K., Evangelista, R. L., Strathmann, T. J., . . . Sharma, B. K. (2013). Complete Utilization of Spent Coffee Grounds To Produce

Biodiesel, Bio-Oil, and Biochar. *ACS Sustainable Chemistry & Engineering, 1*(10), 1286-1294.

Viana, H., Cohen, W. B., Lopes, D., & Aranha, J. (2010). Assessment of forest biomass for use as energy. GIS-based analysis of geographical availability and locations of wood-fired power plants in Portugal. *Applied Energy, 87*(8), 2551-2560.

Weldekidan, H., Strezov, V., Kan, T., Kumar, R., He, J., & Town, G. (2019). Solar assisted catalytic pyrolysis of chicken-litter waste with in-situ and ex-situ loading of CaO and char. *Fuel, 246*, 408-416.

Weldekidan, H., Strezov, V., Kan, T., & Town, G. (2018a). Waste to Energy Conversion of Chicken Litter through a Solar-Driven Pyrolysis Process. *Energy & Fuels, 32*(4), 4341-4349.

Weldekidan, H., Strezov, V., & Town, G. (2018b). Review of solar energy for biofuel extraction. *Renewable and Sustainable Energy Reviews, 88*, 184-192.

Weldekidan, H., Strezov, V., Town, G., & Kan, T. (2018c). Production and analysis of fuels and chemicals obtained from rice husk pyrolysis with concentrated solar radiation. *Fuel, 233*, 396-403.

Werder, M., & Steinfeld, A. (2000). Life cycle assessment of the conventional and solar thermal production of zinc and synthesis gas. *Energy, 25*(5), 395-409.

Whitely, N., Ozao, R., Cao, Y., & Pan, W.-P. (2006). Multi-utilization of Chicken Litter as a Biomass Source. Part II. Pyrolysis. *Energy & Fuels, 20*(6), 2666-2671.

Wu, H., Gauthier, D., Yu, Y., Gao, X., & Flamant, G. (2018). Solar-Thermal Pyrolysis of Mallee Wood at High Temperatures. *Energy & Fuels, 32*(4), 4350-4356.

Zhang, Y., Li, B., Li, H., & Liu, H. (2011). Thermodynamic evaluation of biomass gasification with air in autothermal gasifiers. *Thermochimica Acta, 519*(1), 65-71.

Zhong, M., Zhang, Z., Zhou, Q., Yue, J., Gao, S., & Xu, G. (2012). Continuous high-temperature fluidized bed pyrolysis of coal in complex atmospheres: Product distribution and pyrolysis gas. *Journal of Analytical and Applied Pyrolysis, 97*, 123-129.

Chapter 9: Conclusions and recommendations

In this PhD thesis solar parabolic dish with 1.8 m aperture diameter and a focal length at 0.655 m was designed and manufactured to concentrate solar radiation for the purpose of producing solar fuels from organic waste through a thermochemical conversion process. Temperatures as high as 1100°C were achieved using glass and stainless steel tube reactors placed at the focal zone. Biomass pyrolysis requires temperatures in the range of 300 to 700°C, thus the generated temperature from the setup was sufficient to perform the pyrolysis process.

Following this, different set of pyrolysis experiments were conducted to study the effects of various operating parameters and the products generated from the pyrolysis of chicken-litter waste and rice husk feedstocks under the solar conditions.

Temperature was found to be the most important factor which drastically affected the yield and composition of the pyrolysis products. For example, the gas yield in the chicken litter pyrolysis was observed to increase with temperature from around 45 wt.% at 560°C to 59 wt. % at 860°C. Similarly, the gas yield from the pyrolysis of rice husk increased from 14 wt.% to 26 wt.% with temperature. CO_2, CO and H_2 were the dominant gas products obtained throughout all pyrolysis temperatures. Concentration of CO_2 was significantly reduced to CO with the application of CaO and char catalysts at higher temperatures, moreover experiments performed at 1600°C and 500°C/s produced more combustible gases with higher heating values than at lower ranges of temperatures. It was further noticed that the contents of CO and H_2 increased with rise in temperature for both biomass types and particle sizes. The addition of CaO and char in the solar pyrolysis of chicken litter also deoxygenated the fatty acid fractions of the bio-oil and increased the alcoholic and phenolic components.

Bio-oil and bio-char were the other significant yields obtained from the pyrolysis of the rice husk which could be associated with the higher lignin and cellulose component of the feedstock. The bio-oils generated from both feedstocks were highly oxygenated and acidic which require further downstream thermal or catalytic treatment for direct application in engines as transportation fuels. The bio-oils can be applied to produce industrial solvents, cleaning agents, pharmaceutical commodities and to dehydrate natural gas.

Morphology and functional groups of generated bio-chars were modified at each pyrolysis temperature with various pore size and structures evolved as the temperature increased. Bio-chars produced from the pyrolysis of rice husk had large glass-like cylindrical wholes and

important elements, such as potassium, magnesium, calcium, carbon and silicon, with concentrations generally observed to increase with temperature. Similarly, in the solar pyrolysis of chicken-litter waste, the bio-char yield was observed to significantly decrease with temperate.

Overall, it can be concluded that solar pyrolysis of biomass can become viable potential for converting organic waste into fuels and important chemicals with nearly zero GHGs emissions.

Future research work is needed to upgrade the quality of the bio-oil through hydrothermal or catalytic treatments. Moreover, the pyrolytic gas is concentrated with CO_2 which also requires further treatments to reduce it to other combustible gases. The high heating rate and temperature, which can only be obtained under the solar irradiation, can facilitate the secondary cracking reaction of tar and then improve the production of CO and H_2. Biomass gasification is another process which should be tested under the concentrated solar radiation with different types of carbonaceous feedstocks. Testing the performance of the solar pyrolysis products as well as scaling up the solar-assisted pyrolysis system can be an interesting future work.

Appendix I

Literature review on biomass thermochemical processes with concentrated solar radiation: Recent developments

Detailed literature reviews on solar-assisted thermochemical conversion of biomass has been given in Chapter 2. This is a supplementary information which provides recent R&Ds on biomass pyrolysis with concentrated solar radiation.

Depending on the oxygen and temperature requirements biomass thermochemical conversion routes can be broadly classified as combustion, gasification and pyrolysis. Among these, pyrolysis is attaining greater emphasis due to process simplification and production of different types of chemicals and fuels including pyrolytic gases, bio-oil and bio-char. It is possible to convert almost any type of organic material into the different products at relatively lower temperatures (300 to 700°C) via pyrolysis process. With this direction of progress, several solar pyrolysis technologies were developed at laboratory scale in recent years.

The influence of temperature and heating rate of solar pyrolysis in the properties of chars produced from an agave biomass were studied by Ayala-Cortés *et al.*, (2019). The solar reactor was spherically-shaped borosilicate glass of 25 L capacity and placed at the focal zone of IER-UNAM solar furnace which can generate 25 kW power and peak concentrations of 18,000 kW/m^2. Results indicated that the structure, surface area and electrochemical response of the produced char were highly affected by the solar temperature and heating rates. Particularly temperatures above 650°C tend to destroy the macroporosity of the char which could be associated with plastic transformations.

Experimental studies aimed at comparing the effect of different pellet sizes on the yield and composition of syngas and tar were performed during high temperature fast pyrolysis of sawdust (Soria *et al.*, 2019). The experiments were conducted at PROMES-CNRS using the solar configuration described in Chapter 7 of this thesis. Temperatures and heating rates in the range of 800 to 1600°C and 10 to 50°C/s, respectively, were considered. It was found that an increase in pellet size improved syngas quality and chemical energy content at all operating conditions. The highest syngas yield (~ 59 wt%) was found for a 15 mm pellet height at 1600°C and 50°C/s. On the contrary tar yield (~ 60 wt%) was maximum at 800°C and 10°C/s for a 5 mm pellet height.

The same experimental setup was also employed to drive steam gasification of different lignocellulosic biomass feedstocks continuously fed to the reactor at different rates ranging from 0.8 to 2.7 g/min (Chuayboon *et al.*, 2019). The syngas yield was observed to increase with the feeding rate and reached a maximum value of 83.2 mmol/gbiomass at 2.7 g/min rate.

Solar pyrolysis of scrap tire was performed at lower ranges of pyrolysis temperatures (300 to 500°C) in a vertical solar furnace made from sun tracking heliostat and parabolic concentrator (Rahman & Aziz, 2018). A shutter and PID controller were used to monitor heating rate and final temperatures in the reactor. The highest pyrolysis gas (~19 wt%) was found at 500°C while the bio-char and bio-oil yields were maximum (49 wt% and 45 wt%, respectively) at 300°C.

Appendix II

Solar towers for large scale biomass pyrolysis

Different types of solar technologies can be applied to concentrate the available solar radiation for biomass pyrolysis. Predominantly parabolic trough, parabolic dish or Scheffler dish, Fresnel lens and Heliostat have been extensively studied for solar pyrolysis technology. The main advantage of these types of concentrators is the provision of symmetrical solar beam distribution around the focal point (pyrolysis reactor) which ensure uniform heat flux distribution throughout the biomass sample and reduces temperature gradient in the biomass during pyrolysis. However, these solar concentrators could be employed for pilot scale demonstrations in the range of 10–1000 kW solar input.

Central-receiver solar thermal technology is used to provide high temperature sources for large scale pyrolysis applications (Zheng & Xu, 2018). These types of technologies are called solar towers and are used for commercial scale operations. Solar towers, also known as central tower power plants, have receivers mounted on top of towers. Array of movable mirrors (heliostats) which track the sun at all times of the day are used to focus the sun's rays to the receiver-rector affixed on the top of the tower. The arrangement can concentrate the available solar radiation up to 2000 kW/m^2 and allow a commercial scale pyrolysis reactor to achieve and sustain extremely high temperatures of up to 1700 K (Koepf *et al.*, 2017).

The solar tower technology plant is growing rapidly and many demonstration and commercial plants have been built all over the world (Du *et al.*, 2016). A 30 MW commercial plant was installed in Rehovot–Israel following the successful demonstration of a 5 MW solar tower plant (Wieckert *et al.*, 2006). The system has 62, 000 m^2 circular field that focus the sun's rays onto a hyperbolical reflector located 120 m above the ground which re-direct the sunlight to a two-cavity solar reactor situated on the ground level. The configuration was able to produce solar carbotherml Zn at a rate of 11.1 t/h by reducing ZnO with carbonaceous materials.

Likewise, a solar tower with similar design and configuration but small scale, was installed at the Plataforma Solar de Almeria (PSA). A field of sun tracking heliostats focused the sunrays toward a solar reactor situated on a 46 m high tower and provided 150 kW power which produced high quality syngas from the gasification of various feedstock (Wieckert *et al.*, 2013).

Solar gasification of biomass was carried out in a large-scale solar pyrolysis reactor installed at the top of a central tower surrounded by circular array of heliostats that focused sunlight

onto the reactor (Adinberg *et al.*, 2004). Temperatures of up to 1223 K were achieved to drive the gasification of cellulose particles which produced CO, CO_2 and CH_4 with a relatively higher fraction of hydrogen (26% vol%) than the other gas species.

Appendix III

Reactors for solar pyrolysis

Biomass pyrolysis technologies driven by concentrated solar radiation have two main parts; the concentrator and reactor. As thoroughly discussed in Chapter 2, solar concentrators could be parabolic dish, troughs, heliostat or Fresnel lens while solar reactors are designed based on the type of concentrator and the solar flux map created at the focal zone of the solar collector. Solar receivers when used for biomass pyrolysis are called pyrolysis rectors (Sánchez *et al.*, 2018). Different shape and sizes of solar reactors have been made and tested. For example Rony *et al.*, (2018) designed a cylindrical, two layered, quartz glass reactor with inner and outer diameters of 29 mm and 58 mm respectively. It was used with solar simulator and dish concentrator for the production of fuels and chemicals from the pyrolysis of sawdust at 1000°C. Temperatures were measured with K-type thermocouples and the reactor could operate as both fixed and fluidized bed rector. Same system was employed for the pyrolysis of corn stover at different temperature ranging from 350 to 700°C (Rony *et al.*, 2019). Analysed bio-oils have high contents of phenols and furans while the gas stream contained CO_2, CH_4 H_2 and CO.

Similar designs of different types of materials, listed in Table AIII-1, were adopted in this project as solar absorber-reactors and tested empty for their temperature performance at different radiation levels. K-type thermocouple tip was placed at the centre of the empty reactor where the biomass sample would be placed then the pipe was purged for about 20 min with argon gas, flowing at 100 mL/min to create inert environment inside the reactor. Finally, the reactor was set at the focal region of the concentrator and temperature and radiation data were recorded with TC-08 type of data logger and Campbell pyrometer, respectively. Except for aluminium all the reactors reached pyrolysis temperature with the highest temperatures being in the stainless steel and glass pipes. With parabolic dish as the solar concentrator, flux distribution around the focal region was symmetrical which ensures uniform temperatures and reduced gradient on the biomass during pyrolysis. Figure AII-1 depicts schematic drawing of the glass reactor applied in this project.

Table AIII-1 Dimensions and thermal property of the reactors

Reactor material	Diameter [mm]	Thermal conductivity [W/m.K] at 298 K	Emissivity coefficient (ε) at 298 K	Wall thickens [mm]
glass	12	~1	0.9	0.8
copper	13	401	0.6	0.8
stainless steel	10	16	0.75	0.6
aluminium	10	205	0.25	1
alumina ceramic	7	16	0.8	1

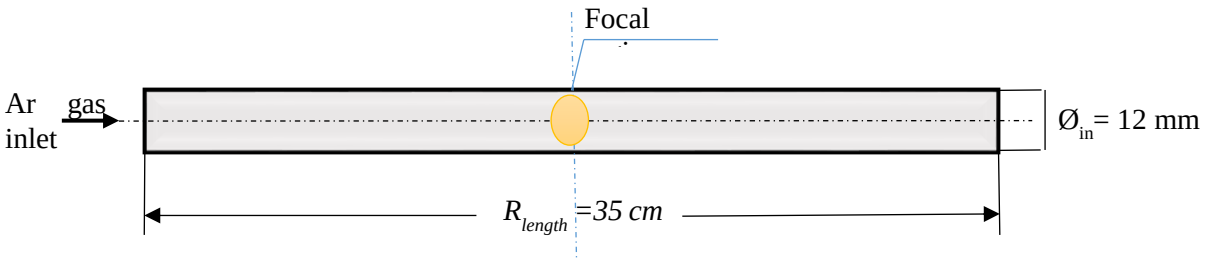

Figure AIII-1 Schematic diagram of the glass reactor

References

Adinberg, R., Epstein, M., & Karni, J. (2004). Solar Gasification of Biomass: A Molten Salt Pyrolysis Study. *Journal of Solar Energy Engineering, 126*(3), 850-857.

Ayala-Cortés, A., Lobato-Peralta, D. R., Arreola-Ramos, C. E., Martínez-Casillas, D. C., Pacheco-Catalán, D. E., Cuentas-Gallegos, A. K., . . . Villafán-Vidales, H. I. (2019). Exploring the influence of solar pyrolysis operation parameters on characteristics of carbon materials. *Journal of Analytical and Applied Pyrolysis, 140*, 290-298.

Chuayboon, S., Abanades, S., & Rodat, S. (2019). Insights into the influence of biomass feedstock type, particle size and feeding rate on thermochemical performances of a continuous solar gasification reactor. *Renewable Energy, 130*, 360-370.

Du, B.-C., He, Y.-L., Zheng, Z.-J., & Cheng, Z.-D. (2016). Analysis of thermal stress and fatigue fracture for the solar tower molten salt receiver. *Applied Thermal Engineering, 99*, 741-750.

Koepf, E., Alxneit, I., Wieckert, C., & Meier, A. (2017). A review of high temperature solar driven reactor technology: 25years of experience in research and development at the Paul Scherrer Institute. *Applied Energy, 188*, 620-651.

Rahman, M. A., & Aziz, M. A. (2018). Solar pyrolysis of scrap tire: optimization of operating parameters. *Journal of Material Cycles and Waste Management, 20*(2), 1207-1215.

Rony, A. H., Kong, L., Lu, W., Dejam, M., Adidharma, H., Gasem, K. A. M., . . . Fan, M. (2019). Kinetics, thermodynamics, and physical characterization of corn stover (Zea mays) for solar biomass pyrolysis potential analysis. *Bioresource Technology, 284*, 466-473.

Rony, A. H., Mosiman, D., Sun, Z., Qin, D., Zheng, Y., Boman, J. H., & Fan, M. (2018). A novel solar powered biomass pyrolysis reactor for producing fuels and chemicals. *Journal of Analytical and Applied Pyrolysis, 132*, 19-32.

Sánchez, M., Clifford, B., & Nixon, J. D. (2018). Modelling and evaluating a solar pyrolysis system. *Renewable Energy, 116*, 630-638.

Soria, J., Li, R., Flamant, G., & Mazza, G. D. (2019). Influence of pellet size on product yields and syngas composition during solar-driven high temperature fast pyrolysis of biomass. *Journal of Analytical and Applied Pyrolysis, 140*, 299-311.

Wieckert, C., Frommherz, U., Kräupl, S., Guillot, E., Olalde, G., Epstein, M., . . . Steinfeld, A. (2006). A 300kW Solar Chemical Pilot Plant for the Carbothermic Production of Zinc. *Journal of Solar Energy Engineering, 129*(2), 190-196.

Wieckert, C., Obrist, A., Zedtwitz, P. v., Maag, G., & Steinfeld, A. (2013). Syngas Production by Thermochemical Gasification of Carbonaceous Waste Materials in a 150 kWth Packed-Bed Solar Reactor. *Energy & Fuels, 27*(8), 4770-4776.

Zheng, Z.-J., & Xu, Y. (2018). A novel system for high-purity hydrogen production based on solar thermal cracking of methane and liquid-metal technology: Thermodynamic analysis. *Energy Conversion and Management, 157*, 562-574.

Appendix IV

Copyright Permission Letters

Permission letters granted from the publisher to include the papers in this PhD thesis are appended here under.

RightsLink®

Home | Create Account | Help | LIVE CHAT

Title:	Waste to Energy Conversion of Chicken Litter through a Solar-Driven Pyrolysis Process
Author:	Haftom Weldekidan, Vladimir Strezov, Tao Kan, et al
Publication:	Energy & Fuels
Publisher:	American Chemical Society
Date:	Apr 1, 2018

LOGIN

If you're a copyright.com user, you can login to RightsLink using your copyright.com credentials.

Already **a RightsLink user** or want to learn more?

PERMISSION/LICENSE IS GRANTED FOR YOUR ORDER AT NO CHARGE

This type of permission/license, instead of the standard Terms & Conditions, is sent to you because no fee is being charged for your order. Please note the following:

- Permission is granted for your request in both print and electronic formats, and translations.
- If figures and/or tables were requested, they may be adapted or used in part.
- Please print this page for your records and send a copy of it to your publisher/graduate school.
- Appropriate credit for the requested material should be given as follows: "Reprinted (adapted) with permission from (COMPLETE REFERENCE CITATION). Copyright (YEAR) American Chemical Society." Insert appropriate information in place of the capitalized words.
- One-time permission is granted only for the use specified in your request. No additional uses are granted (such as derivative works or other editions). For any other uses, please submit a new request.

BACK | CLOSE WINDOW

RightsLink®

Home | Create Account | Help | LIVE CHAT

Title: Energy conversion efficiency of pyrolysis of chicken litter and rice husk biomass

Author: Haftom Weldekidan, Vladimir Strezov, Jing He, et al

Publication: Energy & Fuels

Publisher: American Chemical Society

Date: May 1, 2019

LOGIN

If you're a copyright.com user, you can login to RightsLink using your copyright.com credentials.

Already **a RightsLink user** or want to learn more?

PERMISSION/LICENSE IS GRANTED FOR YOUR ORDER AT NO CHARGE

This type of permission/license, instead of the standard Terms & Conditions, is sent to you because no fee is being charged for your order. Please note the following:

- Permission is granted for your request in both print and electronic formats, and translations.
- If figures and/or tables were requested, they may be adapted or used in part.
- Please print this page for your records and send a copy of it to your publisher/graduate school.
- Appropriate credit for the requested material should be given as follows: "Reprinted (adapted) with permission from (COMPLETE REFERENCE CITATION). Copyright (YEAR) American Chemical Society." Insert appropriate information in place of the capitalized words.
- One-time permission is granted only for the use specified in your request. No additional uses are granted (such as derivative works or other editions). For any other uses, please submit a new request.

BACK CLOSE WINDOW